Abstract

WAN, XIAOHAI. Numerical Simulation Methods for Biological Tissue Interactions. (Under the direction of Dr. Sharon R. Lubkin and Dr. Zhilin Li.)

This thesis describes the Immersed Interface Method (IIM) coupled with the Level Set Method (LSM) for solving viscous two-phase incompressible Stokes equations, with singular interface force and piecewise constant viscosity coefficient. Two-phase Stokes equations appear in many physical and biological applications and we will focus on studying morphogenesis using incompressible Stokes equations.

In this thesis, Stokes equations are used to study the interactions between the mesenchymal and the epithelial tissue in branching morphogenesis. The Stokes equations are decoupled into Poisson equations using the projection method. To use the IIM for the decoupled Poisson equations, we first derive the jump conditions for both the pressure and the velocity in the case where the two fluids may have unequal viscosity coefficients.

Since the jump conditions for the pressure and the velocity can be decoupled by introducing augmented variables, we use the Generalized Minimal Residual (GMRES) method to solve for the augmented variables, and then solve the Stokes equations. For each GMRES iteration, existing fast Poisson solvers can be used and the number of GMRES iterations seems to be independent of the grid size. Thus our algorithm is efficient. Numerical experiments using constructed exact solutions confirm the expected second order accuracy in both 2D and 3D for the Stokes equations.

The interface between two fluid phases is implicitly represented using a level set function. We couple the LSM with IIM for moving interface problems and test the coupled algorithm using mean curvature flow problems for both 2D and 3D. Simulation results show that our moving interface algorithm is efficient and can capture interface dynamics well.

We also study the interactions between mesenchymal and epithelial tissues in the case where the contraction force of mesenchyme is modeled as a body force which deforms the epithelium. We show simulation results for branching morphogenesis with varying parameters.

NUMERICAL SIMULATION METHODS FOR BIOLOGICAL TISSUE INTERACTIONS

by
Xiaohai Wan

a dissertation submitted to the graduate faculty of
north carolina state university
in partial fulfillment of the
requirements for the degree of
doctor of philosophy

biomathematics

raleigh, nc
2006

approved by:

Dr. Mansoor A. Haider	Dr. Julia S. Kimbell
Dr. Sharon R. Lubkin chair of advisory committee	Dr. Zhilin Li co-chair of advisory committee

To my wife and my parents.

Biography

Xiaohai Wan is from Jinhu, Jiangsu province of P.R.China. In 1994, he attended Peking University in China and graduated in 1998 with a Bachelor of Science degree in computational mathematics. He then worked as a college lecturer in Peking University Health Science Center for three years. He came to North Carolina State University to study biomathematics in 2001. In 2003, he received a Master of Science degree in biomathematics with a minor in statistics. He continued his studies towards a Ph.D degree in biomathematics at North Carolina State University and expects to graduate in 2006.

Acknowledgments

I would like to express my deepest gratitude to my advisors: Dr. Sharon R. Lubkin and Dr. Zhilin Li. They have supported me throughout this work and provided valuable ideas, insightful comments, and continuous encouragement. It was really a privilege and a pleasure to be one of their students, and this invaluable experience will definitely benefit me for my future career.

Thanks to Dr. Mansoor A. Haider and Dr. Julia S. Kimbell for being on my Ph.D committee, and for the time they dedicated to reviewing my thesis. Their helpful suggestions have made this dissertation much better. I would also thank Dr. John Bishir for his kindness and helpfulness during my study.

Special thanks to my wife Hanping Song, my father Fuwu Wan and my mother Jiannong Wan. Their love and support have carried me to where I am today.

This work is in part supported by NSF/NIH grant #0201094. I also thank the NSF Institute for Pure & Applied Mathematics (IPAM) at UCLA for a fellowship in the final stage of this work (March - June, 2006).

Table of Contents

List of Figures . . . viii

1 Introduction . . . 1
- 1.1 Biological Tissue Interactions . . . 1
- 1.2 Mathematical Models . . . 2
- 1.3 Our Model for Branching Morphogenesis . . . 4
- 1.4 Outline of the Thesis . . . 7

2 Incompressible Stokes Equations for Flows with Two Viscous Tissues . 9
- 2.1 Navier-Stokes Equations and Stokes Equations . . . 9
  - 2.1.1 Navier-Stokes Equations . . . 9
  - 2.1.2 Nondimensionalization and the Reynolds number . . . 10
  - 2.1.3 Stokes equations for Newtonian incompressible flows . . . 11
- 2.2 The Immersed Interface Problem for Flows with Two Viscous Tissues . . . 12

3 Coordinate Transformations and Jump Conditions for Stokes Equations 15
- 3.1 Local Cartesian Coordinates and Transformations . . . 15
  - 3.1.1 Local Cartesian Coordinates . . . 15
  - 3.1.2 2D Geometry . . . 16
  - 3.1.3 3D Geometry . . . 19
- 3.2 Derivation of Jump Conditions for Stokes Equations . . . 21
  - 3.2.1 Jump Conditions for Stokes Equations . . . 22
  - 3.2.2 2D Geometry . . . 23
  - 3.2.3 3D Geometry . . . 31

4 Immersed Interface Method for Elliptic Differential Equation with Interfaces . . . 41
- 4.1 2D Geometry . . . 41

4.2 3D Geometry . . . 55
4.3 Level Set Approach . . . 71
4.3.1 2D Geometry . . . 72
4.3.2 3D Geometry . . . 75

5 Solving Stokes Equations and Advection Equation . . . 81
5.1 Solving Stokes Equations with an Interface . . . 81
5.1.1 2D Geometry . . . 83
5.1.2 3D Geometry . . . 84
5.2 Solving Advection Equation . . . 86

6 Numerical Implementation: Differencing and Interpolation . . . 87
6.1 2D Geometry . . . 87
6.1.1 Differencing . . . 87
6.1.2 Bilinear interpolation . . . 89
6.1.3 Interface interpolation . . . 89
6.1.4 Residual interpolation . . . 90
6.2 3D Geometry . . . 91
6.2.1 Differencing . . . 91
6.2.2 Bilinear interpolation . . . 93
6.2.3 Interface interpolation . . . 94
6.2.4 Residual interpolation . . . 95

7 Numerical Examples with Fixed Interfaces: Convergence and Efficiency Analysis . . . 98
7.1 2D Geometry . . . 98
7.2 3D Geometry . . . 104

8 Moving Interface Problems: Two-Phase Flow with Surface Tension . . . 112
8.1 Level Set Method for Interface Advection . . . 112
8.2 2D Geometry . . . 113
8.2.1 Ellipse interface . . . 113
8.2.2 Star interface . . . 114
8.3 3D Geometry . . . 118
8.3.1 Ellipsoid interface . . . 118
8.3.2 Cell aggregation implanted in a 3D model gel . . . 121

9 Branching Morphogenesis: Epithelium-Mesenchyme Interactions 124
9.1 2D Geometry 125
9.2 3D Geometry 131

10 Discussion 139

List of References 141

Appendix 146

A Note: Einstein Notation 147

List of Figures

1.1 Digitized image of an E12 Hoxb7/GFP transgenic mouse kidney branching morphogenesis. (b) is imaged approximately 30 hours after (a). Courtesy of Prof. John Bertram with permission. 2

1.2 Epithelium is modeled as the fluid phase inside the interface and mesenchyme is outside the interface. Fibroblast density in the mesenchyme advects with the Stokes flow and produces a traction force in the flow field. 5

1.3 Mesenchymal cells advect in Ω^+ and epithelial cells in Ω^- are in contact with a layer called the basal lamina (Γ). 6

2.1 Interface Γ divides Ω into two disjoint regions: Ω^- and Ω^+. Γ is (a) a closed curve for 2D problems, and (b) a closed surface for 3D problems. 13

3.1 Given a point $\boldsymbol{x}_* \in \Gamma$, a local Cartesian coordinate system $\left(\tilde{x}^\alpha, \tilde{x}^\beta\right)$ is built using $\boldsymbol{x}_*$ as the origin, the unit normal vector $\boldsymbol{n}$ and the unit tangential vector $\boldsymbol{\tau}$ at that point as the two coordinate axes. The normal vector $\boldsymbol{n}$ points from Ω^- to Ω^+ and the tangent vector $\boldsymbol{\tau}$ is counter-clockwise of $\boldsymbol{n}$. 17

3.2 Γ may be parameterized as $\left(\tilde{x}^\alpha = \chi\left(\tilde{x}^\beta\right), \tilde{x}^\beta\right)$. 18

3.3 Given a point $\boldsymbol{x}_* \in \Gamma$, a local Cartesian coordinate system $\left(\tilde{x}^\alpha, \tilde{x}^\beta, \tilde{x}^\gamma\right)$ is built using $\boldsymbol{x}_*$ as the origin, the unit normal vector $\boldsymbol{n}$ and two unit tangent vectors $\boldsymbol{\tau}$ and $\boldsymbol{\eta}$ at that point as the three coordinate axes in sequence. The normal vector $\boldsymbol{n}$ points from Ω^- to Ω^+. $\boldsymbol{n}$, $\boldsymbol{\tau}$ and $\boldsymbol{\eta}$ form a right-handed Cartesian coordinate system $\left(\tilde{x}^\alpha, \tilde{x}^\beta, \tilde{x}^\gamma\right)$. 19

3.4 Γ may be parameterized as $\left(\tilde{x}^\alpha = \chi\left(\tilde{x}^\beta, \tilde{x}^\gamma\right), \tilde{x}^\beta, \tilde{x}^\gamma\right)$. 21

4.1 An open curve cannot be used for the interface Γ, since Ω^+ and Ω^- are not defined (a). Ω^- (shaded region) can be either simply connected (b) or not simply connected (c,d). 42

4.2 Given a point $\boldsymbol{x}_* \in \Gamma$, a local Cartesian coordinate system $\left(\tilde{x}^\alpha, \tilde{x}^\beta\right)$ is built using $\boldsymbol{x}_*$ as the origin, the unit normal vector $\boldsymbol{n}$ and the unit tangential vector $\boldsymbol{\tau}$ at that point as the two coordinate axes. The normal vector $\boldsymbol{n}$ points from Ω^- to Ω^+ and the tangent vector $\boldsymbol{\tau}$ is counter-clockwise of $\boldsymbol{n}$. 45

4.3 An example of the five-point stencil centered at an irregular grid point $\left(x_i^\alpha, x_j^\beta\right) \in \Omega^+$ with only $\left(x_i^\alpha, x_{j-1}^\beta\right) \in \Omega^-$. 46

4.4 An example of the Taylor expansion at the local coordinate system $\left(\tilde{x}^\alpha, \tilde{x}^\beta\right)$. Note that the local origin must be on the interface Γ and close to the five stencil grid points. 47

4.5 The surface Γ needs to be closed and smooth, for example: (a) ring torus (b) union of two intersecting spheroids. 55

4.6 Given a point $\boldsymbol{x}_* \in \Gamma$, a local Cartesian coordinate system $\left(\tilde{x}^\alpha, \tilde{x}^\beta, \tilde{x}^\gamma\right)$ is built using $\boldsymbol{x}_*$ as the origin, the unit normal vector $\boldsymbol{n}$ and two unit tangential vectors $\boldsymbol{\tau}$ and $\boldsymbol{\eta}$ at that point as the three coordinate axes in sequence. The normal vector $\boldsymbol{n}$ points from Ω^- to Ω^+. $\boldsymbol{n}$, $\boldsymbol{\tau}$ and $\boldsymbol{\eta}$ form a right-handed Cartesian coordinate system $\left(\tilde{x}^\alpha, \tilde{x}^\beta, \tilde{x}^\gamma\right)$. 58

4.7 An example of the seven-point stencil centered at an irregular grid point $\left(x_i^\alpha, x_j^\beta, x_l^\gamma\right) \in \Omega^+$ with only $\left(x_i^\alpha, x_j^\beta, x_{l-1}^\gamma\right) \in \Omega^-$. 59

4.8 An example of the Taylor expansion at the local coordinate system $\left(\tilde{x}^\alpha, \tilde{x}^\beta, \tilde{x}^\gamma\right)$. Note that the local origin must be on the interface Γ and close to the seven stencil grid points. 60

4.9 Contour plot of a 2D function $\varphi(x^\alpha, x^\beta) = \sqrt{(x^\alpha)^2 + (x^\beta)^2} - 1.0$ whose zero level set is the unit circle. 71

4.10 An irregular grid point $\boldsymbol{x} = (x_i^\alpha, x_j^\beta)$ and its normal projection point $\boldsymbol{x}_* = (x_*^\alpha, x_*^\beta)$ on the interface Γ. 73

4.11 An irregular grid point $\boldsymbol{x} = (x_i^\alpha, x_j^\beta, x_l^\gamma)$ and its normal projection point $\boldsymbol{x}_* = (x_*^\alpha, x_*^\beta, x_*^\gamma)$ on the interface Γ. 76

7.1 For the equal viscosity case, (a) Convergence analysis in the $\mathcal{L}^\infty$ norm, and (b) CPU time cost. 100

7.2 Convergence analysis in the $\mathcal{L}^\infty$ norm for four cases in log-log scale. The slope of the linear regression line is the convergence rate which is close to number 2.0 for all cases. (a) $\mu^- = 0.001$ and $\mu^+ = 1.0$. (b) $\mu^- = 0.1$ and $\mu^+ = 1.0$. (c) $\mu^- = 10$ and $\mu^+ = 1.0$. (d) $\mu^- = 1000$ and $\mu^+ = 1.0$. Linear regressions $R^2 > 0.98$ for all cases. 101

7.3 The computed solutions for (a) pressure p and (c) velocity component u^α. The error plot of the computed solutions (b) $p - p_{exact}$ and (d) $u^\alpha - u^\alpha_{exact}$. We choose $m = n = 32$ and $\mu^- = 0.8$. 102

7.4 Algorithm efficiency analysis for 100 by 100 through 1600 by 1600 grids. (a): Number of GMRES iterations. (b): CPU cost with unit second. 103

7.5 Grid size is 80 by 80 and the size of the coefficient matrix for the augmented variable $\left[\mu U^i\right]$ is 232 by 232. Region A represents $\mu^- < 1$ where the fluid inside the interface is less viscous than the fluid outside the interface, region B represents $\mu^- > 1$. 103
7.6 Execution time percentage analysis for (a) $\mu^- = 0.1, \mu^+ = 1.0$ and (b) $\mu^- = \mu^+ = 1.0$. We choose $m = n = 100$. 104
7.7 For the equal viscosity case, (a) Convergence analysis in the $\mathcal{L}^\infty$ norm, and (b) CPU time cost. 107
7.8 Convergence analysis in the $\mathcal{L}^\infty$ norm for four cases in log-log scale. The slope of the linear regression line is the convergence rate which is larger than number 2.0 for all cases. (a) $\mu^- = 0.001$ and $\mu^+ = 1.0$. (b) $\mu^- = 0.1$ and $\mu^+ = 1.0$. (c) $\mu^- = 10$ and $\mu^+ = 1.0$. (d) $\mu^- = 100$ and $\mu^+ = 1.0$. Linear regressions $R^2 > 0.95$ for all cases. 108
7.9 The computed solutions sliced at $x^\gamma = 0.0938$ for (a) pressure p and (c) velocity component u^α. The sliced error plot of the computed solutions (b) $p - p_{exact}$ and (d) $u^\alpha - u^\alpha_{exact}$. We choose $m = n = s = 32$ and $\mu^- = 0.8$. . . 109
7.10 Algorithm efficiency analysis for 32^3 through 128^3 grids. (a): Number of GMRES iterations. (b): CPU cost with unit second. 110
7.11 Grid size is 10^3 and the size of the coefficient matrix for the augmented variable $\left[\mu U^i\right]$ is 102 by 102. Region A represents $\mu^- < 1$ where the fluid inside the interface is less viscous than the fluid outside the interface, region B represents $\mu^- > 1$. 110
7.12 Execution time percentage analysis for (a) $\mu^- = 0.1, \mu^+ = 1.0$ and (b) $\mu^- = \mu^+ = 1.0$. We choose $m = n = s = 40$. 111

8.1 Starting from the ellipse, the interface evolves to a circle under surface tension. (a) The interface plotted at $t = 0$ and $t = 100$. (b) Colored pressure profile with streamlines of the velocity field at $t = 25$. Since the pressure is not continuous across the interface, the color plot for the pressure is not smooth near the interface. 114
8.2 Equilibrium pressure field at $t = 100$. Notice the sharp interface for the pressure field. No noise filtering is used to maintain the sharp interface. . . 115
8.3 Colored pressure profile with streamlines of the velocity field at $t = 25$ for (a) $\mu^- = 0.5$ and (b) $\mu^- = 2.0$. 115
8.4 Starting from the five-star shape, the interface relaxes to a circle under surface tension. (a) The interface plotted at $t = 0$ and $t = 98$. The interface with streamlines of the velocity field at (b) $t = 7$ (c) $t = 21$ and (d) $t = 35$. . . . 116
8.5 Pressure field at $t = 7$. Our algorithm captures the highly localized pressure gradient with the presence of complex five-star interface. 117

8.6 Starting from the ellipsoid, the interface evolves to a sphere under surface tension. The interface plotted at (a) $t = 0$ and (b) $t = 100$ with $\mu^- = 1.0$. . 118

8.7 Cone plot of the velocity field at $t = 30$ with $\mu^- = 1.0$. 119

8.8 Comparison of the evolved interface at $t = 50$ for (a) $\mu^- = 0.5$, (b) $\mu^- = 1.0$ and (c) $\mu^- = 2.0$. 120

8.9 Interface initial condition sliced at $x^\gamma = 0.0$ for cell aggregation fusion simulation. 121

8.10 The initial interface (a) and comparison of the evolved interface at $t = 8$ for (b) $\mu^- = 1.0$, (c) $\mu^- = 0.5$ and (d) $\mu^- = 2.0$. 122

8.11 Comparison of the evolved interface at (a) $t = 0$, (b) $t = 2$ and (c) $t = 4$ for $\mu^- = 1.0$. 123

9.1 Initial number density of contractile mesenchymal cells $c\left(x^\alpha, x^\beta\right)$ (red) and initial interface (green circle) separating epithelium and mesenchyme. . . . 126

9.2 The interface with contractile cell number density profile with $\mu^- = 0.1$ at (a) $t = 0.05$ (b) $t = 0.10$ (c) $t = 0.15$ and (d) $t = 0.20$. 127

9.3 The interface with contractile cell number density profile with $\mu^- = 1.0$ at (a) $t = 0.25$ (b) $t = 0.5$ (c) $t = 0.75$ and (d) $t = 1.0$. 128

9.4 The interface with contractile cell number density profile with $\mu^- = 10.0$ at (a) $t = 0.5$ (b) $t = 1$ (c) $t = 1.5$ and (d) $t = 2$. 129

9.5 Comparison of the interface with contractile cell number density profile with (a) $\mu^- = 0.1$ at $t = 0.2$ (b) $\mu^- = 1.0$ at $t = 0.5$ (c) $\mu^- = 10.0$ at $t = 2$. . . . 130

9.6 Level surface (level value: 0.5) of the initial contractile mesenchymal cell number density $c\left(x^\alpha, x^\beta, x^\gamma\right)$ (red) and initial interface (green) separating epithelium and mesenchyme. 131

9.7 Interface evolution with $\mu^- = 0.2$ at (a) $t = 0.05$ (b) $t = 0.1$ (c) $t = 0.15$ and (d) $t = 0.2$. 132

9.8 The interface sliced at $x^\gamma = 0$ (a,c) and $x^\alpha = 0$ (b,d) and sliced color plot of contractile cell number density profile (red) with $\mu^- = 0.2$ at (a,b) $t = 0.05$ (c,d) $t = 0.2$. 133

9.9 Interface evolution with $\mu^- = 1$ at (a) $t = 0.1$ (b) $t = 0.2$ (c) $t = 0.3$ and (d) $t = 0.4$. 134

9.10 The interface sliced at $x^\gamma = 0$ (a,c) and $x^\alpha = 0$ (b,d) and sliced color plot of contractile cell number density profile (red) with $\mu^- = 1.0$ at (a,b) $t = 0.1$ (c,d) $t = 0.4$. 135

9.11 Interface evolution with $\mu^- = 5$ at (a) $t = 0.25$ (b) $t = 0.5$ (c) $t = 0.75$ and (d) $t = 1.0$. 136

9.12 The interface sliced at $x^\gamma = 0$ (a,c) and $x^\alpha = 0$ (b,d) and sliced color plot of contractile cell number density profile (red) with $\mu^- = 5.0$ at (a,b) $t = 0.25$ (c,d) $t = 1.0$. Note that (c,d) is non-physical since the advection equation solver returns negative values for the number density c. We truncated the negative values as zero for comparison with (a,b). 137

Chapter 1

Introduction

Morphogenesis is the generation of form in tissues, organs, and organisms. Understanding morphogenesis is of fundamental importance in developmental biology [53, 2] and tissue engineering research [41]. Many biological experiments involving tissue interactions have been done in the fields of wound healing, angiogenesis and branching morphogenesis. In general, we believe that to fully understand experimental observations made by biologists, one also needs to construct and apply mathematical and physical models to help illustrate underlying principles existing in such complicated biological systems. The ultimate goal of this high level understanding is to help people invent new tools in both biotechnology which involves the application of the principles of engineering and technology to the life sciences, and biotechnics (i.e. organic model of technology).

In this thesis, we use the well-known fluids model to study the interactions of two early embryonic tissues: epithelia and mesenchyme in the context of branching morphogenesis.

1.1 Biological Tissue Interactions

Epithelial tissue is composed of layers of cells and derives from either the ectoderm or the endoderm [2]. Epithelial cells sit on a fibrous membrane called basal lamina secreted by the epithelium. Mesenchyme (embryonic connective tissue), which develops from the mesoderm, contains fibroblasts and a gelatinous extracellular matrix (ECM). Fibroblasts are loosely-packed cells and can develop into various types of cells such as blood cells, endothelial cells and smooth muscle cells. It is known that fibroblasts can secrete collagen fibers, glycosaminoglycans and glycoproteins into the extracellular matrix [2, 8]. Fibroblasts play an important role in both embryonic tissue development by providing ground substance for the ECM and adult tissue regeneration such as wound healing [8].

Experiments on mouse hair follicles, lung, kidney, mammary gland and submandibular gland (SMG) suggest that various components in mouse embryonic model system contribute to the observed epithelial morphogenesis [17]. For example, in the mouse SMG branching morphogenesis experiments, mesenchymal cells of the SMG exert a traction force on collagen fibers and collagen fibers gather and align along the cleft. It is suggested that this mechanical traction force of fibroblasts is an important morphogenetic cue to the clefting and further branching of the epithelium [17]. Also the flowing movement of fibroblasts in groups in the cleft region is shown to be correlated with the branching process [17]. Other components such as epithelial cell growth, epithelial microfilament contraction, epithelial cell adhesions, the basal lamina of the epithelium and other ECM substances (e.g. growth factors) may or may not play necessary roles in this morphogenesis process [17]. See Fig. 1.1 for an example of mouse kidney branching morphogenesis. Note that the SMG epithelium branching is characterized by the formation of narrow and deep clefts [17], which is not seen in the figure.

(a) (b)

Figure 1.1: Digitized image of an E12 Hoxb7/GFP transgenic mouse kidney branching morphogenesis. (b) is imaged approximately 30 hours after (a). Courtesy of Prof. John Bertram with permission.

1.2 Mathematical Models

From previous centrifugation [43, 44, 45] and compression experiments [3, 6, 13, 14, 15] in vitro, it is known that certain embryonic tissues behave both quantitatively and qualitatively like viscoelastic fluids [43, 44, 45, 3, 6, 13, 14, 15], which implies that tissues deform as elastic materials on short time scales and flow as viscous liquids on long time scales. For example, embryonic tissue rounding is driven by surface tension and resisted by cell adhesion in the same way that hydrophobic oil droplets deform in water [36, 48]. Another good example is that one embryonic tissue spreading over the surface of a different tissue mimics the sorting of two immiscible fluids [3]. Therefore it is a good approximation to model embryonic tissue dynamics using fluid mechanics equations in the limit of very viscous flow. Note that it is not appropriate to model mature tissues as viscous fluids [38] since it is known that mechanical responses are different for aged tissue and embryonic tissue [21] and that ECM components become stabilized in maturity.

Existing approaches to modeling tissue dynamics may be grouped into either discrete models or continuum models. In discrete models, tissues are treated as aggregates of cells and empirical, physical, mechanical rules (such as the differential adhesion rule [43, 44]) are enforced for both individual cells and cell-cell interactions. Cellular automata models [42], cellular Potts models [36, 48] and viscoelastic cellular models [42] are all widely used for various biological problems. It is relatively straightforward to incorporate cellular characteristics and extracellular information into discrete models, but such models may produce limited insight for physical reality, and the predictions from such discrete models often do not correspond to physically measurable quantities.

In contrast, continuum models apply viscoelastic equations (e.g. Navier-Stokes equations [11], Stokes equations [34]) to study tissue interactions. Well established fluid models such as multiphase flow theory can be applied with few modifications. Results of such simulations usually have strong physical implications and may well capture the essence of tissue interactions and morphogenesis. Some geometric models may also be considered as continuum models where differential geometry plays a major role in studying morphogenesis [18]. It is also possible to use a hybrid model with both discrete and continuum components [42].

We will use continuum models to model the interactions between epithelial and mesenchymal tissues. Similar models exist in the mixture theory for multiphase material [10]. For example, Murray et. al. [37] have constructed a mathematical model of traction-producing cells advecting within an elastic ECM. Let c be the cell number density per unit volume, ρ be the ECM mass density per unit volume and $\boldsymbol{u}$ be the displacement of the ECM, the balance equation for the cell density c is [37]

$$\frac{\partial c}{\partial t} = -\nabla \cdot \left(D_2 \nabla \left(\nabla^2 c \right) - D_1 \nabla c + \alpha c \nabla \rho + c \frac{\partial \boldsymbol{u}}{\partial t} \right) + rc \left(N - c \right) \tag{1.2.1}$$

where D_1, D_2, α and r are constants. Here $D_2 \nabla \left(\nabla^2 c \right) - D_1 \nabla c$ models random dispersal and contact guidance (i.e. directed locomotion of cells to an anisotropy of the environment) of cells, $\alpha c \nabla \rho$ represents the haptotaxis (i.e. directional motility of cells up the gradient of cellular adhesion sites) movement of cells, $c \frac{\partial \boldsymbol{u}}{\partial t}$ is the advection term and $rc \left(N - c \right)$ models mitosis of cells with carrying capacity N (i.e. the largest equilibrium size for c).

The balance equation for the matrix density ρ is [37]

$$\frac{\partial \rho}{\partial t} = -\nabla \cdot \left(\rho \frac{\partial \boldsymbol{u}}{\partial t} \right). \tag{1.2.2}$$

The force balance equation for both the matrix and the cells is [37]

$$\nabla \cdot \left(\mu \frac{\partial \boldsymbol{e}}{\partial t} + \lambda \frac{\partial \theta}{\partial t} \boldsymbol{I} + \frac{E}{2\,(1+\nu)} \left(\boldsymbol{e} + \frac{\nu}{1-2\nu} \theta \boldsymbol{I} \right) + \tau \rho c \boldsymbol{I} \right) = 0 \tag{1.2.3}$$

where $\boldsymbol{e} = \dfrac{\nabla \boldsymbol{u} + (\nabla \boldsymbol{u})^T}{2}$ is the strain tensor of the matrix, $\theta = \nabla \cdot \boldsymbol{u}$ is the dilatation of the matrix, μ and λ are viscosity coefficients, E is the Young's modulus of the matrix and ν is the Poisson ratio of the matrix material. τ measures the traction force for a single cell. $\boldsymbol{I}$ is the identity matrix.

Lubkin et. al. [32] proposed a multiphase flow model of capsule formation in tumors. In the multiphase flow model, the mesenchyme is modeled as a mixture of cell/fiber phase and aqueous phase, and the velocity of the cells was allowed to be different from the velocity of the aqueous phase. In the limit of a single phase tissue for which the cell/fiber phase is not separable from the aqueous phase, the force balance equation in the model is reduced to

$$\nabla \cdot (\lambda(\nabla \cdot \boldsymbol{v})\boldsymbol{I} + 2\mu\bar{\boldsymbol{e}}) - \nabla p = \nabla(\Upsilon - \Psi). \tag{1.2.4}$$

Here λ and μ are viscosity coefficients, $\boldsymbol{v}$ is the phase velocity, $\bar{\boldsymbol{e}} = \dfrac{\nabla \boldsymbol{v} + (\nabla \boldsymbol{v})^T}{2}$ is the strain rate tensor for the tissue phase, p is the pressure, Υ models the capillary pressure and Ψ models the contractility.

1.3 Our Model for Branching Morphogenesis

We propose a two-phase fluid model for the SMG branching morphogenesis incorporating (1) the viscous fluids model for both the mesenchyme and the epithelium [34], (2) the contraction force fibroblasts exerted on the ECM [37], and (3) confluent flow of fibroblasts along the clefting region of the epithelium [17]. Our model states that the two embryonic tissues are idealized as two-phase Stokes flow where the viscosity coefficient may be different for the two phases. Singular interface forces such as surface tension may exist along the interface separating the two phases. Fibroblasts (tracked by the number density) advect with the flow in the mesenchyme phase and produce a traction force driving the flow. This traction force is modeled as a body force for the two-phase Stokes equations.

If we assume that both mesenchymal and epithelial tissues behave like viscous fluids, from the multiphase flow model [32], we obtain our two-phase Stokes model for the two tissues with mesenchymal contractility as:

$$\frac{\partial c}{\partial t} = -\nabla \cdot (c\boldsymbol{v}) \tag{1.3.1}$$

where c is the spatial number density of contractile mesenchymal cells, and

$$\nabla \cdot (\boldsymbol{\sigma} + \bar{\boldsymbol{\sigma}}) = 0 \tag{1.3.2}$$

where $\boldsymbol{\sigma}$ is the stress tensor for Stokes flow and $\bar{\boldsymbol{\sigma}}$ is the traction stress of mesenchymal cells (as a function of contractile cell number density c). See Fig. 1.2 for the components of our simplified model.

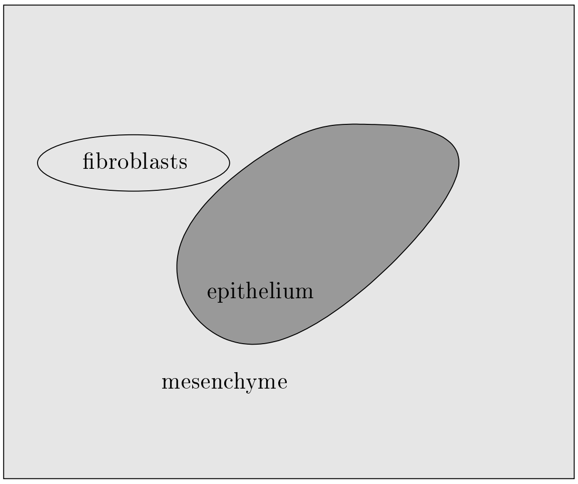

Figure 1.2: Epithelium is modeled as the fluid phase inside the interface and mesenchyme is outside the interface. Fibroblast density in the mesenchyme advects with the Stokes flow and produces a traction force in the flow field.

The confluent flow of fibroblasts along the clefting region of the epithelium [17] is modeled as an advection process. We track the number density of contracting fibroblasts in the mesenchyme phase and the contraction force is treated as a body force term for the two-phase Stokes equations. From Eq. (1.3.1), we have the advection equation in tensor form as

$$\frac{\partial c}{\partial t} = -\frac{\partial \left(cu^i\right)}{\partial x^i} \tag{1.3.3}$$

where $c = c(\boldsymbol{x}, t)$ is the mesenchymal cell number density, t is time coordinate, x^i is spatial coordinates, and u^i is the advection velocity field which is obtained by solving the Stokes flow equations. We use tensor notation throughout the thesis; see Appendix A for the explanations of tensor symbols used. Since for incompressible Stokes flow the velocity field is solenoidal, i.e.

$$\frac{\partial u^i}{\partial x^i} = 0, \tag{1.3.4}$$

substituting Eq. (1.3.4) into Eq. (1.3.3), we get the advection equation in dimensionless form

$$\frac{\partial c}{\partial t} = -u^i \frac{\partial c}{\partial x^i}. \tag{1.3.5}$$

Note that in the multiphase mixture model [32], the incompressibility condition Eq. (1.3.4) is no longer valid and needs to be replaced by a mixture (or group) incompressibility condition. If there is no growth or death for the mesenchymal cell population, we expect that the total number of mesenchymal cells is conserved, i.e.

$$\int_\Omega c\, d\boldsymbol{x} = c^* \tag{1.3.6}$$

where c^* is a normalization constant.

An initial boundary value problem for mesenchymal cellular dynamics

Let the mesenchymal tissue occupy the space of Ω^+ and the epithelial tissue occupy Ω^-. See Fig. 1.3 for the geometry of the problem.

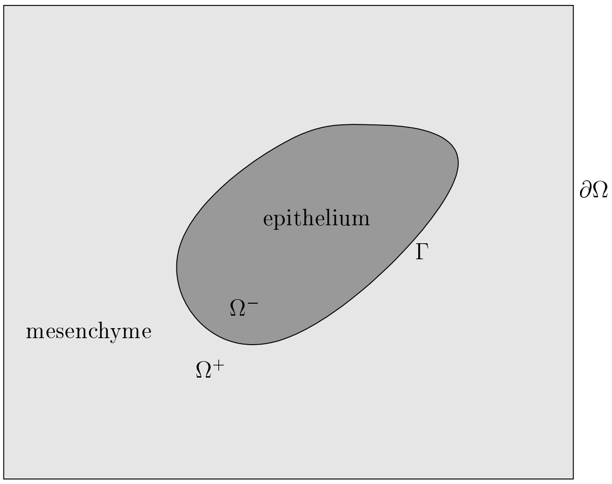

Figure 1.3: Mesenchymal cells advect in Ω^+ and epithelial cells in Ω^- are in contact with a layer called the basal lamina (Γ).

Given an initial condition for the number density c of mesenchymal cells, we solve the advection equation (1.3.5) with periodic boundary condition on $\partial\Omega$. This formulates the initial boundary value problem (IBVP) for mesenchymal cellular dynamics.

Mesenchymal-epithelial interactions

Mesenchymal-epithelial interactions have been studied extensively in biology. We assume that the mesenchymal contractility can be modeled as a contractile stress

$$\bar{\sigma}_{ij} = p_c \delta_{ij} \tag{1.3.7}$$

where p_c depends on the spatial number density c of contractile mesenchymal cells.

For branching morphogenesis using the two-phase Stokes flow model, we will not model the swelling force and the simplest form of p_c is just a linear function of c:

$$p_c = \tau c \tag{1.3.8}$$

where τ measures the traction force a fibroblast cell exerts on the ECM.

Incorporating the contractile stress in the Stokes flow, we can find that p_c may be treated as a body force g^i for the Stokes flow with

$$g^i = \frac{\partial p_c}{\partial x^i}. \tag{1.3.9}$$

Therefore the mesenchymal cells are advected by the Stokes flow and the condensation of mesenchymal cells feeds back as a body force for the Stokes flow.

To summarize, our branching morphogenesis model includes the incompressible Stokes equations, the contraction force as a body force for the Stokes equations and the advection equation for the contractile cell number density c:

$$\boxed{\begin{aligned} -\frac{\partial p}{\partial x^i} + \frac{\partial}{\partial x^j}\left(\mu\left(\frac{\partial u^i}{\partial x^j} + \frac{\partial u^j}{\partial x^i}\right)\right) + g^i &= 0, \\ \frac{\partial u^i}{\partial x^i} &= 0, \\ g^i &= \frac{\partial(\tau c)}{\partial x^i}, \\ \frac{\partial c}{\partial t} &= -u^i\frac{\partial c}{\partial x^i}. \end{aligned}} \tag{1.3.10}$$

1.4 Outline of the Thesis

In Chapter 2, classical fluid mechanics equations (i.e. Navier-Stokes equations and Stokes equations) are derived using Einstein notation and the immersed interface problem for two-phase flow is proposed in the end.

Local Cartesian parameterization of a curve in 2D or a surface in 3D is introduced in Chapter 3 and this local parameterization approach is indispensable to the development of accurate sharp interface methods such as the immersed interface method (IIM) used in the thesis. Jump conditions for Stokes equations are derived in Chapter 3 using both Einstein notation and the local parameterization.

IIM for elliptic equations with interfaces in both 2D and 3D are derived in Chapter 4 with emphasis on the case where the interface is represented implicitly using a level set function. For the case where the viscosity coefficients of the two fluid phases are not equal, the GMRES iteration method is used to solve for augmented variables of the Stokes equations and this method is explained in Chapter 5. In Chapter 6, numerical implementation details such as finite difference schemes and various interpolations are shown in detail.

Grid refinement analysis for fixed interface problems where exact solutions are constructed is shown in Chapter 7. For moving interface problems, the two-phase Stokes solver is coupled with the level set method (LSM). In Chapter 8, we show the surface tension relaxation test simulations in 2D with both ellipse and star interfaces, and in 3D with both ellipsoid and sphere-ring interfaces. We study branching morphogenesis by incorporating the mesenchyme contraction dynamics with the Stokes solver and show simulation results with varying parameters in Chapter 9. Finally, in Chapter 10 we discuss the biological implications of the branching simulations and some future work.

Chapter 2

Incompressible Stokes Equations for Flows with Two Viscous Tissues

We use fluid mechanics equations to model viscous tissues as a continuum. Under the assumptions that tissues may be modeled as Newtonian fluids with very high viscosity coefficient, we choose to study the two-phase Stokes flow and propose the mathematical formulation for the problem.

2.1 Navier-Stokes Equations and Stokes Equations

2.1.1 Navier-Stokes Equations

Most real world objects are classified as solids and fluids. Fluids are different from solids from a mechanics point of view in that a fluid takes the shape of its container while a solid has a reference shape. Fluid dynamics has been studied extensively using a set of differential equations derived from conservation of mass, momentum and energy. In our study, energy dynamics are not of interest. So we will only study equations for conservation of mass and linear momentum.

The mass conservation equation for a fluid is [46]

$$\frac{\partial \rho}{\partial t} + \frac{\partial \left(\rho u^i\right)}{\partial x^i} = 0 \tag{2.1.1}$$

where ρ is fluid density, u^i is fluid velocity, x^i is Cartesian coordinates and t is the time coordinate. The linear momentum conservation equation for a compressible or incompressible fluid follows Cauchy's equation [46]

$$\rho \frac{Du^i}{Dt} = \frac{\partial \sigma_{ij}}{\partial x^j} + \rho g^i \tag{2.1.2}$$

where g^i is a body force such as gravity. The material derivative $\dfrac{Du^i}{Dt}$ is defined as [46]

$$\frac{Du^i}{Dt} = \frac{\partial u^i}{\partial t} + u^j \frac{\partial u^i}{\partial x^j}. \tag{2.1.3}$$

For an incompressible fluid, the mathematical statement of incompressibility is [46]

$$\frac{D\rho}{Dt} = \frac{\partial \rho}{\partial t} + u^j \frac{\partial \rho}{\partial x^j} = 0, \tag{2.1.4}$$

plugging Eq. (2.1.4) into Eq. (2.1.1), we get the incompressibility or continuity equation

$$\frac{\partial u^i}{\partial x^i} = 0. \tag{2.1.5}$$

The stress tensor σ_{ij} for an incompressible Newtonian fluid is

$$\sigma_{ij} = -p\delta_{ij} + \mu 2 e_{ij} \tag{2.1.6}$$

where p is the thermodynamic fluid pressure, μ is a fluid dynamic viscosity coefficient, and δ_{ij} is the Kronecker delta symbol. The rate of deformation tensor e_{ij} is

$$e_{ij} = \frac{1}{2}\left(\frac{\partial u^i}{\partial x^j} + \frac{\partial u^j}{\partial x^i}\right). \tag{2.1.7}$$

Plugging Eqs. (2.1.3, 2.1.6, 2.1.7) into Eq. (2.1.2), we get the well-known Navier-Stokes equation

$$\rho\left(\frac{\partial u^i}{\partial t} + u^j \frac{\partial u^i}{\partial x^j}\right) = -\frac{\partial p}{\partial x^i} + \frac{\partial}{\partial x^j}\left(\mu\left(\frac{\partial u^i}{\partial x^j} + \frac{\partial u^j}{\partial x^i}\right)\right) + \rho g^i \tag{2.1.8}$$

or in vector form

$$\rho\left(\frac{\partial \boldsymbol{u}}{\partial t} + \boldsymbol{u}\cdot\nabla\boldsymbol{u}\right) = -\nabla p + \nabla\mu\left(\nabla\boldsymbol{u} + (\nabla\boldsymbol{u})^T\right) + \rho\boldsymbol{g}. \tag{2.1.9}$$

2.1.2 Nondimensionalization and the Reynolds number

It is expected that the velocity and pressure field for flows in similar domains may be deduced from one another by simply rescaling [46]. Therefore it is helpful to nondimensionalize the Navier-Stokes equations (2.1.8, 2.1.5) for incompressible Newtonian fluids. Assuming that L is the characteristic space scale and U is the characteristic velocity scale, let us introduce the dimensionless variables as follows

$$\hat{x}^i = \frac{x^i}{L}, \quad \hat{t} = \frac{U}{L}t, \quad \hat{u}^i = \frac{u^i}{U}, \quad \hat{p} = \frac{1}{\rho U^2}p, \quad \hat{g}^i = \frac{L}{U^2}g^i \tag{2.1.10}$$

and plug them into the Navier-Stokes equations (2.1.8, 2.1.5) to get the dimensionless form

$$\frac{\partial \hat{u}^i}{\partial \hat{t}} + \hat{u}^j \frac{\partial \hat{u}^i}{\partial \hat{x}^j} = -\frac{\partial \hat{p}}{\partial \hat{x}^i} + \frac{\partial}{\partial \hat{x}^j}\left(\frac{1}{Re}\left(\frac{\partial \hat{u}^i}{\partial \hat{x}^j} + \frac{\partial \hat{u}^j}{\partial \hat{x}^i}\right)\right) + \hat{g}^i \qquad (2.1.11)$$

where the Reynolds number (with no units) is

$$Re = \frac{\rho U L}{\mu} = \frac{UL}{\nu}. \qquad (2.1.12)$$

Here $\nu = \dfrac{\mu}{\rho}$ is the kinematic viscosity coefficient. The dimensionless continuity equation is

$$\frac{\partial \hat{u}^i}{\partial \hat{x}^i} = 0. \qquad (2.1.13)$$

2.1.3 Stokes equations for Newtonian incompressible flows

Under the conditions of extremely low Reynolds number appropriate for modeling morphogenesis [33], viscosity coefficient μ is very large and velocity U is very small. Although it is possible to work with the Navier-Stokes equations, we may be able to model the creeping flow phenomenon using an approximated version of the Navier-Stokes equations, known as the Stokes equations.

Note that the nondimensionalization of the Navier-Stokes equations (2.1.11, 2.1.13) is not unique. For example, since the Reynolds number Re has no units, we may multiply (or divide) any dimensionless variables (e.g. $\hat{p}$) using Re to get new sets of dimensionless variables. Of course, it is preferred to have a dimensionless form with physical meanings. First we assume that the dimensionless forms of spatial coordinate x^i, time coordinate t and velocity u^i are unambiguously chosen as

$$\hat{x}^i = \frac{x^i}{L}, \quad \hat{t} = \frac{U}{L}t, \quad \hat{u}^i = \frac{u^i}{U}. \qquad (2.1.14)$$

And it is clear from Eq. (2.1.11) that the Reynolds number Re can be used to measure the relative importance of inertial forces

$$\frac{D\hat{u}^i}{Dt} = \frac{\partial \hat{u}^i}{\partial \hat{t}} + \hat{u}^j \frac{\partial \hat{u}^i}{\partial \hat{x}^j} \qquad (2.1.15)$$

and viscous forces

$$\frac{\partial}{\partial \hat{x}^j}\left(\frac{\partial \hat{u}^i}{\partial \hat{x}^j} + \frac{\partial \hat{u}^j}{\partial \hat{x}^i}\right). \qquad (2.1.16)$$

If we have $Re \ll 1$, it is expected that the inertial term in Eq. (2.1.11) may be neglected without introducing noticeable errors to the solutions. The dimensionless form of pressure p is rather arbitrary [46], for example,

$$\hat{p} = \frac{1}{\rho U^2} p \qquad (2.1.17)$$

used in Eq. (2.1.10) surely is one version of the dimensionless forms for pressure. We can also use Re to get other versions such as

$$\hat{p}^* = \frac{Re}{\rho U^2} p = \frac{L}{\mu U} p \tag{2.1.18}$$

or more aggressively

$$\hat{p}^{**} = \frac{(Re)^2}{\rho U^2} p = \frac{\rho L^2}{\mu^2} p. \tag{2.1.19}$$

There are two major points observed here: (1) nondimensionalization of pressure p is arbitrary, therefore it is not right to say that we can get only the viscous term left by multiplying Re at both sides of Eq. (2.1.11) and taking the limit of $Re \to 0$; (2) from Eqs. (2.1.18, 2.1.19) it is clear that the pressure term scales as a viscous force and therefore must be kept for the limit of very viscous flow. The same reasoning applies to the body force g^i.

Now by ignoring only the inertia term, we can get the Stokes equation in dimensional form

$$-\frac{\partial p}{\partial x^i} + \frac{\partial}{\partial x^j}\left(\mu\left(\frac{\partial u^i}{\partial x^j} + \frac{\partial u^j}{\partial x^i}\right)\right) + \rho g^i = 0 \tag{2.1.20}$$

with the incompressibility condition

$$\frac{\partial u^i}{\partial x^i} = 0. \tag{2.1.21}$$

We will use the dimensionless form of (2.1.20, 2.1.21) with the same set of notations and call

$$-\frac{\partial p}{\partial x^i} + \frac{\partial}{\partial x^j}\left(\mu\left(\frac{\partial u^i}{\partial x^j} + \frac{\partial u^j}{\partial x^i}\right)\right) + g^i = 0 \tag{2.1.22}$$

and

$$\frac{\partial u^i}{\partial x^i} = 0 \tag{2.1.23}$$

the incompressible Stokes equations.

2.2 The Immersed Interface Problem for Flows with Two Viscous Tissues

We can model epithelio-mesenchymal interactions as creeping flow of two fluids in domains Ω^+ and Ω^- separated by a massless interface Γ. See Fig. 2.1 for an illustration.

We assume that the Stokes equations describe tissue dynamics in both Ω^- and Ω^+, i.e. Eqs. (2.1.22, 2.1.23) are valid for both $\boldsymbol{x} \in \Omega^-$ and $\boldsymbol{x} \in \Omega^+$. Since the Stokes differential equations only admit smooth solutions, we know that the pressure and the velocity for both $\boldsymbol{x} \in \Omega^-$ and $\boldsymbol{x} \in \Omega^+$ are smooth. But we do not know whether the pressure and the velocity

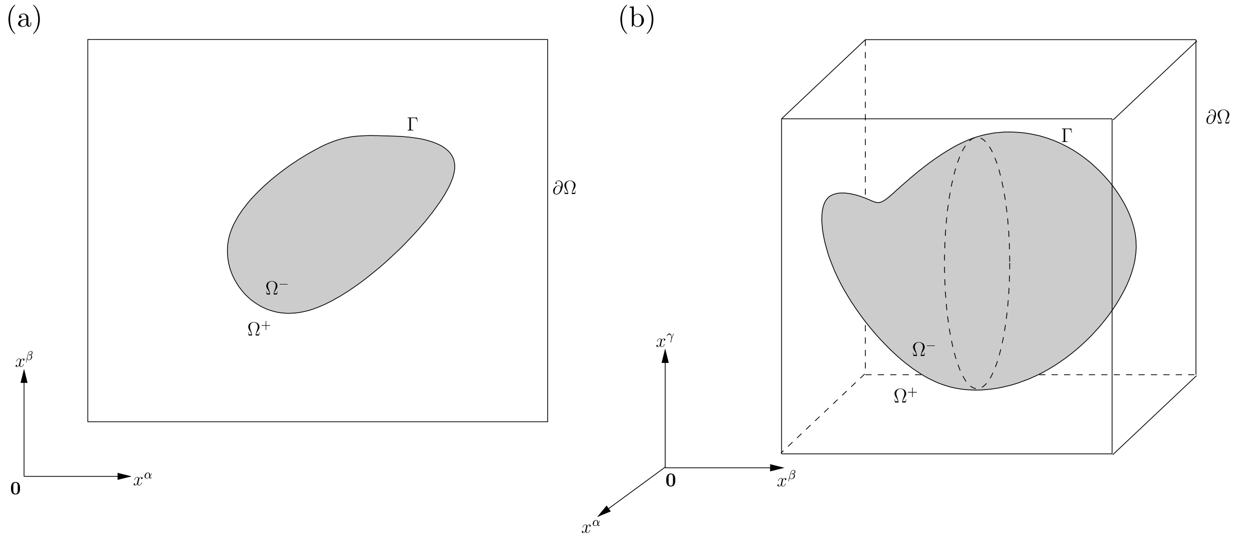

Figure 2.1: Interface Γ divides Ω into two disjoint regions: Ω^- and Ω^+. Γ is (a) a closed curve for 2D problems, and (b) a closed surface for 3D problems.

are smooth or not over the whole domain Ω. Also we know that a fluid property, such as the viscosity coefficient μ, may be different for the two phases across the interface. To retain generality, we express quantities such as pressure and velocity in terms of smooth functions in Ω^+ and Ω^- separately. For example,

$$p = \begin{cases} p^+, & \boldsymbol{x} \in \Omega^+, \\ p^-, & \boldsymbol{x} \in \Omega^- \end{cases} \tag{2.2.1}$$

where p^+ and p^- are sufficiently smooth functions. Also note that

$$\left(\frac{\partial p}{\partial x^i}\right)^+ \equiv \frac{\partial p^+}{\partial x^i}. \tag{2.2.2}$$

For $\boldsymbol{x}_* \in \Gamma$, we can choose $p(\boldsymbol{x}_*)$ as either the limit from Ω^- or the limit from Ω^+. In other words, p can be chosen as either “inner-continuous” or “outer-continuous”. To be consistent, we choose p to be “outer-continuous” throughout the thesis, i.e.

$$p(\boldsymbol{x}_*) = \lim_{\boldsymbol{x} \to \boldsymbol{x}_*} p^+(\boldsymbol{x}). \tag{2.2.3}$$

To summarize, the immersed interface problem for two viscous tissues may be formulated as

$$-\frac{\partial p^+}{\partial x^i} + \frac{\partial}{\partial x^j}\left(\mu^+\left(\frac{\partial\left(u^i\right)^+}{\partial x^j} + \frac{\partial\left(u^j\right)^+}{\partial x^i}\right)\right) + \left(g^i\right)^+ = 0, \quad \boldsymbol{x} \in \Omega^+, \tag{2.2.4}$$

$$\frac{\partial \left(u^i\right)^+}{\partial x^i} = 0, \quad \boldsymbol{x} \in \Omega^+; \tag{2.2.5}$$

and

$$-\frac{\partial p^-}{\partial x^i} + \frac{\partial}{\partial x^j}\left(\mu^-\left(\frac{\partial \left(u^i\right)^-}{\partial x^j} + \frac{\partial \left(u^j\right)^-}{\partial x^i}\right)\right) + \left(g^i\right)^- = 0, \quad \boldsymbol{x} \in \Omega^-, \tag{2.2.6}$$

$$\frac{\partial \left(u^i\right)^-}{\partial x^i} = 0, \quad \boldsymbol{x} \in \Omega^-. \tag{2.2.7}$$

Also, balancing of the surface force along the interface Γ requires [47]

$$\left[\sigma_{ij} n^j\right] + f^i = 0 \tag{2.2.8}$$

where f^i is the singular interface force (e.g. surface tension and Marangoni traction) and n^j is the unit interface normal vector pointing from Ω^- to Ω^+, σ_{ij} is the stress tensor (2.1.6), and the $[\cdot]$ symbol defines the difference of the limiting values across the interface for a given quantity. For example, given $\boldsymbol{x}_* \in \Gamma$ with Γ being the interface, $[p]$ is defined as

$$\begin{aligned}[p]\left(\boldsymbol{x} = \boldsymbol{x}_*\right) &= \lim_{\boldsymbol{x} \to \boldsymbol{x}_*} p^+\left(\boldsymbol{x}\right) - \lim_{\boldsymbol{x} \to \boldsymbol{x}_*} p^-\left(\boldsymbol{x}\right) \\ &= p_\Gamma^+\left(\boldsymbol{x} = \boldsymbol{x}_*\right) - p_\Gamma^-\left(\boldsymbol{x} = \boldsymbol{x}_*\right).\end{aligned} \tag{2.2.9}$$

Chapter 3

Coordinate Transformations and Jump Conditions for Stokes Equations

3.1 Local Cartesian Coordinates and Transformations

We use local Cartesian coordinates defined along the interface and tensor notation to address interface geometry in our problem. Compared with using a non-Cartesian curvilinear coordinate system, our approach makes derivations rather elementary and requires less differential geometry expertise. Note that local Cartesian coordinates and tensor notation are used throughout the thesis.

3.1.1 Local Cartesian Coordinates

Stokes equations for two viscous tissues involve the interface Γ which is a closed smooth curve for 2D problems or a closed smooth surface for 3D problems. For most interface problems, we need to parameterize the interface in some way.

One method is to use non-Cartesian curvilinear coordinates. For example, a closed curve in 2D may be parameterized naturally using the arc length parameter s as

$$\Big(x^{\alpha}(s), x^{\beta}(s)\Big)$$

and this parameterization is unique up to shift of parameter. As a special case, a unit circle with center at the origin may be defined using the polar angle parameter θ as

$$(\cos\theta, \sin\theta)$$

where θ actually measures the arc length for the unit circle. Comparably, a closed surface in 3D may be parameterized under curvilinear coordinates such as cylindrical coordinates and spherical coordinates. As an example, a sphere with center at the origin may be specified in spherical coordinates by

$$\left(x^{\alpha}(\theta,\phi) = r\cos\theta\sin\phi, x^{\beta}(\theta,\phi) = r\sin\theta\sin\phi, x^{\gamma}(\phi) = r\cos\phi\right)$$

where r is a given constant radius, θ is an azimuthal coordinate running from 0 to 2π and ϕ is a colatitude coordinate running from 0 to π.

Another method to parameterize the interface Γ is to use a local Cartesian coordinate system which is a special case of curvilinear coordinates. The reasons that we adopt local Cartesian coordinates are: (1) Γ can be specified in a convenient form within a local region surrounding the Cartesian coordinate origin [24], and (2) calculus operations such as differentiation are straightforward for Cartesian coordinates. Since we have both the original Cartesian coordinates and the "new" local Cartesian coordinates, it is necessary to study the transformation rules between them. Using tensor notations, Cartesian coordinates transformation rules are explained in detail for both 2D and 3D cases in the following sections.

3.1.2 2D Geometry

Let $\boldsymbol{x}_* \in \Gamma$ where Γ is the interface curve. We can build a local Cartesian coordinate system $\left(\tilde{x}^{\alpha}, \tilde{x}^{\beta}\right)$ by using the unit normal direction $n^i\left(\boldsymbol{x}_*\right)$ pointing from Ω^- to Ω^+ and the unit tangential direction $\tau^i\left(\boldsymbol{x}_*\right)$ counter-clockwise of $n^i\left(\boldsymbol{x}_*\right)$. See Fig. 3.1 for an illustration of the coordinate transformation between the original Cartesian coordinates $\left(x^{\alpha}, x^{\beta}\right)$ and the local Cartesian coordinates $\left(\tilde{x}^{\alpha}, \tilde{x}^{\beta}\right)$.

The coordinate transformation matrix A therefore is

$$A = \begin{pmatrix} n^{\alpha}(\boldsymbol{x}_*) & \tau^{\alpha}(\boldsymbol{x}_*) \\ n^{\beta}(\boldsymbol{x}_*) & \tau^{\beta}(\boldsymbol{x}_*) \end{pmatrix}. \tag{3.1.1}$$

Note that A is a special orthogonal matrix with $\det A = 1$, and $A^{-1} = A^T$. We define the local Cartesian coordinate system as $\left(\tilde{x}^{\alpha}, \tilde{x}^{\beta}\right)$ and the coordinate transformation rule is [51]

$$\tilde{x}^i = \left(A^{-1}\right)^i_j \left(x^j - x^j_*\right). \tag{3.1.2}$$

As a special case, the point $\boldsymbol{x}_*$ in $\left(x^{\alpha}, x^{\beta}\right)$ maps to the origin $\tilde{\mathbf{0}}$ in the local coordinate system $\left(\tilde{x}^{\alpha}, \tilde{x}^{\beta}\right)$. For vectors and vector fields such as the velocity field u^i, the transformation rule is [51]

$$\tilde{u}^i = \left(A^{-1}\right)^i_j u^j. \tag{3.1.3}$$

For any functions piecewise differentiable in both Ω^+ and Ω^-, such as the pressure p, we have

$$p = p\left(x^{\alpha}, x^{\beta}\right) = p\left(\tilde{x}^{\alpha}, \tilde{x}^{\beta}\right). \tag{3.1.4}$$

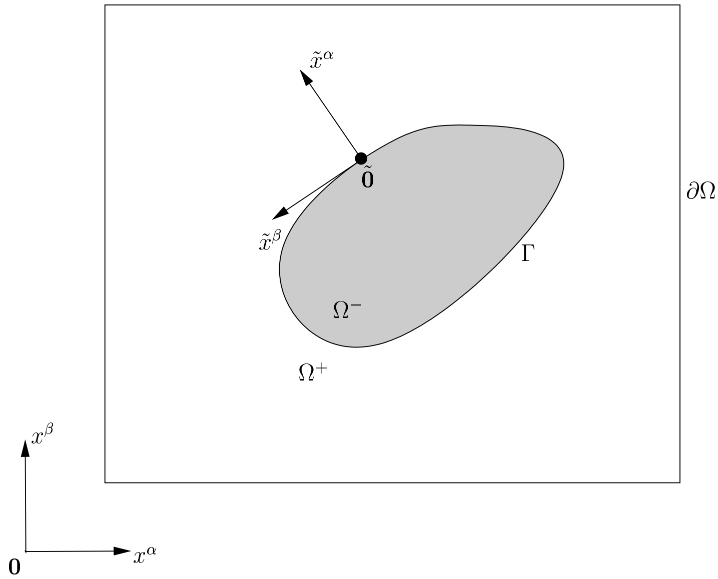

Figure 3.1: Given a point $\boldsymbol{x}_* \in \Gamma$, a local Cartesian coordinate system $\left(\tilde{x}^\alpha, \tilde{x}^\beta\right)$ is built using $\boldsymbol{x}_*$ as the origin, the unit normal vector $\boldsymbol{n}$ and the unit tangential vector $\boldsymbol{\tau}$ at that point as the two coordinate axes. The normal vector $\boldsymbol{n}$ points from Ω^- to Ω^+ and the tangent vector $\boldsymbol{\tau}$ is counter-clockwise of $\boldsymbol{n}$.

We know that $p\left(x^\alpha, x^\beta\right)$ and $p\left(\tilde{x}^\alpha, \tilde{x}^\beta\right)$ represent the same physical quantity while the former one is in terms of x^i and the latter one is in terms of $\tilde{x}^i$, and they are equivalent under Eq. (3.1.2) and its inverse mapping:

$$x^i = A^i_j \tilde{x}^j + x^i_*. \tag{3.1.5}$$

To simplify our notation, we use the same symbol p for the two coordinate systems as in Eq. (3.1.4). First-order coordinate derivatives for p follow the rule:

$$\frac{\partial p}{\partial \tilde{x}^i} = (A)^j_i \frac{\partial p}{\partial x^j} = \left(A^{-1}\right)^i_j \frac{\partial p}{\partial x^j} \tag{3.1.6}$$

and transformation rules for higher order derivatives can be derived easily using the tensor notation. The directional derivative such as the normal derivative for pressure p in $\left(x^\alpha, x^\beta\right)$ is defined as

$$\frac{\partial p}{\partial n} = \nabla p \cdot \boldsymbol{n} = \frac{\partial p}{\partial x^k} n^k. \tag{3.1.7}$$

Accordingly, in the local coordinates $\left(\tilde{x}^\alpha, \tilde{x}^\beta\right)$, since $\boldsymbol{n}$ is a vector, we need to use Eq. (3.1.3) to transform $\boldsymbol{n}$ to $\tilde{\boldsymbol{n}}$ and define the same directional derivative as

$$\frac{\partial p}{\partial \tilde{n}} = \tilde{\nabla} p \cdot \tilde{\boldsymbol{n}} = \frac{\partial p}{\partial \tilde{x}^k} \tilde{n}^k. \tag{3.1.8}$$

The major benefit of introducing the local Cartesian coordinate system is that in the neighborhood of the local origin $\tilde{\mathbf{0}}$, the interface curve Γ may be parameterized as [24]

$$\Gamma = \left(\chi\left(\tilde{x}^{\beta}\right), \tilde{x}^{\beta}\right) \tag{3.1.9}$$

where χ is a sufficiently smooth function of $\tilde{x}^{\beta}$. See Fig. 3.2 for an illustration of the local parameterization of the interface curve Γ. Or we can represent the interface Γ using the

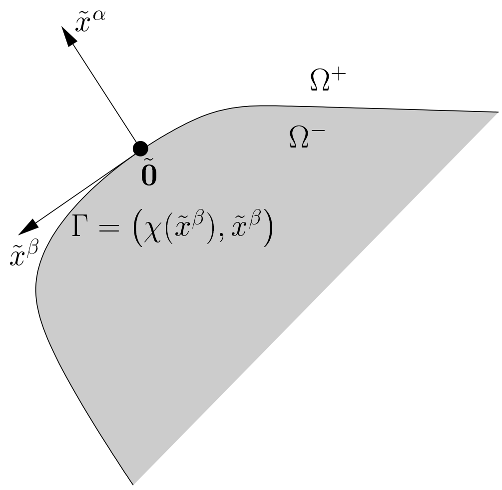

Figure 3.2: In the neighborhood of the local origin $\tilde{\mathbf{0}}$, Γ may be parameterized as $\left(\tilde{x}^{\alpha} = \chi\left(\tilde{x}^{\beta}\right), \tilde{x}^{\beta}\right)$. We also know that $\chi(0) = 0$ and $\frac{d\chi}{d\tilde{x}^{\beta}}(0) = 0$ (see text).

zero level set of the implicit function

$$\varphi\left(\tilde{x}^{\alpha}, \tilde{x}^{\beta}\right) = \tilde{x}^{\alpha} - \chi\left(\tilde{x}^{\beta}\right). \tag{3.1.10}$$

Note that Γ passes through the local origin $\tilde{\mathbf{0}}$ [24], i.e.

$$\chi\left(\tilde{x}^{\beta} = 0\right) = 0 \tag{3.1.11}$$

and the axis $\tilde{x}^{\beta}$ in the local coordinates is tangent to Γ at the local origin $\tilde{\mathbf{0}}$ [24], i.e.

$$\frac{d\chi}{d\tilde{x}^{\beta}}\left(\tilde{x}^{\beta} = 0\right) = 0. \tag{3.1.12}$$

Instead of using a global curvilinear coordinate system, we can define jump conditions for quantities such as the pressure p in the local Cartesian coordinate system $\left(\tilde{x}^{\alpha}, \tilde{x}^{\beta}\right)$ as

$$\begin{aligned} [p] &= p_{\Gamma}^{+}\left(\chi\left(\tilde{x}^{\beta}\right), \tilde{x}^{\beta}\right) - p_{\Gamma}^{-}\left(\chi\left(\tilde{x}^{\beta}\right), \tilde{x}^{\beta}\right) \\ &= p_{\Gamma}^{+} - p_{\Gamma}^{-}. \end{aligned} \tag{3.1.13}$$

For a function w with support only on the interface Γ, we have

$$w = w_\Gamma\left(\tilde{x}^\beta\right). \tag{3.1.14}$$

3.1.3 3D Geometry

Let $\boldsymbol{x}_* \in \Gamma$ where Γ is the interface surface. We can build a local Cartesian coordinate system $\left(\tilde{x}^\alpha, \tilde{x}^\beta, \tilde{x}^\gamma\right)$ by using the unit normal direction $n^i\left(\boldsymbol{x}_*\right)$ pointing from Ω^- to Ω^+ and the two unit tangential directions $\tau^i\left(\boldsymbol{x}_*\right)$ and $\eta^i\left(\boldsymbol{x}_*\right)$ together forming a right-handed Cartesian coordinate system. See Fig. 3.3 for an illustration of the coordinate transformation between the original Cartesian coordinates $\left(x^\alpha, x^\beta, x^\gamma\right)$ and the local Cartesian coordinates $\left(\tilde{x}^\alpha, \tilde{x}^\beta, \tilde{x}^\gamma\right)$.

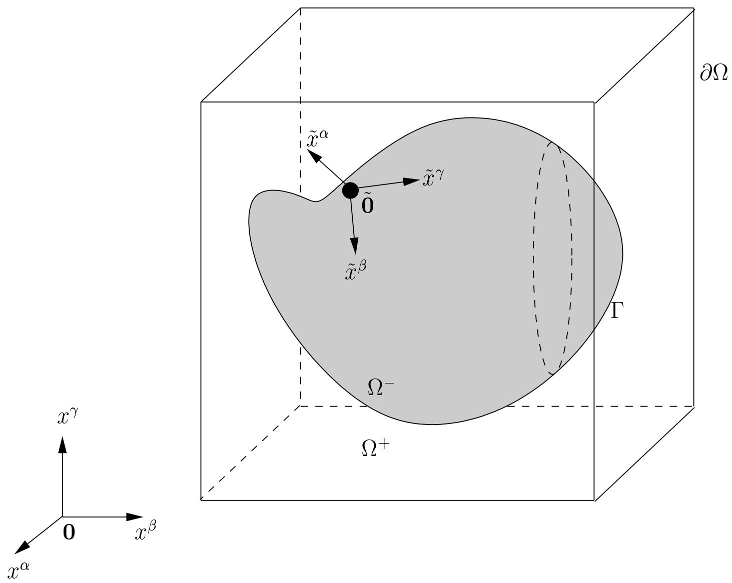

Figure 3.3: Given a point $\boldsymbol{x}_* \in \Gamma$, a local Cartesian coordinate system $\left(\tilde{x}^\alpha, \tilde{x}^\beta, \tilde{x}^\gamma\right)$ is built using $\boldsymbol{x}_*$ as the origin, the unit normal vector $\boldsymbol{n}$ and two unit tangent vectors $\boldsymbol{\tau}$ and $\boldsymbol{\eta}$ at that point as the three coordinate axes in sequence. The normal vector $\boldsymbol{n}$ points from Ω^- to Ω^+. $\boldsymbol{n}$, $\boldsymbol{\tau}$ and $\boldsymbol{\eta}$ form a right-handed Cartesian coordinate system $\left(\tilde{x}^\alpha, \tilde{x}^\beta, \tilde{x}^\gamma\right)$.

The coordinate transformation matrix A therefore is

$$A = \begin{pmatrix} n^\alpha(\boldsymbol{x}_*) & \tau^\alpha(\boldsymbol{x}_*) & \eta^\alpha(\boldsymbol{x}_*) \\ n^\beta(\boldsymbol{x}_*) & \tau^\beta(\boldsymbol{x}_*) & \eta^\beta(\boldsymbol{x}_*) \\ n^\gamma(\boldsymbol{x}_*) & \tau^\gamma(\boldsymbol{x}_*) & \eta^\gamma(\boldsymbol{x}_*) \end{pmatrix}. \tag{3.1.15}$$

Note that A is a special orthogonal matrix with $\det A = 1$, and $A^{-1} = A^T$. We define the local Cartesian coordinate system as $\left(\tilde{x}^\alpha, \tilde{x}^\beta, \tilde{x}^\gamma\right)$ and the coordinate transformation rule is

[51]

$$\tilde{x}^i = \left(A^{-1}\right)^i_j \left(x^j - x^j_*\right). \tag{3.1.16}$$

For vectors and vector fields such as the velocity field u^i, the transformation rule is the same as in the 2D case (3.1.3).

For any function piecewise differentiable in Ω^+ and Ω^-, such as the pressure p, we have

$$p = p\left(x^\alpha, x^\beta, x^\gamma\right) = p\left(\tilde{x}^\alpha, \tilde{x}^\beta, \tilde{x}^\gamma\right). \tag{3.1.17}$$

Note that $p\left(x^\alpha, x^\beta, x^\gamma\right)$ and $p\left(\tilde{x}^\alpha, \tilde{x}^\beta, \tilde{x}^\gamma\right)$ represent the same physical quantity while the former one is in terms of x^i and the latter one is in terms of $\tilde{x}^i$, and they are equivalent under Eq. (3.1.16) and its inverse mapping:

$$x^i = A^i_j \tilde{x}^j + x^i_*. \tag{3.1.18}$$

To simplify our notation, we use the same symbol p for the two coordinate systems. First-order coordinate derivatives for p follow the same rule as in the 2D case (3.1.6). The directional derivative such as the normal derivative for pressure p in $\left(x^\alpha, x^\beta, x^\gamma\right)$ is defined in the same way as the 2D case (3.1.7).

The major benefit of introducing the local Cartesian coordinate system is that in the neighborhood of the local origin $\tilde{\mathbf{0}}$, the interface surface Γ may be parameterized as [24]

$$\Gamma = \left(\chi\left(\tilde{x}^\beta, \tilde{x}^\gamma\right), \tilde{x}^\beta, \tilde{x}^\gamma\right) \tag{3.1.19}$$

where χ is a sufficiently smooth function of $\tilde{x}^\beta$ and $\tilde{x}^\gamma$. See Fig. 3.4 for an illustration of the local parameterization of the interface surface Γ. Or we can represent the interface Γ using the zero level set of the implicit function

$$\varphi\left(\tilde{x}^\alpha, \tilde{x}^\beta, \tilde{x}^\gamma\right) = \tilde{x}^\alpha - \chi\left(\tilde{x}^\beta, \tilde{x}^\gamma\right). \tag{3.1.20}$$

Note that Γ passes through the local origin $\tilde{\mathbf{0}}$ [24], i.e.

$$\chi\left(\tilde{x}^\beta = 0, \tilde{x}^\gamma = 0\right) = 0 \tag{3.1.21}$$

and the two axes $\tilde{x}^\beta$ and $\tilde{x}^\gamma$ in the local coordinate system are tangent to Γ at the local origin $\tilde{\mathbf{0}}$ [24], i.e.

$$\frac{\partial \chi}{\partial \tilde{x}^\beta}\left(\tilde{x}^\beta = 0, \tilde{x}^\gamma = 0\right) = 0, \quad \frac{\partial \chi}{\partial \tilde{x}^\gamma}\left(\tilde{x}^\beta = 0, \tilde{x}^\gamma = 0\right) = 0. \tag{3.1.22}$$

Instead of using a global curvilinear coordinate system, we can define jump conditions for quantities such as the pressure p in the local Cartesian coordinate system $\left(\tilde{x}^\alpha, \tilde{x}^\beta, \tilde{x}^\gamma\right)$ as

$$\begin{aligned} [p] &= p^+_\Gamma\left(\chi\left(\tilde{x}^\beta, \tilde{x}^\gamma\right), \tilde{x}^\beta, \tilde{x}^\gamma\right) - p^-_\Gamma\left(\chi\left(\tilde{x}^\beta, \tilde{x}^\gamma\right), \tilde{x}^\beta, \tilde{x}^\gamma\right) \\ &= p^+_\Gamma - p^-_\Gamma. \end{aligned} \tag{3.1.23}$$

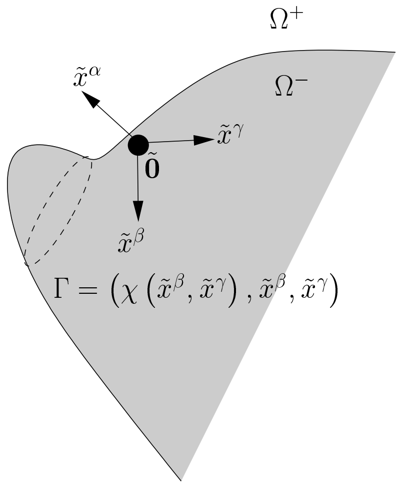

Figure 3.4: In the neighborhood of the local origin $\tilde{\mathbf{0}}$, Γ may be parameterized as $\left(\tilde{x}^\alpha = \chi\left(\tilde{x}^\beta, \tilde{x}^\gamma\right), \tilde{x}^\beta, \tilde{x}^\gamma\right)$. We also know that $\chi(0,0) = 0$ and $\dfrac{\partial \chi}{\partial \tilde{x}^\beta}(0,0) = 0$, $\dfrac{\partial \chi}{\partial \tilde{x}^\gamma}(0,0) = 0$ (see text).

For a function w with support only on the interface Γ, we have

$$w = w_\Gamma\left(\tilde{x}^\beta, \tilde{x}^\gamma\right). \tag{3.1.24}$$

3D geometry is surely more complicated than the 2D case. Since we adopt the tensor notation, it is much easier to show the similarities and differences between 3D problems and their 2D counterparts.

3.2 Derivation of Jump Conditions for Stokes Equations

To use the Immersed Interface Method (IIM) for the Stokes equations, we need to know the jump conditions of both pressure p and velocity u^i. Since the jump conditions for interface problems play almost the same role as boundary conditions for partial differential equations (PDEs), it is necessary to derive jump conditions for a given interface problem in order to capture the dynamics along the interfaces. Our result of jump conditions for the Stokes equations is a generalization for the equal viscosity case [22, 56] and is consistent with existing results [19, 20].

3.2.1 Jump Conditions for Stokes Equations

The formulation for incompressible Stokes equations with two phases includes the Stokes equations [46]

$$-\frac{\partial p}{\partial x^i} + \frac{\partial}{\partial x^j}\left(\mu\left(\frac{\partial u^i}{\partial x^j} + \frac{\partial u^j}{\partial x^i}\right)\right) + g^i = 0, \quad \boldsymbol{x} \in \Omega^+ \cup \Omega^-; \tag{3.2.1}$$

the incompressibility condition [46]

$$\frac{\partial u^i}{\partial x^i} = 0, \quad \boldsymbol{x} \in \Omega^+ \cup \Omega^-; \tag{3.2.2}$$

and the surface force balance equation [47]

$$\left[\sigma_{ij} n^j\right] + f^i = 0 \tag{3.2.3}$$

across Γ. Note that the stress tensor σ_{ij} for a Newtonian fluid is

$$\sigma_{ij} = -p\delta_{ij} + \mu\left(\frac{\partial u^i}{\partial x^j} + \frac{\partial u^j}{\partial x^i}\right). \tag{3.2.4}$$

Plugging Eq. (3.2.4) into Eq. (3.2.3), we can get

$$\left[-pn^i + \mu\left(\frac{\partial u^i}{\partial x^j} + \frac{\partial u^j}{\partial x^i}\right) n^j\right] + f^i = 0. \tag{3.2.5}$$

We know that velocity across the interface is continuous, and this condition is stated in terms of jump conditions as:

$$\left[u^i\right] = 0. \tag{3.2.6}$$

In order to use Immersed Interface Method (IIM) to solve the two-phase Stokes equations in 2D and 3D numerically, we need to know the jump conditions for both pressure p and velocity u^i, i.e. the following jump conditions are needed [29]:

$$[p], \quad \left[\frac{\partial p}{\partial n}\right], \quad \left[\mu u^i\right], \quad \left[\frac{\partial\left(\mu u^i\right)}{\partial n}\right]. \tag{3.2.7}$$

It might be possible to use

$$\left[u^i\right], \quad \left[\frac{\partial u^i}{\partial n}\right] \tag{3.2.8}$$

as a set of jump conditions for velocity u^i and apply IIM, but we will not take this approach in this thesis. In following sections, we will derive the jump conditions (3.2.7) (except for $\left[\mu u^i\right]$) from Eqs. (3.2.1, 3.2.2, 3.2.5) for both 2D and 3D geometry.

3.2.2 2D Geometry

Let $\boldsymbol{x}_* \in \Gamma$ where Γ is the interface curve. We use a local Cartesian coordinate system $\left(\tilde{x}^\alpha, \tilde{x}^\beta\right)$ introduced in Chapter 3.1. Note that the origin of the local coordinates is $\boldsymbol{x}_*$ and the two local coordinate axes are formed by normal vector n^i and tangent vector τ^i of the interface Γ at point $\boldsymbol{x}_*$. In the local coordinates $\left(\tilde{x}^\alpha, \tilde{x}^\beta\right)$, the interface curve Γ may be parameterized in the neighborhood of the local origin $\tilde{\mathbf{0}}$ as

$$\Gamma = \left(\chi\left(\tilde{x}^\beta\right), \tilde{x}^\beta\right). \tag{3.2.9}$$

The unit tangent is given by

$$\tilde{\boldsymbol{\tau}} = \frac{1}{\sqrt{1+\left(\frac{d\chi}{d\tilde{x}^\beta}\right)^2}}\left(\frac{d\chi}{d\tilde{x}^\beta}, 1\right) \tag{3.2.10}$$

and the unit normal direction is

$$\tilde{\boldsymbol{n}} = \frac{1}{\sqrt{1+\left(\frac{d\chi}{d\tilde{x}^\beta}\right)^2}}\left(1, -\frac{d\chi}{d\tilde{x}^\beta}\right). \tag{3.2.11}$$

First we have the following coordinate transformation results for normal directional derivatives:

Lemma 3.2.1.

$$\frac{\partial\left(\mu u^i\right)}{\partial n} = \frac{\partial\left(\mu u^i\right)}{\partial \tilde{n}}, \quad i = \alpha, \beta; \quad \boldsymbol{x} \in \Omega^+ \ or\ \Omega^-. \tag{3.2.12}$$

Proof.

$$\begin{aligned}
\frac{\partial\left(\mu u^i\right)}{\partial \tilde{n}} &= \frac{\partial\left(\mu u^i\right)}{\partial \tilde{x}^k}\tilde{n}^k \\
&= (A)_k^l \frac{\partial\left(\mu u^i\right)}{\partial x^l}\left(A^{-1}\right)_j^k n^j \\
&= \delta_{lj}\frac{\partial\left(\mu u^i\right)}{\partial x^l}n^j = \frac{\partial\left(\mu u^i\right)}{\partial x^j}n^j = \frac{\partial\left(\mu u^i\right)}{\partial n}.
\end{aligned} \tag{3.2.13}$$

□

Remark 3.2.2. *This result is also true for general directional derivatives, e.g. tangential directional derivatives.*

The invariance of incompressibility for velocity under coordinates transformation states:

Lemma 3.2.3.

$$\frac{\partial u^i}{\partial x^i} = \frac{\partial \tilde{u}^i}{\partial \tilde{x}^i} = 0, \quad \boldsymbol{x} \in \Omega^+ \ or\ \Omega^-. \tag{3.2.14}$$

Proof.

$$\begin{aligned}\frac{\partial \tilde{u}^i}{\partial \tilde{x}^i} &= \left(A^{-1}\right)^i_k \frac{\partial u^k}{\partial \tilde{x}^i} \\ &= \left(A^{-1}\right)^i_k A^l_i \frac{\partial u^k}{\partial x^l} \\ &= \frac{\partial u^i}{\partial x^i} = 0.\end{aligned} \tag{3.2.15}$$

□

Lemma 3.2.4.

$$\left[\frac{\partial\left(\mu u^i\right)}{\partial n}\right](0) = \left[\frac{\partial\left(\mu u^i\right)}{\partial \tilde{x}^\alpha}\right](0), \quad i = \alpha, \beta; \quad \boldsymbol{x} \in \Omega^+ \ \textit{or}\ \Omega^-. \tag{3.2.16}$$

Proof.

$$\begin{aligned}\left[\frac{\partial\left(\mu u^i\right)}{\partial n}\right](0) &= \left[\frac{\partial\left(\mu u^i\right)}{\partial \tilde{n}}\right](0) \\ &= \left[\frac{1}{\sqrt{1+\left(\frac{d\chi}{d\tilde{x}^\beta}\right)^2}}\left(\frac{\partial\left(\mu u^i\right)}{\partial \tilde{x}^\alpha} - \frac{\partial\left(\mu u^i\right)}{\partial \tilde{x}^\beta}\frac{d\chi}{d\tilde{x}^\beta}\right)\right](0) \\ &= \left[\frac{\partial\left(\mu u^i\right)}{\partial \tilde{x}^\alpha}\right](0).\end{aligned} \tag{3.2.17}$$

□

Lemma 3.2.5.

$$\left[\frac{\partial\left(\mu u^i\right)}{\partial \tilde{x}^\beta}\right](0) = \frac{d\left[\mu u^i\right]}{d\tilde{x}^\beta}(0), \quad i = \alpha, \beta. \tag{3.2.18}$$

Proof.

$$\begin{aligned}\frac{d\left[\mu u^i\right]}{d\tilde{x}^\beta}(0) &= \frac{d\left(\mu u^i\right)^+_\Gamma}{d\tilde{x}^\beta}(0) - \frac{d\left(\mu u^i\right)^-_\Gamma}{d\tilde{x}^\beta}(0) \\ &= \left(\frac{\partial\left(\mu u^i\right)}{\partial \tilde{x}^\alpha}\right)^+_\Gamma(0)\frac{d\chi}{d\tilde{x}^\beta}(0) + \left(\frac{\partial\left(\mu u^i\right)}{\partial \tilde{x}^\beta}\right)^+_\Gamma(0) \\ &\quad - \left(\left(\frac{\partial\left(\mu u^i\right)}{\partial \tilde{x}^\alpha}\right)^-_\Gamma(0)\frac{d\chi}{d\tilde{x}^\beta}(0) + \left(\frac{\partial\left(\mu u^i\right)}{\partial \tilde{x}^\beta}\right)^-_\Gamma(0)\right) \\ &= \left[\frac{\partial\left(\mu u^i\right)}{\partial \tilde{x}^\beta}\right](0).\end{aligned} \tag{3.2.19}$$

$\square$

Remark 3.2.6. *Higher order derivatives with respect to $\tilde{x}^\beta$ have similar results, for example,*

$$\frac{d^2\left[\mu u^i\right]}{d\tilde{x}^\beta d\tilde{x}^\beta}(0) = \left[\frac{\partial^2\left(\mu u^i\right)}{\partial\tilde{x}^\beta\partial\tilde{x}^\beta}\right](0) + \left[\frac{\partial\left(\mu u^i\right)}{\partial\tilde{x}^\alpha}\right](0)\frac{d^2\chi}{d\tilde{x}^\beta d\tilde{x}^\beta}(0), \quad i = \alpha, \beta. \tag{3.2.20}$$

Note that $\left[\frac{\partial\left(\mu u^i\right)}{\partial\tilde{x}^\alpha}\right](0)$ *will be derived in the following theorem.*

Theorem 3.2.7. *For two-phase Stokes equations in 2D, given an arbitrary point $\boldsymbol{x}_* \in \Gamma$, the following jump conditions for $\frac{\partial\left(\mu u^i\right)}{\partial n}$ hold at point $\boldsymbol{x}_*$:*

$$\begin{pmatrix} \left[\dfrac{\partial\left(\mu u^\alpha\right)}{\partial n}\right] \\ \\ \left[\dfrac{\partial\left(\mu u^\beta\right)}{\partial n}\right] \end{pmatrix} = A \begin{pmatrix} -\left(A^{-1}\right)_j^\beta \dfrac{d\left[\mu u^j\right]}{d\tilde{x}^\beta} \\ \\ -\left(A^{-1}\right)_j^\alpha \dfrac{d\left[\mu u^j\right]}{d\tilde{x}^\beta} - \tilde{f}^\beta \end{pmatrix} \tag{3.2.21}$$

where A is the local coordinate transformation matrix.

Proof. Multiply τ^i at both sides of Eq. (3.2.5) to get

$$\left[\mu\left(\frac{\partial u^i}{\partial x^j} + \frac{\partial u^j}{\partial x^i}\right)n^j\tau^i\right] + f^i\tau^i = 0 \tag{3.2.22}$$

or

$$\left[\mu\left(\frac{\partial u^i}{\partial n}\tau^i + \frac{\partial u^j}{\partial \tau}n^j\right)\right] + f^i\tau^i = 0. \tag{3.2.23}$$

Recast Eq. (3.2.23) in $\tilde{x}^i$ coordinate and use Lemma 3.2.1 for both the normal and tangential derivatives to get

$$\left[\mu\left(\frac{\partial \tilde{u}^i}{\partial \tilde{n}}\tilde{\tau}^i + \frac{\partial \tilde{u}^j}{\partial \tilde{\tau}}\tilde{n}^j\right)\right] + \tilde{f}^i\tilde{\tau}^i = 0. \tag{3.2.24}$$

Plugging Eqs. (3.2.10, 3.2.11) into Eq. (3.2.24) we get

$$\left[\mu\frac{1}{\sqrt{1+\left(\frac{d\chi}{d\tilde{x}^\beta}\right)^2}}\left(\frac{\partial\tilde{u}^\alpha}{\partial\tilde{n}}\frac{d\chi}{d\tilde{x}^\beta} + \frac{\partial\tilde{u}^\beta}{\partial\tilde{n}} + \frac{\partial\tilde{u}^\alpha}{\partial\tilde{\tau}} - \frac{\partial\tilde{u}^\beta}{\partial\tilde{\tau}}\frac{d\chi}{d\tilde{x}^\beta}\right)\right] + \frac{1}{\sqrt{1+\left(\frac{d\chi}{d\tilde{x}^\beta}\right)^2}}\left(\tilde{f}^\alpha\frac{d\chi}{d\tilde{x}^\beta} + \tilde{f}^\beta\right) = 0. \tag{3.2.25}$$

We can evaluate Eq. (3.2.25) at $\tilde{x}^\beta = 0$ to get

$$\left[\mu\left(\frac{\partial \tilde{u}^\beta}{\partial \tilde{n}} + \frac{\partial \tilde{u}^\alpha}{\partial \tilde{\tau}}\right)\right](0) + \tilde{f}^\beta(0) = 0. \tag{3.2.26}$$

Since the viscosity coefficient μ is piecewise constant, we can write Eq. (3.2.26) as

$$\left[\frac{\partial\left(\mu\tilde{u}^\beta\right)}{\partial \tilde{n}} + \frac{\partial\left(\mu\tilde{u}^\alpha\right)}{\partial \tilde{\tau}}\right](0) + \tilde{f}^\beta(0) = 0. \tag{3.2.27}$$

Then we can expand the directional derivatives in Eq. (3.2.27) to get

$$\left[\frac{\partial\left(\mu\tilde{u}^\beta\right)}{\partial \tilde{x}^\alpha} + \frac{\partial\left(\mu\tilde{u}^\alpha\right)}{\partial \tilde{x}^\beta}\right](0) + \tilde{f}^\beta(0) = 0. \tag{3.2.28}$$

From Lemma 3.2.3 we know that

$$\left[\frac{\partial\left(\mu\tilde{u}^i\right)}{\partial \tilde{x}^i}\right](0) = 0. \tag{3.2.29}$$

Eqs. (3.2.28, 3.2.29) form a system of equations for $\left[\frac{\partial\left(\mu u^i\right)}{\partial \tilde{x}^\alpha}\right](0)$ and the coefficient matrix is A^{-1} which is non-singular. By solving this system of equations, we can get

$$\begin{pmatrix} \left[\frac{\partial\left(\mu u^\alpha\right)}{\partial \tilde{x}^\alpha}\right](0) \\ \\ \left[\frac{\partial\left(\mu u^\beta\right)}{\partial \tilde{x}^\alpha}\right](0) \end{pmatrix} = A \begin{pmatrix} -\left[\left(A^{-1}\right)_j^\beta \frac{\partial\left(\mu u^j\right)}{\partial \tilde{x}^\beta}\right](0) \\ \\ -\left[\left(A^{-1}\right)_j^\alpha \frac{\partial\left(\mu u^j\right)}{\partial \tilde{x}^\beta}\right](0) - \tilde{f}^\beta(0) \end{pmatrix}. \tag{3.2.30}$$

Using Lemma 3.2.4, 3.2.5 and suppress the sign for evaluation at the local origin, we reach Eq. (3.2.21). $\square$

For pressure p, we have the following result:

Theorem 3.2.8. *For two-phase Stokes equations in 2D, given an arbitrary point $\boldsymbol{x}_* \in \Gamma$, the following jump condition for pressure p holds at point $\boldsymbol{x}_*$:*

$$[p] = -2\left(A^{-1}\right)_j^\beta \frac{d\left[\mu u^j\right]}{d\tilde{x}^\beta} + \tilde{f}^\alpha. \tag{3.2.31}$$

Proof. Multiply n^i at both sides of Eq. (3.2.5) to get

$$\begin{aligned}
[p] &= \left[\mu\left(\frac{\partial u^i}{\partial x^j}+\frac{\partial u^j}{\partial x^i}\right)n^j n^i\right]+f^i n^i \\
&= \left[\mu\left(\frac{\partial u^i}{\partial n}n^i+\frac{\partial u^j}{\partial n}n^j\right)\right]+f^i n^i \\
&= 2\left[\mu\frac{\partial u^i}{\partial n}n^i\right]+f^i n^i \\
&= 2\left[\frac{\partial\left(\mu u^i\right)}{\partial n}n^i\right]+f^i n^i.
\end{aligned} \tag{3.2.32}$$

Recast Eq. (3.2.32) in $\tilde{x}^i$ coordinate and use Lemma 3.2.1 for the normal derivative to get

$$[p] = 2\left[\frac{\partial\left(\mu\tilde{u}^i\right)}{\partial\tilde{n}}\tilde{n}^i\right]+\tilde{f}^i\tilde{n}^i. \tag{3.2.33}$$

Plugging Eq. (3.2.11) into Eq. (3.2.33) we get

$$[p] = 2\left[\frac{1}{\sqrt{1+\left(\frac{d\chi}{d\tilde{x}^\beta}\right)^2}}\left(\frac{\partial\left(\mu\tilde{u}^\alpha\right)}{\partial\tilde{n}}-\frac{\partial\left(\mu\tilde{u}^\beta\right)}{\partial\tilde{n}}\frac{d\chi}{d\tilde{x}^\beta}\right)\right]+\frac{1}{\sqrt{1+\left(\frac{d\chi}{d\tilde{x}^\beta}\right)^2}}\left(\tilde{f}^\alpha-\tilde{f}^\beta\frac{d\chi}{d\tilde{x}^\beta}\right). \tag{3.2.34}$$

We can evaluate Eq. (3.2.34) at $\tilde{x}^\beta = 0$ to get

$$[p]\,(0) = 2\left[\frac{\partial\left(\mu\tilde{u}^\alpha\right)}{\partial\tilde{n}}\right](0)+\tilde{f}^\alpha(0). \tag{3.2.35}$$

Then we can expand the directional derivatives in Eq. (3.2.35) and use the incompressibility to get

$$\begin{aligned}
[p]\,(0) &= 2\left[\frac{\partial\left(\mu\tilde{u}^\alpha\right)}{\partial\tilde{x}^\alpha}\right](0)+\tilde{f}^\alpha(0) \\
&= -2\left[\frac{\partial\left(\mu\tilde{u}^\beta\right)}{\partial\tilde{x}^\beta}\right](0)+\tilde{f}^\alpha(0).
\end{aligned} \tag{3.2.36}$$

From Lemma 3.2.5, we have

$$[p]\,(0) = -2\frac{d\left[\mu\tilde{u}^\beta\right]}{d\tilde{x}^\beta}(0)+\tilde{f}^\alpha(0). \tag{3.2.37}$$

Using coordinate transformation rule and suppress the sign for evaluation at the local origin, we reach Eq. (3.2.31). □

The jump condition for the normal derivative of pressure p is shown here:

Theorem 3.2.9. *For two-phase Stokes equations in 2D, given an arbitrary point $\boldsymbol{x}_* \in \Gamma$, the following jump condition for $\dfrac{\partial p}{\partial n}$ holds at point $\boldsymbol{x}_*$:*

$$\begin{aligned}\left[\frac{\partial p}{\partial n}\right] = &-2\frac{d^2\chi}{d\tilde{x}^\beta d\tilde{x}^\beta}\left(A^{-1}\right)^\beta_j \frac{d\left[\mu u^j\right]}{d\tilde{x}^\beta} + 2\left(A^{-1}\right)^\alpha_j \frac{d^2\left[\mu u^j\right]}{d\tilde{x}^\beta d\tilde{x}^\beta} \\ &+ \frac{d^2\chi}{d\tilde{x}^\beta d\tilde{x}^\beta}\tilde{f}^\alpha + \frac{d\tilde{f}^\beta}{d\tilde{x}^\beta} + \left[\tilde{g}^\alpha\right].\end{aligned} \tag{3.2.38}$$

Proof. Multiply n^i at both sides of Eq. (3.2.1) for $\boldsymbol{x} \in \Omega^+$ and $\boldsymbol{x} \in \Omega^-$ to get

$$\begin{aligned}\left[\frac{\partial p}{\partial n}\right] &= \left[\frac{\partial}{\partial x^j}\left(\mu\left(\frac{\partial u^i}{\partial x^j} + \frac{\partial u^j}{\partial x^i}\right)\right)n^i\right] + \left[g^i n^i\right] \\ &= \left[\frac{\partial^2\left(\mu u^i\right)}{\partial x^j \partial x^j}n^i\right] + \left[g^i n^i\right].\end{aligned} \tag{3.2.39}$$

Recast Eq. (3.2.39) in $\tilde{x}^i$ coordinate to get

$$\begin{aligned}\left[\frac{\partial p}{\partial n}\right] &= \left[\frac{\partial^2\left(\mu\tilde{u}^i\right)}{\partial\tilde{x}^j \partial\tilde{x}^j}\tilde{n}^i\right] + \left[\tilde{g}^i\tilde{n}^i\right] \\ &= \left[\left(\frac{\partial^2\left(\mu\tilde{u}^i\right)}{\partial\tilde{x}^\alpha\partial\tilde{x}^\alpha} + \frac{\partial^2\left(\mu\tilde{u}^i\right)}{\partial\tilde{x}^\beta\partial\tilde{x}^\beta}\right)\tilde{n}^i\right] + \left[\tilde{g}^i\tilde{n}^i\right].\end{aligned} \tag{3.2.40}$$

Plugging Eq. (3.2.11) into Eq. (3.2.40) we get

$$\begin{aligned}\left[\frac{\partial p}{\partial n}\right] = &\left[\frac{1}{\sqrt{1+\left(\frac{d\chi}{d\tilde{x}^\beta}\right)^2}}\left(\frac{\partial^2\left(\mu\tilde{u}^\alpha\right)}{\partial\tilde{x}^\alpha\partial\tilde{x}^\alpha} + \frac{\partial^2\left(\mu\tilde{u}^\alpha\right)}{\partial\tilde{x}^\beta\partial\tilde{x}^\beta} - \left(\frac{\partial^2\left(\mu\tilde{u}^\beta\right)}{\partial\tilde{x}^\alpha\partial\tilde{x}^\alpha} + \frac{\partial^2\left(\mu\tilde{u}^\beta\right)}{\partial\tilde{x}^\beta\partial\tilde{x}^\beta}\right)\frac{d\chi}{d\tilde{x}^\beta}\right)\right] \\ &+ \left[\frac{1}{\sqrt{1+\left(\frac{d\chi}{d\tilde{x}^\beta}\right)^2}}\left(\tilde{g}^\alpha - \tilde{g}^\beta\frac{d\chi}{d\tilde{x}^\beta}\right)\right].\end{aligned} \tag{3.2.41}$$

We can evaluate Eq. (3.2.41) at $\tilde{x}^\beta = 0$ to get

$$\left[\frac{\partial p}{\partial n}\right](0) = \left[\frac{\partial^2\left(\mu\tilde{u}^\alpha\right)}{\partial\tilde{x}^\alpha\partial\tilde{x}^\alpha} + \frac{\partial^2\left(\mu\tilde{u}^\alpha\right)}{\partial\tilde{x}^\beta\partial\tilde{x}^\beta}\right](0) + \left[\tilde{g}^\alpha\right](0). \tag{3.2.42}$$

Now we take the derivative with respect to $\tilde{x}^\beta$ of both sides of Eq. (3.2.25) to get

$$
\begin{aligned}
&-\left(3\sqrt{1+\left(\frac{d\chi}{d\tilde{x}^\beta}\right)^2}\left(\frac{d\chi}{d\tilde{x}^\beta}\right)^2-\left(\frac{d\chi}{d\tilde{x}^\beta}\right)^2-3\sqrt{1+\left(\frac{d\chi}{d\tilde{x}^\beta}\right)^2}-1\right)\frac{d^2\chi}{d\tilde{x}^\beta d\tilde{x}^\beta}\\
&\bigg/\left(1+\left(\frac{d\chi}{d\tilde{x}^\beta}\right)^2\right)^{\frac{5}{2}}\left[\frac{\partial\left(\mu\tilde{u}^\alpha\right)}{\partial\tilde{x}^\alpha}\right]+\left(3\frac{\frac{d\chi}{d\tilde{x}^\beta}}{1+\left(\frac{d\chi}{d\tilde{x}^\beta}\right)^2}+\frac{\frac{d\chi}{d\tilde{x}^\beta}}{\sqrt{1+\left(\frac{d\chi}{d\tilde{x}^\beta}\right)^2}}\right)\\
&\left[\frac{\partial^2\left(\mu\tilde{u}^\alpha\right)}{\partial\tilde{x}^\alpha\partial\tilde{x}^\alpha}\frac{d\chi}{d\tilde{x}^\beta}+\frac{\partial^2\left(\mu\tilde{u}^\alpha\right)}{\partial\tilde{x}^\alpha\partial\tilde{x}^\beta}\right]-\left(\left(\frac{d\chi}{d\tilde{x}^\beta}\right)^2+1+2\sqrt{1+\left(\frac{d\chi}{d\tilde{x}^\beta}\right)^2}\right)\frac{d^2\chi}{d\tilde{x}^\beta d\tilde{x}^\beta}\frac{d\chi}{d\tilde{x}^\beta}\\
&\bigg/\left(1+\left(\frac{d\chi}{d\tilde{x}^\beta}\right)^2\right)^{\frac{5}{2}}\left[\frac{\partial\left(\mu\tilde{u}^\alpha\right)}{\partial\tilde{x}^\beta}\right]+\left(\frac{1}{\sqrt{1+\left(\frac{d\chi}{d\tilde{x}^\beta}\right)^2}}-\frac{\left(\frac{d\chi}{d\tilde{x}^\beta}\right)^2}{1+\left(\frac{d\chi}{d\tilde{x}^\beta}\right)^2}\right)\\
&\left[\frac{\partial^2\left(\mu\tilde{u}^\alpha\right)}{\partial\tilde{x}^\alpha\partial\tilde{x}^\beta}\frac{d\chi}{d\tilde{x}^\beta}+\frac{\partial^2\left(\mu\tilde{u}^\alpha\right)}{\partial\tilde{x}^\beta\partial\tilde{x}^\beta}\right]-4\frac{\frac{d\chi}{d\tilde{x}^\beta}\frac{d^2\chi}{d\tilde{x}^\beta d\tilde{x}^\beta}}{\left(1+\left(\frac{d\chi}{d\tilde{x}^\beta}\right)^2\right)^2}\left[\frac{\partial\left(\mu\tilde{u}^\beta\right)}{\partial\tilde{x}^\alpha}\right]\\
&+\frac{1-\left(\frac{d\chi}{d\tilde{x}^\beta}\right)^2}{1+\left(\frac{d\chi}{d\tilde{x}^\beta}\right)^2}\left[\frac{\partial^2\left(\mu\tilde{u}^\beta\right)}{\partial\tilde{x}^\alpha\partial\tilde{x}^\alpha}\frac{d\chi}{d\tilde{x}^\beta}+\frac{\partial^2\left(\mu\tilde{u}^\beta\right)}{\partial\tilde{x}^\alpha\partial\tilde{x}^\beta}\right]+\frac{\frac{d^2\chi}{d\tilde{x}^\beta d\tilde{x}^\beta}}{\left(1+\left(\frac{d\chi}{d\tilde{x}^\beta}\right)^2\right)^{\frac{3}{2}}}\tilde{f}^\alpha+\frac{\frac{d\chi}{d\tilde{x}^\beta}}{\sqrt{1+\left(\frac{d\chi}{d\tilde{x}^\beta}\right)^2}}\frac{d\tilde{f}^\alpha}{d\tilde{x}^\beta}\\
&-\frac{\frac{d\chi}{d\tilde{x}^\beta}\frac{d^2\chi}{d\tilde{x}^\beta d\tilde{x}^\beta}}{\left(1+\left(\frac{d\chi}{d\tilde{x}^\beta}\right)^2\right)^{\frac{3}{2}}}\tilde{f}^\beta+\frac{1}{\sqrt{1+\left(\frac{d\chi}{d\tilde{x}^\beta}\right)^2}}\frac{d\tilde{f}^\beta}{d\tilde{x}^\beta}=0.
\end{aligned}
\tag{3.2.43}
$$

We can evaluate Eq. (3.2.43) at $\tilde{x}^\beta=0$ to get

$$
\begin{aligned}
&4\frac{d^2\chi}{d\tilde{x}^\beta d\tilde{x}^\beta}(0)\left[\frac{\partial\left(\mu\tilde{u}^\alpha\right)}{\partial\tilde{x}^\alpha}\right](0)+\left[\frac{\partial^2\left(\mu\tilde{u}^\alpha\right)}{\partial\tilde{x}^\beta\partial\tilde{x}^\beta}\right](0)+\left[\frac{\partial^2\left(\mu\tilde{u}^\beta\right)}{\partial\tilde{x}^\alpha\partial\tilde{x}^\beta}\right](0)\\
&\quad+\frac{d^2\chi}{d\tilde{x}^\beta d\tilde{x}^\beta}(0)\tilde{f}^\alpha(0)+\frac{d\tilde{f}^\beta}{d\tilde{x}^\beta}(0)=0.
\end{aligned}
\tag{3.2.44}
$$

From the incompressibility condition, we know that

$$
\frac{\partial\left(\mu\tilde{u}^\alpha\right)}{\partial\tilde{x}^\alpha}+\frac{\partial\left(\mu\tilde{u}^\beta\right)}{\partial\tilde{x}^\beta}=0,\quad \boldsymbol{x}\in\Omega^+,\ \text{or}\ \Omega^-. \tag{3.2.45}
$$

Taking the derivative of Eq. (3.2.45) with respect to $\tilde{x}^\alpha$ we get

$$
\frac{\partial^2\left(\mu\tilde{u}^\alpha\right)}{\partial\tilde{x}^\alpha\partial\tilde{x}^\alpha}+\frac{\partial^2\left(\mu\tilde{u}^\beta\right)}{\partial\tilde{x}^\alpha\partial\tilde{x}^\beta}=0,\quad \boldsymbol{x}\in\Omega^+,\ \text{or}\ \Omega^-. \tag{3.2.46}
$$

Therefore from Eqs. (3.2.44, 3.2.45, 3.2.46) we get

$$\begin{aligned}\left[\frac{\partial^2\left(\mu\tilde{u}^\alpha\right)}{\partial\tilde{x}^\alpha\partial\tilde{x}^\alpha}\right](0) = &-4\frac{d^2\chi}{d\tilde{x}^\beta d\tilde{x}^\beta}(0)\left[\frac{\partial\left(\mu\tilde{u}^\beta\right)}{\partial\tilde{x}^\beta}\right](0)+\left[\frac{\partial^2\left(\mu\tilde{u}^\alpha\right)}{\partial\tilde{x}^\beta\partial\tilde{x}^\beta}\right](0)\\ &+\frac{d^2\chi}{d\tilde{x}^\beta d\tilde{x}^\beta}(0)\tilde{f}^\alpha(0)+\frac{d\tilde{f}^\beta}{d\tilde{x}^\beta}(0).\end{aligned} \tag{3.2.47}$$

From Eqs. (3.2.42, 3.2.47), we have

$$\begin{aligned}\left[\frac{\partial p}{\partial n}\right](0) = &-4\frac{d^2\chi}{d\tilde{x}^\beta d\tilde{x}^\beta}(0)\left[\frac{\partial\left(\mu\tilde{u}^\beta\right)}{\partial\tilde{x}^\beta}\right](0)+2\left[\frac{\partial^2\left(\mu\tilde{u}^\alpha\right)}{\partial\tilde{x}^\beta\partial\tilde{x}^\beta}\right](0)\\ &+\frac{d^2\chi}{d\tilde{x}^\beta d\tilde{x}^\beta}(0)\tilde{f}^\alpha(0)+\frac{d\tilde{f}^\beta}{d\tilde{x}^\beta}(0)+\left[\tilde{g}^\alpha\right](0).\end{aligned} \tag{3.2.48}$$

Using Lemma 3.2.5 and Eq. (3.2.20), we get

$$\begin{aligned}\left[\frac{\partial p}{\partial n}\right](0) = &-4\frac{d^2\chi}{d\tilde{x}^\beta d\tilde{x}^\beta}(0)\left(A^{-1}\right)^\beta_j\frac{d\left[\mu u^j\right]}{d\tilde{x}^\beta}(0)+2\left(A^{-1}\right)^\alpha_j\left(\frac{d^2\left[\mu u^j\right]}{d\tilde{x}^\beta d\tilde{x}^\beta}(0)-\frac{d^2\chi}{d\tilde{x}^\beta d\tilde{x}^\beta}(0)\left[\frac{\partial\left(\mu u^j\right)}{\partial\tilde{x}^\alpha}\right](0)\right)\\ &+\frac{d^2\chi}{d\tilde{x}^\beta d\tilde{x}^\beta}(0)\tilde{f}^\alpha(0)+\frac{d\tilde{f}^\beta}{d\tilde{x}^\beta}(0)+\left[\tilde{g}^\alpha\right](0).\end{aligned} \tag{3.2.49}$$

From Eq. (3.2.45), Eq. (3.2.49) is simplified as

$$\begin{aligned}\left[\frac{\partial p}{\partial n}\right](0) = &-2\frac{d^2\chi}{d\tilde{x}^\beta d\tilde{x}^\beta}(0)\left(A^{-1}\right)^\beta_j\frac{d\left[\mu u^j\right]}{d\tilde{x}^\beta}(0)+2\left(A^{-1}\right)^\alpha_j\frac{d^2\left[\mu u^j\right]}{d\tilde{x}^\beta d\tilde{x}^\beta}(0)\\ &+\frac{d^2\chi}{d\tilde{x}^\beta d\tilde{x}^\beta}(0)\tilde{f}^\alpha(0)+\frac{d\tilde{f}^\beta}{d\tilde{x}^\beta}(0)+\left[\tilde{g}^\alpha\right](0).\end{aligned} \tag{3.2.50}$$

Suppressing the sign for evaluation at the local origin, we reach Eq. (3.2.38). $\square$

To summarize, for 2D Stokes equations with an interface, we have derived the jump conditions $\left[\frac{\partial\left(\mu u^i\right)}{\partial n}\right]$, $[p]$ and $\left[\frac{\partial p}{\partial n}\right]$ as follows:

$$
\begin{pmatrix} \left[\dfrac{\partial\left(\mu u^{\alpha}\right)}{\partial n}\right] \\ \\ \left[\dfrac{\partial\left(\mu u^{\beta}\right)}{\partial n}\right] \end{pmatrix} = A \begin{pmatrix} -\left(A^{-1}\right)_j^{\beta} \dfrac{d\left[\mu u^j\right]}{d\tilde{x}^{\beta}} \\ \\ -\left(A^{-1}\right)_j^{\alpha} \dfrac{d\left[\mu u^j\right]}{d\tilde{x}^{\beta}} - \tilde{f}^{\beta} \end{pmatrix},
$$

$$
\begin{aligned}
[p] &= -2\left(A^{-1}\right)_j^{\beta} \frac{d\left[\mu u^j\right]}{d\tilde{x}^{\beta}} + \tilde{f}^{\alpha}, \\
\left[\frac{\partial p}{\partial n}\right] &= -2\frac{d^2\chi}{d\tilde{x}^{\beta} d\tilde{x}^{\beta}}\left(A^{-1}\right)_j^{\beta} \frac{d\left[\mu u^j\right]}{d\tilde{x}^{\beta}} + 2\left(A^{-1}\right)_j^{\alpha} \frac{d^2\left[\mu u^j\right]}{d\tilde{x}^{\beta} d\tilde{x}^{\beta}} \\
&\quad + \frac{d^2\chi}{d\tilde{x}^{\beta} d\tilde{x}^{\beta}}\tilde{f}^{\alpha} + \frac{d\tilde{f}^{\beta}}{d\tilde{x}^{\beta}} + \left[\tilde{g}^{\alpha}\right].
\end{aligned} \tag{3.2.51}
$$

3.2.3 3D Geometry

Let $\boldsymbol{x}_* \in \Gamma$ where Γ is the interface surface. We use a local Cartesian coordinate system $\left(\tilde{x}^{\alpha}, \tilde{x}^{\beta}, \tilde{x}^{\gamma}\right)$ introduced in Chapter 3.1. Note that the origin of the local coordinates is $\boldsymbol{x}_*$ and the three local coordinate axes are formed by normal vector n^i and two tangent vectors τ^i and η^i of the interface Γ at point $\boldsymbol{x}_*$. In the local coordinates $\left(\tilde{x}^{\alpha}, \tilde{x}^{\beta}, \tilde{x}^{\gamma}\right)$, the interface surface Γ may be parameterized in the neighborhood of the local origin $\tilde{\mathbf{0}}$ as

$$
\Gamma = \left(\chi\left(\tilde{x}^{\beta}, \tilde{x}^{\gamma}\right), \tilde{x}^{\beta}, \tilde{x}^{\gamma}\right). \tag{3.2.52}
$$

The two unit tangential directions are given by

$$
\tilde{\boldsymbol{\tau}} = \frac{1}{\sqrt{1+\left(\frac{\partial\chi}{\partial\tilde{x}^{\beta}}\right)^2}}\left(\frac{\partial\chi}{\partial\tilde{x}^{\beta}}, 1, 0\right) \tag{3.2.53}
$$

and

$$
\tilde{\boldsymbol{\eta}} = \frac{1}{\sqrt{1+\left(\frac{\partial\chi}{\partial\tilde{x}^{\gamma}}\right)^2}}\left(\frac{\partial\chi}{\partial\tilde{x}^{\gamma}}, 0, 1\right). \tag{3.2.54}
$$

The unit normal direction is

$$
\tilde{\boldsymbol{n}} = \frac{\tilde{\boldsymbol{\tau}} \times \tilde{\boldsymbol{\eta}}}{\|\tilde{\boldsymbol{\tau}} \times \tilde{\boldsymbol{\eta}}\|} = \frac{1}{\sqrt{1+\left(\frac{\partial\chi}{\partial\tilde{x}^{\beta}}\right)^2+\left(\frac{\partial\chi}{\partial\tilde{x}^{\gamma}}\right)^2}}\left(1, -\frac{\partial\chi}{\partial\tilde{x}^{\beta}}, -\frac{\partial\chi}{\partial\tilde{x}^{\gamma}}\right). \tag{3.2.55}
$$

Most results we have shown for 2D geometry are also true for 3D geometry with few modifications.

Lemma 3.2.10.

$$\frac{\partial\left(\mu u^i\right)}{\partial n}=\frac{\partial\left(\mu u^i\right)}{\partial \tilde{n}},\quad i=\alpha,\beta,\gamma;\quad \boldsymbol{x}\in\Omega^+\ \mathit{or}\ \Omega^-. \tag{3.2.56}$$

Proof. See Lemma 3.2.1. □

Lemma 3.2.11.

$$\frac{\partial u^i}{\partial x^i}=\frac{\partial \tilde{u}^i}{\partial \tilde{x}^i}=0,\quad \boldsymbol{x}\in\Omega^+\ \mathit{or}\ \Omega^-. \tag{3.2.57}$$

Proof. See Lemma 3.2.3. □

Lemma 3.2.12.

$$\left[\frac{\partial\left(\mu u^i\right)}{\partial n}\right](0,0)=\left[\frac{\partial\left(\mu u^i\right)}{\partial \tilde{x}^\alpha}\right](0,0),\quad i=\alpha,\beta,\gamma;\quad \boldsymbol{x}\in\Omega^+\ \mathit{or}\ \Omega^-. \tag{3.2.58}$$

Proof.

$$\begin{aligned}
\left[\frac{\partial\left(\mu u^i\right)}{\partial n}\right](0,0)&=\left[\frac{\partial\left(\mu u^i\right)}{\partial \tilde{n}}\right](0,0)\\
&=\left[\frac{1}{\sqrt{1+\left(\frac{\partial\chi}{\partial\tilde{x}^\beta}\right)^2+\left(\frac{\partial\chi}{\partial\tilde{x}^\gamma}\right)^2}}\left(\frac{\partial\left(\mu u^i\right)}{\partial \tilde{x}^\alpha}-\frac{\partial\left(\mu u^i\right)}{\partial \tilde{x}^\beta}\frac{\partial\chi}{\partial\tilde{x}^\beta}-\frac{\partial\left(\mu u^i\right)}{\partial \tilde{x}^\gamma}\frac{\partial\chi}{\partial\tilde{x}^\gamma}\right)\right](0,0)\\
&=\left[\frac{\partial\left(\mu u^i\right)}{\partial \tilde{x}^\alpha}\right](0,0).
\end{aligned} \tag{3.2.59}$$

□

Lemma 3.2.13.

$$\left[\frac{\partial\left(\mu u^i\right)}{\partial \tilde{x}^\beta}\right](0,0)=\frac{\partial\left[\mu u^i\right]}{\partial \tilde{x}^\beta}(0,0),\quad i=\alpha,\beta,\gamma. \tag{3.2.60}$$

Proof.

$$
\begin{aligned}
\frac{\partial\left[\mu u^i\right]}{\partial \tilde{x}^\beta}(0,0) &= \frac{\partial\left(\mu u^i\right)_\Gamma^+}{\partial \tilde{x}^\beta}(0,0) - \frac{\partial\left(\mu u^i\right)_\Gamma^-}{\partial \tilde{x}^\beta}(0,0) \\
&= \left(\frac{\partial\left(\mu u^i\right)}{\partial \tilde{x}^\alpha}\right)_\Gamma^+(0,0)\frac{\partial \chi}{\partial \tilde{x}^\beta}(0,0) + \left(\frac{\partial\left(\mu u^i\right)}{\partial \tilde{x}^\beta}\right)_\Gamma^+(0,0) \\
&\quad - \left(\left(\frac{\partial\left(\mu u^i\right)}{\partial \tilde{x}^\alpha}\right)_\Gamma^-(0,0)\frac{\partial \chi}{\partial \tilde{x}^\beta}(0,0) + \left(\frac{\partial\left(\mu u^i\right)}{\partial \tilde{x}^\beta}\right)_\Gamma^-(0,0)\right) \\
&= \left[\frac{\partial\left(\mu u^i\right)}{\partial \tilde{x}^\beta}\right](0,0).
\end{aligned}
\tag{3.2.61}
$$

$\square$

Remark 3.2.14. *Similarly, we have*

$$
\left[\frac{\partial\left(\mu u^i\right)}{\partial \tilde{x}^\gamma}\right](0,0) = \frac{\partial\left[\mu u^i\right]}{\partial \tilde{x}^\gamma}(0,0), \quad i = \alpha,\beta,\gamma. \tag{3.2.62}
$$

Remark 3.2.15. *For higher order derivatives, we have*

$$
\frac{\partial^2\left[\mu u^i\right]}{\partial \tilde{x}^\beta \partial \tilde{x}^\beta}(0,0) = \left[\frac{\partial^2\left(\mu u^i\right)}{\partial \tilde{x}^\beta \partial \tilde{x}^\beta}\right](0,0) + \left[\frac{\partial\left(\mu u^i\right)}{\partial \tilde{x}^\alpha}\right](0,0)\frac{\partial^2 \chi}{\partial \tilde{x}^\beta \partial \tilde{x}^\beta}(0,0), \quad i = \alpha,\beta,\gamma \tag{3.2.63}
$$

and

$$
\frac{\partial^2\left[\mu u^i\right]}{\partial \tilde{x}^\gamma \partial \tilde{x}^\gamma}(0,0) = \left[\frac{\partial^2\left(\mu u^i\right)}{\partial \tilde{x}^\gamma \partial \tilde{x}^\gamma}\right](0,0) + \left[\frac{\partial\left(\mu u^i\right)}{\partial \tilde{x}^\alpha}\right](0,0)\frac{\partial^2 \chi}{\partial \tilde{x}^\gamma \partial \tilde{x}^\gamma}(0,0), \quad i = \alpha,\beta,\gamma. \tag{3.2.64}
$$

Note that $\left[\frac{\partial\left(\mu u^i\right)}{\partial \tilde{x}^\alpha}\right](0,0)$ *will be derived in the following theorem.*

Theorem 3.2.16. *For two-phase Stokes equations in 3D, given an arbitrary point* $\boldsymbol{x}_* \in \Gamma$, *the following jump conditions for* $\frac{\partial\left(\mu u^i\right)}{\partial n}$ *hold at point* $\boldsymbol{x}_*$:

$$
\begin{pmatrix}
\left[\frac{\partial\left(\mu u^\alpha\right)}{\partial n}\right] \\
\left[\frac{\partial\left(\mu u^\beta\right)}{\partial n}\right] \\
\left[\frac{\partial\left(\mu u^\gamma\right)}{\partial n}\right]
\end{pmatrix}
= A
\begin{pmatrix}
-\left(A^{-1}\right)_j^\beta \frac{\partial\left[\mu u^j\right]}{\partial \tilde{x}^\beta} - \left(A^{-1}\right)_j^\gamma \frac{\partial\left[\mu u^j\right]}{\partial \tilde{x}^\gamma} \\
-\left(A^{-1}\right)_j^\alpha \frac{\partial\left[\mu u^j\right]}{\partial \tilde{x}^\beta} - \tilde{f}^\beta \\
-\left(A^{-1}\right)_j^\alpha \frac{\partial\left[\mu u^j\right]}{\partial \tilde{x}^\gamma} - \tilde{f}^\gamma
\end{pmatrix}
\tag{3.2.65}
$$

where A *is the local coordinate transformation matrix.*

Proof. We can multiply τ^i and η^i separately at both sides of Eq. (3.2.5) and use coordinate transformation to get

$$\left[\mu\left(\frac{\partial \tilde{u}^i}{\partial \tilde{n}}\tilde{\tau}^i + \frac{\partial \tilde{u}^j}{\partial \tilde{\tau}}\tilde{n}^j\right)\right] + \tilde{f}^i\tilde{\tau}^i = 0 \tag{3.2.66}$$

and

$$\left[\mu\left(\frac{\partial \tilde{u}^i}{\partial \tilde{n}}\tilde{\eta}^i + \frac{\partial \tilde{u}^j}{\partial \tilde{\eta}}\tilde{n}^j\right)\right] + \tilde{f}^i\tilde{\eta}^i = 0. \tag{3.2.67}$$

Plugging Eqs. (3.2.53, 3.2.55) into Eq. (3.2.66) we get

$$\begin{aligned}\Bigg[&\frac{1}{\sqrt{1+\left(\frac{\partial\chi}{\partial\tilde{x}^\beta}\right)^2}}\left(\frac{\partial\left(\mu\tilde{u}^\alpha\right)}{\partial\tilde{n}}\frac{\partial\chi}{\partial\tilde{x}^\beta} + \frac{\partial\left(\mu\tilde{u}^\beta\right)}{\partial\tilde{n}}\right) + \frac{1}{\sqrt{1+\left(\frac{\partial\chi}{\partial\tilde{x}^\beta}\right)^2+\left(\frac{\partial\chi}{\partial\tilde{x}^\gamma}\right)^2}}\\ &\left(\frac{\partial\left(\mu\tilde{u}^\alpha\right)}{\partial\tilde{\tau}} - \frac{\partial\left(\mu\tilde{u}^\beta\right)}{\partial\tilde{\tau}}\frac{\partial\chi}{\partial\tilde{x}^\beta} - \frac{\partial\left(\mu\tilde{u}^\gamma\right)}{\partial\tilde{\tau}}\frac{\partial\chi}{\partial\tilde{x}^\gamma}\right)\Bigg] + \frac{1}{\sqrt{1+\left(\frac{\partial\chi}{\partial\tilde{x}^\beta}\right)^2}}\left(\tilde{f}^\alpha\frac{\partial\chi}{\partial\tilde{x}^\beta} + \tilde{f}^\beta\right) = 0.\end{aligned} \tag{3.2.68}$$

We can evaluate Eq. (3.2.68) at $\left(\tilde{x}^\beta, \tilde{x}^\gamma\right) = (0,0)$ to get

$$\left[\frac{\partial\left(\mu\tilde{u}^\beta\right)}{\partial\tilde{n}} + \frac{\partial\left(\mu\tilde{u}^\alpha\right)}{\partial\tilde{\tau}}\right](0,0) + \tilde{f}^\beta(0,0) = 0. \tag{3.2.69}$$

Then we can expand the directional derivatives in Eq. (3.2.69) to get

$$\left[\frac{\partial\left(\mu\tilde{u}^\beta\right)}{\partial\tilde{x}^\alpha} + \frac{\partial\left(\mu\tilde{u}^\alpha\right)}{\partial\tilde{x}^\beta}\right](0,0) + \tilde{f}^\beta(0,0) = 0. \tag{3.2.70}$$

Plugging Eqs. (3.2.54, 3.2.55) into Eq. (3.2.67) we get

$$\begin{aligned}\Bigg[&\frac{1}{\sqrt{1+\left(\frac{\partial\chi}{\partial\tilde{x}^\gamma}\right)^2}}\left(\frac{\partial\left(\mu\tilde{u}^\alpha\right)}{\partial\tilde{n}}\frac{\partial\chi}{\partial\tilde{x}^\gamma} + \frac{\partial\left(\mu\tilde{u}^\gamma\right)}{\partial\tilde{n}}\right) + \frac{1}{\sqrt{1+\left(\frac{\partial\chi}{\partial\tilde{x}^\beta}\right)^2+\left(\frac{\partial\chi}{\partial\tilde{x}^\gamma}\right)^2}}\\ &\left(\frac{\partial\left(\mu\tilde{u}^\alpha\right)}{\partial\tilde{\eta}} - \frac{\partial\left(\mu\tilde{u}^\beta\right)}{\partial\tilde{\eta}}\frac{\partial\chi}{\partial\tilde{x}^\beta} - \frac{\partial\left(\mu\tilde{u}^\gamma\right)}{\partial\tilde{\eta}}\frac{\partial\chi}{\partial\tilde{x}^\gamma}\right)\Bigg] + \frac{1}{\sqrt{1+\left(\frac{\partial\chi}{\partial\tilde{x}^\gamma}\right)^2}}\left(\tilde{f}^\alpha\frac{\partial\chi}{\partial\tilde{x}^\gamma} + \tilde{f}^\gamma\right) = 0.\end{aligned} \tag{3.2.71}$$

We can evaluate Eq. (3.2.71) at $\left(\tilde{x}^\beta, \tilde{x}^\gamma\right) = (0,0)$ to get

$$\left[\frac{\partial\left(\mu\tilde{u}^\gamma\right)}{\partial\tilde{n}} + \frac{\partial\left(\mu\tilde{u}^\alpha\right)}{\partial\tilde{\eta}}\right](0,0) + \tilde{f}^\gamma(0,0) = 0. \tag{3.2.72}$$

Then we can expand the directional derivatives in Eq. (3.2.72) to get

$$\left[\frac{\partial\left(\mu\tilde{u}^\gamma\right)}{\partial\tilde{x}^\alpha} + \frac{\partial\left(\mu\tilde{u}^\alpha\right)}{\partial\tilde{x}^\gamma}\right](0,0) + \tilde{f}^\gamma(0,0) = 0. \tag{3.2.73}$$

From Lemma 3.2.11 we know that

$$\left[\frac{\partial\left(\mu\tilde{u}^i\right)}{\partial\tilde{x}^i}\right](0,0)=0. \tag{3.2.74}$$

Eqs. (3.2.70, 3.2.73, 3.2.74) form a system of equations for $\left[\dfrac{\partial\left(\mu u^i\right)}{\partial\tilde{x}^\alpha}\right](0,0)$ and the coefficient matrix is A^{-1} which is non-singular. By solving this system of equations, we can get

$$\begin{pmatrix} \left[\dfrac{\partial\left(\mu u^\alpha\right)}{\partial\tilde{x}^\alpha}\right](0,0) \\ \\ \left[\dfrac{\partial\left(\mu u^\beta\right)}{\partial\tilde{x}^\alpha}\right](0,0) \\ \\ \left[\dfrac{\partial\left(\mu u^\gamma\right)}{\partial\tilde{x}^\alpha}\right](0,0) \end{pmatrix} = A \begin{pmatrix} -\left[\left(A^{-1}\right)^\beta_j\dfrac{\partial\left(\mu u^j\right)}{\partial\tilde{x}^\beta}\right](0,0)-\left[\left(A^{-1}\right)^\gamma_j\dfrac{\partial\left(\mu u^j\right)}{\partial\tilde{x}^\gamma}\right](0,0) \\ \\ -\left[\left(A^{-1}\right)^\alpha_j\dfrac{\partial\left(\mu u^j\right)}{\partial\tilde{x}^\beta}\right](0,0)-\tilde{f}^\beta(0,0) \\ \\ -\left[\left(A^{-1}\right)^\alpha_j\dfrac{\partial\left(\mu u^j\right)}{\partial\tilde{x}^\gamma}\right](0,0)-\tilde{f}^\gamma(0,0) \end{pmatrix}. \tag{3.2.75}$$

Using Lemma 3.2.12, 3.2.13 and suppress the sign for evaluation at the local origin, we reach Eq. (3.2.65). □

For pressure p, we have the following result:

Theorem 3.2.17. *For two-phase Stokes equations in 3D, given an arbitrary point $\boldsymbol{x}_*\in\Gamma$, the following jump condition for pressure p holds at point $\boldsymbol{x}_*$:*

$$[p]=-2\left(A^{-1}\right)^\beta_j\frac{\partial\left[\mu u^j\right]}{\partial\tilde{x}^\beta}-2\left(A^{-1}\right)^\gamma_j\frac{\partial\left[\mu u^j\right]}{\partial\tilde{x}^\gamma}+\tilde{f}^\alpha. \tag{3.2.76}$$

Proof. We can multiply n^i at both sides of Eq. (3.2.5) and use coordinate transformation to get

$$[p]=2\left[\frac{\partial\left(\mu\tilde{u}^i\right)}{\partial\tilde{n}}\tilde{n}^i\right]+\tilde{f}^i\tilde{n}^i. \tag{3.2.77}$$

Plugging Eq. (3.2.55) into Eq. (3.2.77) we get

$$\begin{aligned}[p]=&\,2\left[\frac{1}{\sqrt{1+\left(\frac{\partial\chi}{\partial\tilde{x}^\beta}\right)^2+\left(\frac{\partial\chi}{\partial\tilde{x}^\gamma}\right)^2}}\left(\frac{\partial\left(\mu\tilde{u}^\alpha\right)}{\partial\tilde{n}}-\frac{\partial\left(\mu\tilde{u}^\beta\right)}{\partial\tilde{n}}\frac{\partial\chi}{\partial\tilde{x}^\beta}-\frac{\partial\left(\mu\tilde{u}^\gamma\right)}{\partial\tilde{n}}\frac{\partial\chi}{\partial\tilde{x}^\gamma}\right)\right] \\ &+\frac{1}{\sqrt{1+\left(\frac{\partial\chi}{\partial\tilde{x}^\beta}\right)^2+\left(\frac{\partial\chi}{\partial\tilde{x}^\gamma}\right)^2}}\left(\tilde{f}^\alpha-\tilde{f}^\beta\frac{\partial\chi}{\partial\tilde{x}^\beta}-\tilde{f}^\gamma\frac{\partial\chi}{\partial\tilde{x}^\gamma}\right).\end{aligned} \tag{3.2.78}$$

We can evaluate Eq. (3.2.78) at $\left(\tilde{x}^\beta, \tilde{x}^\gamma\right) = (0,0)$ to get

$$[p](0,0) = 2\left[\frac{\partial\left(\mu\tilde{u}^\alpha\right)}{\partial\tilde{n}}\right](0,0) + \tilde{f}^\alpha(0,0). \tag{3.2.79}$$

Then we can expand the directional derivatives in Eq. (3.2.79) and use the incompressibility to get

$$\begin{aligned}[p](0,0) &= 2\left[\frac{\partial\left(\mu\tilde{u}^\alpha\right)}{\partial\tilde{x}^\alpha}\right](0,0) + \tilde{f}^\alpha(0,0) \\ &= -2\left[\frac{\partial\left(\mu\tilde{u}^\beta\right)}{\partial\tilde{x}^\beta}\right](0,0) - 2\left[\frac{\partial\left(\mu\tilde{u}^\gamma\right)}{\partial\tilde{x}^\gamma}\right](0,0) + \tilde{f}^\alpha(0,0).\end{aligned} \tag{3.2.80}$$

From Lemma 3.2.13, we have

$$[p](0,0) = -2\frac{\partial\left[\mu\tilde{u}^\beta\right]}{\partial\tilde{x}^\beta}(0,0) - 2\frac{\partial\left[\mu\tilde{u}^\gamma\right]}{\partial\tilde{x}^\gamma}(0,0) + \tilde{f}^\alpha(0,0). \tag{3.2.81}$$

Using coordinate transformation rule and suppress the sign for evaluation at the local origin, we reach Eq. (3.2.76). □

The jump condition for the normal derivative of pressure p is shown here:

Theorem 3.2.18. *For two-phase Stokes equations in 3D, given an arbitrary point $\boldsymbol{x}_* \in \Gamma$, the following jump condition for $\dfrac{\partial p}{\partial n}$ holds at point $\boldsymbol{x}_*$:*

$$\begin{aligned}\left[\frac{\partial p}{\partial n}\right] = &-2\frac{\partial^2\chi}{\partial\tilde{x}^\beta\partial\tilde{x}^\beta}\left(A^{-1}\right)^\beta_j\frac{\partial\left[\mu u^j\right]}{\partial\tilde{x}^\beta} - 2\frac{\partial^2\chi}{\partial\tilde{x}^\gamma\partial\tilde{x}^\gamma}\left(A^{-1}\right)^\gamma_j\frac{\partial\left[\mu u^j\right]}{\partial\tilde{x}^\gamma} \\ &- 2\frac{\partial^2\chi}{\partial\tilde{x}^\beta\partial\tilde{x}^\gamma}\left(A^{-1}\right)^\beta_j\frac{\partial\left[\mu u^j\right]}{\partial\tilde{x}^\gamma} - 2\frac{\partial^2\chi}{\partial\tilde{x}^\beta\partial\tilde{x}^\gamma}\left(A^{-1}\right)^\gamma_j\frac{\partial\left[\mu u^j\right]}{\partial\tilde{x}^\beta} \\ &+ 2\left(A^{-1}\right)^\alpha_j\frac{\partial^2\left[\mu u^j\right]}{\partial\tilde{x}^\beta\partial\tilde{x}^\beta} + 2\left(A^{-1}\right)^\alpha_j\frac{\partial^2\left[\mu u^j\right]}{\partial\tilde{x}^\gamma\partial\tilde{x}^\gamma} \\ &+ \left(\frac{\partial^2\chi}{\partial\tilde{x}^\beta\partial\tilde{x}^\beta} + \frac{\partial^2\chi}{\partial\tilde{x}^\gamma\partial\tilde{x}^\gamma}\right)\tilde{f}^\alpha + \frac{\partial\tilde{f}^\beta}{\partial\tilde{x}^\beta} + \frac{\partial\tilde{f}^\gamma}{\partial\tilde{x}^\gamma} + \left[\tilde{g}^\alpha\right].\end{aligned} \tag{3.2.82}$$

Proof. Multiply n^i at both sides of Eq. (3.2.1) for $\boldsymbol{x} \in \Omega^+$ and $\boldsymbol{x} \in \Omega^-$ to get

$$\begin{aligned}\left[\frac{\partial p}{\partial n}\right] &= \left[\frac{\partial}{\partial x^j}\left(\mu\left(\frac{\partial u^i}{\partial x^j} + \frac{\partial u^j}{\partial x^i}\right)\right)n^i\right] + \left[g^i n^i\right] \\ &= \left[\frac{\partial^2\left(\mu u^i\right)}{\partial x^j\partial x^j}n^i\right] + \left[g^i n^i\right].\end{aligned} \tag{3.2.83}$$

Recast Eq. (3.2.83) in $\tilde{x}^i$ coordinate to get

$$
\begin{aligned}
\left[\frac{\partial p}{\partial n}\right] &= \left[\frac{\partial^2\left(\mu\tilde{u}^i\right)}{\partial\tilde{x}^j\partial\tilde{x}^j}\tilde{n}^i\right] + \left[\tilde{g}^i\tilde{n}^i\right] \\
&= \left[\left(\frac{\partial^2\left(\mu\tilde{u}^i\right)}{\partial\tilde{x}^\alpha\partial\tilde{x}^\alpha} + \frac{\partial^2\left(\mu\tilde{u}^i\right)}{\partial\tilde{x}^\beta\partial\tilde{x}^\beta} + \frac{\partial^2\left(\mu\tilde{u}^i\right)}{\partial\tilde{x}^\gamma\partial\tilde{x}^\gamma}\right)\tilde{n}^i\right] + \left[\tilde{g}^i\tilde{n}^i\right].
\end{aligned}
\tag{3.2.84}
$$

Plugging Eq. (3.2.55) into Eq. (3.2.84) we get

$$
\begin{aligned}
\left[\frac{\partial p}{\partial n}\right] = \Bigg[&\frac{1}{\sqrt{1+\left(\frac{\partial\chi}{\partial\tilde{x}^\beta}\right)^2+\left(\frac{\partial\chi}{\partial\tilde{x}^\gamma}\right)^2}}\left(\frac{\partial^2\left(\mu\tilde{u}^\alpha\right)}{\partial\tilde{x}^\alpha\partial\tilde{x}^\alpha} + \frac{\partial^2\left(\mu\tilde{u}^\alpha\right)}{\partial\tilde{x}^\beta\partial\tilde{x}^\beta} + \frac{\partial^2\left(\mu\tilde{u}^\alpha\right)}{\partial\tilde{x}^\gamma\partial\tilde{x}^\gamma}\right. \\
&-\left(\frac{\partial^2\left(\mu\tilde{u}^\beta\right)}{\partial\tilde{x}^\alpha\partial\tilde{x}^\alpha} + \frac{\partial^2\left(\mu\tilde{u}^\beta\right)}{\partial\tilde{x}^\beta\partial\tilde{x}^\beta} + \frac{\partial^2\left(\mu\tilde{u}^\beta\right)}{\partial\tilde{x}^\gamma\partial\tilde{x}^\gamma}\right)\frac{\partial\chi}{\partial\tilde{x}^\beta} \\
&\left.-\left(\frac{\partial^2\left(\mu\tilde{u}^\gamma\right)}{\partial\tilde{x}^\alpha\partial\tilde{x}^\alpha} + \frac{\partial^2\left(\mu\tilde{u}^\gamma\right)}{\partial\tilde{x}^\beta\partial\tilde{x}^\beta} + \frac{\partial^2\left(\mu\tilde{u}^\gamma\right)}{\partial\tilde{x}^\gamma\partial\tilde{x}^\gamma}\right)\frac{\partial\chi}{\partial\tilde{x}^\gamma}\right)\Bigg] \\
&+\left[\frac{1}{\sqrt{1+\left(\frac{\partial\chi}{\partial\tilde{x}^\beta}\right)^2+\left(\frac{\partial\chi}{\partial\tilde{x}^\gamma}\right)^2}}\left(\tilde{g}^\alpha - \tilde{g}^\beta\frac{\partial\chi}{\partial\tilde{x}^\beta} - \tilde{g}^\gamma\frac{\partial\chi}{\partial\tilde{x}^\gamma}\right)\right].
\end{aligned}
\tag{3.2.85}
$$

We can evaluate Eq. (3.2.85) at $\left(\tilde{x}^\beta, \tilde{x}^\gamma\right) = (0,0)$ to get

$$
\left[\frac{\partial p}{\partial n}\right](0,0) = \left[\frac{\partial^2\left(\mu\tilde{u}^\alpha\right)}{\partial\tilde{x}^\alpha\partial\tilde{x}^\alpha} + \frac{\partial^2\left(\mu\tilde{u}^\alpha\right)}{\partial\tilde{x}^\beta\partial\tilde{x}^\beta} + \frac{\partial^2\left(\mu\tilde{u}^\alpha\right)}{\partial\tilde{x}^\gamma\partial\tilde{x}^\gamma}\right](0,0) + \left[\tilde{g}^\alpha\right](0,0). \tag{3.2.86}
$$

Now we take the derivative with respect to $\tilde{x}^\beta$ of both sides of Eq. (3.2.68) and evaluate at $\left(\tilde{x}^\beta, \tilde{x}^\gamma\right) = (0,0)$ to get

$$
\begin{aligned}
&2\frac{\partial^2\chi}{\partial\tilde{x}^\beta\partial\tilde{x}^\beta}(0,0)\left[\frac{\partial\left(\mu\tilde{u}^\alpha\right)}{\partial\tilde{x}^\alpha}\right](0,0) + \left[\frac{\partial^2\left(\mu\tilde{u}^\alpha\right)}{\partial\tilde{x}^\beta\partial\tilde{x}^\beta}\right](0,0) + \left[\frac{\partial^2\left(\mu\tilde{u}^\beta\right)}{\partial\tilde{x}^\alpha\partial\tilde{x}^\beta}\right](0,0) \\
&-2\frac{\partial^2\chi}{\partial\tilde{x}^\beta\partial\tilde{x}^\beta}(0,0)\left[\frac{\partial\left(\mu\tilde{u}^\beta\right)}{\partial\tilde{x}^\beta}\right](0,0) - \frac{\partial^2\chi}{\partial\tilde{x}^\beta\partial\tilde{x}^\gamma}(0,0)\left[\frac{\partial\left(\mu\tilde{u}^\beta\right)}{\partial\tilde{x}^\gamma}\right](0,0) \\
&-\frac{\partial^2\chi}{\partial\tilde{x}^\beta\partial\tilde{x}^\gamma}(0,0)\left[\frac{\partial\left(\mu\tilde{u}^\gamma\right)}{\partial\tilde{x}^\beta}\right](0,0) + \frac{\partial^2\chi}{\partial\tilde{x}^\beta\partial\tilde{x}^\beta}(0,0)\tilde{f}^\alpha(0,0) + \frac{\partial\tilde{f}^\beta}{\partial\tilde{x}^\beta}(0,0) = 0.
\end{aligned}
\tag{3.2.87}
$$

Next we take the derivative with respect to $\tilde{x}^\gamma$ of both sides of Eq. (3.2.71) and evaluate at $\left(\tilde{x}^\beta, \tilde{x}^\gamma\right) = (0,0)$ to get

$$
\begin{aligned}
&2\frac{\partial^2\chi}{\partial\tilde{x}^\gamma\partial\tilde{x}^\gamma}(0,0)\left[\frac{\partial\left(\mu\tilde{u}^\alpha\right)}{\partial\tilde{x}^\alpha}\right](0,0)+\left[\frac{\partial^2\left(\mu\tilde{u}^\alpha\right)}{\partial\tilde{x}^\gamma\partial\tilde{x}^\gamma}\right](0,0)+\left[\frac{\partial^2\left(\mu\tilde{u}^\gamma\right)}{\partial\tilde{x}^\alpha\partial\tilde{x}^\gamma}\right](0,0)\\
&\quad-2\frac{\partial^2\chi}{\partial\tilde{x}^\gamma\partial\tilde{x}^\gamma}(0,0)\left[\frac{\partial\left(\mu\tilde{u}^\gamma\right)}{\partial\tilde{x}^\gamma}\right](0,0)-\frac{\partial^2\chi}{\partial\tilde{x}^\beta\partial\tilde{x}^\gamma}(0,0)\left[\frac{\partial\left(\mu\tilde{u}^\gamma\right)}{\partial\tilde{x}^\beta}\right](0,0)\\
&\quad-\frac{\partial^2\chi}{\partial\tilde{x}^\beta\partial\tilde{x}^\gamma}(0,0)\left[\frac{\partial\left(\mu\tilde{u}^\beta\right)}{\partial\tilde{x}^\gamma}\right](0,0)+\frac{\partial^2\chi}{\partial\tilde{x}^\gamma\partial\tilde{x}^\gamma}(0,0)\tilde{f}^\alpha(0,0)+\frac{\partial\tilde{f}^\gamma}{\partial\tilde{x}^\gamma}(0,0)=0.
\end{aligned}
\tag{3.2.88}
$$

From the incompressibility condition, we know that

$$
\frac{\partial\left(\mu\tilde{u}^\alpha\right)}{\partial\tilde{x}^\alpha}+\frac{\partial\left(\mu\tilde{u}^\beta\right)}{\partial\tilde{x}^\beta}+\frac{\partial\left(\mu\tilde{u}^\gamma\right)}{\partial\tilde{x}^\gamma}=0,\quad \boldsymbol{x}\in\Omega^+,\ \text{or }\Omega^-. \tag{3.2.89}
$$

Taking the derivative of Eq. (3.2.89) with respect to $\tilde{x}^\alpha$ we get

$$
\frac{\partial^2\left(\mu\tilde{u}^\alpha\right)}{\partial\tilde{x}^\alpha\partial\tilde{x}^\alpha}+\frac{\partial^2\left(\mu\tilde{u}^\beta\right)}{\partial\tilde{x}^\alpha\partial\tilde{x}^\beta}+\frac{\partial^2\left(\mu\tilde{u}^\gamma\right)}{\partial\tilde{x}^\alpha\partial\tilde{x}^\gamma}=0,\quad \boldsymbol{x}\in\Omega^+,\ \text{or }\Omega^-. \tag{3.2.90}
$$

Therefore from Eqs. (3.2.90, 3.2.87, 3.2.88) we get

$$
\begin{aligned}
\left[\frac{\partial^2\left(\mu\tilde{u}^\alpha\right)}{\partial\tilde{x}^\alpha\partial\tilde{x}^\alpha}\right](0,0)&=-2\left(2\frac{\partial^2\chi}{\partial\tilde{x}^\beta\partial\tilde{x}^\beta}(0,0)+\frac{\partial^2\chi}{\partial\tilde{x}^\gamma\partial\tilde{x}^\gamma}(0,0)\right)\left[\frac{\partial\left(\mu\tilde{u}^\beta\right)}{\partial\tilde{x}^\beta}\right](0,0)\\
&\quad-2\left(\frac{\partial^2\chi}{\partial\tilde{x}^\beta\partial\tilde{x}^\beta}(0,0)+2\frac{\partial^2\chi}{\partial\tilde{x}^\gamma\partial\tilde{x}^\gamma}(0,0)\right)\left[\frac{\partial\left(\mu\tilde{u}^\gamma\right)}{\partial\tilde{x}^\gamma}\right](0,0)\\
&\quad+\left[\frac{\partial^2\left(\mu\tilde{u}^\alpha\right)}{\partial\tilde{x}^\beta\partial\tilde{x}^\beta}\right](0,0)+\left[\frac{\partial^2\left(\mu\tilde{u}^\alpha\right)}{\partial\tilde{x}^\gamma\partial\tilde{x}^\gamma}\right](0,0)\\
&\quad-2\frac{\partial^2\chi}{\partial\tilde{x}^\beta\partial\tilde{x}^\gamma}(0,0)\left[\frac{\partial\left(\mu\tilde{u}^\beta\right)}{\partial\tilde{x}^\gamma}\right](0,0)-2\frac{\partial^2\chi}{\partial\tilde{x}^\beta\partial\tilde{x}^\gamma}(0,0)\left[\frac{\partial\left(\mu\tilde{u}^\gamma\right)}{\partial\tilde{x}^\beta}\right](0,0)\\
&\quad+\left(\frac{\partial^2\chi}{\partial\tilde{x}^\beta\partial\tilde{x}^\beta}(0,0)+\frac{\partial^2\chi}{\partial\tilde{x}^\gamma\partial\tilde{x}^\gamma}(0,0)\right)\tilde{f}^\alpha(0,0)+\frac{\partial\tilde{f}^\beta}{\partial\tilde{x}^\beta}(0,0)+\frac{\partial\tilde{f}^\gamma}{\partial\tilde{x}^\gamma}(0,0).
\end{aligned}
\tag{3.2.91}
$$

From Eqs. (3.2.86, 3.2.91), we have

$$\begin{aligned}\left[\frac{\partial p}{\partial n}\right](0,0) = &-2\left(2\frac{\partial^2\chi}{\partial\tilde{x}^\beta\partial\tilde{x}^\beta}(0,0)+\frac{\partial^2\chi}{\partial\tilde{x}^\gamma\partial\tilde{x}^\gamma}(0,0)\right)\left[\frac{\partial\left(\mu\tilde{u}^\beta\right)}{\partial\tilde{x}^\beta}\right](0,0)\\
&-2\left(\frac{\partial^2\chi}{\partial\tilde{x}^\beta\partial\tilde{x}^\beta}(0,0)+2\frac{\partial^2\chi}{\partial\tilde{x}^\gamma\partial\tilde{x}^\gamma}(0,0)\right)\left[\frac{\partial\left(\mu\tilde{u}^\gamma\right)}{\partial\tilde{x}^\gamma}\right](0,0)\\
&+2\left[\frac{\partial^2\left(\mu\tilde{u}^\alpha\right)}{\partial\tilde{x}^\beta\partial\tilde{x}^\beta}\right](0,0)+2\left[\frac{\partial^2\left(\mu\tilde{u}^\alpha\right)}{\partial\tilde{x}^\gamma\partial\tilde{x}^\gamma}\right](0,0)\\
&-2\frac{\partial^2\chi}{\partial\tilde{x}^\beta\partial\tilde{x}^\gamma}(0,0)\left[\frac{\partial\left(\mu\tilde{u}^\beta\right)}{\partial\tilde{x}^\gamma}\right](0,0)-2\frac{\partial^2\chi}{\partial\tilde{x}^\beta\partial\tilde{x}^\gamma}(0,0)\left[\frac{\partial\left(\mu\tilde{u}^\gamma\right)}{\partial\tilde{x}^\beta}\right](0,0)\\
&+\left(\frac{\partial^2\chi}{\partial\tilde{x}^\beta\partial\tilde{x}^\beta}(0,0)+\frac{\partial^2\chi}{\partial\tilde{x}^\gamma\partial\tilde{x}^\gamma}(0,0)\right)\tilde{f}^\alpha(0,0)+\frac{\partial\tilde{f}^\beta}{\partial\tilde{x}^\beta}(0,0)+\frac{\partial\tilde{f}^\gamma}{\partial\tilde{x}^\gamma}(0,0)+\left[\tilde{g}^\alpha\right](0,0).
\end{aligned}\tag{3.2.92}$$

Using Lemma 3.2.13 and Eq. (3.2.92), we get

$$\begin{aligned}\left[\frac{\partial p}{\partial n}\right](0,0) = &-2\left(2\frac{\partial^2\chi}{\partial\tilde{x}^\beta\partial\tilde{x}^\beta}(0,0)+\frac{\partial^2\chi}{\partial\tilde{x}^\gamma\partial\tilde{x}^\gamma}(0,0)\right)\left(A^{-1}\right)_j^\beta\frac{\partial\left[\mu u^j\right]}{\partial\tilde{x}^\beta}(0,0)\\
&-2\left(\frac{\partial^2\chi}{\partial\tilde{x}^\beta\partial\tilde{x}^\beta}(0,0)+2\frac{\partial^2\chi}{\partial\tilde{x}^\gamma\partial\tilde{x}^\gamma}(0,0)\right)\left(A^{-1}\right)_j^\gamma\frac{\partial\left[\mu u^j\right]}{\partial\tilde{x}^\gamma}(0,0)\\
&+2\left(A^{-1}\right)_j^\alpha\left(\frac{\partial^2\left[\mu u^j\right]}{\partial\tilde{x}^\beta\partial\tilde{x}^\beta}(0,0)-\frac{\partial^2\chi}{\partial\tilde{x}^\beta\partial\tilde{x}^\beta}(0,0)\left[\frac{\partial\left(\mu u^j\right)}{\partial\tilde{x}^\alpha}\right](0,0)\right)\\
&+2\left(A^{-1}\right)_j^\alpha\left(\frac{\partial^2\left[\mu u^j\right]}{\partial\tilde{x}^\gamma\partial\tilde{x}^\gamma}(0,0)-\frac{\partial^2\chi}{\partial\tilde{x}^\gamma\partial\tilde{x}^\gamma}(0,0)\left[\frac{\partial\left(\mu u^j\right)}{\partial\tilde{x}^\alpha}\right](0,0)\right)\\
&-2\frac{\partial^2\chi}{\partial\tilde{x}^\beta\partial\tilde{x}^\gamma}(0,0)\left(A^{-1}\right)_j^\beta\frac{\partial\left[\mu u^j\right]}{\partial\tilde{x}^\gamma}(0,0)-2\frac{\partial^2\chi}{\partial\tilde{x}^\beta\partial\tilde{x}^\gamma}(0,0)\left(A^{-1}\right)_j^\gamma\frac{\partial\left[\mu u^j\right]}{\partial\tilde{x}^\beta}(0,0)\\
&+\left(\frac{\partial^2\chi}{\partial\tilde{x}^\beta\partial\tilde{x}^\beta}(0,0)+\frac{\partial^2\chi}{\partial\tilde{x}^\gamma\partial\tilde{x}^\gamma}(0,0)\right)\tilde{f}^\alpha(0,0)+\frac{\partial\tilde{f}^\beta}{\partial\tilde{x}^\beta}(0,0)+\frac{\partial\tilde{f}^\gamma}{\partial\tilde{x}^\gamma}(0,0)+\left[\tilde{g}^\alpha\right](0,0).
\end{aligned}\tag{3.2.93}$$

Using Eq. (3.2.89) and suppressing the sign for evaluation at the local origin, we reach Eq. (3.2.82). □

Remark 3.2.19. *Notice that in Eq. (3.2.82), we have*

$$\begin{aligned}&-2\frac{\partial^2\chi}{\partial\tilde{x}^\beta\partial\tilde{x}^\beta}\left(A^{-1}\right)_j^\beta\frac{\partial\left[\mu u^j\right]}{\partial\tilde{x}^\beta}-2\frac{\partial^2\chi}{\partial\tilde{x}^\gamma\partial\tilde{x}^\gamma}\left(A^{-1}\right)_j^\gamma\frac{\partial\left[\mu u^j\right]}{\partial\tilde{x}^\gamma}-2\frac{\partial^2\chi}{\partial\tilde{x}^\beta\partial\tilde{x}^\gamma}\left(A^{-1}\right)_j^\beta\frac{\partial\left[\mu u^j\right]}{\partial\tilde{x}^\gamma}\\
&-2\frac{\partial^2\chi}{\partial\tilde{x}^\beta\partial\tilde{x}^\gamma}\left(A^{-1}\right)_j^\gamma\frac{\partial\left[\mu u^j\right]}{\partial\tilde{x}^\beta}
\end{aligned}\tag{3.2.94}$$

which equals the trace of the following matrix product

$$-2\begin{pmatrix} \dfrac{\partial^2\chi}{\partial\tilde{x}^\beta\partial\tilde{x}^\beta} & \dfrac{\partial^2\chi}{\partial\tilde{x}^\beta\partial\tilde{x}^\gamma} \\ \dfrac{\partial^2\chi}{\partial\tilde{x}^\beta\partial\tilde{x}^\gamma} & \dfrac{\partial^2\chi}{\partial\tilde{x}^\gamma\partial\tilde{x}^\gamma} \end{pmatrix}\begin{pmatrix} \left(A^{-1}\right)^\beta_j \dfrac{\partial\left[\mu u^j\right]}{\partial\tilde{x}^\beta} & \left(A^{-1}\right)^\beta_j \dfrac{\partial\left[\mu u^j\right]}{\partial\tilde{x}^\gamma} \\ \left(A^{-1}\right)^\gamma_j \dfrac{\partial\left[\mu u^j\right]}{\partial\tilde{x}^\beta} & \left(A^{-1}\right)^\gamma_j \dfrac{\partial\left[\mu u^j\right]}{\partial\tilde{x}^\gamma} \end{pmatrix}. \tag{3.2.95}$$

To summarize, for 3D Stokes equations with interface, we have derived the jump conditions $\left[\dfrac{\partial\left(\mu u^i\right)}{\partial n}\right]$, $[p]$ and $\left[\dfrac{\partial p}{\partial n}\right]$ as follows:

$$\boxed{\begin{aligned}
\begin{pmatrix} \left[\dfrac{\partial\left(\mu u^\alpha\right)}{\partial n}\right] \\ \left[\dfrac{\partial\left(\mu u^\beta\right)}{\partial n}\right] \\ \left[\dfrac{\partial\left(\mu u^\gamma\right)}{\partial n}\right] \end{pmatrix} &= A\begin{pmatrix} -\left(A^{-1}\right)^\beta_j \dfrac{\partial\left[\mu u^j\right]}{\partial\tilde{x}^\beta} - \left(A^{-1}\right)^\gamma_j \dfrac{\partial\left[\mu u^j\right]}{\partial\tilde{x}^\gamma} \\ -\left(A^{-1}\right)^\alpha_j \dfrac{\partial\left[\mu u^j\right]}{\partial\tilde{x}^\beta} - \tilde{f}^\beta \\ -\left(A^{-1}\right)^\alpha_j \dfrac{\partial\left[\mu u^j\right]}{\partial\tilde{x}^\gamma} - \tilde{f}^\gamma \end{pmatrix}, \\
[p] &= -2\left(A^{-1}\right)^\beta_j \frac{\partial\left[\mu u^j\right]}{\partial\tilde{x}^\beta} - 2\left(A^{-1}\right)^\gamma_j \frac{\partial\left[\mu u^j\right]}{\partial\tilde{x}^\gamma} + \tilde{f}^\alpha, \qquad (3.2.96) \\
\left[\frac{\partial p}{\partial n}\right] &= -2\frac{\partial^2\chi}{\partial\tilde{x}^\beta\partial\tilde{x}^\beta}\left(A^{-1}\right)^\beta_j \frac{\partial\left[\mu u^j\right]}{\partial\tilde{x}^\beta} - 2\frac{\partial^2\chi}{\partial\tilde{x}^\gamma\partial\tilde{x}^\gamma}\left(A^{-1}\right)^\gamma_j \frac{\partial\left[\mu u^j\right]}{\partial\tilde{x}^\gamma} \\
&\quad - 2\frac{\partial^2\chi}{\partial\tilde{x}^\beta\partial\tilde{x}^\gamma}\left(A^{-1}\right)^\beta_j \frac{\partial\left[\mu u^j\right]}{\partial\tilde{x}^\gamma} - 2\frac{\partial^2\chi}{\partial\tilde{x}^\beta\partial\tilde{x}^\gamma}\left(A^{-1}\right)^\gamma_j \frac{\partial\left[\mu u^j\right]}{\partial\tilde{x}^\beta} \\
&\quad + 2\left(A^{-1}\right)^\alpha_j \frac{\partial^2\left[\mu u^j\right]}{\partial\tilde{x}^\beta\partial\tilde{x}^\beta} + 2\left(A^{-1}\right)^\alpha_j \frac{\partial^2\left[\mu u^j\right]}{\partial\tilde{x}^\gamma\partial\tilde{x}^\gamma} \\
&\quad + \left(\frac{\partial^2\chi}{\partial\tilde{x}^\beta\partial\tilde{x}^\beta} + \frac{\partial^2\chi}{\partial\tilde{x}^\gamma\partial\tilde{x}^\gamma}\right)\tilde{f}^\alpha + \frac{\partial\tilde{f}^\beta}{\partial\tilde{x}^\beta} + \frac{\partial\tilde{f}^\gamma}{\partial\tilde{x}^\gamma} + \left[\tilde{g}^\alpha\right].
\end{aligned}}$$

Chapter 4

Immersed Interface Method for Elliptic Differential Equation with Interfaces

We can solve the Stokes equations for two viscous tissues by solving an elliptic equation with interfaces using the Immersed Interface Method (IIM). Although the IIM scheme for both 2D and 3D elliptic problems can be found in the literature [26, 24, 27, 7], here we show the derivation of the scheme with tensor notation and some new results.

We begin by considering the non-homogeneous elliptic equation in the invariant form

$$\nabla^2 u + \lambda u + f = 0 \tag{4.0.1}$$

with the constant $\lambda \leq 0$. If $\lambda = 0$, we get the Poisson equation

$$\nabla^2 u + f = 0 \tag{4.0.2}$$

and the Laplace equation is a special case of the Poisson equation with $f = 0$. Here f is a known function of spatial variable $\boldsymbol{x}$.

4.1 2D Geometry

The 2D elliptic equation is

$$\frac{\partial^2 u}{\partial x^\alpha \partial x^\alpha} + \frac{\partial^2 u}{\partial x^\beta \partial x^\beta} + \lambda u + f = 0. \tag{4.1.1}$$

We consider a rectangular domain $\Omega = [x_b^\alpha, x_e^\alpha] \times [x_b^\beta, x_e^\beta]$ with a curved interface $\Gamma \subset \Omega$. Γ divides Ω into Ω^+ outside the interface and Ω^- inside the interface. For example, see Fig. 4.1 for a case where an open curve cannot be used for Γ since Ω^+ and Ω^- are not well defined. On the other hand, the interface curve Γ can be either simply connected, or not simply connected; see Fig. 4.1 for examples.

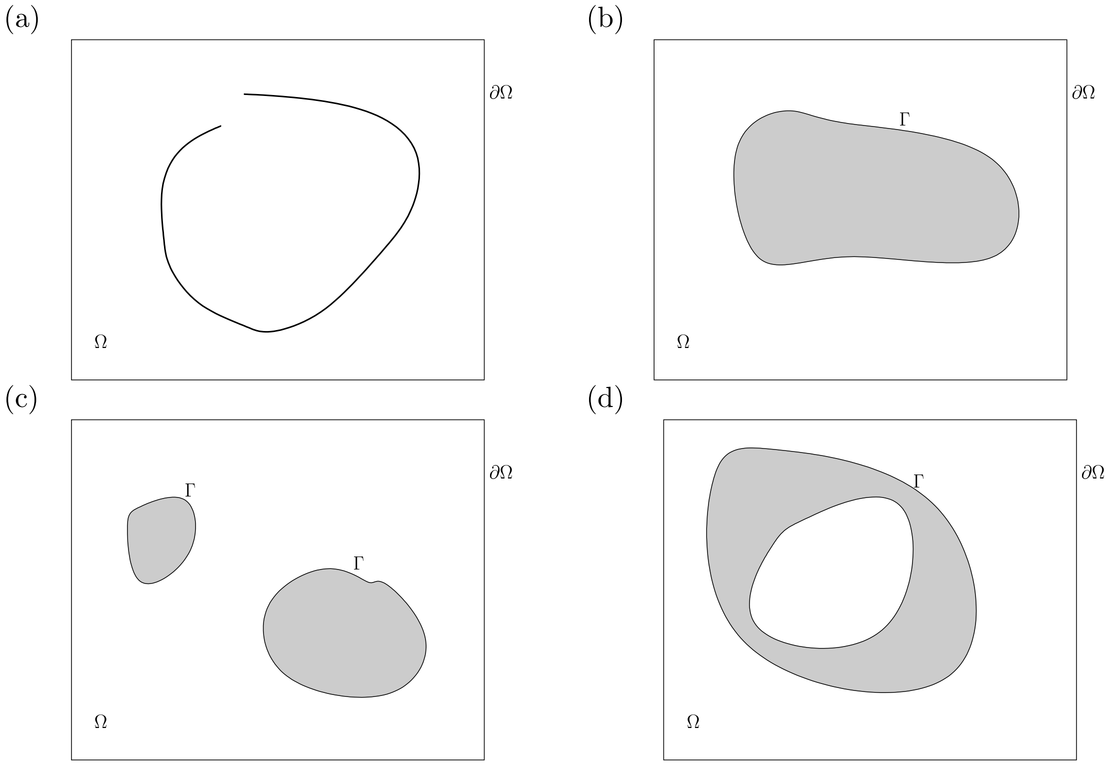

Figure 4.1: An open curve cannot be used for the interface Γ, since Ω^+ and Ω^- are not defined (a). Ω^- (shaded region) can be either simply connected (b) or not simply connected (c,d).

Because u might be discontinuous or non-smooth across the interface Γ, it is more convenient to express u in terms of smooth functions in Ω^+ and Ω^- separately. Namely,

$$u = \begin{cases} u^+, & \boldsymbol{x} \in \Omega^+, \\ u^-, & \boldsymbol{x} \in \Omega^-. \end{cases} \tag{4.1.2}$$

Similar notations are used for other discontinuous or non-smooth quantities. Eq. (4.1.1) now becomes

$$\left(\frac{\partial^2 u}{\partial x^\alpha \partial x^\alpha}\right)^+ + \left(\frac{\partial^2 u}{\partial x^\beta \partial x^\beta}\right)^+ + \lambda^+ u^+ + f^+ = 0, \quad \boldsymbol{x} \in \Omega^+ \tag{4.1.3}$$

and

$$\left(\frac{\partial^2 u}{\partial x^\alpha \partial x^\alpha}\right)^- + \left(\frac{\partial^2 u}{\partial x^\beta \partial x^\beta}\right)^- + \lambda^- u^- + f^- = 0, \quad \boldsymbol{x} \in \Omega^-. \tag{4.1.4}$$

We also assume that the following two jump conditions are known:

$$[u] = w, \quad \left[\frac{\partial u}{\partial n}\right] = v. \tag{4.1.5}$$

Note that we have

$$\left(\frac{\partial^2 u}{\partial x^\alpha \partial x^\alpha}\right)^+ = \frac{\partial^2 u^+}{\partial x^\alpha \partial x^\alpha} \tag{4.1.6}$$

etc. Without loss of generality, we define

$$u(\boldsymbol{x}), \quad \boldsymbol{x} \in \Gamma \tag{4.1.7}$$

as the limit of u on the interface from the side of Ω^+, which may be written as

$$u(\boldsymbol{x}) = u_\Gamma^+, \quad \boldsymbol{x} \in \Gamma. \tag{4.1.8}$$

In other words, $u(\boldsymbol{x})$ is defined to be continuous from the side of Ω^+. The notation u_Γ^- simply means the limit of u on the interface from the side of Ω^-.

The domain Ω is discretized as

$$\Omega_h = \left\{ \left(x_i^\alpha = x_b^\alpha + ih, x_j^\beta = x_b^\beta + jh \right) \Big| i = 0, 1, \ldots, m; j = 0, 1, \cdots, n \right\} \tag{4.1.9}$$

using a uniform grid width h. A grid point $\left(x_i^\alpha, x_j^\beta\right)$, which is on one side of the interface Γ, is called a *regular grid point* if the difference stencil centered at $\left(x_i^\alpha, x_j^\beta\right)$ contains no grid points on the other side of the interface. Intuitively, at those majority regular grid points, if we use a finite difference scheme such as the five-point stencil

$$\frac{U_{i,j-1} + U_{i,j+1} + U_{i-1,j} + U_{i+1,j} - 4U_{i,j}}{h^2} + \lambda U_{i,j} + f_{i,j} = 0, \tag{4.1.10}$$

using Taylor expansion at grid point $\left(x_i^\alpha, x_j^\beta\right)$, we know that the local truncation error for $(x_i^\alpha, x_j^\beta) \in \Omega^+$ is

$$
\begin{aligned}
T &= \frac{u_{i,j-1}^+ + u_{i,j+1}^+ + u_{i-1,j}^+ + u_{i+1,j}^+ - 4u_{i,j}^+}{h^2} + \lambda^+ u_{i,j}^+ + f_{i,j}^+ \\
&= \left(\frac{\partial^2 u}{\partial x^\alpha \partial x^\alpha}\right)^+ (x_i^\alpha, x_j^\beta) + \left(\frac{\partial^2 u}{\partial x^\beta \partial x^\beta}\right)^+ (x_i^\alpha, x_j^\beta) + \lambda^+ u_{i,j}^+ + f_{i,j}^+ + O(h^2) \\
&= O(h^2).
\end{aligned}
\tag{4.1.11}
$$

The same conclusion holds for regular grid points in Ω^-.

At those minority *irregular grid points* either close to or on the interface Γ, we hope that the same second order scheme still works. To facilitate derivations, we locate an interface point $\boldsymbol{x}_* \in \Gamma$ close to the five stencil grid points and define a local Cartesian coordinate system $(\tilde{x}^\alpha, \tilde{x}^\beta)$ centered at $\boldsymbol{x}_*$ as

$$\tilde{x}^i = \left(A^{-1}\right)_j^i \left(x^j - x_*^j\right) \tag{4.1.12}$$

where the coordinate transformation matrix is

$$A = \begin{pmatrix} n^\alpha(\boldsymbol{x}_*) & \tau^\alpha(\boldsymbol{x}_*) \\ n^\beta(\boldsymbol{x}_*) & \tau^\beta(\boldsymbol{x}_*) \end{pmatrix}. \tag{4.1.13}$$

Here $n^i(\boldsymbol{x}_*)$ is the unit normal direction pointing from Ω^- to Ω^+, $\tau^i(\boldsymbol{x}_*)$ is the unit tangential direction counter-clockwise of $n^i(\boldsymbol{x}_*)$. See Fig. 4.2 for an illustration of the change of coordinates.

Lemma 4.1.1.

$$\frac{\partial^2 u}{\partial \tilde{x}^\alpha \partial \tilde{x}^\alpha} + \frac{\partial^2 u}{\partial \tilde{x}^\beta \partial \tilde{x}^\beta} + \lambda u + f = 0. \tag{4.1.14}$$

Proof.

$$
\begin{aligned}
\frac{\partial^2 u}{\partial \tilde{x}^\alpha \partial \tilde{x}^\alpha} + \frac{\partial^2 u}{\partial \tilde{x}^\beta \partial \tilde{x}^\beta} = \frac{\partial^2 u}{\partial \tilde{x}^i \partial \tilde{x}^i} &= \frac{\partial}{\partial \tilde{x}^i}\left((A)_i^l \frac{\partial u}{\partial x^l}\right) \\
&= (A)_i^l (A)_i^k \frac{\partial^2 u}{\partial x^k \partial x^l} \\
&= \left(A^{-1}\right)_l^i (A)_i^k \frac{\partial^2 u}{\partial x^k \partial x^l} \\
&= \delta_{kl} \frac{\partial^2 u}{\partial x^k \partial x^l} = \frac{\partial^2 u}{\partial x^k \partial x^k}.
\end{aligned}
\tag{4.1.15}
$$

So

$$\frac{\partial^2 u}{\partial \tilde{x}^\alpha \partial \tilde{x}^\alpha} + \frac{\partial^2 u}{\partial \tilde{x}^\beta \partial \tilde{x}^\beta} + \lambda u + f = \frac{\partial^2 u}{\partial x^\alpha \partial x^\alpha} + \frac{\partial^2 u}{\partial x^\beta \partial x^\beta} + \lambda u + f = 0. \tag{4.1.16}$$

□

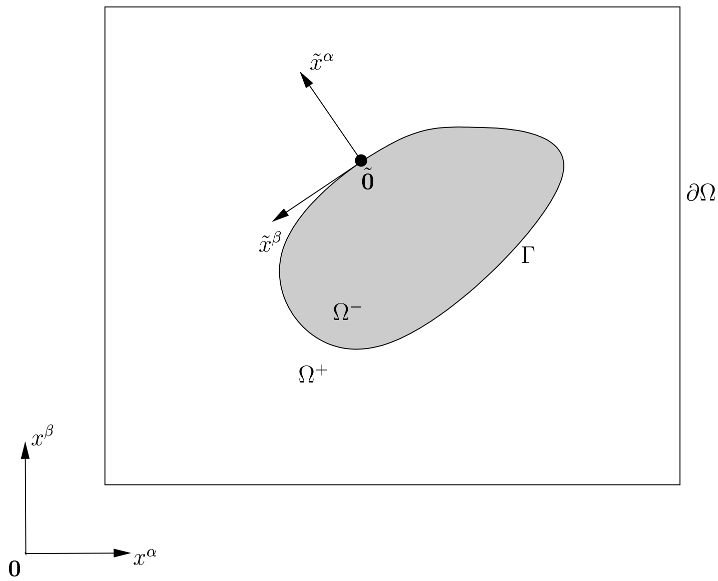

Figure 4.2: Given a point $\boldsymbol{x}_* \in \Gamma$, a local Cartesian coordinate system $\left(\tilde{x}^\alpha, \tilde{x}^\beta\right)$ is built using $\boldsymbol{x}_*$ as the origin, the unit normal vector $\boldsymbol{n}$ and the unit tangential vector $\boldsymbol{\tau}$ at that point as the two coordinate axes. The normal vector $\boldsymbol{n}$ points from Ω^- to Ω^+ and the tangent vector $\boldsymbol{\tau}$ is counter-clockwise of $\boldsymbol{n}$.

Remark 4.1.2. *It is also possible to prove this lemma using the trace invariance under a similarity transformation.*

Let us consider an irregular grid point $(x_i^\alpha, x_j^\beta) \in \Omega^+$, whose coordinates in the local coordinate system $\left(\tilde{x}^\alpha, \tilde{x}^\beta\right)$ is denoted as $(\tilde{x}_{i,j}^\alpha, \tilde{x}_{i,j}^\beta)$. Now the truncation error is

$$T = \frac{u_{i,j-1} + u_{i,j+1} + u_{i-1,j} + u_{i+1,j} - 4u_{i,j}^+}{h^2} + \lambda^+ u_{i,j}^+ + f_{i,j}^+. \tag{4.1.17}$$

For the other four stencil grid points, without loss of generality, we assume that only

$$(\tilde{x}_{i,j-1}^\alpha, \tilde{x}_{i,j-1}^\beta) \in \Omega^-. \tag{4.1.18}$$

See Fig. 4.3 for an example of the difference stencil at the irregular grid point $\left(x_i^\alpha, x_j^\beta\right)$.

Now it is determined that

$$T = \frac{u_{i,j-1}^- + u_{i,j+1}^+ + u_{i-1,j}^+ + u_{i+1,j}^+ - 4u_{i,j}^+}{h^2} + \lambda^+ u_{i,j}^+ + f_{i,j}^+. \tag{4.1.19}$$

Instead of applying Taylor expansion at grid point $(\tilde{x}_{i,j}^\alpha, \tilde{x}_{i,j}^\beta)$, we can expand at the interface point $\boldsymbol{x}_*$, or equivalently the origin $\tilde{\mathbf{0}}$ in the local coordinates $\left(\tilde{x}^\alpha, \tilde{x}^\beta\right)$. Note that the

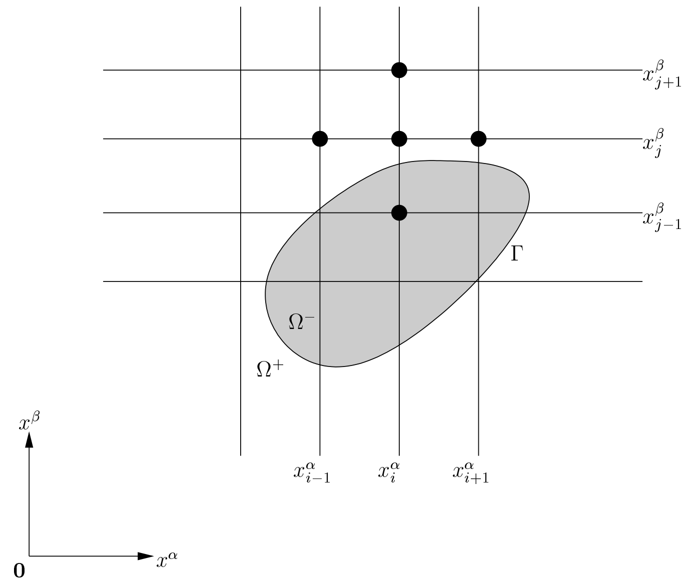

Figure 4.3: An example of the five-point stencil centered at an irregular grid point $\left(x_i^\alpha, x_j^\beta\right) \in \Omega^+$ with only $\left(x_i^\alpha, x_{j-1}^\beta\right) \in \Omega^-$.

interface Γ is parameterized in the local coordinates as

$$\Gamma = \left(\chi(\tilde{x}^\beta), \tilde{x}^\beta\right) \tag{4.1.20}$$

and the limit on the interface for a 2D function from the side of either Ω^+ or Ω^- is parameterized only by $\tilde{x}^\beta$. For example,

$$\begin{aligned} u^-_{i,j-1} = u^-_\Gamma(0) &+ \left(\tilde{x}^\alpha_{i,j-1}\left(\frac{\partial u}{\partial \tilde{x}^\alpha}\right)^-_\Gamma(0) + \tilde{x}^\beta_{i,j-1}\left(\frac{\partial u}{\partial \tilde{x}^\beta}\right)^-_\Gamma(0)\right) \\ &+ \frac{1}{2}\left(\left(\tilde{x}^\alpha_{i,j-1}\right)^2\left(\frac{\partial^2 u}{\partial \tilde{x}^\alpha \partial \tilde{x}^\alpha}\right)^-_\Gamma(0) + 2\tilde{x}^\alpha_{i,j-1}\tilde{x}^\beta_{i,j-1}\left(\frac{\partial^2 u}{\partial \tilde{x}^\alpha \partial \tilde{x}^\beta}\right)^-_\Gamma(0)\right. \\ &+ \left.\left(\tilde{x}^\beta_{i,j-1}\right)^2\left(\frac{\partial^2 u}{\partial \tilde{x}^\beta \partial \tilde{x}^\beta}\right)^-_\Gamma(0)\right) + O(h^3). \end{aligned} \tag{4.1.21}$$

See Fig. 4.4 for an example of the Taylor expansion at the local coordinate system.

Note that the jump conditions (4.1.5) locally can be expressed as

$$[u] = w_\Gamma(\tilde{x}^\beta), \quad \text{or} \quad u^+_\Gamma\left(\chi(\tilde{x}^\beta), \tilde{x}^\beta\right) - u^-_\Gamma\left(\chi(\tilde{x}^\beta), \tilde{x}^\beta\right) = w_\Gamma(\tilde{x}^\beta) \tag{4.1.22}$$

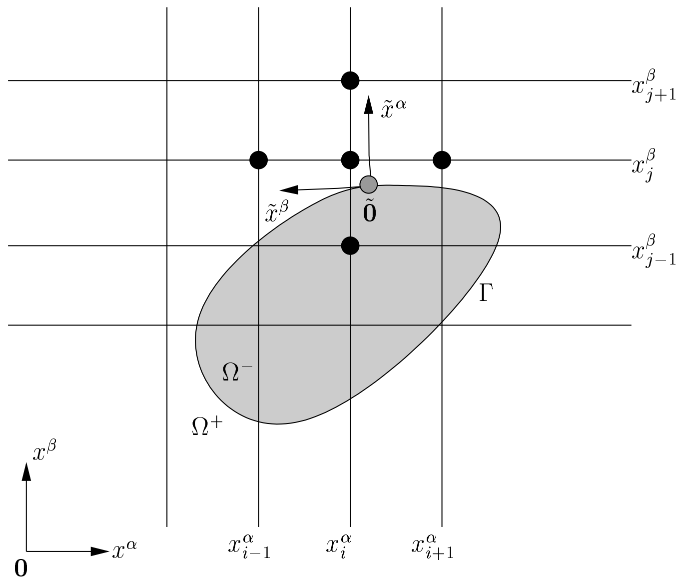

Figure 4.4: An example of the Taylor expansion at the local coordinate system $\left(\tilde{x}^\alpha, \tilde{x}^\beta\right)$. Note that the local origin must be on the interface Γ and close to the five stencil grid points.

and

$$\left[\frac{\partial u}{\partial n}\right] = v_\Gamma(\tilde{x}^\beta), \quad \text{or} \quad \left(\frac{\partial u}{\partial n}\right)^+_\Gamma \left(\chi(\tilde{x}^\beta), \tilde{x}^\beta\right) - \left(\frac{\partial u}{\partial n}\right)^-_\Gamma \left(\chi(\tilde{x}^\beta), \tilde{x}^\beta\right) = v_\Gamma(\tilde{x}^\beta). \quad (4.1.23)$$

We can take the derivative of Eq. (4.1.22) with respect to $\tilde{x}^\beta$ to get

$$\left(\frac{\partial u}{\partial \tilde{x}^\alpha}\right)^+_\Gamma \left(\frac{d\chi}{d\tilde{x}^\beta}\right)_\Gamma + \left(\frac{\partial u}{\partial \tilde{x}^\beta}\right)^+_\Gamma - \left(\left(\frac{\partial u}{\partial \tilde{x}^\alpha}\right)^-_\Gamma \left(\frac{d\chi}{d\tilde{x}^\beta}\right)_\Gamma + \left(\frac{\partial u}{\partial \tilde{x}^\beta}\right)^-_\Gamma\right) = \left(\frac{dw}{d\tilde{x}^\beta}\right)_\Gamma \quad (4.1.24)$$

or in compact form

$$\left[\frac{\partial u}{\partial \tilde{x}^\alpha}\frac{d\chi}{d\tilde{x}^\beta} + \frac{\partial u}{\partial \tilde{x}^\beta}\right] = \left(\frac{dw}{d\tilde{x}^\beta}\right)_\Gamma . \quad (4.1.25)$$

Since

$$\frac{d\chi}{d\tilde{x}^\beta}(0) = 0, \quad (4.1.26)$$

Eq. (4.1.25) evaluated at the local origin $\tilde{\mathbf{0}}$ is

$$\left[\frac{\partial u}{\partial \tilde{x}^\beta}\right](0) = \left(\frac{dw}{d\tilde{x}^\beta}\right)_\Gamma (0) . \quad (4.1.27)$$

Then we take the derivative of Eq. (4.1.24) with respect to $\tilde{x}^\beta$ to get:

$$\left[\frac{\partial u}{\partial \tilde{x}^\alpha}\frac{d^2\chi}{d\tilde{x}^\beta d\tilde{x}^\beta} + \frac{\partial^2 u}{\partial \tilde{x}^\alpha \partial \tilde{x}^\alpha}\left(\frac{d\chi}{d\tilde{x}^\beta}\right)^2 + 2\frac{\partial^2 u}{\partial \tilde{x}^\alpha \partial \tilde{x}^\beta}\frac{d\chi}{d\tilde{x}^\beta} + \frac{\partial^2 u}{\partial \tilde{x}^\beta \partial \tilde{x}^\beta}\right] = \left(\frac{d^2 w}{d\tilde{x}^\beta d\tilde{x}^\beta}\right)_\Gamma \quad (4.1.28)$$

whose value at the local origin $\tilde{\mathbf{0}}$ is

$$\left[\frac{\partial u}{\partial \tilde{x}^{\alpha}} \frac{d^2 \chi}{d\tilde{x}^{\beta} d\tilde{x}^{\beta}} + \frac{\partial^2 u}{\partial \tilde{x}^{\beta} \partial \tilde{x}^{\beta}}\right](0) = \left(\frac{d^2 w}{d\tilde{x}^{\beta} d\tilde{x}^{\beta}}\right)_{\Gamma}(0). \tag{4.1.29}$$

For the jump condition $\left[\frac{\partial u}{\partial n}\right]$, we first introduce the following result:

Lemma 4.1.3.

$$\frac{\partial u}{\partial n} = \frac{\partial u}{\partial \tilde{n}}. \tag{4.1.30}$$

Proof.

$$\begin{aligned} \frac{\partial u}{\partial \tilde{n}} &= \frac{\partial u}{\partial \tilde{x}^{k}} \tilde{n}^{k} \\ &= (A)_{k}^{l} \frac{\partial u}{\partial x^{l}} \left(A^{-1}\right)_{j}^{k} n^{j} \\ &= \delta_{lj} \frac{\partial u}{\partial x^{l}} n^{j} = \frac{\partial u}{\partial x^{j}} n^{j} = \frac{\partial u}{\partial n}. \end{aligned} \tag{4.1.31}$$

□

The unit tangential direction is given by

$$\tilde{\boldsymbol{\tau}} = \frac{1}{\sqrt{1 + \left(\frac{d\chi}{d\tilde{x}^{\beta}}\right)^2}} \left(\frac{d\chi}{d\tilde{x}^{\beta}}, 1\right) \tag{4.1.32}$$

and the unit normal direction is

$$\tilde{\boldsymbol{n}} = \frac{1}{\sqrt{1 + \left(\frac{d\chi}{d\tilde{x}^{\beta}}\right)^2}} \left(1, -\frac{d\chi}{d\tilde{x}^{\beta}}\right). \tag{4.1.33}$$

Note that

$$\begin{aligned} \frac{\partial u}{\partial \tilde{n}} &= \frac{\partial u}{\partial \tilde{x}^{i}} \tilde{n}^{i} \\ &= \frac{\partial u}{\partial \tilde{x}^{\alpha}} \frac{1}{\sqrt{1 + \left(\frac{d\chi}{d\tilde{x}^{\beta}}\right)^2}} - \frac{\partial u}{\partial \tilde{x}^{\beta}} \frac{1}{\sqrt{1 + \left(\frac{d\chi}{d\tilde{x}^{\beta}}\right)^2}} \frac{d\chi}{d\tilde{x}^{\beta}}. \end{aligned} \tag{4.1.34}$$

So from Lemma 4.1.3 and Eq. (4.1.23) we have

$$\left[\frac{\partial u}{\partial \tilde{x}^{\alpha}} \frac{1}{\sqrt{1 + \left(\frac{d\chi}{d\tilde{x}^{\beta}}\right)^2}} - \frac{\partial u}{\partial \tilde{x}^{\beta}} \frac{1}{\sqrt{1 + \left(\frac{d\chi}{d\tilde{x}^{\beta}}\right)^2}} \frac{d\chi}{d\tilde{x}^{\beta}}\right] = v_{\Gamma} \tag{4.1.35}$$

whose value at the local origin $\tilde{\mathbf{0}}$ is

$$\left[\frac{\partial u}{\partial \tilde{x}^{\alpha}}\right](0) = v_{\Gamma}(0)\,. \tag{4.1.36}$$

We can take the derivative of Eq. (4.1.23) or Eq. (4.1.35) with respect to $\tilde{x}^{\beta}$ to get

$$\Bigg[\frac{1}{\sqrt{1+\left(\frac{d\chi}{d\tilde{x}^{\beta}}\right)^{2}}}\left(\frac{\partial^2 u}{\partial \tilde{x}^{\alpha}\partial \tilde{x}^{\alpha}}\frac{d\chi}{d\tilde{x}^{\beta}} + \left(1-\left(\frac{d\chi}{d\tilde{x}^{\beta}}\right)^{2}\right)\frac{\partial^2 u}{\partial \tilde{x}^{\alpha}\partial \tilde{x}^{\beta}} - \frac{\partial^2 u}{\partial \tilde{x}^{\beta}\partial \tilde{x}^{\beta}}\frac{d\chi}{d\tilde{x}^{\beta}} - \frac{\partial u}{\partial \tilde{x}^{\beta}}\frac{d^2\chi}{d\tilde{x}^{\beta}d\tilde{x}^{\beta}}\right)$$
$$-\frac{1}{\left(1+\left(\frac{d\chi}{d\tilde{x}^{\beta}}\right)^{2}\right)^{3/2}}\frac{d\chi}{d\tilde{x}^{\beta}}\frac{d^2\chi}{d\tilde{x}^{\beta}d\tilde{x}^{\beta}}\left(\frac{\partial u}{\partial \tilde{x}^{\alpha}} - \frac{\partial u}{\partial \tilde{x}^{\beta}}\frac{d\chi}{d\tilde{x}^{\beta}}\right)\Bigg] = \left(\frac{dv}{d\tilde{x}^{\beta}}\right)_{\Gamma} \tag{4.1.37}$$

whose value at the local origin $\tilde{\mathbf{0}}$ is simplified as

$$\left[\frac{\partial^2 u}{\partial \tilde{x}^{\alpha}\partial \tilde{x}^{\beta}} - \frac{\partial u}{\partial \tilde{x}^{\beta}}\frac{d^2\chi}{d\tilde{x}^{\beta}d\tilde{x}^{\beta}}\right](0) = \left(\frac{dv}{d\tilde{x}^{\beta}}\right)_{\Gamma}(0)\,. \tag{4.1.38}$$

To summarize, at the local origin $\tilde{\mathbf{0}}$, we have the following six jump conditions from Eqs. (4.1.22, 4.1.27, 4.1.29, 4.1.36, 4.1.38) and Lemma 4.1.1:

$$[u](0) = w_{\Gamma}(0)\,, \tag{4.1.39}$$

$$\left[\frac{\partial u}{\partial \tilde{x}^{\beta}}\right](0) = \left(\frac{dw}{d\tilde{x}^{\beta}}\right)_{\Gamma}(0)\,, \tag{4.1.40}$$

$$\left[\frac{\partial u}{\partial \tilde{x}^{\alpha}}\frac{d^2\chi}{d\tilde{x}^{\beta}d\tilde{x}^{\beta}} + \frac{\partial^2 u}{\partial \tilde{x}^{\beta}\partial \tilde{x}^{\beta}}\right](0) = \left(\frac{d^2 w}{d\tilde{x}^{\beta}d\tilde{x}^{\beta}}\right)_{\Gamma}(0)\,, \tag{4.1.41}$$

$$\left[\frac{\partial u}{\partial \tilde{x}^{\alpha}}\right](0) = v_{\Gamma}(0)\,, \tag{4.1.42}$$

$$\left[\frac{\partial^2 u}{\partial \tilde{x}^{\alpha}\partial \tilde{x}^{\beta}} - \frac{\partial u}{\partial \tilde{x}^{\beta}}\frac{d^2\chi}{d\tilde{x}^{\beta}d\tilde{x}^{\beta}}\right](0) = \left(\frac{dv}{d\tilde{x}^{\beta}}\right)_{\Gamma}(0)\,, \tag{4.1.43}$$

$$\left[\frac{\partial^2 u}{\partial \tilde{x}^{\alpha}\partial \tilde{x}^{\alpha}} + \frac{\partial^2 u}{\partial \tilde{x}^{\beta}\partial \tilde{x}^{\beta}} + \lambda u + f\right](0) = 0. \tag{4.1.44}$$

Lemma 4.1.4.

$$[\lambda u] = u_{\Gamma}^{-}[\lambda] + \lambda_{\Gamma}^{+}[u]\,. \tag{4.1.45}$$

Proof.

$$\begin{aligned} u_\Gamma^- [\lambda] + \lambda_\Gamma^+ [u] &= u_\Gamma^- \left(\lambda_\Gamma^+ - \lambda_\Gamma^-\right) + \lambda_\Gamma^+ \left(u_\Gamma^+ - u_\Gamma^-\right) \\ &= \lambda_\Gamma^+ u_\Gamma^+ - \lambda_\Gamma^- u_\Gamma^- \\ &= [\lambda u] . \end{aligned} \tag{4.1.46}$$

□

Using algebraic manipulations and Lemma 4.1.4, we can decouple the six jump conditions (4.1.39 - 4.1.44) to get:

$$[u](0) = w_\Gamma(0), \tag{4.1.47}$$

$$\left[\frac{\partial u}{\partial \tilde{x}^\alpha}\right](0) = v_\Gamma(0), \tag{4.1.48}$$

$$\left[\frac{\partial u}{\partial \tilde{x}^\beta}\right](0) = \left(\frac{dw}{d\tilde{x}^\beta}\right)_\Gamma (0), \tag{4.1.49}$$

$$\begin{aligned} \left[\frac{\partial^2 u}{\partial \tilde{x}^\alpha \partial \tilde{x}^\alpha}\right](0) &= -\left(\frac{d^2 w}{d\tilde{x}^\beta d\tilde{x}^\beta}\right)_\Gamma (0) + v_\Gamma(0) \left(\frac{d^2 \chi}{d\tilde{x}^\beta d\tilde{x}^\beta}\right)_\Gamma (0) \\ &\quad - u_\Gamma^-(0)[\lambda](0) - \lambda_\Gamma^+(0) w_\Gamma(0) - [f](0) \\ &= -\left(\frac{d^2 w}{d\tilde{x}^\beta d\tilde{x}^\beta}\right)_\Gamma (0) + v_\Gamma(0) \left(\frac{d^2 \chi}{d\tilde{x}^\beta d\tilde{x}^\beta}\right)_\Gamma (0) \\ &\quad - \left(u_\Gamma^+(0) - w_\Gamma(0)\right)[\lambda](0) - \lambda_\Gamma^+(0) w_\Gamma(0) - [f](0), \end{aligned} \tag{4.1.50}$$

$$\left[\frac{\partial^2 u}{\partial \tilde{x}^\beta \partial \tilde{x}^\beta}\right](0) = \left(\frac{d^2 w}{d\tilde{x}^\beta d\tilde{x}^\beta}\right)_\Gamma (0) - v_\Gamma(0) \left(\frac{d^2 \chi}{d\tilde{x}^\beta d\tilde{x}^\beta}\right)_\Gamma (0), \tag{4.1.51}$$

$$\left[\frac{\partial^2 u}{\partial \tilde{x}^\alpha \partial \tilde{x}^\beta}\right](0) = \left(\frac{dw}{d\tilde{x}^\beta}\right)_\Gamma (0) \frac{d^2 \chi}{d\tilde{x}^\beta d\tilde{x}^\beta}(0) + \left(\frac{dv}{d\tilde{x}^\beta}\right)_\Gamma (0). \tag{4.1.52}$$

Using the decoupled jump conditions (4.1.47 - 4.1.52), Eq. (4.1.21) becomes

$$\begin{aligned}
u^-_{i,j-1} &= u^+_\Gamma(0) - w_\Gamma(0) + \tilde{x}^\alpha_{i,j-1}\left(\frac{\partial u}{\partial \tilde{x}^\alpha}\right)^+_\Gamma(0) - \tilde{x}^\alpha_{i,j-1} v_\Gamma(0) + \tilde{x}^\beta_{i,j-1}\left(\frac{\partial u}{\partial \tilde{x}^\beta}\right)^+_\Gamma(0) \\
&\quad - \tilde{x}^\beta_{i,j-1}\left(\frac{dw}{d\tilde{x}^\beta}\right)_\Gamma(0) + \frac{1}{2}\left(\tilde{x}^\alpha_{i,j-1}\right)^2\left(\frac{\partial^2 u}{\partial \tilde{x}^\alpha \partial \tilde{x}^\alpha}\right)^+_\Gamma(0) - \frac{1}{2}\left(\tilde{x}^\alpha_{i,j-1}\right)^2\left(-\left(\frac{d^2 w}{d\tilde{x}^\beta d\tilde{x}^\beta}\right)_\Gamma(0)\right. \\
&\quad \left. + v_\Gamma(0)\left(\frac{d^2\chi}{d\tilde{x}^\beta d\tilde{x}^\beta}\right)_\Gamma(0) - \left(u^+_\Gamma(0) - w_\Gamma(0)\right)[\lambda](0) - \lambda^+_\Gamma(0)\, w_\Gamma(0) - [f](0)\right) \\
&\quad + \tilde{x}^\alpha_{i,j-1}\tilde{x}^\beta_{i,j-1}\left(\frac{\partial^2 u}{\partial \tilde{x}^\alpha \partial \tilde{x}^\beta}\right)^+_\Gamma(0) - \tilde{x}^\alpha_{i,j-1}\tilde{x}^\beta_{i,j-1}\left(\left(\frac{dw}{d\tilde{x}^\beta}\right)_\Gamma(0)\frac{d^2\chi}{d\tilde{x}^\beta d\tilde{x}^\beta}(0) + \left(\frac{dv}{d\tilde{x}^\beta}\right)_\Gamma(0)\right) \\
&\quad + \frac{1}{2}\left(\tilde{x}^\beta_{i,j-1}\right)^2\left(\frac{\partial^2 u}{\partial \tilde{x}^\beta \partial \tilde{x}^\beta}\right)^+_\Gamma(0) - \frac{1}{2}\left(\tilde{x}^\beta_{i,j-1}\right)^2\left(\left(\frac{d^2 w}{d\tilde{x}^\beta d\tilde{x}^\beta}\right)_\Gamma(0) - v_\Gamma(0)\left(\frac{d^2\chi}{d\tilde{x}^\beta d\tilde{x}^\beta}\right)_\Gamma(0)\right) \\
&\quad + O(h^3).
\end{aligned} \tag{4.1.53}$$

We can collect terms related to jump conditions in Eq. (4.1.53) to get

$$\begin{aligned}
u^-_{i,j-1} &= u^+_\Gamma(0) + \tilde{x}^\alpha_{i,j-1}\left(\frac{\partial u}{\partial \tilde{x}^\alpha}\right)^+_\Gamma(0) + \tilde{x}^\beta_{i,j-1}\left(\frac{\partial u}{\partial \tilde{x}^\beta}\right)^+_\Gamma(0) + \frac{1}{2}\left(\tilde{x}^\alpha_{i,j-1}\right)^2\left(\frac{\partial^2 u}{\partial \tilde{x}^\alpha \partial \tilde{x}^\alpha}\right)^+_\Gamma(0) \\
&\quad + \tilde{x}^\alpha_{i,j-1}\tilde{x}^\beta_{i,j-1}\left(\frac{\partial^2 u}{\partial \tilde{x}^\alpha \partial \tilde{x}^\beta}\right)^+_\Gamma(0) + \frac{1}{2}\left(\tilde{x}^\beta_{i,j-1}\right)^2\left(\frac{\partial^2 u}{\partial \tilde{x}^\beta \partial \tilde{x}^\beta}\right)^+_\Gamma(0) \\
&\quad - \left(w_\Gamma(0) + \tilde{x}^\alpha_{i,j-1} v_\Gamma(0) + \tilde{x}^\beta_{i,j-1}\left(\frac{dw}{d\tilde{x}^\beta}\right)_\Gamma(0) + \frac{1}{2}\left(\tilde{x}^\alpha_{i,j-1}\right)^2\left(-\left(\frac{d^2 w}{d\tilde{x}^\beta d\tilde{x}^\beta}\right)_\Gamma(0)\right.\right. \\
&\quad \left. + v_\Gamma(0)\left(\frac{d^2\chi}{d\tilde{x}^\beta d\tilde{x}^\beta}\right)_\Gamma(0) - \left(u^+_\Gamma(0) - w_\Gamma(0)\right)[\lambda](0) - \lambda^+_\Gamma(0)\, w_\Gamma(0) - [f](0)\right) \\
&\quad + \tilde{x}^\alpha_{i,j-1}\tilde{x}^\beta_{i,j-1}\left(\left(\frac{dw}{d\tilde{x}^\beta}\right)_\Gamma(0)\frac{d^2\chi}{d\tilde{x}^\beta d\tilde{x}^\beta}(0) + \left(\frac{dv}{d\tilde{x}^\beta}\right)_\Gamma(0)\right) \\
&\quad \left. + \frac{1}{2}\left(\tilde{x}^\beta_{i,j-1}\right)^2\left(\left(\frac{d^2 w}{d\tilde{x}^\beta d\tilde{x}^\beta}\right)_\Gamma(0) - v_\Gamma(0)\left(\frac{d^2\chi}{d\tilde{x}^\beta d\tilde{x}^\beta}\right)_\Gamma(0)\right)\right) \\
&\quad + O(h^3).
\end{aligned} \tag{4.1.54}$$

Lemma 4.1.5.

$$\tilde{x}^k_{i,j-1} + \tilde{x}^k_{i,j+1} + \tilde{x}^k_{i-1,j} + \tilde{x}^k_{i+1,j} - 4\tilde{x}^k_{i,j} = 0, \quad k = \alpha, \beta. \tag{4.1.55}$$

Proof.

$$\begin{aligned}
\tilde{x}^k_{i,j-1} &= \left(A^{-1}\right)^k_\alpha\left(x^\alpha_i - x^\alpha_*\right) + \left(A^{-1}\right)^k_\beta\left(x^\beta_{j-1} - x^\beta_*\right) \\
&= \left(A^{-1}\right)^k_\alpha\left(x^\alpha_i - x^\alpha_*\right) + \left(A^{-1}\right)^k_\beta\left(x^\beta_j - h - x^\beta_*\right).
\end{aligned} \tag{4.1.56}$$

So

$$
\begin{aligned}
&\tilde{x}^k_{i,j-1} + \tilde{x}^k_{i,j+1} + \tilde{x}^k_{i-1,j} + \tilde{x}^k_{i+1,j} - 4\tilde{x}^k_{i,j} \\
=& \left(A^{-1}\right)^k_\alpha \left(x^\alpha_i - x^\alpha_* + x^\alpha_i - x^\alpha_* + x^\alpha_i - h - x^\alpha_* + x^\alpha_i + h - x^\alpha_* - 4\left(x^\alpha_i - x^\alpha_*\right)\right) \\
&+ \left(A^{-1}\right)^k_\beta \left(x^\beta_j - h - x^\beta_* + x^\beta_j + h - x^\beta_* + x^\beta_j - x^\beta_* + x^\beta_j - x^\beta_* - 4\left(x^\beta_j - x^\beta_*\right)\right) \\
=& 0.
\end{aligned}
\tag{4.1.57}
$$

□

Lemma 4.1.6.

$$
\left(\tilde{x}^k_{i,j-1}\right)^2 + \left(\tilde{x}^k_{i,j+1}\right)^2 + \left(\tilde{x}^k_{i-1,j}\right)^2 + \left(\tilde{x}^k_{i+1,j}\right)^2 - 4\left(\tilde{x}^k_{i,j}\right)^2 = 2h^2, \quad k = \alpha, \beta. \tag{4.1.58}
$$

Proof.

$$
\begin{aligned}
\left(\tilde{x}^k_{i,j-1}\right)^2 =& \left(\left(A^{-1}\right)^k_\alpha\right)^2 \left(x^\alpha_i - x^\alpha_*\right)^2 + \left(\left(A^{-1}\right)^k_\beta\right)^2 \left(x^\beta_j - x^\beta_*\right)^2 \\
&+ 2\left(A^{-1}\right)^k_\alpha \left(A^{-1}\right)^k_\beta \left(x^\alpha_i - x^\alpha_*\right)\left(x^\beta_j - x^\beta_*\right) - 2\left(\left(A^{-1}\right)^k_\beta\right)^2 h \left(x^\beta_j - x^\beta_*\right) \\
&+ \left(\left(A^{-1}\right)^k_\beta\right)^2 h^2 - 2\left(A^{-1}\right)^k_\alpha \left(A^{-1}\right)^k_\beta \left(x^\alpha_i - x^\alpha_*\right) h \\
=& \left(\tilde{x}^k_{i,j}\right)^2 - 2\left(\left(A^{-1}\right)^k_\beta\right)^2 h \left(x^\beta_j - x^\beta_*\right) + \left(\left(A^{-1}\right)^k_\beta\right)^2 h^2 \\
&- 2\left(A^{-1}\right)^k_\alpha \left(A^{-1}\right)^k_\beta \left(x^\alpha_i - x^\alpha_*\right) h.
\end{aligned}
\tag{4.1.59}
$$

So

$$
\left(\tilde{x}^k_{i,j-1}\right)^2 + \left(\tilde{x}^k_{i,j+1}\right)^2 = 2\left(\tilde{x}^k_{i,j}\right)^2 + 2\left(\left(A^{-1}\right)^k_\beta\right)^2 h^2. \tag{4.1.60}
$$

Similarly,

$$
\left(\tilde{x}^k_{i-1,j}\right)^2 + \left(\tilde{x}^k_{i+1,j}\right)^2 = 2\left(\tilde{x}^k_{i,j}\right)^2 + 2\left(\left(A^{-1}\right)^k_\alpha\right)^2 h^2. \tag{4.1.61}
$$

Finally,

$$
\begin{aligned}
&\left(\tilde{x}^k_{i,j-1}\right)^2 + \left(\tilde{x}^k_{i,j+1}\right)^2 + \left(\tilde{x}^k_{i-1,j}\right)^2 + \left(\tilde{x}^k_{i+1,j}\right)^2 - 4\left(\tilde{x}^k_{i,j}\right)^2 \\
&= 2\left(\left(A^{-1}\right)^k_\beta\right)^2 h^2 + 2\left(\left(A^{-1}\right)^k_\alpha\right)^2 h^2 \\
&= 2h^2.
\end{aligned}
\tag{4.1.62}
$$

□

Lemma 4.1.7.

$$
\tilde{x}^\alpha_{i,j-1}\tilde{x}^\beta_{i,j-1} + \tilde{x}^\alpha_{i,j+1}\tilde{x}^\beta_{i,j+1} + \tilde{x}^\alpha_{i-1,j}\tilde{x}^\beta_{i-1,j} + \tilde{x}^\alpha_{i+1,j}\tilde{x}^\beta_{i+1,j} - 4\tilde{x}^\alpha_{i,j}\tilde{x}^\beta_{i,j} = 0. \tag{4.1.63}
$$

Proof.

$$\tilde{x}^{\alpha}_{i,j-1}\tilde{x}^{\beta}_{i,j-1} = \tilde{x}^{\alpha}_{i,j}\tilde{x}^{\beta}_{i,j} - \left(A^{-1}\right)^{\beta}_{\beta} h\tilde{x}^{\alpha}_{i,j} - \left(A^{-1}\right)^{\alpha}_{\beta} h\tilde{x}^{\beta}_{i,j} + \left(A^{-1}\right)^{\alpha}_{\beta}\left(A^{-1}\right)^{\beta}_{\beta} h^2. \tag{4.1.64}$$

So

$$\tilde{x}^{\alpha}_{i,j-1}\tilde{x}^{\beta}_{i,j-1} + \tilde{x}^{\alpha}_{i,j+1}\tilde{x}^{\beta}_{i,j+1} = 2\tilde{x}^{\alpha}_{i,j}\tilde{x}^{\beta}_{i,j} + 2\left(A^{-1}\right)^{\alpha}_{\beta}\left(A^{-1}\right)^{\beta}_{\beta} h^2. \tag{4.1.65}$$

Similarly,

$$\tilde{x}^{\alpha}_{i-1,j}\tilde{x}^{\beta}_{i-1,j} + \tilde{x}^{\alpha}_{i+1,j}\tilde{x}^{\beta}_{i+1,j} = 2\tilde{x}^{\alpha}_{i,j}\tilde{x}^{\beta}_{i,j} + 2\left(A^{-1}\right)^{\alpha}_{\alpha}\left(A^{-1}\right)^{\beta}_{\alpha} h^2. \tag{4.1.66}$$

Finally,

$$\begin{aligned}
&\tilde{x}^{\alpha}_{i,j-1}\tilde{x}^{\beta}_{i,j-1} + \tilde{x}^{\alpha}_{i,j+1}\tilde{x}^{\beta}_{i,j+1} + \tilde{x}^{\alpha}_{i-1,j}\tilde{x}^{\beta}_{i-1,j} + \tilde{x}^{\alpha}_{i+1,j}\tilde{x}^{\beta}_{i+1,j} - 4\tilde{x}^{\alpha}_{i,j}\tilde{x}^{\beta}_{i,j}\\
&= 2\left(A^{-1}\right)^{\alpha}_{\alpha}\left(A^{-1}\right)^{\beta}_{\alpha} h^2 + 2\left(A^{-1}\right)^{\alpha}_{\beta}\left(A^{-1}\right)^{\beta}_{\beta} h^2\\
&= 0.
\end{aligned} \tag{4.1.67}$$

□

By expanding $u^{-}_{i,j-1}, u^{+}_{i,j+1}, u^{+}_{i-1,j}, u^{+}_{i+1,j}, u^{+}_{i,j}$ and $\lambda^{+}, f^{+}_{i,j}$ in a Taylor series about the local origin $\tilde{\mathbf{0}}$ and applying Lemma 4.1.5 - 4.1.7, the truncation error (4.1.19) is found to be

$$\begin{aligned}
T &= \left(\frac{\partial^2 u}{\partial\tilde{x}^{\alpha}\partial\tilde{x}^{\alpha}}\right)^{+}_{\Gamma}(0) + \left(\frac{\partial^2 u}{\partial\tilde{x}^{\beta}\partial\tilde{x}^{\beta}}\right)^{+}_{\Gamma}(0) + \left(\frac{\left(\tilde{x}^{\alpha}_{i,j-1}\right)^2}{2h^2}[\lambda](0) + \lambda^{+}_{\Gamma}(0)\right)u^{+}_{\Gamma}(0)\\
&\quad + f^{+}_{\Gamma}(0) + C^{+} + O(h)\\
&= \frac{\left(\tilde{x}^{\alpha}_{i,j-1}\right)^2}{2h^2}[\lambda](0)\,u^{+}_{\Gamma}(0) + C^{+} + O(h)\\
&= C^{+} + O(h) \quad (\text{if } [\lambda] = 0)
\end{aligned} \tag{4.1.68}$$

where

$$\begin{aligned}
C^{+} = &-\frac{1}{h^2}\left(w_{\Gamma}(0) + \tilde{x}^{\alpha}_{i,j-1}v_{\Gamma}(0) + \tilde{x}^{\beta}_{i,j-1}\left(\frac{dw}{d\tilde{x}^{\beta}}\right)_{\Gamma}(0) + \frac{1}{2}\left(\tilde{x}^{\alpha}_{i,j-1}\right)^2\left(-\left(\frac{d^2 w}{d\tilde{x}^{\beta}d\tilde{x}^{\beta}}\right)_{\Gamma}(0)\right.\right.\\
&+v_{\Gamma}(0)\left(\frac{d^2\chi}{d\tilde{x}^{\beta}d\tilde{x}^{\beta}}\right)_{\Gamma}(0) + w_{\Gamma}(0)[\lambda](0) - \lambda^{+}_{\Gamma}(0)\,w_{\Gamma}(0) - [f](0)\Bigg)\\
&+\tilde{x}^{\alpha}_{i,j-1}\tilde{x}^{\beta}_{i,j-1}\left(\left(\frac{dw}{d\tilde{x}^{\beta}}\right)_{\Gamma}(0)\frac{d^2\chi}{d\tilde{x}^{\beta}d\tilde{x}^{\beta}}(0) + \left(\frac{dv}{d\tilde{x}^{\beta}}\right)_{\Gamma}(0)\right)\\
&\left.+\frac{1}{2}\left(\tilde{x}^{\beta}_{i,j-1}\right)^2\left(\left(\frac{d^2 w}{d\tilde{x}^{\beta}d\tilde{x}^{\beta}}\right)_{\Gamma}(0) - v_{\Gamma}(0)\left(\frac{d^2\chi}{d\tilde{x}^{\beta}d\tilde{x}^{\beta}}\right)_{\Gamma}(0)\right)\right).
\end{aligned} \tag{4.1.69}$$

If $-C^{+}$ is added to the difference scheme (4.1.10) at the irregular outer grid point $\left(x_i^{\alpha}, x_j^{\beta}\right)$, the truncation error $T = O(h)$. The consistency of the discretization is guaranteed. It is also clear that $-C^{+}$ needs to be added for each stencil point $\notin \Omega^{+}$.

For an irregular grid point $\left(x_i^{\alpha}, x_j^{\beta}\right) \in \Omega^{-}$ with only $\left(x_i^{\alpha}, x_{j-1}^{\beta}\right) \in \Omega^{+}$, following the same steps we can show that

$$
\begin{aligned}
T = & \left(\frac{\partial^2 u}{\partial \tilde{x}^{\alpha} \partial \tilde{x}^{\alpha}}\right)_{\Gamma}^{-}(0) + \left(\frac{\partial^2 u}{\partial \tilde{x}^{\beta} \partial \tilde{x}^{\beta}}\right)_{\Gamma}^{-}(0) + \left(-\frac{\left(\tilde{x}_{i,j-1}^{\alpha}\right)^2}{2h^2}[\lambda](0) + \lambda_{\Gamma}^{-}(0)\right) u_{\Gamma}^{-}(0) \\
& + f_{\Gamma}^{-}(0) + C^{-} + O(h) \\
= & -\frac{\left(\tilde{x}_{i,j-1}^{\alpha}\right)^2}{2h^2}[\lambda](0)\, u_{\Gamma}^{-}(0) + C^{-} + O(h) \\
= & \; C^{-} + O(h) \quad (\text{if } [\lambda] = 0)
\end{aligned}
\tag{4.1.70}
$$

where

$$
\begin{aligned}
C^{-} = & \frac{1}{h^2}\left(w_{\Gamma}(0) + \tilde{x}_{i,j-1}^{\alpha} v_{\Gamma}(0) + \tilde{x}_{i,j-1}^{\beta}\left(\frac{dw}{d\tilde{x}^{\beta}}\right)_{\Gamma}(0) + \frac{1}{2}\left(\tilde{x}_{i,j-1}^{\alpha}\right)^2\left(-\left(\frac{d^2 w}{d\tilde{x}^{\beta} d\tilde{x}^{\beta}}\right)_{\Gamma}(0)\right.\right. \\
& \left. + v_{\Gamma}(0)\left(\frac{d^2 \chi}{d\tilde{x}^{\beta} d\tilde{x}^{\beta}}\right)_{\Gamma}(0) - \lambda_{\Gamma}^{+}(0)\, w_{\Gamma}(0) - [f](0)\right) \\
& + \tilde{x}_{i,j-1}^{\alpha} \tilde{x}_{i,j-1}^{\beta}\left(\left(\frac{dw}{d\tilde{x}^{\beta}}\right)_{\Gamma}(0)\, \frac{d^2 \chi}{d\tilde{x}^{\beta} d\tilde{x}^{\beta}}(0) + \left(\frac{dv}{d\tilde{x}^{\beta}}\right)_{\Gamma}(0)\right) \\
& \left. + \frac{1}{2}\left(\tilde{x}_{i,j-1}^{\beta}\right)^2\left(\left(\frac{d^2 w}{d\tilde{x}^{\beta} d\tilde{x}^{\beta}}\right)_{\Gamma}(0) - v_{\Gamma}(0)\left(\frac{d^2 \chi}{d\tilde{x}^{\beta} d\tilde{x}^{\beta}}\right)_{\Gamma}(0)\right)\right).
\end{aligned}
\tag{4.1.71}
$$

If $-C^{-}$ is added to the difference scheme (4.1.10) at the irregular inner grid point $\left(x_i^{\alpha}, x_j^{\beta}\right)$, the truncation error $T = O(h)$. The consistency of the discretization is guaranteed. It is also clear that $-C^{-}$ needs to be added for each stencil point $\notin \Omega^{-}$. Note that without the $\frac{1}{2}\left(\tilde{x}_{i,j-1}^{\alpha}\right)^2 \frac{w_{\Gamma}(0)[\lambda](0)}{h^2}$ term (which is the case if $[\lambda] = 0$), $C^{+} = -C^{-}$.

To summarize, for the 2D elliptic equation (4.1.1) with an interface Γ and λ being a constant, the consistent finite difference scheme is [24]

$$
\frac{U_{i,j-1} + U_{i,j+1} + U_{i-1,j} + U_{i+1,j} - 4U_{i,j}}{h^2} + \lambda U_{i,j} + f_{i,j} + C = 0 \tag{4.1.72}
$$

where the correction term C is

$$C = \begin{cases} 0, & (x_i^\alpha, x_j^\beta) \text{ is a regular grid point,} \\ \\ -C^+, & (x_i^\alpha, x_j^\beta) \text{ is an irregular grid point in } \Omega^+, \\ \\ -C^-, & (x_i^\alpha, x_j^\beta) \text{ is an irregular grid point in } \Omega^-. \end{cases} \tag{4.1.73}$$

4.2 3D Geometry

The 3D elliptic equation is

$$\frac{\partial^2 u}{\partial x^\alpha \partial x^\alpha} + \frac{\partial^2 u}{\partial x^\beta \partial x^\beta} + \frac{\partial^2 u}{\partial x^\gamma \partial x^\gamma} + \lambda u + f = 0. \tag{4.2.1}$$

We consider a rectangular prism domain $\Omega = [x_b^\alpha, x_e^\alpha] \times [x_b^\beta, x_e^\beta] \times [x_b^\gamma, x_e^\gamma]$ with a surface interface $\Gamma \subset \Omega$. Γ divides Ω into Ω^+ which is outside the surface and Ω^- which is inside the interface. We require the surface Γ to be a closed orientable surface without singularities. See Fig. 4.5 for examples of admissible surfaces.

(a) (b)

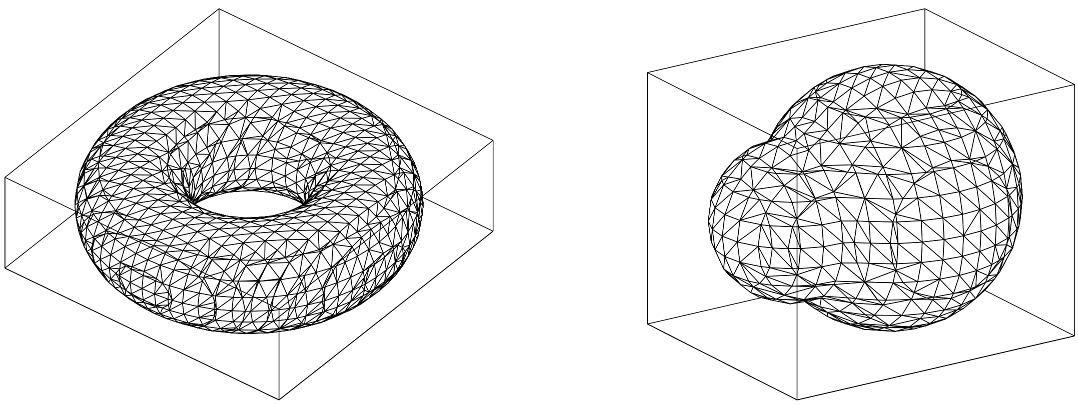

Figure 4.5: The surface Γ needs to be closed and smooth, for example: (a) ring torus (b) union of two intersecting spheroids.

Because u might be discontinuous or non-smooth across the interface Γ, it is more convenient to express u in terms of smooth functions in Ω^+ and Ω^- separately. Namely,

$$u = \begin{cases} u^+, & \boldsymbol{x} \in \Omega^+, \\ u^-, & \boldsymbol{x} \in \Omega^-. \end{cases} \tag{4.2.2}$$

Similar notations are used for other discontinuous or non-smooth quantities. Eq. (4.2.1) now becomes

$$\left(\frac{\partial^2 u}{\partial x^\alpha \partial x^\alpha}\right)^+ + \left(\frac{\partial^2 u}{\partial x^\beta \partial x^\beta}\right)^+ + \left(\frac{\partial^2 u}{\partial x^\gamma \partial x^\gamma}\right)^+ + \lambda^+ u^+ + f^+ = 0, \quad \boldsymbol{x} \in \Omega^+ \tag{4.2.3}$$

and

$$\left(\frac{\partial^2 u}{\partial x^\alpha \partial x^\alpha}\right)^- + \left(\frac{\partial^2 u}{\partial x^\beta \partial x^\beta}\right)^- + \left(\frac{\partial^2 u}{\partial x^\gamma \partial x^\gamma}\right)^- + \lambda^- u^- + f^- = 0, \quad \boldsymbol{x} \in \Omega^-. \tag{4.2.4}$$

We also assume that the following two jump conditions are known:

$$[u] = w, \qquad \left[\frac{\partial u}{\partial n}\right] = v. \tag{4.2.5}$$

Note that we have

$$\left(\frac{\partial^2 u}{\partial x^\alpha \partial x^\alpha}\right)^+ = \frac{\partial^2 u^+}{\partial x^\alpha \partial x^\alpha} \tag{4.2.6}$$

etc. Without loss of generality, we define

$$u(\boldsymbol{x}), \quad \boldsymbol{x} \in \Gamma \tag{4.2.7}$$

as the limit of u on the interface from the side of Ω^+, which may be written as

$$u(\boldsymbol{x}) = u_\Gamma^+, \quad \boldsymbol{x} \in \Gamma. \tag{4.2.8}$$

In other words, $u(\boldsymbol{x})$ is defined to be continuous from the side of Ω^+. The notation u_Γ^- simply means the limit of u on the interface from the side of Ω^-.

The domain Ω is discretized as

$$\begin{aligned}\Omega_h = \Big\{ \Big(x_i^\alpha = x_b^\alpha + ih, x_j^\beta = x_b^\beta + jh, x_l^\gamma = x_b^\gamma + lh \Big) \Big| i = 0, 1, \ldots, m; \\ j = 0, 1, \cdots, n; l = 0, 1, \cdots, s \Big\}\end{aligned} \tag{4.2.9}$$

using a uniform grid width h. A grid point $(x_i^\alpha, x_j^\beta, x_l^\gamma)$, which is on one side of the interface Γ, is called a *regular grid point* if the difference stencil centered at $(x_i^\alpha, x_j^\beta, x_l^\gamma)$ contains no grid points on the other side of the interface. Intuitively, at those majority regular grid points, if we use a finite difference scheme such as the seven-point stencil

$$\frac{U_{i,j,l-1} + U_{i,j,l+1} + U_{i,j-1,l} + U_{i,j+1,l} + U_{i-1,j,l} + U_{i+1,j,l} - 6U_{i,j,l}}{h^2} + \lambda U_{i,j,l} + f_{i,j,l} = 0, \tag{4.2.10}$$

using Taylor expansion at grid point $(x_i^\alpha, x_j^\beta, x_l^\gamma)$, we know that the local truncation error for $(x_i^\alpha, x_j^\beta, x_l^\gamma) \in \Omega^+$ is

$$\begin{aligned}
T &= \frac{u^+_{i,j,l-1} + u^+_{i,j,l+1} + u^+_{i,j-1,l} + u^+_{i,j+1,l} + u^+_{i-1,j,l} + u^+_{i+1,j,l} - 6u^+_{i,j,l}}{h^2} + \lambda^+ u^+_{i,j,l} + f^+_{i,j,l} \\
&= \left(\frac{\partial^2 u}{\partial x^\alpha \partial x^\alpha}\right)^+ (x_i^\alpha, x_j^\beta, x_l^\gamma) + \left(\frac{\partial^2 u}{\partial x^\beta \partial x^\beta}\right)^+ (x_i^\alpha, x_j^\beta, x_l^\gamma) + \left(\frac{\partial^2 u}{\partial x^\gamma \partial x^\gamma}\right)^+ (x_i^\alpha, x_j^\beta, x_l^\gamma) \\
&\quad + \lambda^+ u^+_{i,j,l} + f^+_{i,j,l} + O(h^2) \\
&= O(h^2).
\end{aligned} \tag{4.2.11}$$

The same conclusion holds for regular grid points in Ω^-.

At those minority *irregular grid points* either close to or on the interface Γ, we hope that the same second order scheme still works. To facilitate derivations, we locate an interface point $\boldsymbol{x}_* \in \Gamma$ close to the seven stencil grid points and define a local Cartesian coordinate system $(\tilde{x}^\alpha, \tilde{x}^\beta, \tilde{x}^\gamma)$ centered at $\boldsymbol{x}_*$ as

$$\tilde{x}^i = \left(A^{-1}\right)^i_j \left(x^j - x^j_*\right) \tag{4.2.12}$$

where the coordinate transformation matrix is

$$A = \begin{pmatrix} n^\alpha(\boldsymbol{x}_*) & \tau^\alpha(\boldsymbol{x}_*) & \eta^\alpha(\boldsymbol{x}_*) \\ n^\beta(\boldsymbol{x}_*) & \tau^\beta(\boldsymbol{x}_*) & \eta^\beta(\boldsymbol{x}_*) \\ n^\gamma(\boldsymbol{x}_*) & \tau^\gamma(\boldsymbol{x}_*) & \eta^\gamma(\boldsymbol{x}_*) \end{pmatrix}. \tag{4.2.13}$$

Here $n^i(\boldsymbol{x}_*)$ is the unit normal direction pointing from Ω^- to Ω^+, $\tau^i(\boldsymbol{x}_*)$ and $\eta^i(\boldsymbol{x}_*)$ are two orthogonal unit tangential directions forming a right-handed Cartesian coordinate system together with $n^i(\boldsymbol{x}_*)$. See Fig. 4.6 for an illustration of the change of coordinates.

Lemma 4.2.1.

$$\frac{\partial^2 u}{\partial \tilde{x}^\alpha \partial \tilde{x}^\alpha} + \frac{\partial^2 u}{\partial \tilde{x}^\beta \partial \tilde{x}^\beta} + \frac{\partial^2 u}{\partial \tilde{x}^\gamma \partial \tilde{x}^\gamma} + \lambda u + f = 0. \tag{4.2.14}$$

Proof. Similar to the 2D case; see Lemma 4.1.1. □

Let us consider an irregular grid point $(x_i^\alpha, x_j^\beta, x_l^\gamma) \in \Omega^+$, whose coordinates in the local coordinate system $\left(\tilde{x}^\alpha, \tilde{x}^\beta, \tilde{x}^\gamma\right)$ are denoted as $(\tilde{x}^\alpha_{i,j,l}, \tilde{x}^\beta_{i,j,l}, \tilde{x}^\gamma_{i,j,l})$. Now the truncation error is

$$T = \frac{u_{i,j,l-1} + u_{i,j,l+1} + u_{i,j-1,l} + u_{i,j+1,l} + u_{i-1,j,l} + u_{i+1,j,l} - 6u^+_{i,j,l}}{h^2} + \lambda^+ u^+_{i,j,l} + f^+_{i,j,l}. \tag{4.2.15}$$

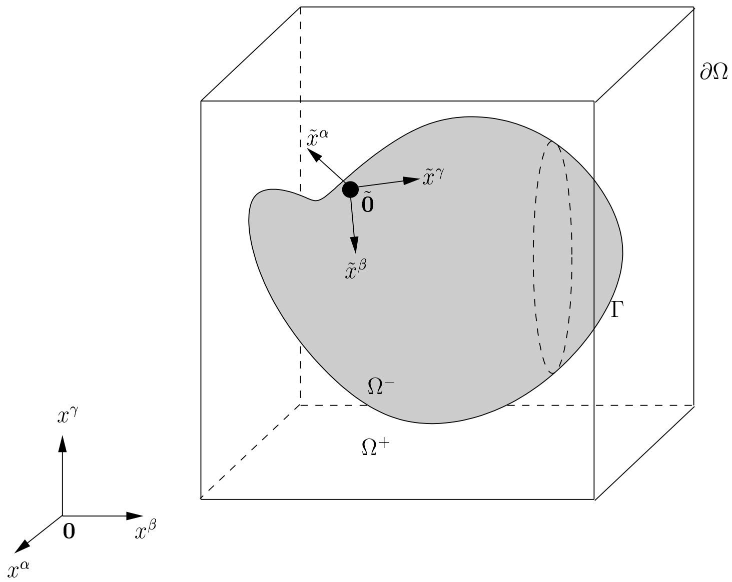

Figure 4.6: Given a point $\boldsymbol{x}_* \in \Gamma$, a local Cartesian coordinate system $\left(\tilde{x}^{\alpha}, \tilde{x}^{\beta}, \tilde{x}^{\gamma}\right)$ is built using $\boldsymbol{x}_*$ as the origin, the unit normal vector $\boldsymbol{n}$ and two unit tangential vectors $\boldsymbol{\tau}$ and $\boldsymbol{\eta}$ at that point as the three coordinate axes in sequence. The normal vector $\boldsymbol{n}$ points from Ω^- to Ω^+. $\boldsymbol{n}$, $\boldsymbol{\tau}$ and $\boldsymbol{\eta}$ form a right-handed Cartesian coordinate system $\left(\tilde{x}^{\alpha}, \tilde{x}^{\beta}, \tilde{x}^{\gamma}\right)$.

For the other six stencil grid points, without loss of generality, we assume that only

$$(\tilde{x}^{\alpha}_{i,j,l-1}, \tilde{x}^{\beta}_{i,j,l-1}, \tilde{x}^{\gamma}_{i,j,l-1}) \in \Omega^-. \tag{4.2.16}$$

See Fig. 4.7 for for an example of the difference stencil at the irregular grid point $\left(x_i^{\alpha}, x_j^{\beta}, x_l^{\gamma}\right)$.

Now it is determined that

$$T = \frac{u^-_{i,j,l-1} + u^+_{i,j,l+1} + u^+_{i,j-1,l} + u^+_{i,j+1,l} + u^+_{i-1,j,l} + u^+_{i+1,j,l} - 6u^+_{i,j,l}}{h^2} + \lambda^+ u^+_{i,j,l} + f^+_{i,j,l}. \tag{4.2.17}$$

Instead of applying Taylor expansion at grid point $(\tilde{x}^{\alpha}_{i,j,l}, \tilde{x}^{\beta}_{i,j,l}, \tilde{x}^{\gamma}_{i,j,l})$, we can expand at the interface point $\boldsymbol{x}_*$, or equivalently the origin $\tilde{\mathbf{0}}$ in the local coordinates $\left(\tilde{x}^{\alpha}, \tilde{x}^{\beta}, \tilde{x}^{\gamma}\right)$. Note that the interface Γ is parameterized in the local coordinates as

$$\Gamma = \left(\chi\left(\tilde{x}^{\beta}, \tilde{x}^{\gamma}\right), \tilde{x}^{\beta}, \tilde{x}^{\gamma}\right) \tag{4.2.18}$$

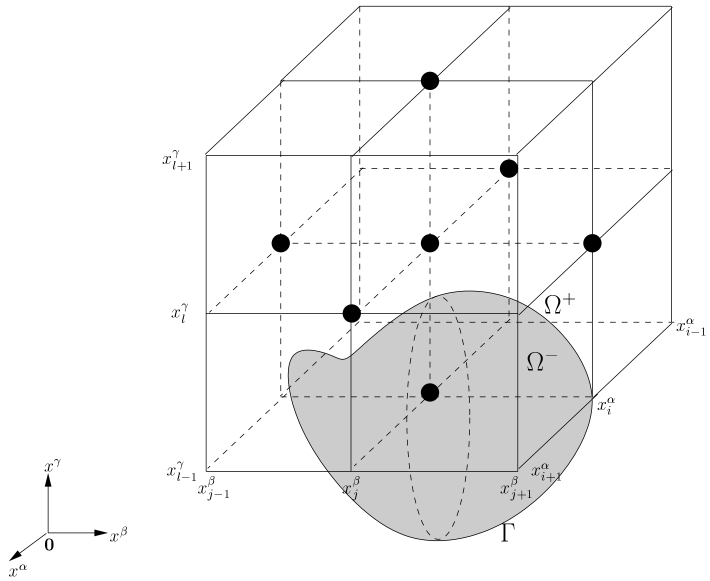

Figure 4.7: An example of the seven-point stencil centered at an irregular grid point $\left(x_i^{\alpha}, x_j^{\beta}, x_l^{\gamma}\right) \in \Omega^+$ with only $\left(x_i^{\alpha}, x_j^{\beta}, x_{l-1}^{\gamma}\right) \in \Omega^-$.

and the limit on the interface for a 3D function from the side of either Ω^+ or Ω^- is parameterized only by $\left(\tilde{x}^{\beta}, \tilde{x}^{\gamma}\right)$. For example,

$$\begin{aligned}
u^-_{i,j,l-1} = u^-_{\Gamma}(0,0) &+ \left(\tilde{x}^{\alpha}_{i,j,l-1}\left(\frac{\partial u}{\partial \tilde{x}^{\alpha}}\right)^-_{\Gamma}(0,0) + \tilde{x}^{\beta}_{i,j,l-1}\left(\frac{\partial u}{\partial \tilde{x}^{\beta}}\right)^-_{\Gamma}(0,0) + \tilde{x}^{\gamma}_{i,j,l-1}\left(\frac{\partial u}{\partial \tilde{x}^{\gamma}}\right)^-_{\Gamma}(0,0)\right) \\
&+ \frac{1}{2}\left(\left(\tilde{x}^{\alpha}_{i,j,l-1}\right)^2\left(\frac{\partial^2 u}{\partial \tilde{x}^{\alpha}\partial \tilde{x}^{\alpha}}\right)^-_{\Gamma}(0,0) + \left(\tilde{x}^{\beta}_{i,j,l-1}\right)^2\left(\frac{\partial^2 u}{\partial \tilde{x}^{\beta}\partial \tilde{x}^{\beta}}\right)^-_{\Gamma}(0,0)\right. \\
&+ \left.\left(\tilde{x}^{\gamma}_{i,j,l-1}\right)^2\left(\frac{\partial^2 u}{\partial \tilde{x}^{\gamma}\partial \tilde{x}^{\gamma}}\right)^-_{\Gamma}(0,0)\right) + \left(\tilde{x}^{\alpha}_{i,j,l-1}\tilde{x}^{\beta}_{i,j,l-1}\left(\frac{\partial^2 u}{\partial \tilde{x}^{\alpha}\partial \tilde{x}^{\beta}}\right)^-_{\Gamma}(0,0)\right. \\
&+ \left.\tilde{x}^{\alpha}_{i,j,l-1}\tilde{x}^{\gamma}_{i,j,l-1}\left(\frac{\partial^2 u}{\partial \tilde{x}^{\alpha}\partial \tilde{x}^{\gamma}}\right)^-_{\Gamma}(0,0) + \tilde{x}^{\beta}_{i,j,l-1}\tilde{x}^{\gamma}_{i,j,l-1}\left(\frac{\partial^2 u}{\partial \tilde{x}^{\beta}\partial \tilde{x}^{\gamma}}\right)^-_{\Gamma}(0,0)\right) + O(h^3).
\end{aligned} \tag{4.2.19}$$

See Fig. 4.8 for an example of the Taylor expansion at the local coordinate system.

Note that the jump conditions (4.2.5) locally can be expressed as

$$[u] = w_{\Gamma}(\tilde{x}^{\beta}, \tilde{x}^{\gamma}), \tag{4.2.20}$$

or

$$u^+_{\Gamma}\left(\chi(\tilde{x}^{\beta}, \tilde{x}^{\gamma}), \tilde{x}^{\beta}, \tilde{x}^{\gamma}\right) - u^-_{\Gamma}\left(\chi(\tilde{x}^{\beta}, \tilde{x}^{\gamma}), \tilde{x}^{\beta}, \tilde{x}^{\gamma}\right) = w_{\Gamma}(\tilde{x}^{\beta}, \tilde{x}^{\gamma}); \tag{4.2.21}$$

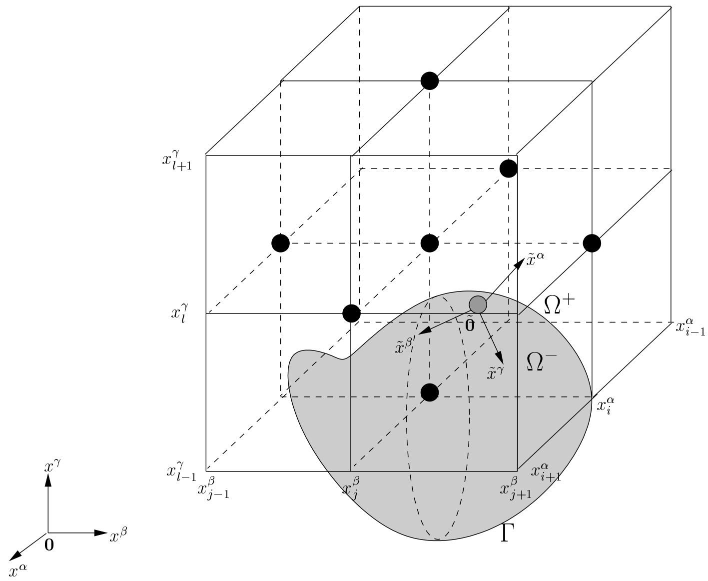

Figure 4.8: An example of the Taylor expansion at the local coordinate system $\left(\tilde{x}^{\alpha}, \tilde{x}^{\beta}, \tilde{x}^{\gamma}\right)$. Note that the local origin must be on the interface Γ and close to the seven stencil grid points.

and

$$\left[\frac{\partial u}{\partial n}\right] = v_{\Gamma}(\tilde{x}^{\beta}, \tilde{x}^{\gamma}), \tag{4.2.22}$$

or

$$\left(\frac{\partial u}{\partial n}\right)^{+}_{\Gamma} \left(\chi(\tilde{x}^{\beta}, \tilde{x}^{\gamma}), \tilde{x}^{\beta}, \tilde{x}^{\gamma}\right) - \left(\frac{\partial u}{\partial n}\right)^{-}_{\Gamma} \left(\chi(\tilde{x}^{\beta}, \tilde{x}^{\gamma}), \tilde{x}^{\beta}, \tilde{x}^{\gamma}\right) = v_{\Gamma}(\tilde{x}^{\beta}, \tilde{x}^{\gamma}). \tag{4.2.23}$$

We can take the derivative of Eq. (4.2.20) with respect to $\tilde{x}^{\beta}$ to get

$$\left(\frac{\partial u}{\partial \tilde{x}^{\alpha}}\right)^{+}_{\Gamma} \left(\frac{\partial \chi}{\partial \tilde{x}^{\beta}}\right)_{\Gamma} + \left(\frac{\partial u}{\partial \tilde{x}^{\beta}}\right)^{+}_{\Gamma} - \left(\left(\frac{\partial u}{\partial \tilde{x}^{\alpha}}\right)^{-}_{\Gamma} \left(\frac{\partial \chi}{\partial \tilde{x}^{\beta}}\right)_{\Gamma} + \left(\frac{\partial u}{\partial \tilde{x}^{\beta}}\right)^{-}_{\Gamma}\right) = \left(\frac{\partial w}{\partial \tilde{x}^{\beta}}\right)_{\Gamma} \tag{4.2.24}$$

or in compact form

$$\left[\frac{\partial u}{\partial \tilde{x}^{\alpha}} \frac{\partial \chi}{\partial \tilde{x}^{\beta}} + \frac{\partial u}{\partial \tilde{x}^{\beta}}\right] = \left(\frac{\partial w}{\partial \tilde{x}^{\beta}}\right)_{\Gamma}. \tag{4.2.25}$$

Since

$$\frac{\partial \chi}{\partial \tilde{x}^{\beta}}(0,0) = 0, \tag{4.2.26}$$

Eq. (4.2.25) evaluated at the local origin $\tilde{\mathbf{0}}$ is

$$\left[\frac{\partial u}{\partial \tilde{x}^{\beta}}\right](0,0) = \left(\frac{\partial w}{\partial \tilde{x}^{\beta}}\right)_{\Gamma}(0,0). \tag{4.2.27}$$

Similarly, we can take the derivative of Eq. (4.2.20) with respect to $\tilde{x}^\gamma$ to get

$$\left[\frac{\partial u}{\partial \tilde{x}^\alpha}\frac{\partial \chi}{\partial \tilde{x}^\gamma}+\frac{\partial u}{\partial \tilde{x}^\gamma}\right]=\left(\frac{\partial w}{\partial \tilde{x}^\gamma}\right)_\Gamma . \tag{4.2.28}$$

Since

$$\frac{\partial \chi}{\partial \tilde{x}^\gamma}(0,0)=0, \tag{4.2.29}$$

Eq. (4.2.28) evaluated at the local origin $\tilde{\mathbf{O}}$ is

$$\left[\frac{\partial u}{\partial \tilde{x}^\gamma}\right](0,0)=\left(\frac{\partial w}{\partial \tilde{x}^\gamma}\right)_\Gamma (0,0)\,. \tag{4.2.30}$$

Then we take the derivative of Eq. (4.2.24) with respect to $\tilde{x}^\beta$ to get

$$\left[\frac{\partial u}{\partial \tilde{x}^\alpha}\frac{\partial^2 \chi}{\partial \tilde{x}^\beta\partial \tilde{x}^\beta}+\frac{\partial^2 u}{\partial \tilde{x}^\alpha\partial \tilde{x}^\alpha}\left(\frac{\partial \chi}{\partial \tilde{x}^\beta}\right)^2+2\frac{\partial^2 u}{\partial \tilde{x}^\alpha\partial \tilde{x}^\beta}\frac{\partial \chi}{\partial \tilde{x}^\beta}+\frac{\partial^2 u}{\partial \tilde{x}^\beta\partial \tilde{x}^\beta}\right]=\left(\frac{\partial^2 w}{\partial \tilde{x}^\beta\partial \tilde{x}^\beta}\right)_\Gamma \tag{4.2.31}$$

whose value at the local origin $\tilde{\mathbf{O}}$ is

$$\left[\frac{\partial u}{\partial \tilde{x}^\alpha}\frac{\partial^2 \chi}{\partial \tilde{x}^\beta\partial \tilde{x}^\beta}+\frac{\partial^2 u}{\partial \tilde{x}^\beta\partial \tilde{x}^\beta}\right](0,0)=\left(\frac{\partial^2 w}{\partial \tilde{x}^\beta\partial \tilde{x}^\beta}\right)_\Gamma (0,0)\,. \tag{4.2.32}$$

Taking the derivative of Eq. (4.2.24) with respect to $\tilde{x}^\gamma$ we get

$$\left[\frac{\partial u}{\partial \tilde{x}^\alpha}\frac{\partial^2 \chi}{\partial \tilde{x}^\beta\partial \tilde{x}^\gamma}+\frac{\partial^2 u}{\partial \tilde{x}^\alpha\partial \tilde{x}^\alpha}\frac{\partial \chi}{\partial \tilde{x}^\beta}\frac{\partial \chi}{\partial \tilde{x}^\gamma}+\frac{\partial^2 u}{\partial \tilde{x}^\alpha\partial \tilde{x}^\gamma}\frac{\partial \chi}{\partial \tilde{x}^\beta}+\frac{\partial^2 u}{\partial \tilde{x}^\alpha\partial \tilde{x}^\beta}\frac{\partial \chi}{\partial \tilde{x}^\gamma}+\frac{\partial^2 u}{\partial \tilde{x}^\beta\partial \tilde{x}^\gamma}\right]=\left(\frac{\partial^2 w}{\partial \tilde{x}^\beta\partial \tilde{x}^\gamma}\right)_\Gamma \tag{4.2.33}$$

whose value at the local origin $\tilde{\mathbf{O}}$ is

$$\left[\frac{\partial u}{\partial \tilde{x}^\alpha}\frac{\partial^2 \chi}{\partial \tilde{x}^\beta\partial \tilde{x}^\gamma}+\frac{\partial^2 u}{\partial \tilde{x}^\beta\partial \tilde{x}^\gamma}\right](0,0)=\left(\frac{\partial^2 w}{\partial \tilde{x}^\beta\partial \tilde{x}^\gamma}\right)_\Gamma (0,0)\,. \tag{4.2.34}$$

Taking the derivative of Eq. (4.2.28) with respect to $\tilde{x}^\gamma$ we get

$$\left[\frac{\partial u}{\partial \tilde{x}^\alpha}\frac{\partial^2 \chi}{\partial \tilde{x}^\gamma\partial \tilde{x}^\gamma}+\frac{\partial^2 u}{\partial \tilde{x}^\alpha\partial \tilde{x}^\alpha}\left(\frac{\partial \chi}{\partial \tilde{x}^\gamma}\right)^2+2\frac{\partial^2 u}{\partial \tilde{x}^\alpha\partial \tilde{x}^\gamma}\frac{\partial \chi}{\partial \tilde{x}^\gamma}+\frac{\partial^2 u}{\partial \tilde{x}^\gamma\partial \tilde{x}^\gamma}\right]=\left(\frac{\partial^2 w}{\partial \tilde{x}^\gamma\partial \tilde{x}^\gamma}\right)_\Gamma \tag{4.2.35}$$

whose value at the local origin $\tilde{\mathbf{O}}$ is

$$\left[\frac{\partial u}{\partial \tilde{x}^\alpha}\frac{\partial^2 \chi}{\partial \tilde{x}^\gamma\partial \tilde{x}^\gamma}+\frac{\partial^2 u}{\partial \tilde{x}^\gamma\partial \tilde{x}^\gamma}\right](0,0)=\left(\frac{\partial^2 w}{\partial \tilde{x}^\gamma\partial \tilde{x}^\gamma}\right)_\Gamma (0,0)\,. \tag{4.2.36}$$

For the jump condition $\left[\frac{\partial u}{\partial n}\right]$, we first introduce the following result:

Lemma 4.2.2.

$$\frac{\partial u}{\partial n} = \frac{\partial u}{\partial \tilde{n}}. \tag{4.2.37}$$

Proof. Same as the 2D case, see Lemma 4.1.3. $\square$

The two unit tangential directions are given by

$$\tilde{\boldsymbol{\tau}} = \frac{1}{\sqrt{1+\left(\frac{\partial \chi}{\partial \tilde{x}^\beta}\right)^2}} \left(\frac{\partial \chi}{\partial \tilde{x}^\beta}, 1, 0\right) \tag{4.2.38}$$

and

$$\tilde{\boldsymbol{\eta}} = \frac{1}{\sqrt{1+\left(\frac{\partial \chi}{\partial \tilde{x}^\gamma}\right)^2}} \left(\frac{\partial \chi}{\partial \tilde{x}^\gamma}, 0, 1\right). \tag{4.2.39}$$

Note that these two tangential directions are orthogonal to each other at the local origin $\tilde{\mathbf{0}}$ and may not be so elsewhere. Since $\|\tilde{\boldsymbol{\tau}} \times \tilde{\boldsymbol{\eta}}\| > 0$, we know that $\tilde{\boldsymbol{\tau}}$ and $\tilde{\boldsymbol{\eta}}$ span the tangent plane. The unit normal direction is

$$\tilde{\boldsymbol{n}} = \frac{\tilde{\boldsymbol{\tau}} \times \tilde{\boldsymbol{\eta}}}{\|\tilde{\boldsymbol{\tau}} \times \tilde{\boldsymbol{\eta}}\|} = \frac{1}{\sqrt{1+\left(\frac{\partial \chi}{\partial \tilde{x}^\beta}\right)^2+\left(\frac{\partial \chi}{\partial \tilde{x}^\gamma}\right)^2}} \left(1, -\frac{\partial \chi}{\partial \tilde{x}^\beta}, -\frac{\partial \chi}{\partial \tilde{x}^\gamma}\right). \tag{4.2.40}$$

Note that

$$\begin{aligned}
\frac{\partial u}{\partial \tilde{n}} &= \frac{\partial u}{\partial \tilde{x}^i}\tilde{n}^i \\
&= \frac{\partial u}{\partial \tilde{x}^\alpha}\frac{1}{\sqrt{1+\left(\frac{\partial \chi}{\partial \tilde{x}^\beta}\right)^2+\left(\frac{\partial \chi}{\partial \tilde{x}^\gamma}\right)^2}} - \frac{\partial u}{\partial \tilde{x}^\beta}\frac{1}{\sqrt{1+\left(\frac{\partial \chi}{\partial \tilde{x}^\beta}\right)^2+\left(\frac{\partial \chi}{\partial \tilde{x}^\gamma}\right)^2}}\frac{\partial \chi}{\partial \tilde{x}^\beta} \\
&- \frac{\partial u}{\partial \tilde{x}^\gamma}\frac{1}{\sqrt{1+\left(\frac{\partial \chi}{\partial \tilde{x}^\beta}\right)^2+\left(\frac{\partial \chi}{\partial \tilde{x}^\gamma}\right)^2}}\frac{\partial \chi}{\partial \tilde{x}^\gamma}.
\end{aligned} \tag{4.2.41}$$

So from Lemma 4.2.2 and Eq. (4.2.22) we have

$$\begin{aligned}
&\left[\frac{\partial u}{\partial \tilde{x}^\alpha}\frac{1}{\sqrt{1+\left(\frac{\partial \chi}{\partial \tilde{x}^\beta}\right)^2+\left(\frac{\partial \chi}{\partial \tilde{x}^\gamma}\right)^2}} - \frac{\partial u}{\partial \tilde{x}^\beta}\frac{1}{\sqrt{1+\left(\frac{\partial \chi}{\partial \tilde{x}^\beta}\right)^2+\left(\frac{\partial \chi}{\partial \tilde{x}^\gamma}\right)^2}}\frac{\partial \chi}{\partial \tilde{x}^\beta}\right. \\
&\left. -\frac{\partial u}{\partial \tilde{x}^\gamma}\frac{1}{\sqrt{1+\left(\frac{\partial \chi}{\partial \tilde{x}^\beta}\right)^2+\left(\frac{\partial \chi}{\partial \tilde{x}^\gamma}\right)^2}}\frac{\partial \chi}{\partial \tilde{x}^\gamma}\right] = v_\Gamma
\end{aligned} \tag{4.2.42}$$

whose value at the local origin $\tilde{\mathbf{0}}$ is

$$\left[\frac{\partial u}{\partial \tilde{x}^{\alpha}}\right](0,0) = v_{\Gamma}\,(0,0)\,. \tag{4.2.43}$$

We can take the derivative of Eq. (4.2.42) with respect to $\tilde{x}^{\beta}$ to get

$$\begin{aligned}
&\Bigg[-\frac{1}{\left(1+\left(\frac{\partial \chi}{\partial \tilde{x}^{\beta}}\right)^{2}+\left(\frac{\partial \chi}{\partial \tilde{x}^{\gamma}}\right)^{2}\right)^{3/2}}\left(\frac{\partial \chi}{\partial \tilde{x}^{\beta}}\frac{\partial^{2} \chi}{\partial \tilde{x}^{\beta}\partial \tilde{x}^{\beta}}+\frac{\partial \chi}{\partial \tilde{x}^{\gamma}}\frac{\partial^{2} \chi}{\partial \tilde{x}^{\beta}\tilde{x}^{\gamma}}\right)\left(\frac{\partial u}{\partial \tilde{x}^{\alpha}}-\frac{\partial u}{\partial \tilde{x}^{\beta}}\frac{\partial \chi}{\partial \tilde{x}^{\beta}}-\frac{\partial u}{\partial \tilde{x}^{\gamma}}\frac{\partial \chi}{\partial \tilde{x}^{\gamma}}\right)\\
&+\frac{1}{\sqrt{1+\left(\frac{\partial \chi}{\partial \tilde{x}^{\beta}}\right)^{2}+\left(\frac{\partial \chi}{\partial \tilde{x}^{\gamma}}\right)^{2}}}\left(\frac{\partial^{2} u}{\partial \tilde{x}^{\alpha}\partial \tilde{x}^{\alpha}}\frac{\partial \chi}{\partial \tilde{x}^{\beta}}+\frac{\partial^{2} u}{\partial \tilde{x}^{\alpha}\partial \tilde{x}^{\beta}}-\left(\frac{\partial^{2} u}{\partial \tilde{x}^{\alpha}\partial \tilde{x}^{\beta}}\frac{\partial \chi}{\partial \tilde{x}^{\beta}}+\frac{\partial^{2} u}{\partial \tilde{x}^{\beta}\partial \tilde{x}^{\beta}}\right)\frac{\partial \chi}{\partial \tilde{x}^{\beta}}\right.\\
&\left.-\frac{\partial u}{\partial \tilde{x}^{\beta}}\frac{\partial^{2} \chi}{\partial \tilde{x}^{\beta}\partial \tilde{x}^{\beta}}-\left(\frac{\partial^{2} u}{\partial \tilde{x}^{\alpha}\partial \tilde{x}^{\gamma}}\frac{\partial \chi}{\partial \tilde{x}^{\beta}}+\frac{\partial^{2} u}{\partial \tilde{x}^{\beta}\partial \tilde{x}^{\gamma}}\right)\frac{\partial \chi}{\partial \tilde{x}^{\gamma}}-\frac{\partial u}{\partial \tilde{x}^{\gamma}}\frac{\partial^{2} \chi}{\partial \tilde{x}^{\beta}\partial \tilde{x}^{\gamma}}\right)\Bigg]=\frac{\partial v_{\Gamma}}{\partial \tilde{x}^{\beta}}
\end{aligned} \tag{4.2.44}$$

whose value at the local origin $\tilde{\mathbf{0}}$ is simplified to

$$\left[\frac{\partial^{2} u}{\partial \tilde{x}^{\alpha}\partial \tilde{x}^{\beta}}-\frac{\partial u}{\partial \tilde{x}^{\beta}}\frac{\partial^{2} \chi}{\partial \tilde{x}^{\beta}\partial \tilde{x}^{\beta}}-\frac{\partial u}{\partial \tilde{x}^{\gamma}}\frac{\partial^{2} \chi}{\partial \tilde{x}^{\beta}\partial \tilde{x}^{\gamma}}\right](0,0)=\frac{\partial v_{\Gamma}}{\partial \tilde{x}^{\beta}}\,(0,0)\,. \tag{4.2.45}$$

Taking the derivative of Eq. (4.2.42) with respect to $\tilde{x}^{\gamma}$ we get

$$\begin{aligned}
&\Bigg[-\frac{1}{\left(1+\left(\frac{\partial \chi}{\partial \tilde{x}^{\beta}}\right)^{2}+\left(\frac{\partial \chi}{\partial \tilde{x}^{\gamma}}\right)^{2}\right)^{3/2}}\left(\frac{\partial \chi}{\partial \tilde{x}^{\beta}}\frac{\partial^{2} \chi}{\partial \tilde{x}^{\beta}\partial \tilde{x}^{\gamma}}+\frac{\partial \chi}{\partial \tilde{x}^{\gamma}}\frac{\partial^{2} \chi}{\partial \tilde{x}^{\gamma}\tilde{x}^{\gamma}}\right)\left(\frac{\partial u}{\partial \tilde{x}^{\alpha}}-\frac{\partial u}{\partial \tilde{x}^{\beta}}\frac{\partial \chi}{\partial \tilde{x}^{\beta}}-\frac{\partial u}{\partial \tilde{x}^{\gamma}}\frac{\partial \chi}{\partial \tilde{x}^{\gamma}}\right)\\
&+\frac{1}{\sqrt{1+\left(\frac{\partial \chi}{\partial \tilde{x}^{\beta}}\right)^{2}+\left(\frac{\partial \chi}{\partial \tilde{x}^{\gamma}}\right)^{2}}}\left(\frac{\partial^{2} u}{\partial \tilde{x}^{\alpha}\partial \tilde{x}^{\alpha}}\frac{\partial \chi}{\partial \tilde{x}^{\gamma}}+\frac{\partial^{2} u}{\partial \tilde{x}^{\alpha}\partial \tilde{x}^{\gamma}}-\left(\frac{\partial^{2} u}{\partial \tilde{x}^{\alpha}\partial \tilde{x}^{\beta}}\frac{\partial \chi}{\partial \tilde{x}^{\gamma}}+\frac{\partial^{2} u}{\partial \tilde{x}^{\beta}\partial \tilde{x}^{\gamma}}\right)\frac{\partial \chi}{\partial \tilde{x}^{\beta}}\right.\\
&\left.-\frac{\partial u}{\partial \tilde{x}^{\beta}}\frac{\partial^{2} \chi}{\partial \tilde{x}^{\beta}\partial \tilde{x}^{\gamma}}-\left(\frac{\partial^{2} u}{\partial \tilde{x}^{\alpha}\partial \tilde{x}^{\gamma}}\frac{\partial \chi}{\partial \tilde{x}^{\gamma}}+\frac{\partial^{2} u}{\partial \tilde{x}^{\gamma}\partial \tilde{x}^{\gamma}}\right)\frac{\partial \chi}{\partial \tilde{x}^{\gamma}}-\frac{\partial u}{\partial \tilde{x}^{\gamma}}\frac{\partial^{2} \chi}{\partial \tilde{x}^{\gamma}\partial \tilde{x}^{\gamma}}\right)\Bigg]=\frac{\partial v_{\Gamma}}{\partial \tilde{x}^{\gamma}}
\end{aligned} \tag{4.2.46}$$

whose value at the local origin $\tilde{\mathbf{0}}$ is simplified to

$$\left[\frac{\partial^{2} u}{\partial \tilde{x}^{\alpha}\partial \tilde{x}^{\gamma}}-\frac{\partial u}{\partial \tilde{x}^{\beta}}\frac{\partial^{2} \chi}{\partial \tilde{x}^{\beta}\partial \tilde{x}^{\gamma}}-\frac{\partial u}{\partial \tilde{x}^{\gamma}}\frac{\partial^{2} \chi}{\partial \tilde{x}^{\gamma}\partial \tilde{x}^{\gamma}}\right](0,0)=\frac{\partial v_{\Gamma}}{\partial \tilde{x}^{\gamma}}\,(0,0)\,. \tag{4.2.47}$$

To summarize, at the local origin $\tilde{\mathbf{0}}$, we have the following ten jump conditions from Lemma 4.2.1 and Eqs. (4.2.20, 4.2.27, 4.2.30, 4.2.32, 4.2.34, 4.2.36, 4.2.43, 4.2.45, 4.2.47):

$$[u]\,(0,0) = w_\Gamma(0,0), \tag{4.2.48}$$

$$\left[\frac{\partial u}{\partial \tilde{x}^\beta}\right](0,0) = \left(\frac{\partial w}{\partial \tilde{x}^\beta}\right)_\Gamma (0,0)\,, \tag{4.2.49}$$

$$\left[\frac{\partial u}{\partial \tilde{x}^\gamma}\right](0,0) = \left(\frac{\partial w}{\partial \tilde{x}^\gamma}\right)_\Gamma (0,0)\,, \tag{4.2.50}$$

$$\left[\frac{\partial u}{\partial \tilde{x}^\alpha}\frac{\partial^2 \chi}{\partial \tilde{x}^\beta \partial \tilde{x}^\beta} + \frac{\partial^2 u}{\partial \tilde{x}^\beta \partial \tilde{x}^\beta}\right](0,0) = \left(\frac{\partial^2 w}{\partial \tilde{x}^\beta \partial \tilde{x}^\beta}\right)_\Gamma (0,0)\,, \tag{4.2.51}$$

$$\left[\frac{\partial u}{\partial \tilde{x}^\alpha}\frac{\partial^2 \chi}{\partial \tilde{x}^\beta \partial \tilde{x}^\gamma} + \frac{\partial^2 u}{\partial \tilde{x}^\beta \partial \tilde{x}^\gamma}\right](0,0) = \left(\frac{\partial^2 w}{\partial \tilde{x}^\beta \partial \tilde{x}^\gamma}\right)_\Gamma (0,0)\,, \tag{4.2.52}$$

$$\left[\frac{\partial u}{\partial \tilde{x}^\alpha}\frac{\partial^2 \chi}{\partial \tilde{x}^\gamma \partial \tilde{x}^\gamma} + \frac{\partial^2 u}{\partial \tilde{x}^\gamma \partial \tilde{x}^\gamma}\right](0,0) = \left(\frac{\partial^2 w}{\partial \tilde{x}^\gamma \partial \tilde{x}^\gamma}\right)_\Gamma (0,0)\,, \tag{4.2.53}$$

$$\left[\frac{\partial u}{\partial \tilde{x}^\alpha}\right](0,0) = v_\Gamma\,(0,0)\,, \tag{4.2.54}$$

$$\left[\frac{\partial^2 u}{\partial \tilde{x}^\alpha \partial \tilde{x}^\beta} - \frac{\partial u}{\partial \tilde{x}^\beta}\frac{\partial^2 \chi}{\partial \tilde{x}^\beta \partial \tilde{x}^\beta} - \frac{\partial u}{\partial \tilde{x}^\gamma}\frac{\partial^2 \chi}{\partial \tilde{x}^\beta \partial \tilde{x}^\gamma}\right](0,0) = \left(\frac{\partial v}{\partial \tilde{x}^\beta}\right)_\Gamma (0,0)\,, \tag{4.2.55}$$

$$\left[\frac{\partial^2 u}{\partial \tilde{x}^\alpha \partial \tilde{x}^\gamma} - \frac{\partial u}{\partial \tilde{x}^\beta}\frac{\partial^2 \chi}{\partial \tilde{x}^\beta \partial \tilde{x}^\gamma} - \frac{\partial u}{\partial \tilde{x}^\gamma}\frac{\partial^2 \chi}{\partial \tilde{x}^\gamma \partial \tilde{x}^\gamma}\right](0,0) = \left(\frac{\partial v}{\partial \tilde{x}^\gamma}\right)_\Gamma (0,0)\,, \tag{4.2.56}$$

$$\left[\frac{\partial^2 u}{\partial \tilde{x}^\alpha \partial \tilde{x}^\alpha} + \frac{\partial^2 u}{\partial \tilde{x}^\beta \partial \tilde{x}^\beta} + \frac{\partial^2 u}{\partial \tilde{x}^\gamma \partial \tilde{x}^\gamma} + \lambda u + f\right](0,0) = 0. \tag{4.2.57}$$

Using algebraic manipulations and Lemma 4.1.4, we can decouple the ten jump conditions (4.2.48 - 4.2.57) as:

$$[u]\,(0,0) = w_\Gamma(0,0), \tag{4.2.58}$$

$$\left[\frac{\partial u}{\partial \tilde{x}^\alpha}\right](0,0) = v_\Gamma\,(0,0)\,, \tag{4.2.59}$$

$$\left[\frac{\partial u}{\partial \tilde{x}^\beta}\right](0,0) = \left(\frac{\partial w}{\partial \tilde{x}^\beta}\right)_\Gamma (0,0)\,, \tag{4.2.60}$$

$$\left[\frac{\partial u}{\partial \tilde{x}^\gamma}\right](0,0) = \left(\frac{\partial w}{\partial \tilde{x}^\gamma}\right)_\Gamma (0,0)\,, \tag{4.2.61}$$

$$
\begin{aligned}
\left[\frac{\partial^2 u}{\partial\tilde{x}^\alpha\partial\tilde{x}^\alpha}\right](0,0) &= v_\Gamma(0,0)\left(\frac{\partial^2\chi}{\partial\tilde{x}^\beta\partial\tilde{x}^\beta}\right)_\Gamma(0,0) - \left(\frac{\partial^2 w}{\partial\tilde{x}^\beta\partial\tilde{x}^\beta}\right)_\Gamma(0,0) + v_\Gamma(0,0)\left(\frac{\partial^2\chi}{\partial\tilde{x}^\gamma\partial\tilde{x}^\gamma}\right)_\Gamma(0,0) \\
&\quad - \left(\frac{\partial^2 w}{\partial\tilde{x}^\gamma\partial\tilde{x}^\gamma}\right)_\Gamma(0,0) - u_\Gamma^-(0,0)\left[\lambda\right](0,0) - \lambda_\Gamma^+(0,0)w_\Gamma(0,0) - \left[f\right](0,0) \\
&= v_\Gamma(0,0)\left(\frac{\partial^2\chi}{\partial\tilde{x}^\beta\partial\tilde{x}^\beta}\right)_\Gamma(0,0) - \left(\frac{\partial^2 w}{\partial\tilde{x}^\beta\partial\tilde{x}^\beta}\right)_\Gamma(0,0) + v_\Gamma(0,0)\left(\frac{\partial^2\chi}{\partial\tilde{x}^\gamma\partial\tilde{x}^\gamma}\right)_\Gamma(0,0) \\
&\quad - \left(\frac{\partial^2 w}{\partial\tilde{x}^\gamma\partial\tilde{x}^\gamma}\right)_\Gamma(0,0) - \big(u_\Gamma^+(0,0) - w_\Gamma(0,0)\big)\left[\lambda\right](0,0) \\
&\quad - \lambda_\Gamma^+(0,0)w_\Gamma(0,0) - \left[f\right](0,0),
\end{aligned} \tag{4.2.62}
$$

$$
\left[\frac{\partial^2 u}{\partial\tilde{x}^\beta\partial\tilde{x}^\beta}\right](0,0) = -v_\Gamma(0,0)\left(\frac{\partial^2\chi}{\partial\tilde{x}^\beta\partial\tilde{x}^\beta}\right)_\Gamma(0,0) + \left(\frac{\partial^2 w}{\partial\tilde{x}^\beta\partial\tilde{x}^\beta}\right)_\Gamma(0,0), \tag{4.2.63}
$$

$$
\left[\frac{\partial^2 u}{\partial\tilde{x}^\gamma\partial\tilde{x}^\gamma}\right](0,0) = -v_\Gamma(0,0)\left(\frac{\partial^2\chi}{\partial\tilde{x}^\gamma\partial\tilde{x}^\gamma}\right)_\Gamma(0,0) + \left(\frac{\partial^2 w}{\partial\tilde{x}^\gamma\partial\tilde{x}^\gamma}\right)_\Gamma(0,0), \tag{4.2.64}
$$

$$
\begin{aligned}
\left[\frac{\partial^2 u}{\partial\tilde{x}^\alpha\partial\tilde{x}^\beta}\right](0,0) &= \left(\frac{\partial w}{\partial\tilde{x}^\beta}\right)_\Gamma(0,0)\left(\frac{\partial^2\chi}{\partial\tilde{x}^\beta\partial\tilde{x}^\beta}\right)_\Gamma(0,0) + \left(\frac{\partial w}{\partial\tilde{x}^\gamma}\right)_\Gamma(0,0)\left(\frac{\partial^2\chi}{\partial\tilde{x}^\beta\partial\tilde{x}^\gamma}\right)_\Gamma(0,0) \\
&\quad + \left(\frac{\partial v}{\partial\tilde{x}^\beta}\right)_\Gamma(0,0),
\end{aligned} \tag{4.2.65}
$$

$$
\begin{aligned}
\left[\frac{\partial^2 u}{\partial\tilde{x}^\alpha\partial\tilde{x}^\gamma}\right](0,0) &= \left(\frac{\partial w}{\partial\tilde{x}^\beta}\right)_\Gamma(0,0)\left(\frac{\partial^2\chi}{\partial\tilde{x}^\beta\partial\tilde{x}^\gamma}\right)_\Gamma(0,0) + \left(\frac{\partial w}{\partial\tilde{x}^\gamma}\right)_\Gamma(0,0)\left(\frac{\partial^2\chi}{\partial\tilde{x}^\gamma\partial\tilde{x}^\gamma}\right)_\Gamma(0,0) \\
&\quad + \left(\frac{\partial v}{\partial\tilde{x}^\gamma}\right)_\Gamma(0,0),
\end{aligned} \tag{4.2.66}
$$

$$
\left[\frac{\partial^2 u}{\partial\tilde{x}^\beta\partial\tilde{x}^\gamma}\right](0,0) = -v_\Gamma(0,0)\left(\frac{\partial^2\chi}{\partial\tilde{x}^\beta\partial\tilde{x}^\gamma}\right)_\Gamma(0,0) + \left(\frac{\partial^2 w}{\partial\tilde{x}^\beta\partial\tilde{x}^\gamma}\right)_\Gamma(0,0). \tag{4.2.67}
$$

Using the decoupled jump conditions (4.2.58 - 4.2.67), Eq. (4.2.19) becomes

$$
\begin{aligned}
u^-_{i,j,l-1} = {} & u^+_\Gamma(0,0) - w_\Gamma(0,0) + \tilde{x}^\alpha_{i,j,l-1}\left(\frac{\partial u}{\partial \tilde{x}^\alpha}\right)^+_\Gamma(0,0) - \tilde{x}^\alpha_{i,j,l-1} v_\Gamma(0,0) + \tilde{x}^\beta_{i,j,l-1}\left(\frac{\partial u}{\partial \tilde{x}^\beta}\right)^+_\Gamma(0,0) \\
& - \tilde{x}^\beta_{i,j,l-1}\left(\frac{\partial w}{\partial \tilde{x}^\beta}\right)_\Gamma(0,0) + \tilde{x}^\gamma_{i,j,l-1}\left(\frac{\partial u}{\partial \tilde{x}^\gamma}\right)^+_\Gamma(0,0) - \tilde{x}^\gamma_{i,j,l-1}\left(\frac{\partial w}{\partial \tilde{x}^\gamma}\right)_\Gamma(0,0) \\
& + \frac{1}{2}\left(\tilde{x}^\alpha_{i,j,l-1}\right)^2\left(\frac{\partial^2 u}{\partial \tilde{x}^\alpha \partial \tilde{x}^\alpha}\right)^+_\Gamma(0,0) - \frac{1}{2}\left(\tilde{x}^\alpha_{i,j,l-1}\right)^2\Bigg(v_\Gamma(0,0)\left(\frac{\partial^2 \chi}{\partial \tilde{x}^\beta \partial \tilde{x}^\beta}\right)_\Gamma(0,0) \\
& - \left(\frac{\partial^2 w}{\partial \tilde{x}^\beta \partial \tilde{x}^\beta}\right)_\Gamma(0,0) + v_\Gamma(0,0)\left(\frac{\partial^2 \chi}{\partial \tilde{x}^\gamma \partial \tilde{x}^\gamma}\right)_\Gamma(0,0) - \left(\frac{\partial^2 w}{\partial \tilde{x}^\gamma \partial \tilde{x}^\gamma}\right)_\Gamma(0,0) \\
& - \left(u^+_\Gamma(0,0) - w_\Gamma(0,0)\right)[\lambda](0,0) - \lambda^+_\Gamma(0,0) w_\Gamma(0,0) - [f](0,0)\Bigg) \\
& + \frac{1}{2}\left(\tilde{x}^\beta_{i,j,l-1}\right)^2\left(\frac{\partial^2 u}{\partial \tilde{x}^\beta \partial \tilde{x}^\beta}\right)^+_\Gamma(0,0) - \frac{1}{2}\left(\tilde{x}^\beta_{i,j,l-1}\right)^2\Bigg(-v_\Gamma(0,0)\left(\frac{\partial^2 \chi}{\partial \tilde{x}^\beta \partial \tilde{x}^\beta}\right)_\Gamma(0,0) \\
& + \left(\frac{\partial^2 w}{\partial \tilde{x}^\beta \partial \tilde{x}^\beta}\right)_\Gamma(0,0)\Bigg) + \frac{1}{2}\left(\tilde{x}^\gamma_{i,j,l-1}\right)^2\left(\frac{\partial^2 u}{\partial \tilde{x}^\gamma \partial \tilde{x}^\gamma}\right)^+_\Gamma(0,0) - \frac{1}{2}\left(\tilde{x}^\gamma_{i,j,l-1}\right)^2 \\
& \Bigg(-v_\Gamma(0,0)\left(\frac{\partial^2 \chi}{\partial \tilde{x}^\gamma \partial \tilde{x}^\gamma}\right)_\Gamma(0,0) + \left(\frac{\partial^2 w}{\partial \tilde{x}^\gamma \partial \tilde{x}^\gamma}\right)_\Gamma(0,0)\Bigg) + \tilde{x}^\alpha_{i,j,l-1}\tilde{x}^\beta_{i,j,l-1}\left(\frac{\partial^2 u}{\partial \tilde{x}^\alpha \partial \tilde{x}^\beta}\right)^+_\Gamma(0,0) \\
& - \tilde{x}^\alpha_{i,j,l-1}\tilde{x}^\beta_{i,j,l-1}\Bigg(\left(\frac{\partial w}{\partial \tilde{x}^\beta}\right)_\Gamma(0,0)\left(\frac{\partial^2 \chi}{\partial \tilde{x}^\beta \partial \tilde{x}^\beta}\right)_\Gamma(0,0) + \left(\frac{\partial w}{\partial \tilde{x}^\gamma}\right)_\Gamma(0,0)\left(\frac{\partial^2 \chi}{\partial \tilde{x}^\beta \partial \tilde{x}^\gamma}\right)_\Gamma(0,0) \\
& + \left(\frac{\partial v}{\partial \tilde{x}^\beta}\right)_\Gamma(0,0)\Bigg) + \tilde{x}^\alpha_{i,j,l-1}\tilde{x}^\gamma_{i,j,l-1}\left(\frac{\partial^2 u}{\partial \tilde{x}^\alpha \partial \tilde{x}^\gamma}\right)^+_\Gamma(0,0) - \tilde{x}^\alpha_{i,j,l-1}\tilde{x}^\gamma_{i,j,l-1} \\
& \Bigg(\left(\frac{\partial w}{\partial \tilde{x}^\beta}\right)_\Gamma(0,0)\left(\frac{\partial^2 \chi}{\partial \tilde{x}^\beta \partial \tilde{x}^\gamma}\right)_\Gamma(0,0) + \left(\frac{\partial w}{\partial \tilde{x}^\gamma}\right)_\Gamma(0,0)\left(\frac{\partial^2 \chi}{\partial \tilde{x}^\gamma \partial \tilde{x}^\gamma}\right)_\Gamma(0,0) + \left(\frac{\partial v}{\partial \tilde{x}^\gamma}\right)_\Gamma(0,0)\Bigg) \\
& + \tilde{x}^\beta_{i,j,l-1}\tilde{x}^\gamma_{i,j,l-1}\left(\frac{\partial^2 u}{\partial \tilde{x}^\beta \partial \tilde{x}^\gamma}\right)^+_\Gamma(0,0) - \tilde{x}^\beta_{i,j,l-1}\tilde{x}^\gamma_{i,j,l-1} \\
& \Bigg(-v_\Gamma(0,0)\left(\frac{\partial^2 \chi}{\partial \tilde{x}^\beta \partial \tilde{x}^\gamma}\right)_\Gamma(0,0) + \left(\frac{\partial^2 w}{\partial \tilde{x}^\beta \partial \tilde{x}^\gamma}\right)_\Gamma(0,0)\Bigg) + O(h^3).
\end{aligned}
\tag{4.2.68}
$$

We can collect terms related to jump conditions in Eq. (4.2.68) to get

$$
\begin{aligned}
u^-_{i,j,l-1} = {} & u^+_\Gamma(0,0) + \tilde{x}^\alpha_{i,j,l-1}\left(\frac{\partial u}{\partial \tilde{x}^\alpha}\right)^+_\Gamma(0,0) + \tilde{x}^\beta_{i,j,l-1}\left(\frac{\partial u}{\partial \tilde{x}^\beta}\right)^+_\Gamma(0,0) + \tilde{x}^\gamma_{i,j,l-1}\left(\frac{\partial u}{\partial \tilde{x}^\gamma}\right)^+_\Gamma(0,0) \\
& + \frac{1}{2}\left(\tilde{x}^\alpha_{i,j,l-1}\right)^2\left(\frac{\partial^2 u}{\partial \tilde{x}^\alpha \partial \tilde{x}^\alpha}\right)^+_\Gamma(0,0) + \frac{1}{2}\left(\tilde{x}^\beta_{i,j,l-1}\right)^2\left(\frac{\partial^2 u}{\partial \tilde{x}^\beta \partial \tilde{x}^\beta}\right)^+_\Gamma(0,0) \\
& + \frac{1}{2}\left(\tilde{x}^\gamma_{i,j,l-1}\right)^2\left(\frac{\partial^2 u}{\partial \tilde{x}^\gamma \partial \tilde{x}^\gamma}\right)^+_\Gamma(0,0) + \tilde{x}^\alpha_{i,j,l-1}\tilde{x}^\beta_{i,j,l-1}\left(\frac{\partial^2 u}{\partial \tilde{x}^\alpha \partial \tilde{x}^\beta}\right)^+_\Gamma(0,0) \\
& + \tilde{x}^\alpha_{i,j,l-1}\tilde{x}^\gamma_{i,j,l-1}\left(\frac{\partial^2 u}{\partial \tilde{x}^\alpha \partial \tilde{x}^\gamma}\right)^+_\Gamma(0,0) + \tilde{x}^\beta_{i,j,l-1}\tilde{x}^\gamma_{i,j,l-1}\left(\frac{\partial^2 u}{\partial \tilde{x}^\beta \partial \tilde{x}^\gamma}\right)^+_\Gamma(0,0) \\
& - \Bigg(w_\Gamma(0,0) + \tilde{x}^\alpha_{i,j,l-1} v_\Gamma(0,0) + \tilde{x}^\beta_{i,j,l-1}\left(\frac{\partial w}{\partial \tilde{x}^\beta}\right)_\Gamma(0,0) + \tilde{x}^\gamma_{i,j,l-1}\left(\frac{\partial w}{\partial \tilde{x}^\gamma}\right)_\Gamma(0,0) \\
& + \frac{1}{2}\left(\tilde{x}^\alpha_{i,j,l-1}\right)^2\Bigg(v_\Gamma(0,0)\left(\frac{\partial^2 \chi}{\partial \tilde{x}^\beta \partial \tilde{x}^\beta}\right)_\Gamma(0,0) - \left(\frac{\partial^2 w}{\partial \tilde{x}^\beta \partial \tilde{x}^\beta}\right)_\Gamma(0,0) \\
& + v_\Gamma(0,0)\left(\frac{\partial^2 \chi}{\partial \tilde{x}^\gamma \partial \tilde{x}^\gamma}\right)_\Gamma(0,0) - \left(\frac{\partial^2 w}{\partial \tilde{x}^\gamma \partial \tilde{x}^\gamma}\right)_\Gamma(0,0) - \left(u^+_\Gamma(0,0) - w_\Gamma(0,0)\right)[\lambda](0,0) \\
& -\lambda^+_\Gamma(0,0) w_\Gamma(0,0) - [f](0,0)\Bigg) \\
& + \frac{1}{2}\left(\tilde{x}^\beta_{i,j,l-1}\right)^2\left(-v_\Gamma(0,0)\left(\frac{\partial^2 \chi}{\partial \tilde{x}^\beta \partial \tilde{x}^\beta}\right)_\Gamma(0,0) + \left(\frac{\partial^2 w}{\partial \tilde{x}^\beta \partial \tilde{x}^\beta}\right)_\Gamma(0,0)\right) \\
& + \frac{1}{2}\left(\tilde{x}^\gamma_{i,j,l-1}\right)^2\left(-v_\Gamma(0,0)\left(\frac{\partial^2 \chi}{\partial \tilde{x}^\gamma \partial \tilde{x}^\gamma}\right)_\Gamma(0,0) + \left(\frac{\partial^2 w}{\partial \tilde{x}^\gamma \partial \tilde{x}^\gamma}\right)_\Gamma(0,0)\right) + \tilde{x}^\alpha_{i,j,l-1}\tilde{x}^\beta_{i,j,l-1} \\
& \left(\left(\frac{\partial w}{\partial \tilde{x}^\beta}\right)_\Gamma(0,0)\left(\frac{\partial^2 \chi}{\partial \tilde{x}^\beta \partial \tilde{x}^\beta}\right)_\Gamma(0,0) + \left(\frac{\partial w}{\partial \tilde{x}^\gamma}\right)_\Gamma(0,0)\left(\frac{\partial^2 \chi}{\partial \tilde{x}^\beta \partial \tilde{x}^\gamma}\right)_\Gamma(0,0) + \left(\frac{\partial v}{\partial \tilde{x}^\beta}\right)_\Gamma(0,0)\right) \\
& + \tilde{x}^\alpha_{i,j,l-1}\tilde{x}^\gamma_{i,j,l-1}\left(\left(\frac{\partial w}{\partial \tilde{x}^\beta}\right)_\Gamma(0,0)\left(\frac{\partial^2 \chi}{\partial \tilde{x}^\beta \partial \tilde{x}^\gamma}\right)_\Gamma(0,0) + \left(\frac{\partial w}{\partial \tilde{x}^\gamma}\right)_\Gamma(0,0)\left(\frac{\partial^2 \chi}{\partial \tilde{x}^\gamma \partial \tilde{x}^\gamma}\right)_\Gamma(0,0)\right. \\
& \left. + \left(\frac{\partial v}{\partial \tilde{x}^\gamma}\right)_\Gamma(0,0)\right) + \tilde{x}^\beta_{i,j,l-1}\tilde{x}^\gamma_{i,j,l-1}\left(-v_\Gamma(0,0)\left(\frac{\partial^2 \chi}{\partial \tilde{x}^\beta \partial \tilde{x}^\gamma}\right)_\Gamma(0,0) + \left(\frac{\partial^2 w}{\partial \tilde{x}^\beta \partial \tilde{x}^\gamma}\right)_\Gamma(0,0)\right)\Bigg) \\
& + O(h^3).
\end{aligned}
\tag{4.2.69}
$$

Lemma 4.2.3.

$$\tilde{x}^k_{i,j,l-1} + \tilde{x}^k_{i,j,l+1} + \tilde{x}^k_{i,j-1,l} + \tilde{x}^k_{i,j+1,l} + \tilde{x}^k_{i-1,j,l} + \tilde{x}^k_{i+1,j,l} - 6\tilde{x}^k_{i,j,l} = 0, \quad k = \alpha, \beta, \gamma. \tag{4.2.70}$$

Proof. Similar to the 2D case, see Lemma 4.1.5. $\square$

Lemma 4.2.4.

$$\left(\tilde{x}^k_{i,j,l-1}\right)^2 + \left(\tilde{x}^k_{i,j,l+1}\right)^2 + \left(\tilde{x}^k_{i,j-1,l}\right)^2 + \left(\tilde{x}^k_{i,j+1,l}\right)^2 + \left(\tilde{x}^k_{i-1,j,l}\right)^2 + \left(\tilde{x}^k_{i+1,j,l}\right)^2 - 6\left(\tilde{x}^k_{i,j,l}\right)^2 = 2h^2,$$
$$k = \alpha, \beta, \gamma. \tag{4.2.71}$$

Proof. Similar to the 2D case, see Lemma 4.1.6. □

Lemma 4.2.5.

$$\tilde{x}^p_{i,j,l-1}\tilde{x}^q_{i,j,l-1} + \tilde{x}^p_{i,j,l+1}\tilde{x}^q_{i,j,l+1} + \tilde{x}^p_{i,j-1,l}\tilde{x}^q_{i,j-1,l} + \tilde{x}^p_{i,j+1,l}\tilde{x}^q_{i,j+1,l} + \tilde{x}^p_{i-1,j,l}\tilde{x}^q_{i-1,j,l} + \tilde{x}^p_{i+1,j,l}\tilde{x}^q_{i+1,j,l}$$
$$- 6\tilde{x}^p_{i,j,l}\tilde{x}^q_{i,j,l} = 0, \quad (p,q) = (\alpha,\beta), (\alpha,\gamma) \textit{ or } (\beta,\gamma). \tag{4.2.72}$$

Proof. Similar to the 2D case, see Lemma 4.1.7. □

By expanding $u^-_{i,j,l-1}, u^+_{i,j,l+1}, u^+_{i,j-1,l}, u^+_{i,j+1,l}, u^+_{i-1,j,l}, u^+_{i+1,j,l}, u^+_{i,j,l}$ and $\lambda^+, f^+_{i,j,l}$ in a Taylor series about the local origin $\tilde{\mathbf{0}}$ and applying Lemma 4.2.3 - 4.2.5, the truncation error (4.2.17) is found to be

$$\begin{aligned}
T &= \left(\frac{\partial^2 u}{\partial \tilde{x}^\alpha \partial \tilde{x}^\alpha}\right)^+_\Gamma (0,0) + \left(\frac{\partial^2 u}{\partial \tilde{x}^\beta \partial \tilde{x}^\beta}\right)^+_\Gamma (0,0) + \left(\frac{\partial^2 u}{\partial \tilde{x}^\gamma \partial \tilde{x}^\gamma}\right)^+_\Gamma (0,0) \\
&\quad + \left(\frac{\left(\tilde{x}^\alpha_{i,j,l-1}\right)^2}{2h^2} [\lambda](0,0) + \lambda^+_\Gamma(0,0)\right) u^+_\Gamma(0,0) + f^+_\Gamma(0,0) + C^+ + O(h) \\
&= \frac{\left(\tilde{x}^\alpha_{i,j,l-1}\right)^2}{2h^2} [\lambda](0,0) u^+_\Gamma(0,0) + C^+ + O(h) \\
&= C^+ + O(h) \quad (\text{if } [\lambda] = 0)
\end{aligned} \tag{4.2.73}$$

where

$$
\begin{aligned}
C^{+} = & -\frac{1}{h^2}\left(w_\Gamma(0,0)+\tilde{x}^{\alpha}_{i,j,l-1}v_\Gamma(0,0)+\tilde{x}^{\beta}_{i,j,l-1}\left(\frac{\partial w}{\partial\tilde{x}^{\beta}}\right)_\Gamma(0,0)+\tilde{x}^{\gamma}_{i,j,l-1}\left(\frac{\partial w}{\partial\tilde{x}^{\gamma}}\right)_\Gamma(0,0)\right.\\
& +\frac{1}{2}\left(\tilde{x}^{\alpha}_{i,j,l-1}\right)^2\left(v_\Gamma(0,0)\left(\frac{\partial^2\chi}{\partial\tilde{x}^{\beta}\partial\tilde{x}^{\beta}}\right)_\Gamma(0,0)-\left(\frac{\partial^2 w}{\partial\tilde{x}^{\beta}\partial\tilde{x}^{\beta}}\right)_\Gamma(0,0)+v_\Gamma(0,0)\left(\frac{\partial^2\chi}{\partial\tilde{x}^{\gamma}\partial\tilde{x}^{\gamma}}\right)_\Gamma(0,0)\right.\\
& \left.-\left(\frac{\partial^2 w}{\partial\tilde{x}^{\gamma}\partial\tilde{x}^{\gamma}}\right)_\Gamma(0,0)+w_\Gamma(0,0)\left[\lambda\right](0,0)-\lambda^{+}_\Gamma(0,0)w_\Gamma(0,0)-\left[f\right](0,0)\right)\\
& +\frac{1}{2}\left(\tilde{x}^{\beta}_{i,j,l-1}\right)^2\left(-v_\Gamma(0,0)\left(\frac{\partial^2\chi}{\partial\tilde{x}^{\beta}\partial\tilde{x}^{\beta}}\right)_\Gamma(0,0)+\left(\frac{\partial^2 w}{\partial\tilde{x}^{\beta}\partial\tilde{x}^{\beta}}\right)_\Gamma(0,0)\right)\\
& +\frac{1}{2}\left(\tilde{x}^{\gamma}_{i,j,l-1}\right)^2\left(-v_\Gamma(0,0)\left(\frac{\partial^2\chi}{\partial\tilde{x}^{\gamma}\partial\tilde{x}^{\gamma}}\right)_\Gamma(0,0)+\left(\frac{\partial^2 w}{\partial\tilde{x}^{\gamma}\partial\tilde{x}^{\gamma}}\right)_\Gamma(0,0)\right)\\
& +\tilde{x}^{\alpha}_{i,j,l-1}\tilde{x}^{\beta}_{i,j,l-1}\left(\left(\frac{\partial w}{\partial\tilde{x}^{\beta}}\right)_\Gamma(0,0)\left(\frac{\partial^2\chi}{\partial\tilde{x}^{\beta}\partial\tilde{x}^{\beta}}\right)_\Gamma(0,0)+\left(\frac{\partial w}{\partial\tilde{x}^{\gamma}}\right)_\Gamma(0,0)\left(\frac{\partial^2\chi}{\partial\tilde{x}^{\beta}\partial\tilde{x}^{\gamma}}\right)_\Gamma(0,0)\right.\\
& \left.+\left(\frac{\partial v}{\partial\tilde{x}^{\beta}}\right)_\Gamma(0,0)\right)+\tilde{x}^{\alpha}_{i,j,l-1}\tilde{x}^{\gamma}_{i,j,l-1}\left(\left(\frac{\partial w}{\partial\tilde{x}^{\beta}}\right)_\Gamma(0,0)\left(\frac{\partial^2\chi}{\partial\tilde{x}^{\beta}\partial\tilde{x}^{\gamma}}\right)_\Gamma(0,0)\right.\\
& \left.+\left(\frac{\partial w}{\partial\tilde{x}^{\gamma}}\right)_\Gamma(0,0)\left(\frac{\partial^2\chi}{\partial\tilde{x}^{\gamma}\partial\tilde{x}^{\gamma}}\right)_\Gamma(0,0)+\left(\frac{\partial v}{\partial\tilde{x}^{\gamma}}\right)_\Gamma(0,0)\right)\\
& \left.+\tilde{x}^{\beta}_{i,j,l-1}\tilde{x}^{\gamma}_{i,j,l-1}\left(-v_\Gamma(0,0)\left(\frac{\partial^2\chi}{\partial\tilde{x}^{\beta}\partial\tilde{x}^{\gamma}}\right)_\Gamma(0,0)+\left(\frac{\partial^2 w}{\partial\tilde{x}^{\beta}\partial\tilde{x}^{\gamma}}\right)_\Gamma(0,0)\right)\right).
\end{aligned}
\tag{4.2.74}
$$

If $-C^{+}$ is added to the difference scheme (4.2.10) at the irregular outer grid point $\left(x^{\alpha}_i, x^{\beta}_j, x^{\gamma}_l\right)$, the truncation error $T = O(h)$. The consistency of the discretization is guaranteed. It is also clear that $-C^{+}$ needs to be added for each stencil point $\notin \Omega^{+}$.

For an irregular grid point $\left(x^{\alpha}_i, x^{\beta}_j, x^{\gamma}_l\right) \in \Omega^{-}$ with only $\left(x^{\alpha}_i, x^{\beta}_j, x^{\gamma}_{l-1}\right) \in \Omega^{+}$, following the same steps we can show that

$$
\begin{aligned}
T = & \left(\frac{\partial^2 u}{\partial\tilde{x}^{\alpha}\partial\tilde{x}^{\alpha}}\right)^{-}_\Gamma(0,0)+\left(\frac{\partial^2 u}{\partial\tilde{x}^{\beta}\partial\tilde{x}^{\beta}}\right)^{-}_\Gamma(0,0)+\left(\frac{\partial^2 u}{\partial\tilde{x}^{\gamma}\partial\tilde{x}^{\gamma}}\right)^{-}_\Gamma(0,0)\\
& +\left(-\frac{\left(\tilde{x}^{\alpha}_{i,j,l-1}\right)^2}{2h^2}\left[\lambda\right](0,0)+\lambda^{-}_\Gamma(0,0)\right)u^{-}_\Gamma(0,0)+f^{-}_\Gamma(0,0)+C^{-}+O(h)\\
= & -\frac{\left(\tilde{x}^{\alpha}_{i,j,l-1}\right)^2}{2h^2}\left[\lambda\right](0,0)u^{-}_\Gamma(0,0)+C^{-}+O(h)\\
= & \, C^{-}+O(h) \quad (\text{if } \left[\lambda\right]=0)
\end{aligned}
\tag{4.2.75}
$$

where

$$
\begin{aligned}
C^{-} = \frac{1}{h^2} \Bigg(& w_\Gamma(0,0) + \tilde{x}^{\alpha}_{i,j,l-1} v_\Gamma(0,0) + \tilde{x}^{\beta}_{i,j,l-1} \left(\frac{\partial w}{\partial \tilde{x}^{\beta}}\right)_\Gamma (0,0) + \tilde{x}^{\gamma}_{i,j,l-1} \left(\frac{\partial w}{\partial \tilde{x}^{\gamma}}\right)_\Gamma (0,0) \\
& + \frac{1}{2} \left(\tilde{x}^{\alpha}_{i,j,l-1}\right)^2 \Bigg(v_\Gamma(0,0) \left(\frac{\partial^2 \chi}{\partial \tilde{x}^{\beta} \partial \tilde{x}^{\beta}}\right)_\Gamma (0,0) - \left(\frac{\partial^2 w}{\partial \tilde{x}^{\beta} \partial \tilde{x}^{\beta}}\right)_\Gamma (0,0) + v_\Gamma(0,0) \left(\frac{\partial^2 \chi}{\partial \tilde{x}^{\gamma} \partial \tilde{x}^{\gamma}}\right)_\Gamma (0,0) \\
& - \left(\frac{\partial^2 w}{\partial \tilde{x}^{\gamma} \partial \tilde{x}^{\gamma}}\right)_\Gamma (0,0) - \lambda^{+}_\Gamma(0,0) w_\Gamma(0,0) - [f](0,0) \Bigg) \\
& + \frac{1}{2} \left(\tilde{x}^{\beta}_{i,j,l-1}\right)^2 \left(-v_\Gamma(0,0) \left(\frac{\partial^2 \chi}{\partial \tilde{x}^{\beta} \partial \tilde{x}^{\beta}}\right)_\Gamma (0,0) + \left(\frac{\partial^2 w}{\partial \tilde{x}^{\beta} \partial \tilde{x}^{\beta}}\right)_\Gamma (0,0) \right) \\
& + \frac{1}{2} \left(\tilde{x}^{\gamma}_{i,j,l-1}\right)^2 \left(-v_\Gamma(0,0) \left(\frac{\partial^2 \chi}{\partial \tilde{x}^{\gamma} \partial \tilde{x}^{\gamma}}\right)_\Gamma (0,0) + \left(\frac{\partial^2 w}{\partial \tilde{x}^{\gamma} \partial \tilde{x}^{\gamma}}\right)_\Gamma (0,0) \right) \\
& + \tilde{x}^{\alpha}_{i,j,l-1} \tilde{x}^{\beta}_{i,j,l-1} \Bigg(\left(\frac{\partial w}{\partial \tilde{x}^{\beta}}\right)_\Gamma (0,0) \left(\frac{\partial^2 \chi}{\partial \tilde{x}^{\beta} \partial \tilde{x}^{\beta}}\right)_\Gamma (0,0) + \left(\frac{\partial w}{\partial \tilde{x}^{\gamma}}\right)_\Gamma (0,0) \left(\frac{\partial^2 \chi}{\partial \tilde{x}^{\beta} \partial \tilde{x}^{\gamma}}\right)_\Gamma (0,0) \\
& + \left(\frac{\partial v}{\partial \tilde{x}^{\beta}}\right)_\Gamma (0,0) \Bigg) + \tilde{x}^{\alpha}_{i,j,l-1} \tilde{x}^{\gamma}_{i,j,l-1} \Bigg(\left(\frac{\partial w}{\partial \tilde{x}^{\beta}}\right)_\Gamma (0,0) \left(\frac{\partial^2 \chi}{\partial \tilde{x}^{\beta} \partial \tilde{x}^{\gamma}}\right)_\Gamma (0,0) \\
& + \left(\frac{\partial w}{\partial \tilde{x}^{\gamma}}\right)_\Gamma (0,0) \left(\frac{\partial^2 \chi}{\partial \tilde{x}^{\gamma} \partial \tilde{x}^{\gamma}}\right)_\Gamma (0,0) + \left(\frac{\partial v}{\partial \tilde{x}^{\gamma}}\right)_\Gamma (0,0) \Bigg) \\
& + \tilde{x}^{\beta}_{i,j,l-1} \tilde{x}^{\gamma}_{i,j,l-1} \left(-v_\Gamma(0,0) \left(\frac{\partial^2 \chi}{\partial \tilde{x}^{\beta} \partial \tilde{x}^{\gamma}}\right)_\Gamma (0,0) + \left(\frac{\partial^2 w}{\partial \tilde{x}^{\beta} \partial \tilde{x}^{\gamma}}\right)_\Gamma (0,0) \right) \Bigg).
\end{aligned}
\tag{4.2.76}
$$

If $-C^-$ is added to the difference scheme (4.2.10) at the irregular inner grid point $\left(x_i^\alpha, x_j^\beta, x_l^\gamma\right)$, the truncation error $T = O(h)$. The consistency of the discretization is guaranteed. It is also clear that $-C^-$ needs to be added for each stencil point $\notin \Omega^+$. Note that without the term $\frac{1}{2}\left(\tilde{x}^{\alpha}_{i,j,l-1}\right)^2 \frac{w_\Gamma(0,0)[\lambda](0,0)}{h^2}$ (which is the case if $[\lambda] = 0$), $C^+ = -C^-$.

To summarize, for the 3D elliptic equation (4.2.1) with an interface Γ and λ being a constant, the consistent finite difference scheme is [24, 7]

$$
\frac{U_{i,j,l-1} + U_{i,j,l+1} + U_{i,j-1,l} + U_{i,j+1,l} + U_{i-1,j,l} + U_{i+1,j,l} - 6U_{i,j,l}}{h^2} + \lambda U_{i,j,l} + f_{i,j,l} + C = 0 \tag{4.2.77}
$$

where the correction term C is

$$
C = \begin{cases} 0, & (x_i^\alpha, x_j^\beta, x_l^\gamma) \text{ is a regular grid point,} \\ -C^+, & (x_i^\alpha, x_j^\beta, x_l^\gamma) \text{ is an irregular grid point in } \Omega^+, \\ -C^-, & (x_i^\alpha, x_j^\beta, x_l^\gamma) \text{ is an irregular grid point in } \Omega^-. \end{cases}
$$

4.3 Level Set Approach

There are two main approaches to modeling moving geometric objects: Lagrangian and Eulerian. The use of implicit surfaces is a popular Eulerian approach in many computer-based 2D and 3D geometric models. From physical intuition, implicit surfaces may be defined by the contour of a field, such as gravitational or electromagnetic field. The field strength at any point in space is the sum of the field strengths due to each source point. Mathematically, the level set of a differentiable function

$$\varphi : \mathbb{R}^n \to \mathbb{R} \tag{4.3.1}$$

corresponding to a real value c is the set of points

$$\left\{(x_1, \cdots, x_n) \in \mathbb{R}^n \middle| \varphi(x_1, \cdots, x_n) = c\right\}. \tag{4.3.2}$$

If $n = 2$, the level set is a plane curve known as a level curve. If $n = 3$, the level set is known as a level surface. See Fig. 4.9 for an example of level curves.

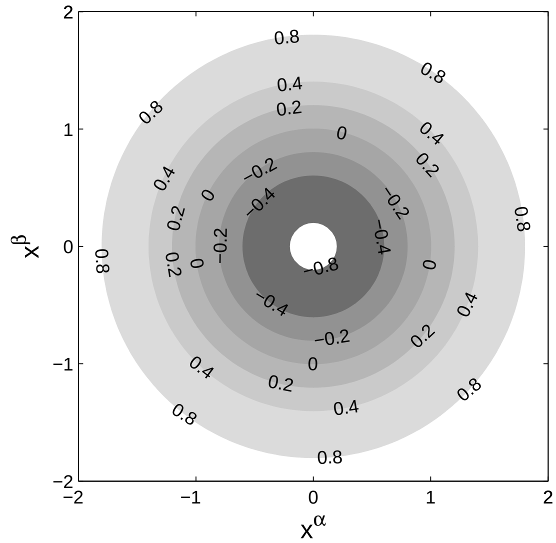

Figure 4.9: Contour plot of a 2D function $\varphi(x^\alpha, x^\beta) = \sqrt{(x^\alpha)^2 + (x^\beta)^2} - 1.0$ whose zero level set is the unit circle.

4.3.1 2D Geometry

Irregular grid points

We denote

$$\Omega^+ = \left\{ \left(x^\alpha, x^\beta\right) \middle| \varphi(x^\alpha, x^\beta) \geq 0 \right\} \tag{4.3.3}$$

and

$$\Omega^- = \left\{ \left(x^\alpha, x^\beta\right) \middle| \varphi(x^\alpha, x^\beta) < 0 \right\}. \tag{4.3.4}$$

For the five-point stencil, a grid point $\left(x_i^\alpha, x_j^\beta\right)$ is an *irregular inner grid point* if and only if

$$\varphi(x_i^\alpha, x_j^\beta) < 0 \tag{4.3.5}$$

and any of the following four inequalities is true:

$$\varphi(x_i^\alpha, x_{j-1}^\beta) \geq 0, \quad \varphi(x_i^\alpha, x_{j+1}^\beta) \geq 0, \quad \varphi(x_{i-1}^\alpha, x_j^\beta) \geq 0, \quad \varphi(x_{i+1}^\alpha, x_j^\beta) \geq 0. \tag{4.3.6}$$

Similarly, a grid point $\left(x_i^\alpha, x_j^\beta\right)$ is an *irregular outer grid point* if and only if

$$\varphi(x_i^\alpha, x_j^\beta) \geq 0 \tag{4.3.7}$$

and any of the following four inequalities is true:

$$\varphi(x_i^\alpha, x_{j-1}^\beta) < 0, \quad \varphi(x_i^\alpha, x_{j+1}^\beta) < 0, \quad \varphi(x_{i-1}^\alpha, x_j^\beta) < 0, \quad \varphi(x_{i+1}^\alpha, x_j^\beta) < 0. \tag{4.3.8}$$

Local Cartesian coordinates

For a given irregular grid point $\boldsymbol{x} = \left(x_i^\alpha, x_j^\beta\right)$ close to the interface, there is a corresponding orthogonal projection point $\boldsymbol{x}_* = \left(x_*^\alpha, x_*^\beta\right)$ on the interface satisfying

$$\boldsymbol{x}_* = \boldsymbol{x} + a\boldsymbol{n}(\boldsymbol{x}) \tag{4.3.9}$$

where a is a real unknown variable and

$$\boldsymbol{n} = \frac{\nabla\varphi}{\|\nabla\varphi\|} = \frac{1}{\sqrt{\left(\frac{\partial\varphi}{\partial x^\alpha}\right)^2 + \left(\frac{\partial\varphi}{\partial x^\beta}\right)^2}} \left(\frac{\partial\varphi}{\partial x^\alpha}, \frac{\partial\varphi}{\partial x^\beta}\right) \tag{4.3.10}$$

is the unit outward normal direction at $\boldsymbol{x}$. See Fig. 4.10 for an illustration.

Since

$$\varphi(\boldsymbol{x}_*) = 0, \tag{4.3.11}$$

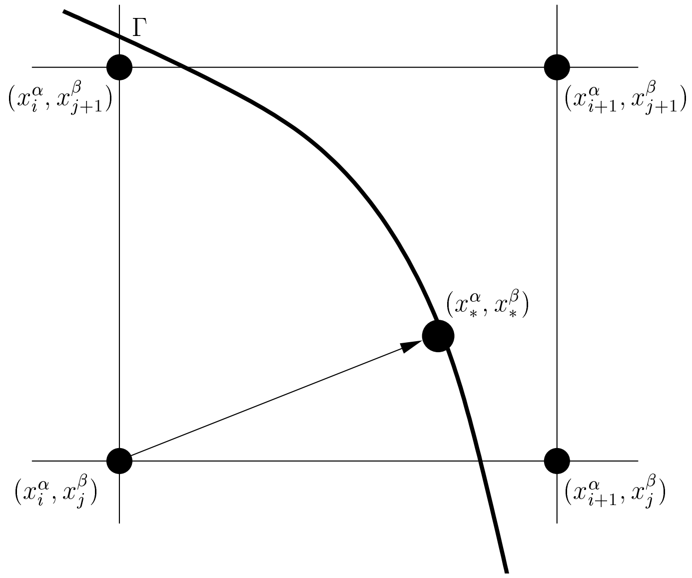

Figure 4.10: An irregular grid point $\boldsymbol{x} = (x_i^\alpha, x_j^\beta)$ and its normal projection point $\boldsymbol{x}_* = (x_*^\alpha, x_*^\beta)$ on the interface Γ.

we have [31]

$$0 = \varphi(\boldsymbol{x} + a\boldsymbol{n}) \approx \varphi(\boldsymbol{x}) + \|\nabla\varphi\| a + \frac{1}{2}\left(\boldsymbol{n}^T \boldsymbol{H}(\varphi)\, \boldsymbol{n}\right) a^2 \tag{4.3.12}$$

where the Hessian matrix $\boldsymbol{H}$ is defined as

$$\boldsymbol{H}(\varphi) = \begin{pmatrix} \dfrac{\partial^2\varphi}{\partial x^\alpha \partial x^\alpha} & \dfrac{\partial^2\varphi}{\partial x^\alpha \partial x^\beta} \\ \dfrac{\partial^2\varphi}{\partial x^\beta \partial x^\alpha} & \dfrac{\partial^2\varphi}{\partial x^\beta \partial x^\beta} \end{pmatrix}. \tag{4.3.13}$$

Eq. (4.3.12) can be solved explicitly to get an approximation of $\boldsymbol{x}_*$ from Eq. (4.3.9).

The unit tangential direction $\boldsymbol{\tau}$ is

$$\boldsymbol{\tau} = \frac{1}{\sqrt{\left(\frac{\partial\varphi}{\partial x^\alpha}\right)^2 + \left(\frac{\partial\varphi}{\partial x^\beta}\right)^2}} \left(-\frac{\partial\varphi}{\partial x^\beta}, \frac{\partial\varphi}{\partial x^\alpha}\right). \tag{4.3.14}$$

Using calculated $\boldsymbol{x}_*$, $\boldsymbol{n}(\boldsymbol{x}_*)$ and $\boldsymbol{\tau}(\boldsymbol{x}_*)$, we can get the Cartesian coordinate transformation formulation which is indispensable to the calculation of the correction term.

Correction term

To calculate the correction term, we need to explain how to calculate the second-order surface derivative $\frac{d^2\chi}{d\tilde{x}^\beta d\tilde{x}^\beta}(0)$. Let φ be the level set function and using the local coordinate system (Chapter 3.1), we know that

$$\varphi(\chi(\tilde{x}^\beta), \tilde{x}^\beta) = 0. \tag{4.3.15}$$

Taking derivatives in the same fashion as deriving the jump conditions, we can get

$$\frac{\partial\varphi}{\partial\tilde{x}^\alpha}(0)\frac{d^2\chi}{d\tilde{x}^\beta d\tilde{x}^\beta}(0) + \frac{\partial^2\varphi}{\partial\tilde{x}^\beta\partial\tilde{x}^\beta}(0) = 0 \tag{4.3.16}$$

which leads to

$$\frac{d^2\chi}{d\tilde{x}^\beta d\tilde{x}^\beta}(0) = -\frac{\partial^2\varphi}{\partial\tilde{x}^\beta\partial\tilde{x}^\beta}(0)\Big/\frac{\partial\varphi}{\partial\tilde{x}^\alpha}(0). \tag{4.3.17}$$

To calculate $\frac{d^2\chi}{d\tilde{x}^\beta d\tilde{x}^\beta}(0)$ using Eq. (4.3.17), note that

$$\frac{\partial\varphi}{\partial\tilde{x}^\alpha} = (A)^l_\alpha \frac{\partial\varphi}{\partial x^l} \tag{4.3.18}$$

and

$$\frac{\partial^2\varphi}{\partial\tilde{x}^\beta\partial\tilde{x}^\beta} = \frac{\partial}{\partial\tilde{x}^\beta}\left((A)^l_\beta \frac{\partial\varphi}{\partial x^l}\right) = (A)^l_\beta (A)^k_\beta \frac{\partial^2\varphi}{\partial x^k\partial x^l}. \tag{4.3.19}$$

Curvature

It is often necessary to obtain extrinsic curvature values for problems such as modeling of mean curvature flow. It is known that the curvature for a 2D curve given implicitly by

$$\varphi(x^\alpha, x^\beta) = 0 \tag{4.3.20}$$

is [40]

$$\kappa = \nabla\cdot\frac{\nabla\varphi}{\|\nabla\varphi\|} = \frac{\frac{\partial^2\varphi}{\partial x^\alpha\partial x^\alpha}\left(\frac{\partial\varphi}{\partial x^\beta}\right)^2 - 2\frac{\partial^2\varphi}{\partial x^\alpha\partial x^\beta}\frac{\partial\varphi}{\partial x^\alpha}\frac{\partial\varphi}{\partial x^\beta} + \frac{\partial^2\varphi}{\partial x^\beta\partial x^\beta}\left(\frac{\partial\varphi}{\partial x^\alpha}\right)^2}{\left(\left(\frac{\partial\varphi}{\partial x^\alpha}\right)^2 + \left(\frac{\partial\varphi}{\partial x^\beta}\right)^2\right)^{\frac{3}{2}}}. \tag{4.3.21}$$

Lemma 4.3.1.

$$\kappa = -\frac{d^2\chi}{d\tilde{x}^\beta d\tilde{x}^\beta}(0). \tag{4.3.22}$$

Proof. By definition, the curvature κ for a plane curve given by Cartesian parametric equations

$$\tilde{x}^\alpha = \chi(\tilde{x}^\beta), \quad \tilde{x}^\beta = \tilde{x}^\beta \tag{4.3.23}$$

at the origin of the local Cartesian coordinates $\left(\tilde{x}^\alpha, \tilde{x}^\beta\right)$ is

$$\kappa = \frac{\dfrac{d\tilde{x}^\alpha}{d\tilde{x}^\beta}\dfrac{d^2\tilde{x}^\beta}{d\tilde{x}^\beta d\tilde{x}^\beta} - \dfrac{d\tilde{x}^\beta}{d\tilde{x}^\beta}\dfrac{d^2\tilde{x}^\alpha}{d\tilde{x}^\beta d\tilde{x}^\beta}}{\left(\left(\dfrac{d\tilde{x}^\alpha}{d\tilde{x}^\beta}\right)^2 + \left(\dfrac{d\tilde{x}^\beta}{d\tilde{x}^\beta}\right)^2\right)^{\frac{3}{2}}}(0) = \frac{-\dfrac{d^2\chi}{d\tilde{x}^\beta d\tilde{x}^\beta}}{\left(\left(\dfrac{d\chi}{d\tilde{x}^\beta}\right)^2 + 1\right)^{\frac{3}{2}}}(0) = -\frac{d^2\chi}{d\tilde{x}^\beta d\tilde{x}^\beta}(0). \tag{4.3.24}$$

□

Remark 4.3.2. *For 2D geometry, the second-order surface derivative* $\dfrac{d^2\chi}{d\tilde{x}^\beta d\tilde{x}^\beta}(0)$ *in the correction term can be calculated using either the curvature formula (4.3.21) or the formula (4.3.17).*

4.3.2 3D Geometry

Irregular grid points

We denote

$$\Omega^+ = \left\{\left(x^\alpha, x^\beta, x^\gamma\right) \middle| \varphi(x^\alpha, x^\beta, x^\gamma) \geq 0\right\} \tag{4.3.25}$$

and

$$\Omega^- = \left\{\left(x^\alpha, x^\beta, x^\gamma\right) \middle| \varphi(x^\alpha, x^\beta, x^\gamma) < 0\right\}. \tag{4.3.26}$$

For the seven-point stencil, a grid point $\left(x_i^\alpha, x_j^\beta, x_l^\gamma\right)$ is an *irregular inner grid point* if and only if

$$\varphi(x_i^\alpha, x_j^\beta, x_l^\gamma) < 0 \tag{4.3.27}$$

and any of the following six inequalities is true:

$$\begin{aligned} &\varphi(x_i^\alpha, x_j^\beta, x_{l-1}^\gamma) \geq 0, \quad \varphi(x_i^\alpha, x_j^\beta, x_{l+1}^\gamma) \geq 0, \quad \varphi(x_i^\alpha, x_{j-1}^\beta, x_l^\gamma) \geq 0, \\ &\varphi(x_i^\alpha, x_{j+1}^\beta, x_l^\gamma) \geq 0, \quad \varphi(x_{i-1}^\alpha, x_j^\beta, x_l^\gamma) \geq 0, \quad \varphi(x_{i+1}^\alpha, x_j^\beta, x_l^\gamma) \geq 0. \end{aligned} \tag{4.3.28}$$

Similarly, a grid point $\left(x_i^\alpha, x_j^\beta, x_l^\gamma\right)$ is an *irregular outer grid point* if and only if

$$\varphi(x_i^\alpha, x_j^\beta, x_l^\gamma) \geq 0 \tag{4.3.29}$$

and any of the following six inequalities is true:

$$\begin{aligned} &\varphi(x_i^\alpha, x_j^\beta, x_{l-1}^\gamma) < 0, \quad \varphi(x_i^\alpha, x_j^\beta, x_{l+1}^\gamma) < 0, \quad \varphi(x_i^\alpha, x_{j-1}^\beta, x_l^\gamma) < 0, \\ &\varphi(x_i^\alpha, x_{j+1}^\beta, x_l^\gamma) < 0, \quad \varphi(x_{i-1}^\alpha, x_j^\beta, x_l^\gamma) < 0, \quad \varphi(x_{i+1}^\alpha, x_j^\beta, x_l^\gamma) < 0. \end{aligned} \tag{4.3.30}$$

Local Cartesian coordinates

For a given irregular grid point $\boldsymbol{x} = \left(x_i^\alpha, x_j^\beta, x_l^\gamma\right)$ close to the interface, there is a corresponding orthogonal projection point $\boldsymbol{x}_* = \left(x_*^\alpha, x_*^\beta, x_*^\gamma\right)$ on the interface satisfying

$$\boldsymbol{x}_* = \boldsymbol{x} + a\boldsymbol{n}(\boldsymbol{x}) \tag{4.3.31}$$

where a is a real unknown variable and

$$\boldsymbol{n} = \frac{\nabla\varphi}{\|\nabla\varphi\|} = \frac{1}{\sqrt{\left(\frac{\partial\varphi}{\partial x^\alpha}\right)^2 + \left(\frac{\partial\varphi}{\partial x^\beta}\right)^2 + \left(\frac{\partial\varphi}{\partial x^\gamma}\right)^2}}\left(\frac{\partial\varphi}{\partial x^\alpha}, \frac{\partial\varphi}{\partial x^\beta}, \frac{\partial\varphi}{\partial x^\gamma}\right) \tag{4.3.32}$$

is the unit outward normal direction at $\boldsymbol{x}$. See Fig. 4.11 for an illustration.

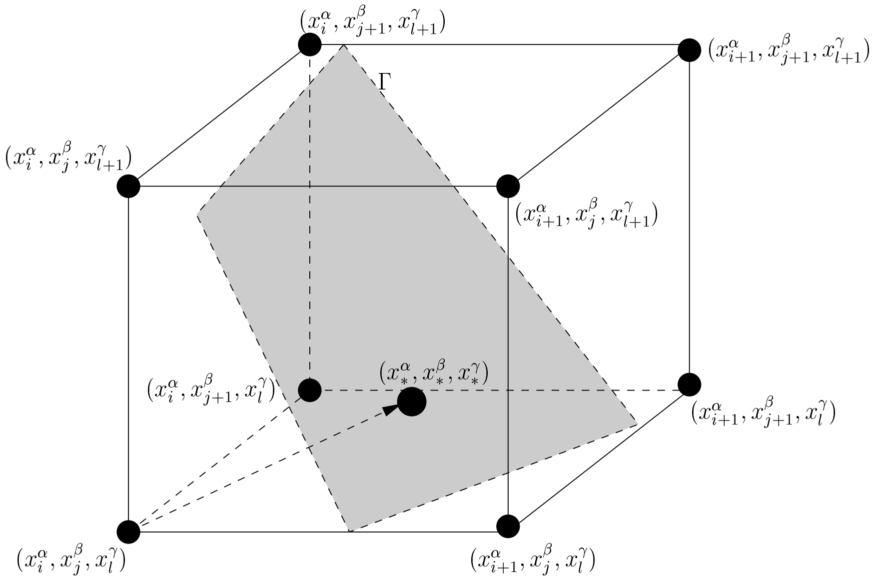

Figure 4.11: An irregular grid point $\boldsymbol{x} = (x_i^\alpha, x_j^\beta, x_l^\gamma)$ and its normal projection point $\boldsymbol{x}_* = (x_*^\alpha, x_*^\beta, x_*^\gamma)$ on the interface Γ.

Since

$$\varphi(\boldsymbol{x}_*) = 0, \tag{4.3.33}$$

we have

$$0 = \varphi(\boldsymbol{x} + a\boldsymbol{n}) \approx \varphi(\boldsymbol{x}) + \|\nabla\varphi\|a + \frac{1}{2}\left(\boldsymbol{n}^T\boldsymbol{H}\left(\varphi\right)\boldsymbol{n}\right)a^2 \tag{4.3.34}$$

where the Hessian matrix $\boldsymbol{H}$ is defined as

$$\boldsymbol{H}(\varphi) = \begin{pmatrix} \dfrac{\partial^2\varphi}{\partial x^\alpha \partial x^\alpha} & \dfrac{\partial^2\varphi}{\partial x^\alpha \partial x^\beta} & \dfrac{\partial^2\varphi}{\partial x^\alpha \partial x^\gamma} \\ \dfrac{\partial^2\varphi}{\partial x^\beta \partial x^\alpha} & \dfrac{\partial^2\varphi}{\partial x^\beta \partial x^\beta} & \dfrac{\partial^2\varphi}{\partial x^\beta \partial x^\gamma} \\ \dfrac{\partial^2\varphi}{\partial x^\gamma \partial x^\alpha} & \dfrac{\partial^2\varphi}{\partial x^\gamma \partial x^\beta} & \dfrac{\partial^2\varphi}{\partial x^\gamma \partial x^\gamma} \end{pmatrix}. \tag{4.3.35}$$

Eq. (4.3.34) can be solved explicitly to get an approximation of $\boldsymbol{x}_*$ from Eq. (4.3.31).

Unlike the 2D case, there is freedom to choose two orthonormal tangential directions $\boldsymbol{\tau}$ and $\boldsymbol{\eta}$ satisfying (1) $\boldsymbol{\tau}$ and $\boldsymbol{\eta}$ cannot be zero vectors, and (2) $\boldsymbol{\tau}$, $\boldsymbol{\eta}$ and $\boldsymbol{n}$ form a right-handed Cartesian coordinate system. For example [7], if

$$\left(\frac{\partial\varphi}{\partial x^\alpha}\right)^2 + \left(\frac{\partial\varphi}{\partial x^\beta}\right)^2 > 0, \tag{4.3.36}$$

we can select $\boldsymbol{\tau}$ as

$$\boldsymbol{\tau} = \frac{1}{\sqrt{\left(\frac{\partial\varphi}{\partial x^\alpha}\right)^2 + \left(\frac{\partial\varphi}{\partial x^\beta}\right)^2}} \left(\frac{\partial\varphi}{\partial x^\beta}, -\frac{\partial\varphi}{\partial x^\alpha}, 0\right), \tag{4.3.37}$$

otherwise we choose

$$\boldsymbol{\tau} = \frac{1}{\sqrt{\left(\frac{\partial\varphi}{\partial x^\alpha}\right)^2 + \left(\frac{\partial\varphi}{\partial x^\gamma}\right)^2}} \left(\frac{\partial\varphi}{\partial x^\gamma}, 0, -\frac{\partial\varphi}{\partial x^\alpha}\right). \tag{4.3.38}$$

Note that this strategy always works provided

$$\left(\frac{\partial\varphi}{\partial x^\alpha}\right)^2 + \left(\frac{\partial\varphi}{\partial x^\beta}\right)^2 + \left(\frac{\partial\varphi}{\partial x^\gamma}\right)^2 > 0, \tag{4.3.39}$$

or equivalently $\|\nabla\varphi\| > 0$ which is true if surface normal exists. After we determine $\boldsymbol{\tau}$, we can get $\boldsymbol{\eta} = \boldsymbol{n} \times \boldsymbol{\tau}$ accordingly as

$$\frac{1}{\sqrt{\left(\frac{\partial\varphi}{\partial x^\alpha}\right)^2 + \left(\frac{\partial\varphi}{\partial x^\beta}\right)^2 + \left(\frac{\partial\varphi}{\partial x^\gamma}\right)^2}} \frac{1}{\sqrt{\left(\frac{\partial\varphi}{\partial x^\alpha}\right)^2 + \left(\frac{\partial\varphi}{\partial x^\beta}\right)^2}} \left(\frac{\partial\varphi}{\partial x^\alpha}\frac{\partial\varphi}{\partial x^\gamma}, \frac{\partial\varphi}{\partial x^\beta}\frac{\partial\varphi}{\partial x^\gamma}, -\left(\frac{\partial\varphi}{\partial x^\alpha}\right)^2 - \left(\frac{\partial\varphi}{\partial x^\beta}\right)^2\right) \tag{4.3.40}$$

or

$$\frac{1}{\sqrt{\left(\frac{\partial\varphi}{\partial x^\alpha}\right)^2 + \left(\frac{\partial\varphi}{\partial x^\beta}\right)^2 + \left(\frac{\partial\varphi}{\partial x^\gamma}\right)^2}} \frac{1}{\sqrt{\left(\frac{\partial\varphi}{\partial x^\alpha}\right)^2 + \left(\frac{\partial\varphi}{\partial x^\gamma}\right)^2}} \left(-\frac{\partial\varphi}{\partial x^\alpha}\frac{\partial\varphi}{\partial x^\beta}, \left(\frac{\partial\varphi}{\partial x^\alpha}\right)^2 + \left(\frac{\partial\varphi}{\partial x^\gamma}\right)^2, -\frac{\partial\varphi}{\partial x^\beta}\frac{\partial\varphi}{\partial x^\gamma}\right). \tag{4.3.41}$$

Using calculated $\boldsymbol{x}_*$, $\boldsymbol{n}(\boldsymbol{x}_*)$, $\boldsymbol{\tau}(\boldsymbol{x}_*)$ and $\boldsymbol{\eta}(\boldsymbol{x}_*)$, we can get the Cartesian coordinate transformation formulation which is indispensable to the calculation of the correction term.

Correction term

To calculate the correction term, we need to explain how to calculate the second-order surface derivatives $\frac{\partial^2 \chi}{\partial \tilde{x}^\beta \partial \tilde{x}^\beta}(0,0)$, $\frac{\partial^2 \chi}{\partial \tilde{x}^\gamma \partial \tilde{x}^\gamma}(0,0)$ and $\frac{\partial^2 \chi}{\partial \tilde{x}^\beta \partial \tilde{x}^\gamma}(0,0)$. Let φ be the level set function and using the local coordinate system, we know that

$$\varphi(\chi(\tilde{x}^\beta, \tilde{x}^\gamma), \tilde{x}^\beta, \tilde{x}^\gamma) = 0. \tag{4.3.42}$$

Taking derivatives in the same fashion as deriving the jump conditions, we can get

$$\frac{\partial \varphi}{\partial \tilde{x}^\alpha}(0,0)\frac{\partial^2 \chi}{\partial \tilde{x}^\beta \partial \tilde{x}^\beta}(0,0) + \frac{\partial^2 \varphi}{\partial \tilde{x}^\beta \partial \tilde{x}^\beta}(0,0) = 0 \tag{4.3.43}$$

which leads to

$$\frac{\partial^2 \chi}{\partial \tilde{x}^\beta \partial \tilde{x}^\beta}(0,0) = -\frac{\partial^2 \varphi}{\partial \tilde{x}^\beta \partial \tilde{x}^\beta}(0,0)\bigg/\frac{\partial \varphi}{\partial \tilde{x}^\alpha}(0,0); \tag{4.3.44}$$

and

$$\frac{\partial \varphi}{\partial \tilde{x}^\alpha}(0,0)\frac{\partial^2 \chi}{\partial \tilde{x}^\beta \partial \tilde{x}^\gamma}(0,0) + \frac{\partial^2 \varphi}{\partial \tilde{x}^\beta \partial \tilde{x}^\gamma}(0,0) = 0 \tag{4.3.45}$$

which leads to

$$\frac{\partial^2 \chi}{\partial \tilde{x}^\beta \partial \tilde{x}^\gamma}(0,0) = -\frac{\partial^2 \varphi}{\partial \tilde{x}^\beta \partial \tilde{x}^\gamma}(0,0)\bigg/\frac{\partial \varphi}{\partial \tilde{x}^\alpha}(0,0); \tag{4.3.46}$$

and

$$\frac{\partial \varphi}{\partial \tilde{x}^\alpha}(0,0)\frac{\partial^2 \chi}{\partial \tilde{x}^\gamma \partial \tilde{x}^\gamma}(0,0) + \frac{\partial^2 \varphi}{\partial \tilde{x}^\gamma \partial \tilde{x}^\gamma}(0,0) = 0 \tag{4.3.47}$$

which leads to

$$\frac{\partial^2 \chi}{\partial \tilde{x}^\gamma \partial \tilde{x}^\gamma}(0,0) = -\frac{\partial^2 \varphi}{\partial \tilde{x}^\gamma \partial \tilde{x}^\gamma}(0,0)\bigg/\frac{\partial \varphi}{\partial \tilde{x}^\alpha}(0,0). \tag{4.3.48}$$

For example, if we want to calculate $\frac{\partial^2 \chi}{\partial \tilde{x}^\beta \partial \tilde{x}^\beta}(0,0)$ using Eq. (4.3.44), note that

$$\frac{\partial \varphi}{\partial \tilde{x}^\alpha} = (A)^l_\alpha \frac{\partial \varphi}{\partial x^l} \tag{4.3.49}$$

and

$$\frac{\partial^2 \varphi}{\partial \tilde{x}^\beta \partial \tilde{x}^\beta} = \frac{\partial}{\partial \tilde{x}^\beta}\left((A)^l_\beta \frac{\partial \varphi}{\partial x^l}\right) = (A)^l_\beta (A)^k_\beta \frac{\partial^2 \varphi}{\partial x^k \partial x^l}. \tag{4.3.50}$$

Curvatures

It is often necessary to obtain curvature values for problems such as modeling of mean curvature flow. It is known that the extrinsic mean curvature κ_M for a 3D surface given implicitly by

$$\varphi(x^\alpha, x^\beta, x^\gamma) = 0 \tag{4.3.51}$$

is

$$\kappa_M = \frac{1}{2}\nabla\cdot\frac{\nabla\varphi}{\|\nabla\varphi\|} = \frac{1}{2}\left(\left(\frac{\partial^2\varphi}{\partial x^\beta\partial x^\beta}+\frac{\partial^2\varphi}{\partial x^\gamma\partial x^\gamma}\right)\left(\frac{\partial\varphi}{\partial x^\alpha}\right)^2+\left(\frac{\partial^2\varphi}{\partial x^\alpha\partial x^\alpha}+\frac{\partial^2\varphi}{\partial x^\gamma\partial x^\gamma}\right)\left(\frac{\partial\varphi}{\partial x^\beta}\right)^2\right.$$
$$+\left(\frac{\partial^2\varphi}{\partial x^\alpha\partial x^\alpha}+\frac{\partial^2\varphi}{\partial x^\beta\partial x^\beta}\right)\left(\frac{\partial\varphi}{\partial x^\gamma}\right)^2-2\left(\frac{\partial\varphi}{\partial x^\alpha}\frac{\partial\varphi}{\partial x^\beta}\frac{\partial^2\varphi}{\partial x^\alpha\partial x^\beta}\right.$$
$$\left.\left.+\frac{\partial\varphi}{\partial x^\alpha}\frac{\partial\varphi}{\partial x^\gamma}\frac{\partial^2\varphi}{\partial x^\alpha\partial x^\gamma}+\frac{\partial\varphi}{\partial x^\beta}\frac{\partial\varphi}{\partial x^\gamma}\frac{\partial^2\varphi}{\partial x^\beta\partial x^\gamma}\right)\right)\Big/\left(\left(\frac{\partial\varphi}{\partial x^\alpha}\right)^2+\left(\frac{\partial\varphi}{\partial x^\beta}\right)^2+\left(\frac{\partial\varphi}{\partial x^\gamma}\right)^2\right)^{\frac{3}{2}}. \tag{4.3.52}$$

By definition, the intrinsic Gaussian curvature κ_G is given by

$$\kappa_G = \frac{\nabla\varphi\cdot\left(\frac{\partial\varphi}{\partial x^\alpha}\left(\frac{\partial(\nabla\varphi)}{\partial x^\beta}\times\frac{\partial(\nabla\varphi)}{\partial x^\gamma}\right)+\frac{\partial\varphi}{\partial x^\beta}\left(\frac{\partial(\nabla\varphi)}{\partial x^\gamma}\times\frac{\partial(\nabla\varphi)}{\partial x^\alpha}\right)+\frac{\partial\varphi}{\partial x^\gamma}\left(\frac{\partial(\nabla\varphi)}{\partial x^\alpha}\times\frac{\partial(\nabla\varphi)}{\partial x^\beta}\right)\right)}{(\nabla\varphi\cdot\nabla\varphi)^2}$$
$$=\left(\left(\frac{\partial\varphi}{\partial x^\alpha}\right)^2\left(\frac{\partial^2\varphi}{\partial x^\beta\partial x^\beta}\frac{\partial^2\varphi}{\partial x^\gamma\partial x^\gamma}-\left(\frac{\partial^2\varphi}{\partial x^\beta\partial x^\gamma}\right)^2\right)+\left(\frac{\partial\varphi}{\partial x^\beta}\right)^2\left(\frac{\partial^2\varphi}{\partial x^\alpha\partial x^\alpha}\frac{\partial^2\varphi}{\partial x^\gamma\partial x^\gamma}-\left(\frac{\partial^2\varphi}{\partial x^\alpha\partial x^\gamma}\right)^2\right)\right.$$
$$+\left(\frac{\partial\varphi}{\partial x^\gamma}\right)^2\left(\frac{\partial^2\varphi}{\partial x^\alpha\partial x^\alpha}\frac{\partial^2\varphi}{\partial x^\beta\partial x^\beta}-\left(\frac{\partial^2\varphi}{\partial x^\alpha\partial x^\beta}\right)^2\right)+2\frac{\partial\varphi}{\partial x^\alpha}\frac{\partial\varphi}{\partial x^\beta}\left(\frac{\partial^2\varphi}{\partial x^\alpha\partial x^\gamma}\frac{\partial^2\varphi}{\partial x^\beta\partial x^\gamma}-\frac{\partial^2\varphi}{\partial x^\alpha\partial x^\beta}\frac{\partial^2\varphi}{\partial x^\gamma\partial x^\gamma}\right)$$
$$+2\frac{\partial\varphi}{\partial x^\beta}\frac{\partial\varphi}{\partial x^\gamma}\left(\frac{\partial^2\varphi}{\partial x^\alpha\partial x^\beta}\frac{\partial^2\varphi}{\partial x^\alpha\partial x^\gamma}-\frac{\partial^2\varphi}{\partial x^\beta\partial x^\gamma}\frac{\partial^2\varphi}{\partial x^\alpha\partial x^\alpha}\right)$$
$$\left.+2\frac{\partial\varphi}{\partial x^\alpha}\frac{\partial\varphi}{\partial x^\gamma}\left(\frac{\partial^2\varphi}{\partial x^\alpha\partial x^\beta}\frac{\partial^2\varphi}{\partial x^\beta\partial x^\gamma}-\frac{\partial^2\varphi}{\partial x^\alpha\partial x^\gamma}\frac{\partial^2\varphi}{\partial x^\beta\partial x^\beta}\right)\right)\Big/\left(\left(\frac{\partial\varphi}{\partial x^\alpha}\right)^2+\left(\frac{\partial\varphi}{\partial x^\beta}\right)^2+\left(\frac{\partial\varphi}{\partial x^\gamma}\right)^2\right)^2. \tag{4.3.53}$$

Theorem 4.3.3. *The principal curvatures κ_1 and κ_2 relate to the Gaussian curvature κ_G and mean curvature κ_M through*

$$\kappa_1 = \kappa_M + \sqrt{\kappa_M^2 - \kappa_G} \tag{4.3.54}$$

and

$$\kappa_2 = \kappa_M - \sqrt{\kappa_M^2 - \kappa_G}. \tag{4.3.55}$$

Equivalently,

$$\kappa_G = \kappa_1\kappa_2 \tag{4.3.56}$$

and

$$\kappa_M = \frac{\kappa_1+\kappa_2}{2}. \tag{4.3.57}$$

Lemma 4.3.4.

$$\kappa_M = -\frac{1}{2}\left(\frac{\partial^2\chi}{\partial\tilde{x}^\beta\partial\tilde{x}^\beta}(0,0)+\frac{\partial^2\chi}{\partial\tilde{x}^\gamma\partial\tilde{x}^\gamma}(0,0)\right), \tag{4.3.58}$$

$$\kappa_G = \frac{\partial^2 \chi}{\partial \tilde{x}^\beta \partial \tilde{x}^\beta}(0,0) \frac{\partial^2 \chi}{\partial \tilde{x}^\gamma \partial \tilde{x}^\gamma}(0,0) - \left(\frac{\partial^2 \chi}{\partial \tilde{x}^\beta \partial \tilde{x}^\gamma}(0,0) \right)^2 . \tag{4.3.59}$$

Proof. By definition, the mean curvature κ_M for a 3D surface given by

$$\varphi\left(\tilde{x}^\alpha, \tilde{x}^\beta, \tilde{x}^\gamma\right) = \tilde{x}^\alpha - \chi\left(\tilde{x}^\beta, \tilde{x}^\gamma\right) \tag{4.3.60}$$

at the origin of the local Cartesian coordinates $\left(\tilde{x}^\alpha, \tilde{x}^\beta, \tilde{x}^\gamma\right)$ is

$$\begin{aligned} \kappa_M &= \frac{1}{2}\left(\frac{\partial^2 \varphi}{\partial \tilde{x}^\beta \partial \tilde{x}^\beta}(0,0) + \frac{\partial^2 \varphi}{\partial \tilde{x}^\gamma \partial \tilde{x}^\gamma}(0,0) \right) \\ &= -\frac{1}{2}\left(\frac{\partial^2 \chi}{\partial \tilde{x}^\beta \partial \tilde{x}^\beta}(0,0) + \frac{\partial^2 \chi}{\partial \tilde{x}^\gamma \partial \tilde{x}^\gamma}(0,0) \right). \end{aligned} \tag{4.3.61}$$

By definition, the Gaussian curvature κ_G at the origin of the local Cartesian coordinates is

$$\begin{aligned} \kappa_G &= \frac{\partial^2 \varphi}{\partial \tilde{x}^\beta \partial x^\beta}(0,0) \frac{\partial^2 \varphi}{\partial \tilde{x}^\gamma \partial x^\gamma}(0,0) - \left(\frac{\partial^2 \varphi}{\partial \tilde{x}^\beta \partial \tilde{x}^\gamma}(0,0) \right)^2 \\ &= \frac{\partial^2 \chi}{\partial \tilde{x}^\beta \partial \tilde{x}^\beta}(0,0) \frac{\partial^2 \chi}{\partial \tilde{x}^\gamma \partial \tilde{x}^\gamma}(0,0) - \left(\frac{\partial^2 \chi}{\partial \tilde{x}^\beta \partial \tilde{x}^\gamma}(0,0) \right)^2 . \end{aligned} \tag{4.3.62}$$

□

Remark 4.3.5. *Let the second-order surface derivative matrix be*

$$S = -\begin{pmatrix} \dfrac{\partial^2 \chi}{\partial \tilde{x}^\beta \partial \tilde{x}^\beta} & \dfrac{\partial^2 \chi}{\partial \tilde{x}^\beta \partial \tilde{x}^\gamma} \\ \dfrac{\partial^2 \chi}{\partial \tilde{x}^\beta \partial \tilde{x}^\gamma} & \dfrac{\partial^2 \chi}{\partial \tilde{x}^\gamma \partial \tilde{x}^\gamma} \end{pmatrix}. \tag{4.3.63}$$

Then

$$2\kappa_M = tr(S) \tag{4.3.64}$$

and

$$\kappa_G = |S|. \tag{4.3.65}$$

This result is well-known in differential geometry.

Chapter 5

Solving Stokes Equations and Advection Equation

The incompressible Stokes equations may be solved using the projection method [4] which decouples the Stokes equations into Poisson elliptic equations. The main difficulty for the two-phase Stokes equations is that the jump conditions $\left[\mu u^i\right]$ are not known except when $\mu^+ = \mu^-$. We choose to solve for $\left[\mu u^i\right]$ (i.e. the augmented variables [25, 27, 28, 30, 54, 29]) using iterative methods first and then solve the two-phase Stokes equations. The advection equation is solved using an upwind scheme.

5.1 Solving Stokes Equations with an Interface

The momentum equation for the Stokes equations is

$$\begin{aligned}\frac{\partial p}{\partial x^i} &= \frac{\partial}{\partial x^j}\left(\mu\left(\frac{\partial u^i}{\partial x^j} + \frac{\partial u^j}{\partial x^i}\right)\right) + g^i, \quad \boldsymbol{x} \in \Omega^+ \text{ or } \Omega^- \\ &= \frac{\partial^2\left(\mu u^i\right)}{\partial x^j \partial x^j} + \frac{\partial^2\left(\mu u^j\right)}{\partial x^j \partial x^i} + g^i \qquad (\mu \text{ is piecewise constant}) \\ &= \frac{\partial^2\left(\mu u^i\right)}{\partial x^j \partial x^j} + g^i. \qquad (\text{incompressibility condition})\end{aligned} \tag{5.1.1}$$

If we apply the divergence operator to both sides of Eq. (5.1.1) and make use of the incompressibility condition in each fluid, we get an elliptic equation for p:

$$\frac{\partial^2 p}{\partial x^i \partial x^i} = \frac{\partial g^i}{\partial x^i}. \tag{5.1.2}$$

We can solve Eq. (5.1.2) if we know the jump conditions $[p]$ and $\left[\dfrac{\partial p}{\partial n}\right]$. After we solve the pressure p, we can rewrite Eq. (5.1.1) as

$$\frac{\partial^2\left(\mu u^i\right)}{\partial x^j \partial x^j} = \frac{\partial p}{\partial x^i} - g^i. \tag{5.1.3}$$

If we know the jump conditions $\left[\mu u^i\right]$ and $\left[\dfrac{\partial\left(\mu u^i\right)}{\partial n}\right]$, we can solve the elliptic equation (5.1.3) for μu^i. The velocity field u^i may be recovered from μu^i by rescaling. This is called the *decoupled Poisson equations approach.*

The jump conditions $[p]$, $\left[\dfrac{\partial p}{\partial n}\right]$ and $\left[\dfrac{\partial\left(\mu u^i\right)}{\partial n}\right]$ have been derived and they depend on the unknown jump condition $\left[\mu u^i\right]$. Therefore if we know $\left[\mu u^i\right]$, the Stokes equations may be solved using the immersed interface methods. Also notice that since $\left[u^i\right]=0$, we have

$$\left[\mu u^i\right] = \left(u^i\right)_\Gamma^+ [\mu] = \left(u^i\right)_\Gamma^- [\mu]. \tag{5.1.4}$$

Eq. (5.1.4) shows that $\left[\mu u^i\right]$ equals $\left(u^i\right)_\Gamma^+$ (or $\left(u^i\right)_\Gamma^-$) rescaled by $[\mu]$.

Proposition 5.1.1. *If, given a guess of $\left[\mu u^i\right]$ for a Stokes flow with boundary conditions on $\partial\Omega$ and with an interface, the solution of Eqs. (5.1.2, 5.1.3) with jump conditions*

$$\left[\mu u^i\right], \quad \left[\frac{\partial\left(\mu u^i\right)}{\partial n}\right], \quad [p], \quad \left[\frac{\partial p}{\partial n}\right] \tag{5.1.5}$$

satisfies the continuity equation

$$\left[u^i\right]=0, \tag{5.1.6}$$

then the given guess of $\left[\mu u^i\right]$ is the actual jump condition for the problem.

Now we will show how to solve for $\left[\mu u^i\right]$ numerically. Let us look at the discretized Stokes equations using the immersed interface method. We denote the values of p and μu^i at grid points as a vector X and $\left[\mu u^i\right]$ for projection points of irregular grid points as a vector Y.

Given Y, we can always use the immersed interface method to solve for X. This means that

$$CY + DX = F \tag{5.1.7}$$

where C and D are two matrices and F is a vector. Note that D is always invertible and the inversion of D is to solve the Stokes equations with interface using the immersed interface method given the jump conditions. So from Eq. (5.1.7)

$$X = D^{-1}\left(F - CY\right). \tag{5.1.8}$$

Given X, we can interpolate $\left[u^i\right]$ for projection points of irregular grid points. We denote the interpolated values of $\left[u^i\right]$ as a vector R and it depends on both X and Y linearly, i.e.

$$R = AY + BX - E \tag{5.1.9}$$

where A and B are two matrices and E is a vector. From Eqs. (5.1.8, 5.1.9), we have

$$\begin{aligned} R(Y) &= AY + BD^{-1}\left(F - CY\right) - E \\ &= \left(A - BD^{-1}C\right)Y + \left(BD^{-1}F - E\right). \end{aligned} \tag{5.1.10}$$

From Proposition 5.1.1, we need to solve the Schur complement equation for Y

$$\left(A - BD^{-1}C\right)Y = \left(E - BD^{-1}F\right). \tag{5.1.11}$$

To solve Eq. (5.1.11), we need to know the coefficient matrix $\left(A - BD^{-1}C\right)$ and the right hand side vector $\left(E - BD^{-1}F\right)$.

We choose to use the Generalized Minimum RESidual (GMRES) method [49] to invert $\left(A - BD^{-1}C\right)$. GMRES is a Krylov based iterative method which has been used to solve large, sparse and non-Hermitian linear systems. To use GMRES, we need to know the matrix-vector product $\left(A - BD^{-1}C\right)V$ for a given vector V and the vector $\left(E - BD^{-1}F\right)$.

Theorem 5.1.1. *Given a vector V, we have*

$$\left(A - BD^{-1}C\right)V = R(Y = V) - R(Y = \mathbf{0}) \tag{5.1.12}$$

and

$$E - BD^{-1}F = -R(Y = \mathbf{0}). \tag{5.1.13}$$

Proof.

$$\begin{aligned} \left(A - BD^{-1}C\right)V &= \left(A - BD^{-1}C\right)V + BD^{-1}F - E \\ &\quad - \left(\left(A - BD^{-1}C\right)\mathbf{0} + BD^{-1}F - E\right) \\ &= R(Y = V) - R(Y = \mathbf{0}). \end{aligned} \tag{5.1.14}$$

It is obvious that Eq. (5.1.13) is true. □

After we solve Eq. (5.1.11) using GMRES (or other methods), we can plug the solution of Y into Eq. (5.1.8) to solve X and this concludes the algorithm.

Since we know how to solve the unknown jump condition $\left[\mu u^i\right]$, now let us focus on the forward problem, that is, assuming that $\left[\mu u^i\right]$ is known, we want to solve the Stokes equations with an interface. Here we explain the details for both 2D and 3D problems.

5.1.1 2D Geometry

For 2D problems, let the coordinate transformation matrix be

$$A = \begin{pmatrix} n^\alpha & \tau^\alpha \\ n^\beta & \tau^\beta \end{pmatrix}. \tag{5.1.15}$$

We have the elliptic equation for pressure p:

$$\frac{\partial^2 p}{\partial x^\alpha \partial x^\alpha} + \frac{\partial^2 p}{\partial x^\beta \partial x^\beta} = \frac{\partial g^\alpha}{\partial x^\alpha} + \frac{\partial g^\beta}{\partial x^\beta} \tag{5.1.16}$$

with jump conditions

$$[p] = -2\left(A^{-1}\right)_j^\beta \frac{d\left[\mu u^j\right]}{d\tilde{x}^\beta} + \tilde{f}^\alpha, \tag{5.1.17}$$

and

$$\begin{aligned}\left[\frac{\partial p}{\partial n}\right] = & -2\frac{d^2\chi}{d\tilde{x}^\beta d\tilde{x}^\beta}\left(A^{-1}\right)_j^\beta \frac{d\left[\mu u^j\right]}{d\tilde{x}^\beta} + 2\left(A^{-1}\right)_j^\alpha \frac{d^2\left[\mu u^j\right]}{d\tilde{x}^\beta d\tilde{x}^\beta} \\ & + \frac{d^2\chi}{d\tilde{x}^\beta d\tilde{x}^\beta}\tilde{f}^\alpha + \frac{d\tilde{f}^\beta}{d\tilde{x}^\beta} + \left[\tilde{g}^\alpha\right].\end{aligned} \tag{5.1.18}$$

There are two elliptic equations for the velocity field $\left(u^\alpha, u^\beta\right)$:

$$\frac{\partial^2\left(\mu u^\alpha\right)}{\partial x^\alpha \partial x^\alpha} + \frac{\partial^2\left(\mu u^\alpha\right)}{\partial x^\beta \partial x^\beta} = \frac{\partial p}{\partial x^\alpha} - g^\alpha \tag{5.1.19}$$

and

$$\frac{\partial^2\left(\mu u^\beta\right)}{\partial x^\alpha \partial x^\alpha} + \frac{\partial^2\left(\mu u^\beta\right)}{\partial x^\beta \partial x^\beta} = \frac{\partial p}{\partial x^\beta} - g^\beta \tag{5.1.20}$$

with jump conditions

$$\left[\mu u^\alpha\right], \quad \left[\mu u^\beta\right] \tag{5.1.21}$$

and

$$\begin{pmatrix} \left[\dfrac{\partial\left(\mu u^\alpha\right)}{\partial n}\right] \\[3ex] \left[\dfrac{\partial\left(\mu u^\beta\right)}{\partial n}\right] \end{pmatrix} = A \begin{pmatrix} -\left(A^{-1}\right)_j^\beta \dfrac{d\left[\mu u^j\right]}{d\tilde{x}^\beta} \\[3ex] -\left(A^{-1}\right)_j^\alpha \dfrac{d\left[\mu u^j\right]}{d\tilde{x}^\beta} - \tilde{f}^\beta \end{pmatrix}. \tag{5.1.22}$$

It is clear that we need to call the IIM solver for elliptic equations three times in order to solve the Stokes equations in 2D with known jump condition $\left[\mu u^i\right]$.

5.1.2 3D Geometry

For 3D problems, let the coordinate transformation matrix be

$$A = \begin{pmatrix} n^\alpha & \tau^\alpha & \eta^\alpha \\ n^\beta & \tau^\beta & \eta^\beta \\ n^\gamma & \tau^\gamma & \eta^\gamma \end{pmatrix}. \tag{5.1.23}$$

We have the elliptic equation for pressure p:

$$\frac{\partial^2 p}{\partial x^\alpha \partial x^\alpha} + \frac{\partial^2 p}{\partial x^\beta \partial x^\beta} + \frac{\partial^2 p}{\partial x^\gamma \partial x^\gamma} = \frac{\partial g^\alpha}{\partial x^\alpha} + \frac{\partial g^\beta}{\partial x^\beta} + \frac{\partial g^\gamma}{\partial x^\gamma} \tag{5.1.24}$$

with jump conditions

$$[p] = -2\left(A^{-1}\right)_j^\beta \frac{\partial\left[\mu u^j\right]}{\partial\tilde{x}^\beta} - 2\left(A^{-1}\right)_j^\gamma \frac{\partial\left[\mu u^j\right]}{\partial\tilde{x}^\gamma} + \tilde{f}^\alpha, \tag{5.1.25}$$

and

$$\begin{aligned}\left[\frac{\partial p}{\partial n}\right] = &-2\frac{\partial^2\chi}{\partial\tilde{x}^\beta\partial\tilde{x}^\beta}\left(A^{-1}\right)_j^\beta \frac{\partial\left[\mu u^j\right]}{\partial\tilde{x}^\beta} - 2\frac{\partial^2\chi}{\partial\tilde{x}^\gamma\partial\tilde{x}^\gamma}\left(A^{-1}\right)_j^\gamma \frac{\partial\left[\mu u^j\right]}{\partial\tilde{x}^\gamma}\\ &- 2\frac{\partial^2\chi}{\partial\tilde{x}^\beta\partial\tilde{x}^\gamma}\left(A^{-1}\right)_j^\beta \frac{\partial\left[\mu u^j\right]}{\partial\tilde{x}^\gamma} - 2\frac{\partial^2\chi}{\partial\tilde{x}^\beta\partial\tilde{x}^\gamma}\left(A^{-1}\right)_j^\gamma \frac{\partial\left[\mu u^j\right]}{\partial\tilde{x}^\beta}\\ &+ 2\left(A^{-1}\right)_j^\alpha \frac{\partial^2\left[\mu u^j\right]}{\partial\tilde{x}^\beta\partial\tilde{x}^\beta} + 2\left(A^{-1}\right)_j^\alpha \frac{\partial^2\left[\mu u^j\right]}{\partial\tilde{x}^\gamma\partial\tilde{x}^\gamma}\\ &+ \left(\frac{\partial^2\chi}{\partial\tilde{x}^\beta\partial\tilde{x}^\beta} + \frac{\partial^2\chi}{\partial\tilde{x}^\gamma\partial\tilde{x}^\gamma}\right)\tilde{f}^\alpha + \frac{\partial\tilde{f}^\beta}{\partial\tilde{x}^\beta} + \frac{\partial\tilde{f}^\gamma}{\partial\tilde{x}^\gamma} + \left[\tilde{g}^\alpha\right].\end{aligned} \tag{5.1.26}$$

There are three elliptic equations for the velocity field $\left(u^\alpha, u^\beta, u^\gamma\right)$:

$$\frac{\partial^2\left(\mu u^\alpha\right)}{\partial x^\alpha\partial x^\alpha} + \frac{\partial^2\left(\mu u^\alpha\right)}{\partial x^\beta\partial x^\beta} + \frac{\partial^2\left(\mu u^\alpha\right)}{\partial x^\gamma\partial x^\gamma} = \frac{\partial p}{\partial x^\alpha} - g^\alpha, \tag{5.1.27}$$

$$\frac{\partial^2\left(\mu u^\beta\right)}{\partial x^\alpha\partial x^\alpha} + \frac{\partial^2\left(\mu u^\beta\right)}{\partial x^\beta\partial x^\beta} + \frac{\partial^2\left(\mu u^\beta\right)}{\partial x^\gamma\partial x^\gamma} = \frac{\partial p}{\partial x^\beta} - g^\beta, \tag{5.1.28}$$

and

$$\frac{\partial^2\left(\mu u^\gamma\right)}{\partial x^\alpha\partial x^\alpha} + \frac{\partial^2\left(\mu u^\gamma\right)}{\partial x^\beta\partial x^\beta} + \frac{\partial^2\left(\mu u^\gamma\right)}{\partial x^\gamma\partial x^\gamma} = \frac{\partial p}{\partial x^\gamma} - g^\gamma \tag{5.1.29}$$

with jump conditions

$$\left[\mu u^\alpha\right], \quad \left[\mu u^\beta\right], \quad \left[\mu u^\gamma\right] \tag{5.1.30}$$

and

$$\begin{pmatrix} \left[\dfrac{\partial\left(\mu u^\alpha\right)}{\partial n}\right] \\ \\ \left[\dfrac{\partial\left(\mu u^\beta\right)}{\partial n}\right] \\ \\ \left[\dfrac{\partial\left(\mu u^\gamma\right)}{\partial n}\right] \end{pmatrix} = A \begin{pmatrix} -\left(A^{-1}\right)_j^\beta \dfrac{\partial\left[\mu u^j\right]}{\partial\tilde{x}^\beta} - \left(A^{-1}\right)_j^\gamma \dfrac{\partial\left[\mu u^j\right]}{\partial\tilde{x}^\gamma} \\ \\ -\left(A^{-1}\right)_j^\alpha \dfrac{\partial\left[\mu u^j\right]}{\partial\tilde{x}^\beta} - \tilde{f}^\beta \\ \\ -\left(A^{-1}\right)_j^\alpha \dfrac{\partial\left[\mu u^j\right]}{\partial\tilde{x}^\gamma} - \tilde{f}^\gamma \end{pmatrix}. \tag{5.1.31}$$

It is clear that we need to call the IIM solver for elliptic equations four times in order to solve the Stokes equations in 3D with known jump condition $\left[\mu u^i\right]$.

5.2 Solving Advection Equation

For the hyperbolic advection equation

$$\frac{\partial c}{\partial t} = -u^i \frac{\partial c}{\partial x^i}, \tag{5.2.1}$$

we use the forward Euler method for the time derivative and upwinding for the advection term. So

$$\frac{\partial c}{\partial t}(t = t_n) \approx \frac{c^{n+1} - c^n}{\Delta t}. \tag{5.2.2}$$

If $u^i > 0$,

$$\frac{\partial c}{\partial x^i}(x^i = x^i_k) \approx \frac{c(x^i = x^i_k) - c(x^i = x^i_{k-1})}{h}, \tag{5.2.3}$$

otherwise

$$\frac{\partial c}{\partial x^i}(x^i = x^i_k) \approx \frac{c(x^i = x^i_{k+1}) - c(x^i = x^i_k)}{h}. \tag{5.2.4}$$

Chapter 6

Numerical Implementation: Differencing and Interpolation

The elliptic solver using the immersed interface method enables us to use a widely available fast Poisson solver to solve the discrete systems of equations. The fast Poisson solver, for example the one from Fishpack [1], only requires $O(Nlog(N))$ operations, where N is the total number of grid points. Therefore the Stokes equations with given jump condition $\left[\mu u^i\right]$ can be solved in $O(3Nlog(N))$ operations for 2D problems and $O(4Nlog(N))$ operations for 3D problems, which corresponds to the cost of one GMRES iteration.

One major step of the IIM solver is to calculate the correction term needed for irregular grid points. For GMRES iterations, the major step is to calculate the residual vector. We explain the details of those two major steps by showing the finite difference and interpolations involved for both 2D and 3D problems.

6.1 2D Geometry

6.1.1 Differencing

To approximate the derivatives for a given grid function which is smooth in Ω such as the level set function φ, we can use the central finite difference schemes:

$$\left.\frac{\partial \varphi}{\partial x^\alpha}\right|_{i,j} \approx \frac{\varphi_{i+1,j} - \varphi_{i-1,j}}{2h}, \tag{6.1.1}$$

$$\left.\frac{\partial \varphi}{\partial x^\beta}\right|_{i,j} \approx \frac{\varphi_{i,j+1} - \varphi_{i,j-1}}{2h}, \tag{6.1.2}$$

$$\left.\frac{\partial^2 \varphi}{\partial x^\alpha \partial x^\alpha}\right|_{i,j} \approx \frac{\varphi_{i+1,j} - 2\varphi_{i,j} + \varphi_{i-1,j}}{h^2}, \tag{6.1.3}$$

$$\left.\frac{\partial^2\varphi}{\partial x^\beta \partial x^\beta}\right|_{i,j} \approx \frac{\varphi_{i,j+1} - 2\varphi_{i,j} + \varphi_{i,j-1}}{h^2}, \tag{6.1.4}$$

$$\left.\frac{\partial^2\varphi}{\partial x^\alpha \partial x^\beta}\right|_{i,j} = \left.\frac{\partial^2\varphi}{\partial x^\beta \partial x^\alpha}\right|_{i,j} \approx \frac{\varphi_{i+1,j+1} + \varphi_{i-1,j-1} - \varphi_{i+1,j-1} - \varphi_{i-1,j+1}}{4h^2}. \tag{6.1.5}$$

If the grid function may be discontinuous in Ω while sufficiently smooth in subregions Ω^+ and Ω^-, such as the body force component g^α in the Stokes equations, we choose to use a one-sided least square scheme to approximate the derivatives at those grid points close to or on the interface where the discontinuity happens. For example, given such a grid point $\boldsymbol{x} = \left(x_i^\alpha, x_j^\beta\right) \in \Omega^+$ and its neighboring grid points $\left\{\left(x_m^\alpha, x_n^\beta\right) \mid \left(x_m^\alpha, x_n^\beta\right) \in \Omega^+\right\}$, we use the following scheme:

$$\sum_{m,n} a_{m,n} g^\alpha_{m,n} \tag{6.1.6}$$

where $a_{m,n}$ is the coefficient to be determined. The Taylor expansion of $g^\alpha_{m,n}$ at $\boldsymbol{x}$ is

$$\begin{aligned} g^\alpha_{m,n} = g^\alpha_{i,j} &+ \left.\frac{\partial g^\alpha}{\partial x^\alpha}\right|_{i,j}\left(x_m^\alpha - x_i^\alpha\right) + \left.\frac{\partial g^\alpha}{\partial x^\beta}\right|_{i,j}\left(x_n^\beta - x_j^\beta\right) + \frac{1}{2}\left.\frac{\partial^2 g^\alpha}{\partial x^\alpha \partial x^\alpha}\right|_{i,j}\left(x_m^\alpha - x_i^\alpha\right)^2 \\ &+ \frac{1}{2}\left.\frac{\partial^2 g^\alpha}{\partial x^\beta \partial x^\beta}\right|_{i,j}\left(x_n^\beta - x_j^\beta\right)^2 + \left.\frac{\partial^2 g^\alpha}{\partial x^\alpha \partial x^\beta}\right|_{i,j}\left(x_m^\alpha - x_i^\alpha\right)\left(x_n^\beta - x_j^\beta\right) + \cdots . \end{aligned} \tag{6.1.7}$$

Substituting Eq. (6.1.7) into Eq. (6.1.6), to approximate $\left.\frac{\partial g^\alpha}{\partial x^\alpha}\right|_{i,j}$, $\left.\frac{\partial g^\alpha}{\partial x^\beta}\right|_{i,j}$, $\left.\frac{\partial^2 g^\alpha}{\partial x^\alpha \partial x^\alpha}\right|_{i,j}$, $\left.\frac{\partial^2 g^\alpha}{\partial x^\beta \partial x^\beta}\right|_{i,j}$ and $\left.\frac{\partial^2 g^\alpha}{\partial x^\alpha \partial x^\beta}\right|_{i,j}$, the coefficients $a_{m,n}$ in the interpolation scheme (6.1.6) are seen to be the solution of the following linear systems of equations :

$$\begin{pmatrix} \sum_{m,n} a_{m,n} \\ \sum_{m,n} (a_{m,n}(x_m^\alpha - x_i^\alpha)) \\ \sum_{m,n} \left(a_{m,n}(x_n^\beta - x_j^\beta)\right) \\ \sum_{m,n} \left(\frac{1}{2} a_{m,n}(x_m^\alpha - x_i^\alpha)^2\right) \\ \sum_{m,n} \left(\frac{1}{2} a_{m,n}(x_n^\beta - x_j^\beta)^2\right) \\ \sum_{m,n} \left(a_{m,n}(x_m^\alpha - x_i^\alpha)(x_n^\beta - x_j^\beta)\right) \end{pmatrix} = \begin{pmatrix} 0 \\ 1 \\ 0 \\ 0 \\ 0 \\ 0 \end{pmatrix}, \cdots, \begin{pmatrix} 0 \\ 0 \\ 0 \\ 0 \\ 0 \\ 1 \end{pmatrix}. \tag{6.1.8}$$

If we choose more than six grid points (including the point $\boldsymbol{x}$) for the interpolation, then the linear system of equations (6.1.8) is underdetermined, that is, there are an infinite number of solutions. We use the singular value decomposition (SVD) method [9] to get the unique solution that has the least 2-norm among all feasible solutions. At the majority regular grid points, the central finite difference schemes (6.1.1 - 6.1.5) can still be used.

6.1.2 Bilinear interpolation

To calculate the local coordinate transformation matrix, we need to approximate the level set derivatives such as $\dfrac{\partial \varphi}{\partial x^{\alpha}}$ at interface projection point $\boldsymbol{x}_* \in \Gamma$ and we choose to use bilinear interpolation here. We label the four grid points surrounding $\boldsymbol{x}_*$ as

$$\left(x_i^{\alpha}, x_j^{\beta}\right), \left(x_{i+1}^{\alpha}, x_j^{\beta}\right), \left(x_i^{\alpha}, x_{j+1}^{\beta}\right), \left(x_{i+1}^{\alpha}, x_{j+1}^{\beta}\right). \tag{6.1.9}$$

If we define

$$a = \frac{2\left(x_*^{\alpha} - x_i^{\alpha}\right)}{h} - 1, \quad b = \frac{2\left(x_*^{\beta} - x_j^{\beta}\right)}{h} - 1, \tag{6.1.10}$$

then we can use the following bilinear interpolation scheme

$$\begin{aligned} \frac{\partial \varphi}{\partial x^{\alpha}}\left(\boldsymbol{x} = \boldsymbol{x}^*\right) \approx \frac{1}{4}\Bigg(& (1-a)(1-b)\left.\frac{\partial \varphi}{\partial x^{\alpha}}\right|_{i,j} + (1+a)(1-b)\left.\frac{\partial \varphi}{\partial x^{\alpha}}\right|_{i+1,j} \\ & + (1-a)(1+b)\left.\frac{\partial \varphi}{\partial x^{\alpha}}\right|_{i,j+1} + (1+a)(1+b)\left.\frac{\partial \varphi}{\partial x^{\alpha}}\right|_{i+1,j+1}\Bigg). \end{aligned} \tag{6.1.11}$$

6.1.3 Interface interpolation

Calculation of the correction term involves both the local Cartesian coordinates $\left(\tilde{x}^{\alpha}, \tilde{x}^{\beta}\right)$ and local derivatives of jump conditions such as $\dfrac{dw}{d\tilde{x}^{\beta}}$ where w is a jump condition. Given an interface point $\boldsymbol{x}_* = \left(x_*^{\alpha}, x_*^{\beta}\right) \in \Gamma$ and its neighboring interface points $\left\{\left(x_i^{\alpha}, x_i^{\beta}\right) \,\middle|\, \left(x_i^{\alpha}, x_i^{\beta}\right) \in \Gamma\right\}$, using the local coordinate system centered at $\boldsymbol{x}_*$, the least square interpolation scheme to approximate $\dfrac{dw}{d\tilde{x}^{\beta}}$ at the local origin can be written as

$$\sum_i a_i w(\tilde{x}_i^{\beta}) \tag{6.1.12}$$

where a_i are the coefficients to be determined and $\tilde{x}_i^{\beta} = \left(A^{-1}\right)_j^{\beta}\left(x_i^j - x_*^j\right)$. Substituting the Taylor expansion of $w(\tilde{x}_i^{\beta})$ at the local origin

$$w(\tilde{x}_i^{\beta}) = w(0) + \frac{dw}{d\tilde{x}^{\beta}}(0)\tilde{x}_i^{\beta} + \frac{1}{2}\frac{d^2 w}{d\tilde{x}^{\beta} d\tilde{x}^{\beta}}(0)\left(\tilde{x}_i^{\beta}\right)^2 + \cdots \tag{6.1.13}$$

into Eq. (6.1.12), the coefficients a_i are the solution of the following linear system of equations:

$$\begin{pmatrix} \sum_i a_i \\ \sum_i \left(a_i \tilde{x}_i^\beta\right) \\ \sum_i \left(\frac{1}{2} a_i (\tilde{x}_i^\beta)^2\right) \end{pmatrix} = \begin{pmatrix} 0 \\ 1 \\ 0 \end{pmatrix}. \tag{6.1.14}$$

We can also approximate w and $\dfrac{d^2 w}{d\tilde{x}^\beta d\tilde{x}^\beta}$ at the local origin by changing the right hand side vector to $(1,0,0)^T$ and $(0,0,1)^T$ in Eq. (6.1.14). If we choose more than three interface points for the interpolation, then Eq. (6.1.14) is underdetermined and we use the SVD method to solve it.

6.1.4 Residual interpolation

For projection points from irregular *inner* grid points, the values of unknown jump conditions, such as $\left[\mu u^i\right]$ for the Stokes equations, are discretized and denoted as Y and we use interpolations (6.1.14) to approximate $\left[\mu u^i\right]$ for projection points from irregular *outer* grid points.

To solve for Y, we need to calculate the residual vector R and we use a two-sided least square interpolation method. For example, for Stokes equations, the residual is $\left(u^i\right)_\Gamma^+$ where u^i is the velocity. Given an interface point $\boldsymbol{x}_* = \left(x_*^\alpha, x_*^\beta\right) \in \Gamma$ and its neighboring grid points $\left\{\left(x_m^\alpha, x_n^\beta\right) \middle| \left(x_m^\alpha, x_n^\beta\right) \in \Omega\right\}$, we use the following scheme:

$$\sum_{m,n} a_{m,n} u_{m,n}^i + b \tag{6.1.15}$$

where $a_{m,n}$ are the coefficients to be determined and b is a correction term due to the two-sided scheme. Using the local Cartesian coordinate system centered at $\boldsymbol{x}_*$, the local coordinates for the interpolation grid points are denoted as $\left(\tilde{x}_{m,n}^\alpha, \tilde{x}_{m,n}^\beta\right)$. The Taylor expansion of $u_{m,n}^i$ at the local origin is

$$\begin{aligned} u_{m,n}^i = {} & \left(u^i\right)^\pm(0) + \frac{\partial\left(u^i\right)^\pm}{\partial \tilde{x}^\alpha}(0)\tilde{x}_{m,n}^\alpha + \frac{\partial\left(u^i\right)^\pm}{\partial \tilde{x}^\beta}(0)\tilde{x}_{m,n}^\beta + \frac{1}{2}\frac{\partial^2\left(u^i\right)^\pm}{\partial \tilde{x}^\alpha \partial \tilde{x}^\alpha}(0)\left(\tilde{x}_{m,n}^\alpha\right)^2 \\ & + \frac{1}{2}\frac{\partial^2\left(u^i\right)^\pm}{\partial \tilde{x}^\beta \partial \tilde{x}^\beta}(0)\left(\tilde{x}_{m,n}^\beta\right)^2 + \frac{\partial^2\left(u^i\right)^\pm}{\partial \tilde{x}^\alpha \partial \tilde{x}^\beta}(0)\tilde{x}_{m,n}^\alpha \tilde{x}_{m,n}^\beta + \cdots. \end{aligned} \tag{6.1.16}$$

The $\pm$ sign is determined according to whether $\left(\tilde{x}_{m,n}^\alpha, \tilde{x}_{m,n}^\beta\right) \in \Omega^\pm$. Substituting Eq. (6.1.16) into Eq. (6.1.15), to approximate $\left(u^i\right)_\Gamma^+(0)$, the coefficients $a_{m,n}$ in the interpolation scheme (6.1.15) are the solution of the following linear system of equations:

$$\begin{pmatrix} \sum_{m,n} a_{m,n} \\ \sum_{m,n} \left(a_{m,n}\tilde{x}^{\alpha}_{m,n}\right) \\ \sum_{m,n} \left(a_{m,n}\tilde{x}^{\beta}_{m,n}\right) \\ \sum_{m,n} \left(\frac{1}{2}a_{m,n}(\tilde{x}^{\alpha}_{m,n})^2\right) \\ \sum_{m,n} \left(\frac{1}{2}a_{m,n}(\tilde{x}^{\beta}_{m,n})^2\right) \\ \sum_{m,n} \left(a_{m,n}\tilde{x}^{\alpha}_{m,n}\tilde{x}^{\beta}_{m,n}\right) \end{pmatrix} = \begin{pmatrix} 1 \\ 0 \\ 0 \\ 0 \\ 0 \\ 0 \end{pmatrix}. \tag{6.1.17}$$

The correction term is

$$\begin{aligned} b = \sum_{\left(\tilde{x}^{\alpha}_{m,n},\tilde{x}^{\beta}_{m,n}\right)\in\Omega^-} a_{m,n} \Bigg(& \left[u^i\right](0) + \left[\frac{\partial\left(u^i\right)}{\partial\tilde{x}^{\alpha}}\right](0)\tilde{x}^{\alpha}_{m,n} + \left[\frac{\partial\left(u^i\right)}{\partial\tilde{x}^{\beta}}\right](0)\tilde{x}^{\beta}_{m,n} \\ & + \frac{1}{2}\left[\frac{\partial^2\left(u^i\right)}{\partial\tilde{x}^{\alpha}\partial\tilde{x}^{\alpha}}\right](0)\left(\tilde{x}^{\alpha}_{m,n}\right)^2 + \frac{1}{2}\left[\frac{\partial^2\left(u^i\right)}{\partial\tilde{x}^{\beta}\partial\tilde{x}^{\beta}}\right](0)\left(\tilde{x}^{\beta}_{m,n}\right)^2 + \left[\frac{\partial^2\left(u^i\right)}{\partial\tilde{x}^{\alpha}\partial\tilde{x}^{\beta}}\right](0)\tilde{x}^{\alpha}_{m,n}\tilde{x}^{\beta}_{m,n}\Bigg). \end{aligned} \tag{6.1.18}$$

We choose more than six grid points for the interpolation to get an underdetermined system of equations (6.1.17) which is solved by the SVD method.

6.2 3D Geometry

6.2.1 Differencing

To approximate the derivatives for a given smooth grid function such as the level set function φ, we use the central finite difference schemes:

$$\left.\frac{\partial\varphi}{\partial x^{\alpha}}\right|_{i,j,l} \approx \frac{\varphi_{i+1,j,l} - \varphi_{i-1,j,l}}{2h}, \tag{6.2.1}$$

$$\left.\frac{\partial\varphi}{\partial x^{\beta}}\right|_{i,j,l} \approx \frac{\varphi_{i,j+1,l} - \varphi_{i,j-1,l}}{2h}, \tag{6.2.2}$$

$$\left.\frac{\partial\varphi}{\partial x^{\gamma}}\right|_{i,j,l} \approx \frac{\varphi_{i,j,l+1} - \varphi_{i,j,l-1}}{2h}, \tag{6.2.3}$$

$$\left.\frac{\partial^2\varphi}{\partial x^\alpha\partial x^\alpha}\right|_{i,j,l} \approx \frac{\varphi_{i+1,j,l} - 2\varphi_{i,j,l} + \varphi_{i-1,j,l}}{h^2}, \tag{6.2.4}$$

$$\left.\frac{\partial^2\varphi}{\partial x^\beta\partial x^\beta}\right|_{i,j,l} \approx \frac{\varphi_{i,j+1,l} - 2\varphi_{i,j,l} + \varphi_{i,j-1,l}}{h^2}, \tag{6.2.5}$$

$$\left.\frac{\partial^2\varphi}{\partial x^\gamma\partial x^\gamma}\right|_{i,j,l} \approx \frac{\varphi_{i,j,l+1} - 2\varphi_{i,j,l} + \varphi_{i,j,l-1}}{h^2}, \tag{6.2.6}$$

$$\left.\frac{\partial^2\varphi}{\partial x^\alpha\partial x^\beta}\right|_{i,j,l} = \left.\frac{\partial^2\varphi}{\partial x^\beta\partial x^\alpha}\right|_{i,j,l} \approx \frac{\varphi_{i+1,j+1,l} + \varphi_{i-1,j-1,l} - \varphi_{i+1,j-1,l} - \varphi_{i-1,j+1,l}}{4h^2}, \tag{6.2.7}$$

$$\left.\frac{\partial^2\varphi}{\partial x^\alpha\partial x^\gamma}\right|_{i,j,l} = \left.\frac{\partial^2\varphi}{\partial x^\gamma\partial x^\alpha}\right|_{i,j,l} \approx \frac{\varphi_{i+1,j,l+1} + \varphi_{i-1,j,l-1} - \varphi_{i+1,j,l-1} - \varphi_{i-1,j,l+1}}{4h^2}, \tag{6.2.8}$$

$$\left.\frac{\partial^2\varphi}{\partial x^\beta\partial x^\gamma}\right|_{i,j,l} = \left.\frac{\partial^2\varphi}{\partial x^\gamma\partial x^\beta}\right|_{i,j,l} \approx \frac{\varphi_{i,j+1,l+1} + \varphi_{i,j-1,l-1} - \varphi_{i,j+1,l-1} - \varphi_{i,j-1,l+1}}{4h^2}. \tag{6.2.9}$$

If the grid function may be discontinuous in Ω while still smooth in subregions Ω^+ and Ω^-, such as the body force component g^α in the Stokes equations, we use a one-sided least square scheme to approximate the derivatives at those grid points close to or on the interface where the discontinuity happens. For example, given such a grid point $\boldsymbol{x} = \left(x_i^\alpha,\, x_j^\beta,\, x_l^\gamma\right) \in \Omega^+$ and its neighboring grid points $\left\{\left(x_m^\alpha,\, x_n^\beta,\, x_s^\gamma\right) \in \Omega^+\right\}$, we use the following scheme:

$$\sum_{m,n,s} a_{m,n,s} g^\alpha_{m,n,s} \tag{6.2.10}$$

where $a_{m,n,s}$ is the coefficient to be determined. The Taylor expansion of $g^\alpha_{m,n,s}$ at $\boldsymbol{x}$ is

$$\begin{aligned} g^\alpha_{m,n,s} = {} & g^\alpha_{i,j,l} + \left.\frac{\partial g^\alpha}{\partial x^\alpha}\right|_{i,j,l} \left(x_m^\alpha - x_i^\alpha\right) + \left.\frac{\partial g^\alpha}{\partial x^\beta}\right|_{i,j,l} \left(x_n^\beta - x_j^\beta\right) + \left.\frac{\partial g^\alpha}{\partial x^\gamma}\right|_{i,j,l} \left(x_s^\gamma - x_l^\gamma\right) \\ & + \frac{1}{2}\left.\frac{\partial^2 g^\alpha}{\partial x^\alpha\partial x^\alpha}\right|_{i,j,l} \left(x_m^\alpha - x_i^\alpha\right)^2 + \frac{1}{2}\left.\frac{\partial^2 g^\alpha}{\partial x^\beta\partial x^\beta}\right|_{i,j,l} \left(x_n^\beta - x_j^\beta\right)^2 \\ & + \frac{1}{2}\left.\frac{\partial^2 g^\alpha}{\partial x^\gamma\partial x^\gamma}\right|_{i,j,l} \left(x_s^\gamma - x_l^\gamma\right)^2 + \left.\frac{\partial^2 g^\alpha}{\partial x^\alpha\partial x^\beta}\right|_{i,j,l} \left(x_m^\alpha - x_i^\alpha\right)\left(x_n^\beta - x_j^\beta\right) \\ & + \left.\frac{\partial^2 g^\alpha}{\partial x^\alpha\partial x^\gamma}\right|_{i,j,l} \left(x_m^\alpha - x_i^\alpha\right)\left(x_s^\gamma - x_l^\gamma\right) + \left.\frac{\partial^2 g^\alpha}{\partial x^\beta\partial x^\gamma}\right|_{i,j,l} \left(x_n^\beta - x_j^\beta\right)\left(x_s^\gamma - x_l^\gamma\right) + \cdots . \end{aligned} \tag{6.2.11}$$

Substituting Eq. (6.2.11) into Eq. (6.2.10), to approximate $\left.\frac{\partial g^\alpha}{\partial x^\alpha}\right|_{i,j,l}$, $\left.\frac{\partial g^\alpha}{\partial x^\beta}\right|_{i,j,l}$, $\left.\frac{\partial g^\alpha}{\partial x^\gamma}\right|_{i,j,l}$, $\left.\frac{\partial^2 g^\alpha}{\partial x^\alpha\partial x^\alpha}\right|_{i,j,l}$, $\left.\frac{\partial^2 g^\alpha}{\partial x^\beta\partial x^\beta}\right|_{i,j,l}$, $\left.\frac{\partial^2 g^\alpha}{\partial x^\gamma\partial x^\gamma}\right|_{i,j,l}$, $\left.\frac{\partial^2 g^\alpha}{\partial x^\alpha\partial x^\beta}\right|_{i,j,l}$, $\left.\frac{\partial^2 g^\alpha}{\partial x^\alpha\partial x^\gamma}\right|_{i,j,l}$ and $\left.\frac{\partial^2 g^\alpha}{\partial x^\beta\partial x^\gamma}\right|_{i,j,l}$, the coefficients $a_{m,n,s}$ in the interpolation scheme (6.2.10) are the solution of the following linear systems of equations:

$$\begin{pmatrix} \sum_{m,n,s} a_{m,n,s} \\ \sum_{m,n,s} (a_{m,n,s}(x_m^\alpha - x_i^\alpha)) \\ \sum_{m,n,s} \left(a_{m,n,s}(x_n^\beta - x_j^\beta)\right) \\ \sum_{m,n,s} \left(a_{m,n,s}(x_s^\gamma - x_l^\gamma)\right) \\ \sum_{m,n,s} \left(\frac{1}{2}a_{m,n,s}(x_m^\alpha - x_i^\alpha)^2\right) \\ \sum_{m,n,s} \left(\frac{1}{2}a_{m,n,s}(x_n^\beta - x_j^\beta)^2\right) \\ \sum_{m,n,s} \left(\frac{1}{2}a_{m,n,s}(x_s^\gamma - x_l^\gamma)^2\right) \\ \sum_{m,n,s} \left(a_{m,n,s}(x_m^\alpha - x_i^\alpha)(x_n^\beta - x_j^\beta)\right) \\ \sum_{m,n,s} \left(a_{m,n,s}(x_m^\alpha - x_i^\alpha)(x_s^\gamma - x_l^\gamma)\right) \\ \sum_{m,n,s} \left(a_{m,n,s}(x_n^\beta - x_j^\beta)(x_s^\gamma - x_l^\gamma)\right) \end{pmatrix} = \begin{pmatrix} 0 \\ 1 \\ 0 \\ 0 \\ 0 \\ 0 \\ 0 \\ 0 \\ 0 \\ 0 \end{pmatrix}, \cdots, \begin{pmatrix} 0 \\ 0 \\ 0 \\ 0 \\ 0 \\ 0 \\ 0 \\ 0 \\ 0 \\ 1 \end{pmatrix}. \tag{6.2.12}$$

We choose more than ten grid points (including the point $\boldsymbol{x}$) for the interpolation and solve Eq. (6.2.12) using the SVD method. At the majority regular grid points, the central finite difference schemes (6.2.1 - 6.2.9) can still be used.

6.2.2 Bilinear interpolation

To calculate the local coordinate transformation matrix, we need to approximate the level set derivatives such as $\dfrac{\partial \varphi}{\partial x^\alpha}$ at interface projection point $\boldsymbol{x}_* \in \Gamma$ and we use the bilinear interpolation method. We label the eight grid points surrounding $\boldsymbol{x}_*$ as

$$\begin{aligned} &\left(x_i^\alpha, x_j^\beta, x_l^\gamma\right), \quad \left(x_{i+1}^\alpha, x_j^\beta, x_l^\gamma\right), \quad \left(x_i^\alpha, x_{j+1}^\beta, x_l^\gamma\right), \quad \left(x_i^\alpha, x_j^\beta, x_{l+1}^\gamma\right), \\ &\left(x_{i+1}^\alpha, x_{j+1}^\beta, x_l^\gamma\right), \quad \left(x_{i+1}^\alpha, x_j^\beta, x_{l+1}^\gamma\right), \quad \left(x_i^\alpha, x_{j+1}^\beta, x_{l+1}^\gamma\right), \quad \left(x_{i+1}^\alpha, x_{j+1}^\beta, x_{l+1}^\gamma\right). \end{aligned} \tag{6.2.13}$$

If we define

$$a = \frac{2\left(x_*^\alpha - x_i^\alpha\right)}{h} - 1, \quad b = \frac{2\left(x_*^\beta - x_j^\beta\right)}{h} - 1, \quad c = \frac{2\left(x_*^\gamma - x_l^\gamma\right)}{h} - 1, \tag{6.2.14}$$

then we have the following bilinear interpolation scheme

$$
\begin{aligned}
\frac{\partial\varphi}{\partial x^\alpha}\left(\boldsymbol{x}=\boldsymbol{x}^*\right) \approx \frac{1}{8}\Bigg(& (1-a)(1-b)(1-c)\left.\frac{\partial\varphi}{\partial x^\alpha}\right|_{i,j,l} + (1+a)(1-b)(1-c)\left.\frac{\partial\varphi}{\partial x^\alpha}\right|_{i+1,j,l} \\
& + (1-a)(1+b)(1-c)\left.\frac{\partial\varphi}{\partial x^\alpha}\right|_{i,j+1,l} + (1-a)(1-b)(1+c)\left.\frac{\partial\varphi}{\partial x^\alpha}\right|_{i,j,l+1} \\
& + (1+a)(1+b)(1-c)\left.\frac{\partial\varphi}{\partial x^\alpha}\right|_{i+1,j+1,l} + (1+a)(1-b)(1+c)\left.\frac{\partial\varphi}{\partial x^\alpha}\right|_{i+1,j,l+1} \\
& +(1-a)(1+b)(1+c)\left.\frac{\partial\varphi}{\partial x^\alpha}\right|_{i,j+1,l+1} + (1+a)(1+b)(1+c)\left.\frac{\partial\varphi}{\partial x^\alpha}\right|_{i+1,j+1,l+1}\Bigg).
\end{aligned}
\tag{6.2.15}
$$

6.2.3 Interface interpolation

Calculation of the correction term involves both the local Cartesian coordinates $\left(\tilde{x}^\alpha, \tilde{x}^\beta, \tilde{x}^\gamma\right)$ and local derivatives of jump conditions such as $\dfrac{\partial w}{\partial \tilde{x}^\beta}$ where w is a jump condition. Given an interface point $\boldsymbol{x}_* = \left(x_*^\alpha, x_*^\beta, x_*^\gamma\right) \in \Gamma$ and its neighboring interface points

$$\left\{\left(x_i^\alpha, x_i^\beta, x_i^\gamma\right) \,\middle|\, \left(x_i^\alpha, x_i^\beta, x_i^\gamma\right) \in \Gamma\right\},$$

using the local coordinate system centered at $\boldsymbol{x}_*$, the least square interpolation scheme to approximate $\dfrac{\partial w}{\partial \tilde{x}^\beta}$ at the local origin can be written as

$$\sum_i a_i w(\tilde{x}_i^\beta, \tilde{x}_i^\gamma) \tag{6.2.16}$$

where a_i are the coefficients to be determined and $\tilde{x}_i^k = \left(A^{-1}\right)_j^k \left(x_i^j - x_*^j\right),\ k = \beta, \gamma$. Substituting the Taylor expansion of $w(\tilde{x}_i^\beta, \tilde{x}_i^\gamma)$ at the local origin

$$
\begin{aligned}
w(\tilde{x}_i^\beta, \tilde{x}_i^\gamma) = w(0,0) + \frac{\partial w}{\partial \tilde{x}^\beta}(0,0)\tilde{x}_i^\beta + \frac{\partial w}{\partial \tilde{x}^\gamma}(0,0)\tilde{x}_i^\gamma + \frac{1}{2}\frac{\partial^2 w}{\partial \tilde{x}^\beta \partial \tilde{x}^\beta}(0,0)\left(\tilde{x}_i^\beta\right)^2 \\
+ \frac{1}{2}\frac{\partial^2 w}{\partial \tilde{x}^\gamma \partial \tilde{x}^\gamma}(0,0)\left(\tilde{x}_i^\gamma\right)^2 + \frac{\partial^2 w}{\partial \tilde{x}^\beta \partial \tilde{x}^\gamma}(0,0)\tilde{x}_i^\beta \tilde{x}_i^\gamma + \cdots
\end{aligned}
\tag{6.2.17}
$$

into Eq. (6.2.16), the coefficients a_i are the solution of the following linear system of equations:

$$\begin{pmatrix} \sum_i a_i \\ \sum_i \left(a_i \tilde{x}_i^{\beta}\right) \\ \sum_i \left(a_i \tilde{x}_i^{\gamma}\right) \\ \sum_i \left(\frac{1}{2} a_i (\tilde{x}_i^{\beta})^2\right) \\ \sum_i \left(\frac{1}{2} a_i (\tilde{x}_i^{\gamma})^2\right) \\ \sum_i \left(a_i \tilde{x}_i^{\beta} \tilde{x}_i^{\gamma}\right) \end{pmatrix} = \begin{pmatrix} 0 \\ 1 \\ 0 \\ 0 \\ 0 \\ 0 \end{pmatrix}. \tag{6.2.18}$$

We can also approximate w, $\dfrac{\partial w}{\partial \tilde{x}^{\gamma}}$, $\dfrac{\partial^2 w}{\partial \tilde{x}^{\beta} \partial \tilde{x}^{\beta}}$, $\dfrac{\partial^2 w}{\partial \tilde{x}^{\gamma} \partial \tilde{x}^{\gamma}}$ and $\dfrac{\partial^2 w}{\partial \tilde{x}^{\beta} \partial \tilde{x}^{\gamma}}$ at the local origin by changing the right hand side vector in Eq. (6.2.18). If we choose more than six interface points for the interpolation, then Eq. (6.2.18) is underdetermined and we use the SVD method to solve it.

6.2.4 Residual interpolation

For projection points from irregular *inner* grid points, the values of unknown jump conditions, such as $\left[\mu u^i\right]$ for the Stokes equations, are discretized and denoted as Y and we use interpolations (6.2.18) to approximate $\left[\mu u^i\right]$ for projection points from irregular *outer* grid points.

To solve for Y, we need to calculate the residual vector R and we use a two-sided least square interpolation method. For example, for the Stokes equations, the residual is $\left(u^i\right)_{\Gamma}^{+}$ where u^i is the velocity. Given an interface point $\boldsymbol{x}_* = \left(x_*^{\alpha}, x_*^{\beta}, x_*^{\gamma}\right) \in \Gamma$ and its neighboring grid points $\left\{\left(x_m^{\alpha}, x_n^{\beta}, x_s^{\gamma}\right) \middle| \left(x_m^{\alpha}, x_n^{\beta}, x_s^{\gamma}\right) \in \Omega\right\}$, we use the following scheme:

$$\sum_{m,n,s} a_{m,n,s} \left(u^i\right)_{m,n,s} + b \tag{6.2.19}$$

where $a_{m,n,s}$ are the coefficients to be determined and b is a correction term due to the two-sided scheme. Using the local Cartesian coordinate system centered at $\boldsymbol{x}_*$, the local coordinates for the interpolation grid points are denoted as $\left(\tilde{x}_{m,n,s}^{\alpha}, \tilde{x}_{m,n,s}^{\beta}, \tilde{x}_{m,n,s}^{\gamma}\right)$. The

Taylor expansion of $\left(u^i\right)_{m,n,s}$ at the local origin is

$$\begin{aligned}
\left(u^i\right)_{m,n,s} = \left(u^i\right)^{\pm}(0,0) &+ \frac{\partial\left(u^i\right)^{\pm}}{\partial\tilde{x}^{\alpha}}(0,0)\tilde{x}^{\alpha}_{m,n,s} + \frac{\partial\left(u^i\right)^{\pm}}{\partial\tilde{x}^{\beta}}(0,0)\tilde{x}^{\beta}_{m,n,s} + \frac{\partial\left(u^i\right)^{\pm}}{\partial\tilde{x}^{\gamma}}(0,0)\tilde{x}^{\gamma}_{m,n,s} \\
&+ \frac{1}{2}\frac{\partial^2\left(u^i\right)^{\pm}}{\partial\tilde{x}^{\alpha}\partial\tilde{x}^{\alpha}}(0,0)\left(\tilde{x}^{\alpha}_{m,n,s}\right)^2 + \frac{1}{2}\frac{\partial^2\left(u^i\right)^{\pm}}{\partial\tilde{x}^{\beta}\partial\tilde{x}^{\beta}}(0,0)\left(\tilde{x}^{\beta}_{m,n,s}\right)^2 + \frac{1}{2}\frac{\partial^2\left(u^i\right)^{\pm}}{\partial\tilde{x}^{\gamma}\partial\tilde{x}^{\gamma}}(0,0)\left(\tilde{x}^{\gamma}_{m,n,s}\right)^2 \\
&+ \frac{\partial^2\left(u^i\right)^{\pm}}{\partial\tilde{x}^{\alpha}\partial\tilde{x}^{\beta}}(0,0)\tilde{x}^{\alpha}_{m,n,s}\tilde{x}^{\beta}_{m,n,s} + \frac{\partial^2\left(u^i\right)^{\pm}}{\partial\tilde{x}^{\alpha}\partial\tilde{x}^{\gamma}}(0,0)\tilde{x}^{\alpha}_{m,n,s}\tilde{x}^{\gamma}_{m,n,s} \\
&+ \frac{\partial^2\left(u^i\right)^{\pm}}{\partial\tilde{x}^{\beta}\partial\tilde{x}^{\gamma}}(0,0)\tilde{x}^{\beta}_{m,n,s}\tilde{x}^{\gamma}_{m,n,s} + \cdots .
\end{aligned} \tag{6.2.20}$$

The $\pm$ sign is determined according to whether $\left(\tilde{x}^{\alpha}_{m,n,s}, \tilde{x}^{\beta}_{m,n,s}, \tilde{x}^{\gamma}_{m,n,s}\right) \in \Omega^{\pm}$. Substituting Eq. (6.2.20) into Eq. (6.2.19), to approximate $\left(u^i\right)^{+}_{\Gamma}(0,0)$, the coefficients $a_{m,n,s}$ in the interpolation scheme (6.2.19) are the solution of the following linear system of equations:

$$\begin{pmatrix}
\sum_{m,n,s} a_{m,n,s} \\
\sum_{m,n,s}\left(a_{m,n,s}\tilde{x}^{\alpha}_{m,n,s}\right) \\
\sum_{m,n,s}\left(a_{m,n,s}\tilde{x}^{\beta}_{m,n,s}\right) \\
\sum_{m,n,s}\left(a_{m,n,s}\tilde{x}^{\gamma}_{m,n,s}\right) \\
\sum_{m,n,s}\left(\frac{1}{2}a_{m,n,s}(\tilde{x}^{\alpha}_{m,n,s})^2\right) \\
\sum_{m,n,s}\left(\frac{1}{2}a_{m,n,s}(\tilde{x}^{\beta}_{m,n,s})^2\right) \\
\sum_{m,n,s}\left(\frac{1}{2}a_{m,n,s}(\tilde{x}^{\gamma}_{m,n,s})^2\right) \\
\sum_{m,n,s}\left(a_{m,n,s}\tilde{x}^{\alpha}_{m,n,s}\tilde{x}^{\beta}_{m,n,s}\right) \\
\sum_{m,n,s}\left(a_{m,n,s}\tilde{x}^{\alpha}_{m,n,s}\tilde{x}^{\gamma}_{m,n,s}\right) \\
\sum_{m,n,s}\left(a_{m,n,s}\tilde{x}^{\beta}_{m,n,s}\tilde{x}^{\gamma}_{m,n,s}\right)
\end{pmatrix} = \begin{pmatrix} 1 \\ 0 \\ 0 \\ 0 \\ 0 \\ 0 \\ 0 \\ 0 \\ 0 \\ 0 \end{pmatrix}. \tag{6.2.21}$$

The correction term is

$$b = \sum_{\left(\tilde{x}^{\alpha}_{m,n,s},\tilde{x}^{\beta}_{m,n,s},\tilde{x}^{\gamma}_{m,n,s}\right)\in\Omega^-} a_{m,n,s}\Bigg(\left[u^i\right](0,0) + \left[\frac{\partial\left(u^i\right)}{\partial\tilde{x}^{\alpha}}\right](0,0)\tilde{x}^{\alpha}_{m,n,s} + \left[\frac{\partial\left(u^i\right)}{\partial\tilde{x}^{\beta}}\right](0,0)\tilde{x}^{\beta}_{m,n,s}$$
$$+ \left[\frac{\partial\left(u^i\right)}{\partial\tilde{x}^{\gamma}}\right](0,0)\tilde{x}^{\gamma}_{m,n,s} + \frac{1}{2}\left[\frac{\partial^2\left(u^i\right)}{\partial\tilde{x}^{\alpha}\partial\tilde{x}^{\alpha}}\right](0,0)\left(\tilde{x}^{\alpha}_{m,n,s}\right)^2 + \frac{1}{2}\left[\frac{\partial^2\left(u^i\right)}{\partial\tilde{x}^{\beta}\partial\tilde{x}^{\beta}}\right](0,0)\left(\tilde{x}^{\beta}_{m,n,s}\right)^2$$
$$+ \frac{1}{2}\left[\frac{\partial^2\left(u^i\right)}{\partial\tilde{x}^{\gamma}\partial\tilde{x}^{\gamma}}\right](0,0)\left(\tilde{x}^{\gamma}_{m,n,s}\right)^2 + \left[\frac{\partial^2\left(u^i\right)}{\partial\tilde{x}^{\alpha}\partial\tilde{x}^{\beta}}\right](0,0)\tilde{x}^{\alpha}_{m,n,s}\tilde{x}^{\beta}_{m,n,s}$$
$$+ \left[\frac{\partial^2\left(u^i\right)}{\partial\tilde{x}^{\alpha}\partial\tilde{x}^{\gamma}}\right](0,0)\tilde{x}^{\alpha}_{m,n,s}\tilde{x}^{\gamma}_{m,n,s} + \left[\frac{\partial^2\left(u^i\right)}{\partial\tilde{x}^{\beta}\partial\tilde{x}^{\gamma}}\right](0,0)\tilde{x}^{\beta}_{m,n,s}\tilde{x}^{\gamma}_{m,n,s}\Bigg). \tag{6.2.22}$$

We choose more than ten grid points for the interpolation to get an underdetermined system of equations (6.2.21) which is solved by the SVD method.

Chapter 7

Numerical Examples with Fixed Interfaces: Convergence and Efficiency Analysis

We implement the algorithms for Stokes equations with interfaces described in Chapters 5 and 6 in both 2D and 3D. First we show the convergence and efficiency analysis for problems with fixed interfaces. All the computations are done on a P4 3.20GHz DELL$^{\mathrm{TM}}$ desktop PC with 2GB memory.

7.1 2D Geometry

The computational domain is $\Omega = [-1.5, 1.5] \times [-1.5, 1.5]$. We choose to fix $\mu^+ = 1.0$ while varying μ^-. The interface is an ellipse

$$\varphi\left(x^\alpha, x^\beta\right) = \left(x^\alpha\right)^2 + 4\left(x^\beta\right)^2 - 1.0. \tag{7.1.1}$$

The initial guess of GMRES for the augmented variable $\left[\mu U^i\right]$ takes non-informative zero values. The tolerance of the GMRES iteration is set to be 10^{-5}. Dirichlet boundary conditions are used for both velocity and pressure.

The exact solution of velocity $\boldsymbol{u} = \left(u^{\alpha}, u^{\beta}\right)$ and pressure p is constructed as

$$u^{\alpha} = \begin{cases} x^{\beta} & \text{if } (x^{\alpha})^2 + 4\left(x^{\beta}\right)^2 < 1, \\ x^{\beta}\left((x^{\alpha})^2 + 4\left(x^{\beta}\right)^2\right) & \text{if } (x^{\alpha})^2 + 4\left(x^{\beta}\right)^2 \geq 1; \end{cases}$$

$$u^{\beta} = \begin{cases} \dfrac{x^{\alpha}\left(-1 + (x^{\alpha})^2\right)}{4} & \text{if } (x^{\alpha})^2 + 4\left(x^{\beta}\right)^2 < 1, \\ -x^{\alpha}\left(x^{\beta}\right)^2 & \text{if } (x^{\alpha})^2 + 4\left(x^{\beta}\right)^2 \geq 1; \end{cases} \tag{7.1.2}$$

$$p = \begin{cases} -\dfrac{3x^{\alpha}\left(2(x^{\alpha})^2 - 1\right)x^{\beta}}{8} & \text{if } (x^{\alpha})^2 + 4\left(x^{\beta}\right)^2 < 1, \\ 0 & \text{if } (x^{\alpha})^2 + 4\left(x^{\beta}\right)^2 \geq 1. \end{cases}$$

The body force term $\boldsymbol{g} = \left(g^{\alpha}, g^{\beta}\right)$ is chosen to be

$$g^{\alpha} = \begin{cases} -\dfrac{3\left(6(x^{\alpha})^2 - 1\right)x^{\beta}}{8} & \text{if } (x^{\alpha})^2 + 4\left(x^{\beta}\right)^2 < 1, \\ -26\mu^{+}x^{\beta} & \text{if } (x^{\alpha})^2 + 4\left(x^{\beta}\right)^2 \geq 1; \end{cases}$$

$$g^{\beta} = \begin{cases} -\dfrac{3x^{\alpha}\left(2(x^{\alpha})^2 - 1 + 4\mu^{-}\right)}{8} & \text{if } (x^{\alpha})^2 + 4\left(x^{\beta}\right)^2 < 1, \\ 2\mu^{+}x^{\alpha} & \text{if } (x^{\alpha})^2 + 4\left(x^{\beta}\right)^2 \geq 1. \end{cases} \tag{7.1.3}$$

And the singular interface force terms are

$$\begin{aligned} f^{\alpha} = &\left(\frac{3}{4}(x^{\alpha})^3 x^{\beta} - \frac{3}{8}x^{\alpha}x^{\beta} - 4\mu^{+}x^{\alpha}x^{\beta}\right)n^{\alpha} \\ &+ \left(-\mu^{+}(x^{\alpha})^2 - 11\mu^{+}\left(x^{\beta}\right)^2 + \frac{3}{4}\mu^{-} + \frac{3}{4}\mu^{-}(x^{\alpha})^2\right)n^{\beta} \end{aligned} \tag{7.1.4}$$

and

$$\begin{aligned} f^{\beta} = &\left(\frac{3}{4}(x^{\alpha})^3 x^{\beta} - \frac{3}{8}x^{\alpha}x^{\beta} + 4\mu^{+}x^{\alpha}x^{\beta}\right)n^{\beta} \\ &+ \left(-\mu^{+}(x^{\alpha})^2 - 11\mu^{+}\left(x^{\beta}\right)^2 + \frac{3}{4}\mu^{-} + \frac{3}{4}\mu^{-}(x^{\alpha})^2\right)n^{\alpha}. \end{aligned} \tag{7.1.5}$$

Note that this is a very general fixed interface problem with non-homogeneous jumps for both velocity and pressure.

We use linear regression analysis to find the convergence order of the solution. For this purpose, we choose $m = n = 100, 200, 400, 800$ and 1600 to run the convergence analysis for

$\mu^- = 0.001, 0.1, 10$ and 1000. For the special case when $\mu^- = 1.0$, no GMRES iterations are needed. See Fig. 7.1 for the grid refinement analysis and CPU cost.

(a)

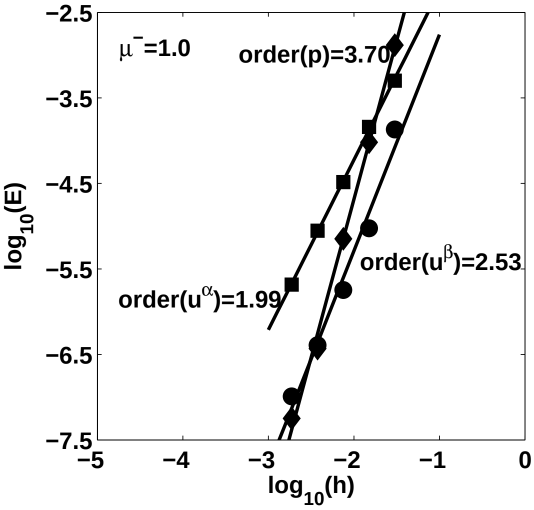

(b)

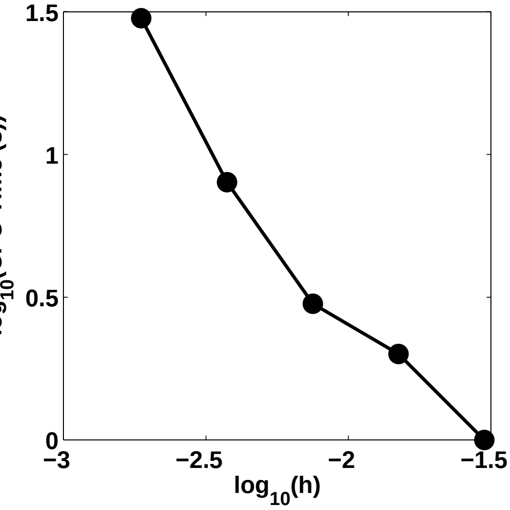

Figure 7.1: For the equal viscosity case, (a) Convergence analysis in the $\mathcal{L}^\infty$ norm, and (b) CPU time cost.

Fig. 7.2 shows the grid refinement analysis of the test problem for the unequal viscosity cases. The error is the $\mathcal{L}^\infty$ error at all grid points. The slope of the linear regression line is the order of the convergence. It is clear from these results that the algorithm is second order or almost second order accurate in both velocity and pressure. For this problem, it also seems that with larger μ^-, the numerical solution for velocity tends to be more accurate than the solution for pressure.

See Fig. 7.3 for the computed solution and error plots with 32 by 32 grids and $\mu^- = 0.8$ for pressure p and velocity component u^α. Fig. 7.4 shows the algorithm efficiency analysis. The number of GMRES iterations remain relatively constant with grid size. In Fig. 7.5, we show the 2-norm condition number of the coefficient matrix for the augmented variable $\left[\mu U^i\right]$. It can be seen that the coefficient matrix is ill-conditioned and future research needs to be done to discover preconditioner techniques for this problem. Note that the condition number is a measure of stability of the coefficient matrix to numerical operations (see Fig. 7.2) and affects the number of GMRES iterations (see Fig. 7.4).

To enhance the performance of the algorithm, it is very useful to discover where the code is spending time as it executes. We use a statistical sampling method to record the location where the code is executing at a predetermined interval. Once we have discovered

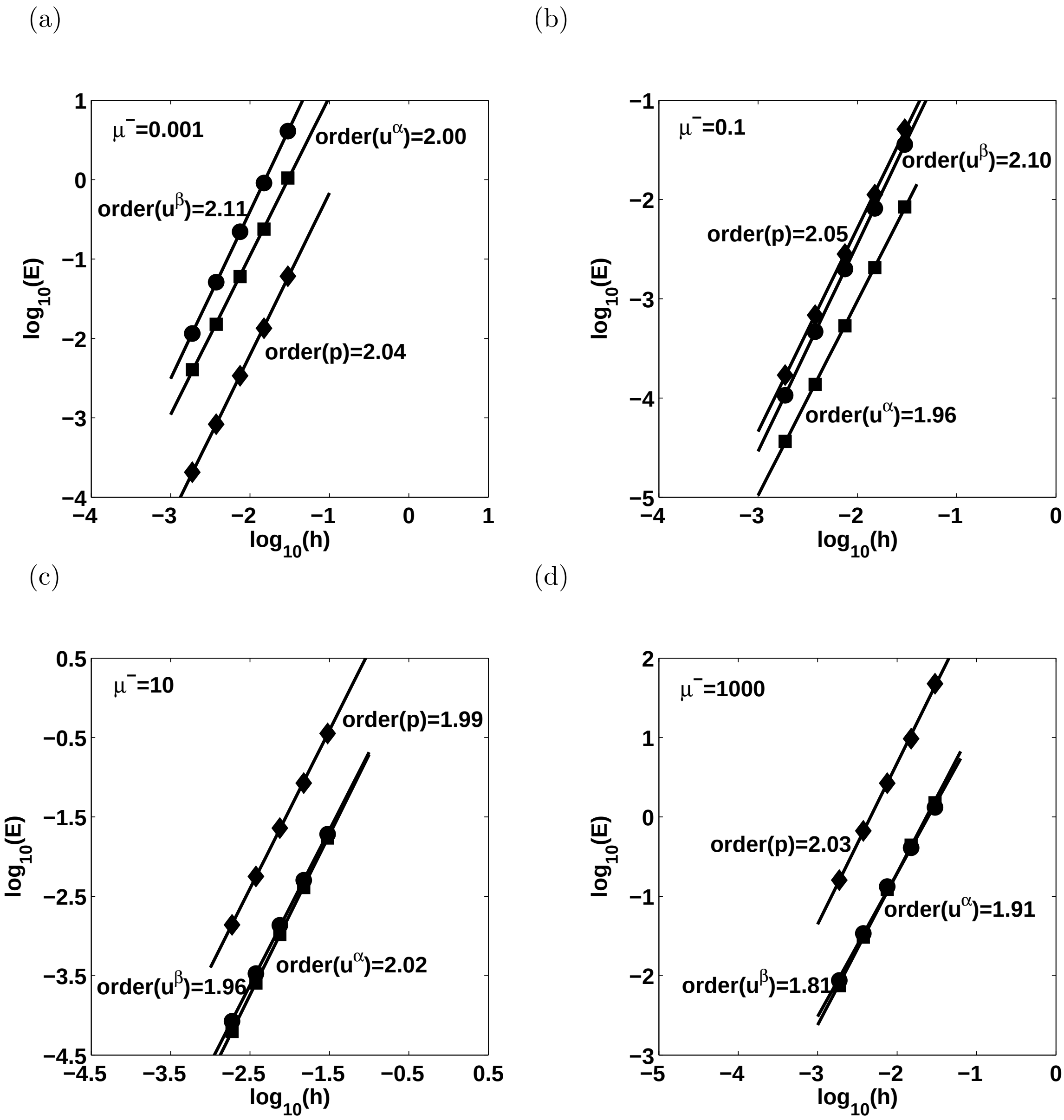

Figure 7.2: Convergence analysis in the $\mathcal{L}^\infty$ norm for four cases in log-log scale. The slope of the linear regression line is the convergence rate which is close to number 2.0 for all cases. (a) $\mu^- = 0.001$ and $\mu^+ = 1.0$. (b) $\mu^- = 0.1$ and $\mu^+ = 1.0$. (c) $\mu^- = 10$ and $\mu^+ = 1.0$. (d) $\mu^- = 1000$ and $\mu^+ = 1.0$. Linear regressions $R^2 > 0.98$ for all cases.

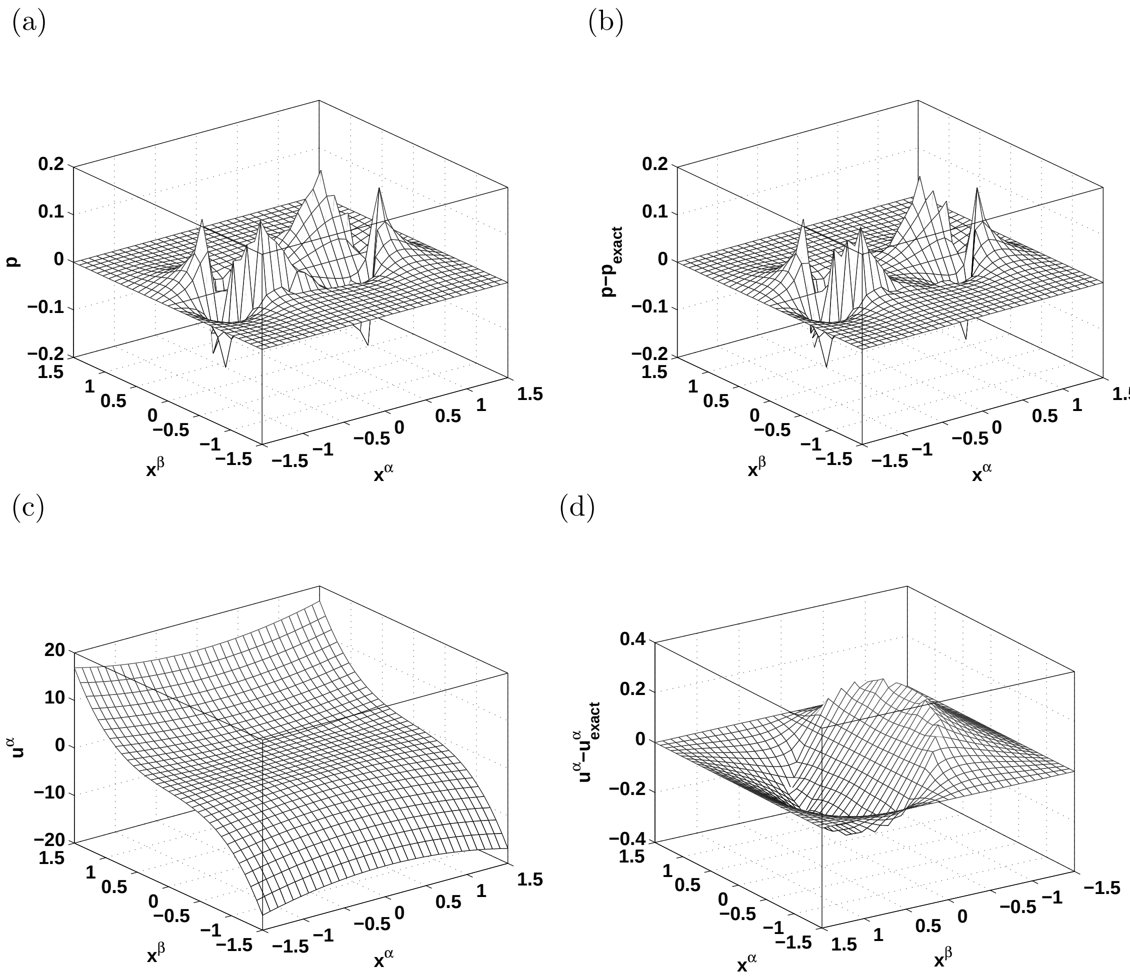

Figure 7.3: The computed solutions for (a) pressure p and (c) velocity component u^{α}. The error plot of the computed solutions (b) $p - p_{exact}$ and (d) $u^{\alpha} - u^{\alpha}_{exact}$. We choose $m = n = 32$ and $\mu^{-} = 0.8$.

(a) (b)

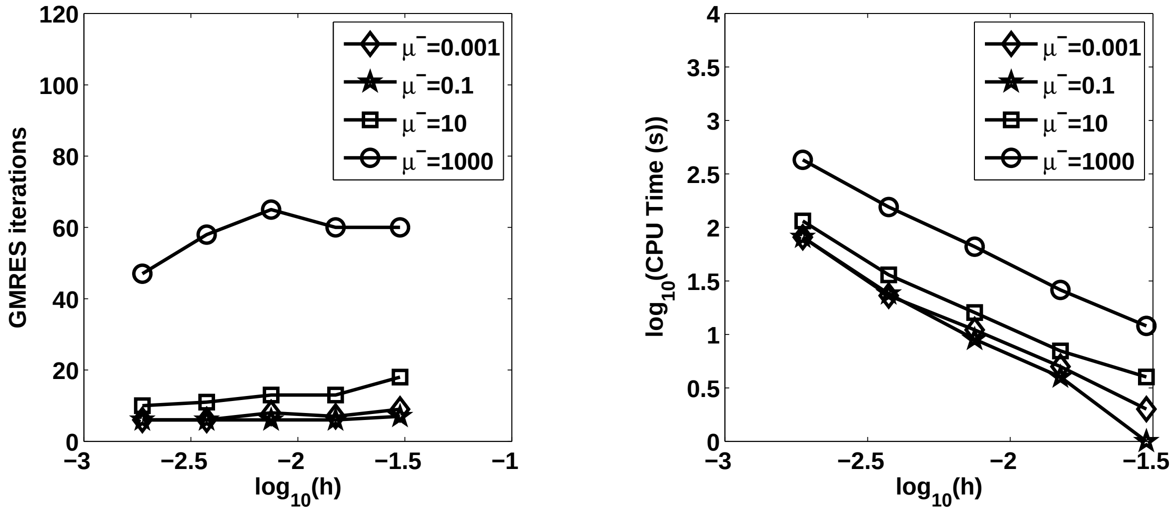

Figure 7.4: Algorithm efficiency analysis for 100 by 100 through 1600 by 1600 grids. (a): Number of GMRES iterations. (b): CPU cost with unit second.

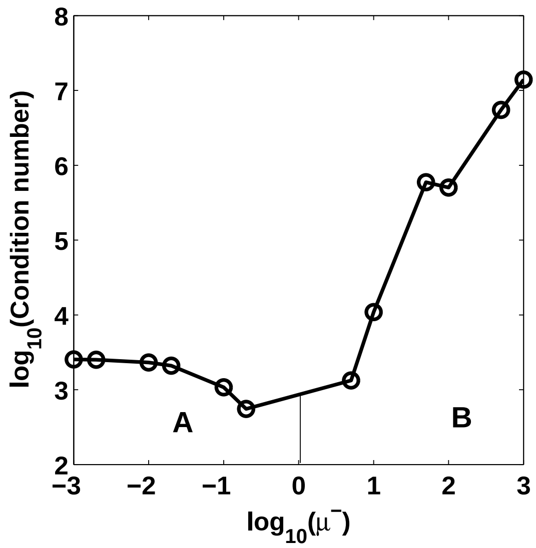

Figure 7.5: Grid size is 80 by 80 and the size of the coefficient matrix for the augmented variable $\left[\mu U^i\right]$ is 232 by 232. Region A represents $\mu^- < 1$ where the fluid inside the interface is less viscous than the fluid outside the interface, region B represents $\mu^- > 1$.

heavily executed portions of the code, we will be able to either adopt a faster algorithm for those portions or fine tune the current implementations. From Fig. 7.6 we can find that a faster Singular Value Decomposition (SVD) implementation will help to improve the performance of our algorithm for cases with either equal viscosity coefficients or unequal viscosity coefficients.

(a) (b)

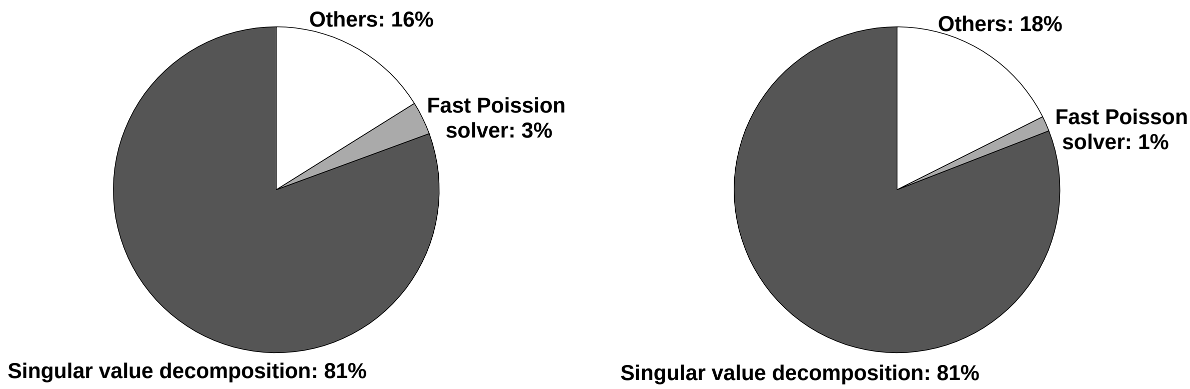

Figure 7.6: Execution time percentage analysis for (a) $\mu^- = 0.1, \mu^+ = 1.0$ and (b) $\mu^- = \mu^+ = 1.0$. We choose $m = n = 100$.

7.2 3D Geometry

The computational domain is $\Omega = [-1.5, 1.5] \times [-1.5, 1.5] \times [-1.5, 1.5]$. We choose to fix $\mu^+ = 1.0$ while varying μ^-. The interface is an ellipsoid

$$\varphi\left(x^\alpha, x^\beta, x^\gamma\right) = (x^\alpha)^2 + 4\left(x^\beta\right)^2 + 4\,(x^\gamma)^2 - 1.0. \tag{7.2.1}$$

The initial guess of GMRES for the augmented variable $\left[\mu U^i\right]$ takes non-informative zero values. The tolerance of the GMRES iteration is set to be 10^{-5}. Dirichlet boundary conditions are used for both velocity and pressure.

The exact solution of velocity $\boldsymbol{u} = \left(u^\alpha, u^\beta, u^\gamma\right)$ and pressure p is constructed as

$$
\begin{aligned}
u^\alpha &= \begin{cases} x^\beta x^\gamma \left(1 - 4\left(x^\gamma\right)^2\right) & \text{if } \left(x^\alpha\right)^2 + 4\left(x^\beta\right)^2 + 4\left(x^\gamma\right)^2 < 1, \\ x^\beta x^\gamma \left(\left(x^\alpha\right)^2 + 4\left(x^\beta\right)^2\right) & \text{if } \left(x^\alpha\right)^2 + 4\left(x^\beta\right)^2 + 4\left(x^\gamma\right)^2 \geq 1; \end{cases} \\
u^\beta &= \begin{cases} -x^\alpha x^\gamma \left(\left(x^\alpha\right)^2 + 4\left(x^\gamma\right)^2\right) & \text{if } \left(x^\alpha\right)^2 + 4\left(x^\beta\right)^2 + 4\left(x^\gamma\right)^2 < 1, \\ -x^\alpha x^\gamma \left(1 - 4\left(x^\beta\right)^2\right) & \text{if } \left(x^\alpha\right)^2 + 4\left(x^\beta\right)^2 + 4\left(x^\gamma\right)^2 \geq 1; \end{cases} \\
u^\gamma &= \begin{cases} \dfrac{5x^\alpha x^\beta \left(-1 + \left(x^\alpha\right)^2 + 4\left(x^\beta\right)^2\right)}{4} & \text{if } \left(x^\alpha\right)^2 + 4\left(x^\beta\right)^2 + 4\left(x^\gamma\right)^2 < 1, \\ -5x^\alpha x^\beta \left(x^\gamma\right)^2 & \text{if } \left(x^\alpha\right)^2 + 4\left(x^\beta\right)^2 + 4\left(x^\gamma\right)^2 \geq 1; \end{cases} \\
p &= \begin{cases} -\dfrac{3x^\alpha \left(2\left(x^\alpha\right)^2 - 1\right) x^\beta \left(x^\gamma\right)^2}{8} & \text{if } \left(x^\alpha\right)^2 + 4\left(x^\beta\right)^2 + 4\left(x^\gamma\right)^2 < 1, \\ 0 & \text{if } \left(x^\alpha\right)^2 + 4\left(x^\beta\right)^2 + 4\left(x^\gamma\right)^2 \geq 1. \end{cases}
\end{aligned}
\tag{7.2.2}
$$

The body force term $\boldsymbol{g} = \left(g^\alpha, g^\beta, g^\gamma\right)$ is chosen to be

$$
\begin{aligned}
g^\alpha &= \begin{cases} -\dfrac{3x^\beta x^\gamma \left(6\left(x^\alpha\right)^2 x^\gamma - x^\gamma - 64\mu^-\right)}{8} & \text{if } \left(x^\alpha\right)^2 + 4\left(x^\beta\right)^2 + 4\left(x^\gamma\right)^2 < 1, \\ -26\mu^+ x^\beta x^\gamma & \text{if } \left(x^\alpha\right)^2 + 4\left(x^\beta\right)^2 + 4\left(x^\gamma\right)^2 \geq 1; \end{cases} \\
g^\beta &= \begin{cases} -\dfrac{3x^\alpha x^\gamma \left(2\left(x^\alpha\right)^2 x^\gamma - x^\gamma - 80\mu^-\right)}{8} & \text{if } \left(x^\alpha\right)^2 + 4\left(x^\beta\right)^2 + 4\left(x^\gamma\right)^2 < 1, \\ -8\mu^+ x^\alpha x^\gamma & \text{if } \left(x^\alpha\right)^2 + 4\left(x^\beta\right)^2 + 4\left(x^\gamma\right)^2 \geq 1; \end{cases} \\
g^\gamma &= \begin{cases} -\dfrac{3x^\alpha x^\beta \left(2\left(x^\alpha\right)^2 x^\gamma - x^\gamma + 50\mu^-\right)}{4} & \text{if } \left(x^\alpha\right)^2 + 4\left(x^\beta\right)^2 + 4\left(x^\gamma\right)^2 < 1, \\ 10\mu^+ x^\alpha x^\beta & \text{if } \left(x^\alpha\right)^2 + 4\left(x^\beta\right)^2 + 4\left(x^\gamma\right)^2 \geq 1. \end{cases}
\end{aligned}
\tag{7.2.3}
$$

And the singular interface force terms are

$$
\begin{aligned}
f^{\alpha} = & \left(\frac{3}{4}\left(x^{\alpha}\right)^{3} x^{\beta}\left(x^{\gamma}\right)^{2}-\frac{3}{8} x^{\alpha} x^{\beta}\left(x^{\gamma}\right)^{2}-4 \mu^{+} x^{\alpha} x^{\beta} x^{\gamma}\right) n^{\alpha}+\left(-\mu^{+}\left(x^{\alpha}\right)^{2} x^{\gamma}\right. \\
& \left.-16 \mu^{+}\left(x^{\beta}\right)^{2} x^{\gamma}+\mu^{+} x^{\gamma}+\mu^{-} x^{\gamma}-8 \mu^{-}\left(x^{\gamma}\right)^{3}-3 \mu^{-}\left(x^{\alpha}\right)^{2} x^{\gamma}\right) n^{\beta} \\
& +\left(-\mu^{+}\left(x^{\alpha}\right)^{2} x^{\beta}-4 \mu^{+}\left(x^{\beta}\right)^{3}+5 \mu^{+} x^{\beta}\left(x^{\gamma}\right)^{2}-\frac{1}{4} \mu^{-} x^{\beta}-12 \mu^{-} x^{\beta}\left(x^{\gamma}\right)^{2}\right. \\
& \left.+\frac{15}{4} \mu^{-}\left(x^{\alpha}\right)^{2} x^{\beta}+5 \mu^{-}\left(x^{\beta}\right)^{3}\right) n^{\gamma},
\end{aligned} \tag{7.2.4}
$$

$$
\begin{aligned}
f^{\beta} = & \left(-\mu^{+}\left(x^{\alpha}\right)^{2} x^{\gamma}-16 \mu^{+}\left(x^{\beta}\right)^{2} x^{\gamma}+\mu^{+} x^{\gamma}+\mu^{-} x^{\gamma}-8 \mu^{-}\left(x^{\gamma}\right)^{3}-3 \mu^{-}\left(x^{\alpha}\right)^{2} x^{\gamma}\right) n^{\alpha} \\
& +\left(\frac{3}{4}\left(x^{\alpha}\right)^{3} x^{\beta}\left(x^{\gamma}\right)^{2}-\frac{3}{8} x^{\alpha} x^{\beta}\left(x^{\gamma}\right)^{2}-16 \mu^{+} x^{\alpha} x^{\beta} x^{\gamma}\right) n^{\beta}+\left(\mu^{+} x^{\alpha}-4 \mu^{+} x^{\alpha}\left(x^{\beta}\right)^{2}\right. \\
& \left.+5 \mu^{+} x^{\alpha}\left(x^{\gamma}\right)^{2}+\frac{1}{4} \mu^{-}\left(x^{\alpha}\right)^{3}-12 \mu^{-} x^{\alpha}\left(x^{\gamma}\right)^{2}-\frac{5}{4} \mu^{-} x^{\alpha}+15 \mu^{-} x^{\alpha}\left(x^{\beta}\right)^{2}\right) n^{\gamma}
\end{aligned} \tag{7.2.5}
$$

and

$$
\begin{aligned}
f^{\gamma} = & \left(-\mu^{+}\left(x^{\alpha}\right)^{2} x^{\beta}-4 \mu^{+}\left(x^{\beta}\right)^{3}+5 \mu^{+} x^{\beta}\left(x^{\gamma}\right)^{2}-\frac{1}{4} \mu^{-} x^{\beta}-12 \mu^{-} x^{\beta}\left(x^{\gamma}\right)^{2}+\frac{15}{4} \mu^{-}\left(x^{\alpha}\right)^{2} x^{\beta}\right. \\
& \left.+5 \mu^{-}\left(x^{\beta}\right)^{3}\right) n^{\alpha}+\left(\mu^{+} x^{\alpha}-4 \mu^{+} x^{\alpha}\left(x^{\beta}\right)^{2}+5 \mu^{+} x^{\alpha}\left(x^{\gamma}\right)^{2}+\frac{1}{4} \mu^{-}\left(x^{\alpha}\right)^{3}\right. \\
& \left.-12 \mu^{-} x^{\alpha}\left(x^{\gamma}\right)^{2}-\frac{5}{4} \mu^{-} x^{\alpha}+15 \mu^{-} x^{\alpha}\left(x^{\beta}\right)^{2}\right) n^{\beta}+\left(\frac{3}{4}\left(x^{\alpha}\right)^{3} x^{\beta}\left(x^{\gamma}\right)^{2}\right. \\
& \left.-\frac{3}{8} x^{\alpha} x^{\beta}\left(x^{\gamma}\right)^{2}+20 \mu^{+} x^{\alpha} x^{\beta} x^{\gamma}\right) n^{\gamma}.
\end{aligned} \tag{7.2.6}
$$

Note that this is a very general fixed interface problem with non-homogeneous jumps for both velocity and pressure.

We use linear regression analysis to find the convergence order of the solution. For this purpose, we choose $m = n = s = 32, 56, 80, 104$ and 128 to run the convergence analysis for $\mu^- = 0.001, 0.1, 10$ and 100. For the special case when $\mu^- = 1.0$, no GMRES iterations are needed and see Fig. 7.7 for the grid refinement analysis and CPU cost.

Fig. 7.8 shows the grid refinement analysis of the test problem for the unequal viscosity cases. The error is the $\mathcal{L}^\infty$ error at all grid points. The slope of the linear regression line is the order of the convergence. It is clear from these results that the algorithm is higher than second order accurate in both velocity and pressure. For this problem, it also seems that with larger μ^-, the numerical solution for velocity tends to be more accurate than the solution for pressure.

(a)

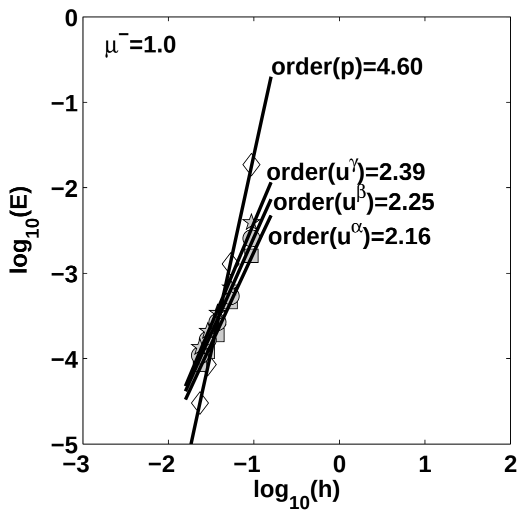

(b)

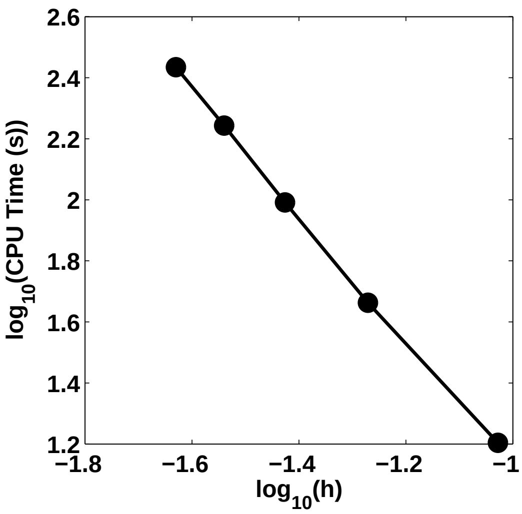

Figure 7.7: For the equal viscosity case, (a) Convergence analysis in the $\mathcal{L}^\infty$ norm, and (b) CPU time cost.

See Fig. 7.9 for the sliced solution and error plots with 32^3 grids and $\mu^- = 0.8$ for pressure p and velocity component u^α. Fig. 7.10 shows the algorithm efficiency analysis. The number of GMRES iterations remains relatively constant with grid size for finer grids. In Fig. 7.11, we show the 2-norm condition number of the coefficient matrix for the augmented variable $\left[\mu U^i\right]$. It can be seen that the coefficient matrix is ill-conditioned and future research needs to be done to discover preconditioner techniques for this problem. Note that the condition number is a measure of stability of the coefficient matrix to numerical operations (see Fig. 7.8) and affects the number of GMRES iterations (see Fig. 7.10).

We use the statistical sampling technique to quantify the CPU cost for different portions of the algorithm. From Fig. 7.12 we can find that a faster SVD implementation will help to improve the overall performance of our algorithm for both equal and unequal viscosity cases.

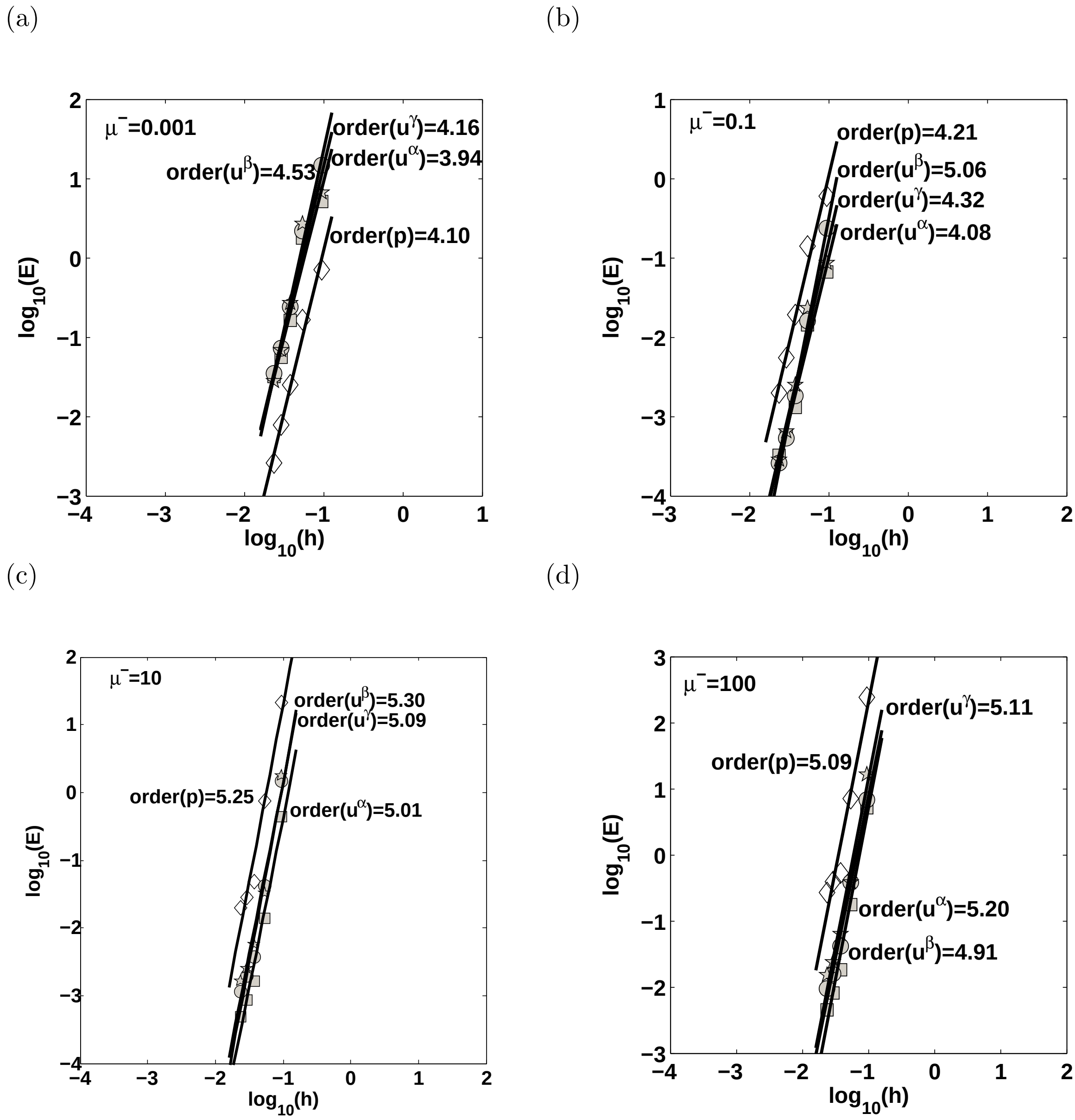

Figure 7.8: Convergence analysis in the $\mathcal{L}^{\infty}$ norm for four cases in log-log scale. The slope of the linear regression line is the convergence rate which is larger than number 2.0 for all cases. (a) $\mu^- = 0.001$ and $\mu^+ = 1.0$. (b) $\mu^- = 0.1$ and $\mu^+ = 1.0$. (c) $\mu^- = 10$ and $\mu^+ = 1.0$. (d) $\mu^- = 100$ and $\mu^+ = 1.0$. Linear regressions $R^2 > 0.95$ for all cases.

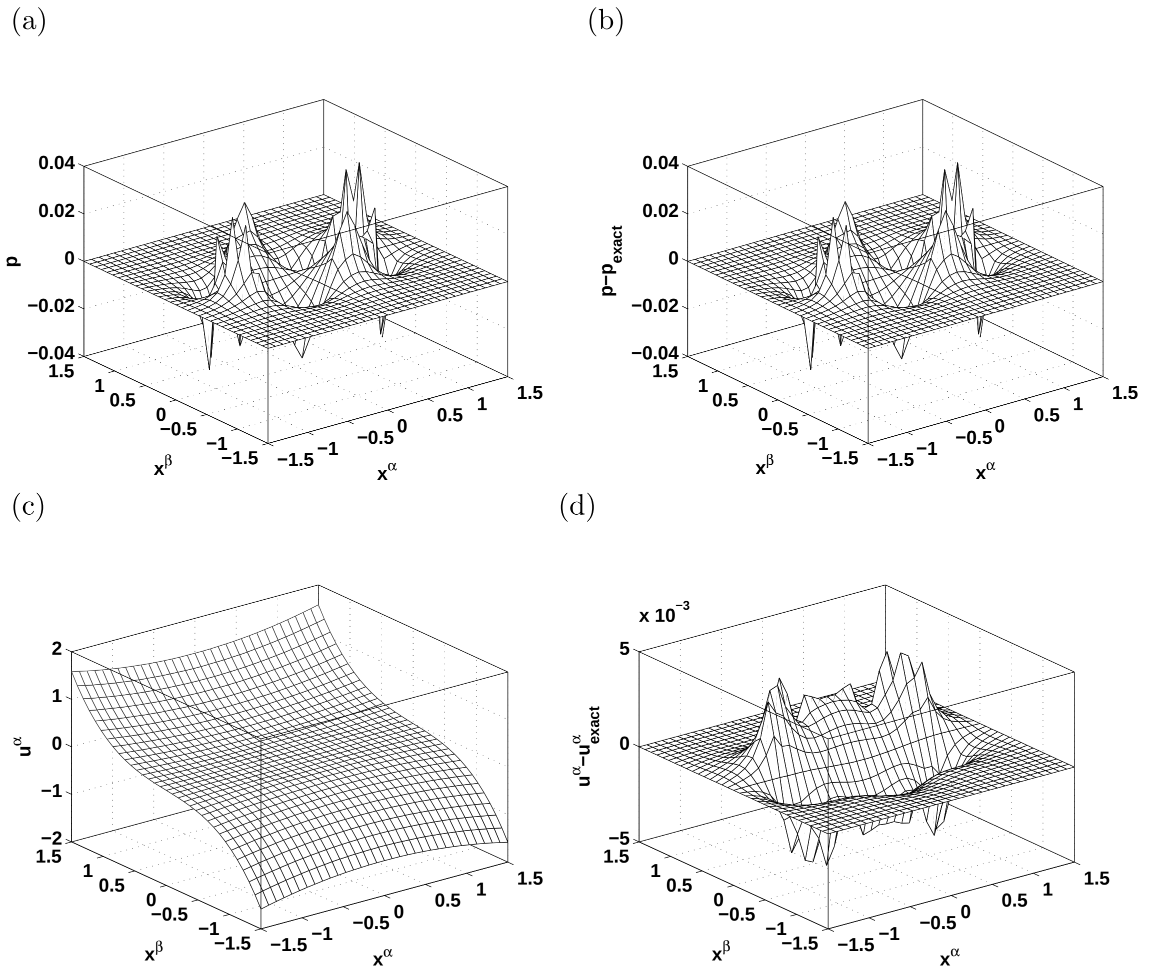

Figure 7.9: The computed solutions sliced at $x^{\gamma} = 0.0938$ for (a) pressure p and (c) velocity component u^{α}. The sliced error plot of the computed solutions (b) $p - p_{exact}$ and (d) $u^{\alpha} - u^{\alpha}_{exact}$. We choose $m = n = s = 32$ and $\mu^{-} = 0.8$.

(a) (b)

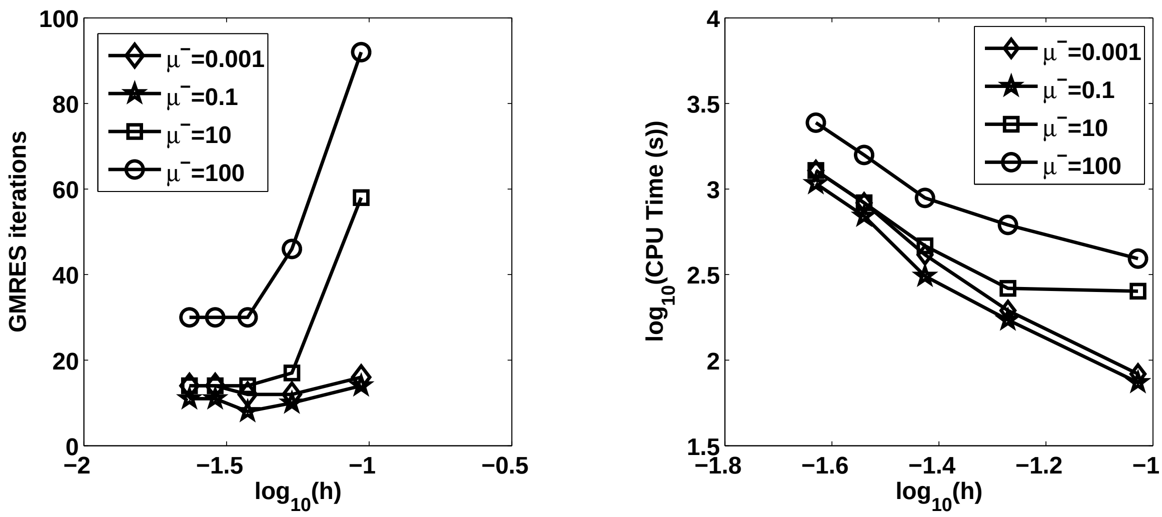

Figure 7.10: Algorithm efficiency analysis for 32^3 through 128^3 grids. (a): Number of GMRES iterations. (b): CPU cost with unit second.

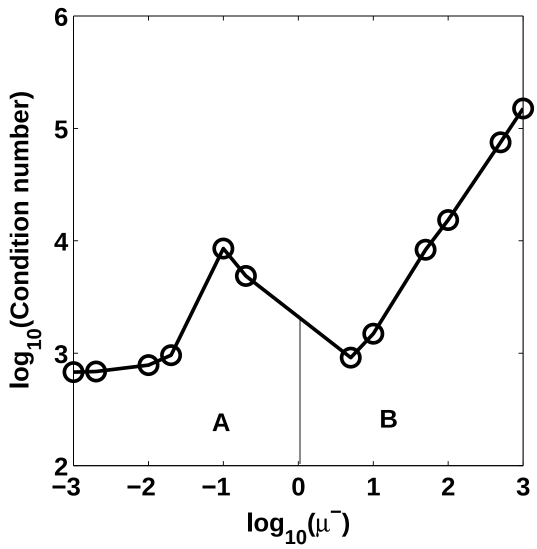

Figure 7.11: Grid size is 10^3 and the size of the coefficient matrix for the augmented variable $\left[\mu U^i\right]$ is 102 by 102. Region A represents $\mu^- < 1$ where the fluid inside the interface is less viscous than the fluid outside the interface, region B represents $\mu^- > 1$.

(a) (b)

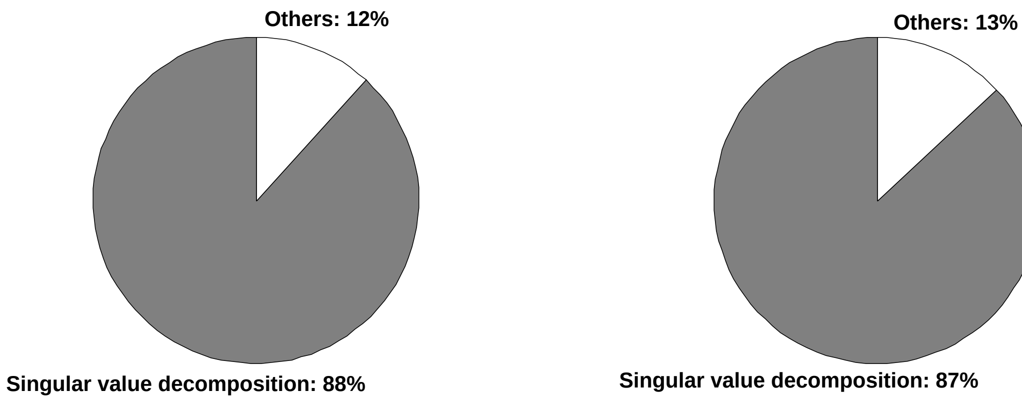

Figure 7.12: Execution time percentage analysis for (a) $\mu^- = 0.1, \mu^+ = 1.0$ and (b) $\mu^- = \mu^+ = 1.0$. We choose $m = n = s = 40$.

Chapter 8

Moving Interface Problems: Two-Phase Flow with Surface Tension

In order to test our two-phase Stokes flow solver for moving interface problems, we choose to use the well-known mean curvature flow cases where the surface tension $f^i n^i$ is proportional to the mean curvature of the interface and the tangential interface force is zero. For the mean curvature flow, in terms of jump condition for pressure p, we have the Young-Laplace equation

$$[p] = \xi \kappa_M \tag{8.0.1}$$

where ξ is the surface tension constant and κ_M is the mean curvature of the interface Γ. We solve the nondimensional incompressible Stokes equations for all the two-phase flow simulations with surface tension.

8.1 Level Set Method for Interface Advection

The interface between two fluid phases is represented implicitly using the level set function as

$$\varphi(x^i, t) = 0 \tag{8.1.1}$$

where $\varphi(\cdot)$ is the level set function, x^i is the spatial coordinates and t is the time coordinates. Since the solution x^i of Eq. (8.1.1) is the interface which depends on t, we can take the derivative of Eq. (8.1.1) with respect to t to get the level set equation [40]

$$0 = \frac{d\varphi}{dt} = \frac{\partial \varphi}{\partial t} + \frac{\partial \varphi}{\partial x^i}\frac{dx^i}{dt} = \frac{\partial \varphi}{\partial t} + \frac{\partial \varphi}{\partial x^i} u^i \tag{8.1.2}$$

where u^i is the advection velocity. We use the third-order accurate Hamilton-Jacobi essentially nonoscillatory (HJ ENO) scheme [40] for the spatial derivative term $\frac{\partial \varphi}{\partial x^i}$ with upwind differencing. The time advancing scheme is the first-order accurate total variation diminishing (TVD) Runge-Kutta (RK) scheme, which is just the forward Euler method. Stability of the time stepping scheme is enforced using the Courant-Friedrichs-Lewy condition (CFL condition) [40]

$$\Delta t = \alpha \frac{h}{\sum_i max|u^i|} \tag{8.1.3}$$

where h is the grid size and α is a constant chosen to be 0.5.

It is necessary to keep the level set function φ close to a signed distance function [50] satisfying

$$\left|\frac{\partial \varphi}{\partial x^i}\right| = 1. \tag{8.1.4}$$

This is enforced by solving the reinitialization equation [40]

$$\frac{\partial \varphi}{\partial t} + S(\varphi_0)\left(\left|\frac{\partial \varphi}{\partial x^i}\right| - 1\right) = 0 \tag{8.1.5}$$

where

$$S(\varphi_0) = \frac{\varphi_0}{\sqrt{\varphi_0^2 + h^2}}. \tag{8.1.6}$$

In the reinitialization equation (8.1.5), t is the pseudo-time variable for iterations and φ_0 is the initial input of the level set function for this iteration. Eq. (8.1.5) is discretized using the Godunov scheme for the level set motion in the normal direction [40].

Volume or area conservation for the two fluid phases separated by the zero level sets is a non-trivial research topic [12, 52, 40]. We adopt the method [16] which iteratively solves the following equation

$$\mathcal{M}(\varphi + \epsilon < 0) = \mathcal{M}_0 \tag{8.1.7}$$

for ϵ. Here $\mathcal{M}(\cdot)$ is the volume or area measure and $\mathcal{M}_0$ is the value of this measure at the initial time of the simulation.

We use the Level Set Method Library (LSMLIB) [5] developed by Kevin T. Chu and Masa Prodanovic and this library is freely available through the Internet.

8.2 2D Geometry

8.2.1 Ellipse interface

The computational domain is $[-1, 1] \times [-1, 1]$ with periodic boundary condition, and the grid size is 64×64. The initial condition of the interface for the two phases is chosen to be an ellipse

$$\varphi(x^\alpha, x^\beta) = \frac{(x^\alpha)^2}{0.8^2} + \frac{\left(x^\beta\right)^2}{0.4^2} - 1.0 = 0, \tag{8.2.1}$$

and the surface tension constant ξ is chosen to be 0.1. We run the simulation to equilibrium (or close to equilibrium) at $t = 100$. We first show the time evolution results for the case when $\mu^- = \mu^+ = 1.0$ in Fig. 8.1 and the final pressure profile in Fig. 8.2. Note that for the equal viscosity coefficient case, no GMRES iterations are needed.

(a) (b)

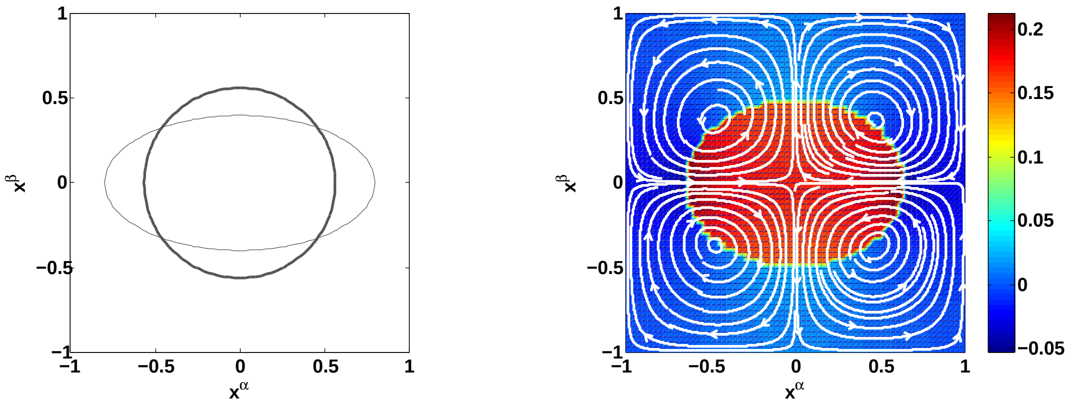

Figure 8.1: Starting from the ellipse, the interface evolves to a circle under surface tension. (a) The interface plotted at $t = 0$ and $t = 100$. (b) Colored pressure profile with streamlines of the velocity field at $t = 25$. Since the pressure is not continuous across the interface, the color plot for the pressure is not smooth near the interface.

We run the same simulations with $\mu^- = 0.5$ and $\mu^- = 2.0$. For $\mu^- = 0.5$, the fluid inside the interface is less viscous than the fluid outside and for $\mu^- = 2.0$ it is the opposite. GMRES iterations per time step for both cases are in the range of 2-5. The computation time for the equal viscosity case is 504 seconds, for $\mu^- = 0.5$ is 940 seconds and for $\mu^+ = 2.0$ is 978 seconds. See Fig. 8.3 for the pressure color plot and velocity streamlines of these two cases. The comparison between Fig. 8.3 and Fig. 8.1(b) clearly illustrates the effects of the viscosity difference for the two-phase flow.

8.2.2 Star interface

It is interesting to see whether our Stokes solver coupled with the LSM can handle flow with complex interfaces such as the five-star interface in the literature [23, 55]. For this experiment, the initial shape of the interface between two fluids with $\mu^- = \mu^+ = 1.0$ is expressed in the polar coordinates (r, θ) as

$$r(\theta) = 0.5(1 + 0.4\sin(5\theta)), \quad 0 \leq \theta \leq 2\pi. \tag{8.2.2}$$

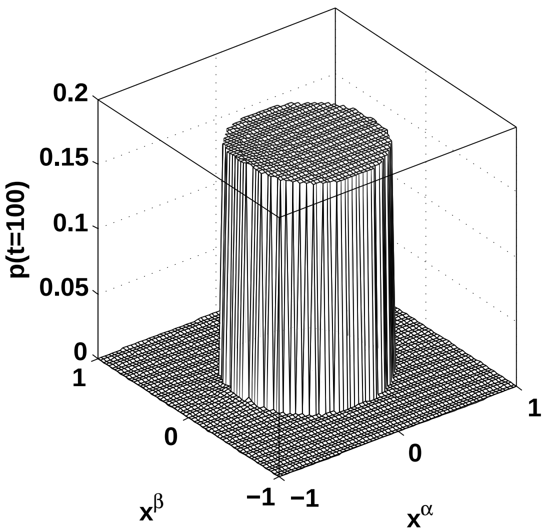

Figure 8.2: Equilibrium pressure field at $t = 100$. Notice the sharp interface for the pressure field. No noise filtering is used to maintain the sharp interface.

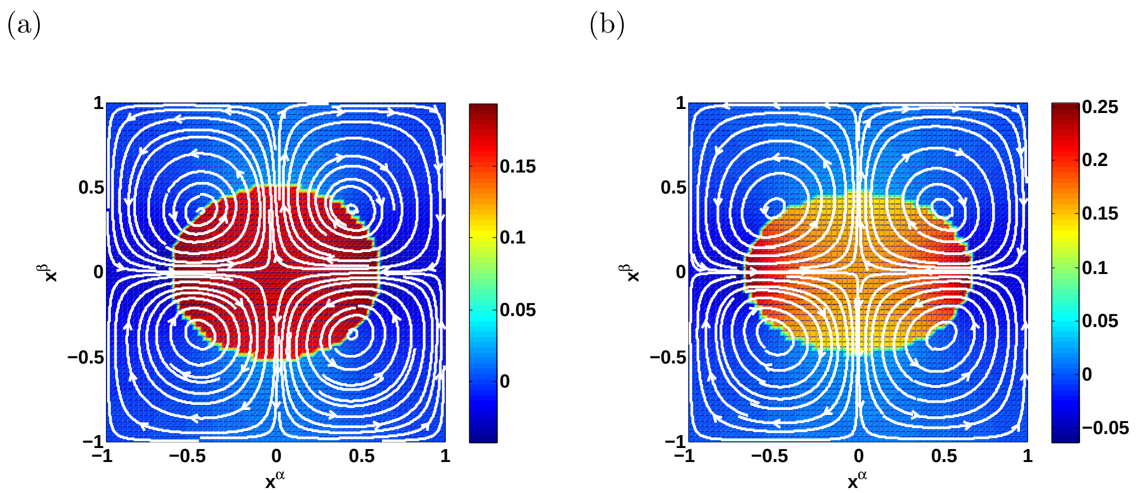

Figure 8.3: Colored pressure profile with streamlines of the velocity field at $t = 25$ for (a) $\mu^- = 0.5$ and (b) $\mu^- = 2.0$.

The computational domain is $[-1,1]\times[-1,1]$ with periodic boundary condition, and the grid size is 320×320. The surface tension constant ξ is chosen to be 0.05. We run the simulation to equilibrium which is set as $t=98$. See Fig. 8.4 for the time evolution results. From Fig. 8.5, it is clear that our algorithm can capture the highly localized discontinuous pressure profile, which is critical for simulating the pressure driven interface. The computation cost is 3350 seconds.

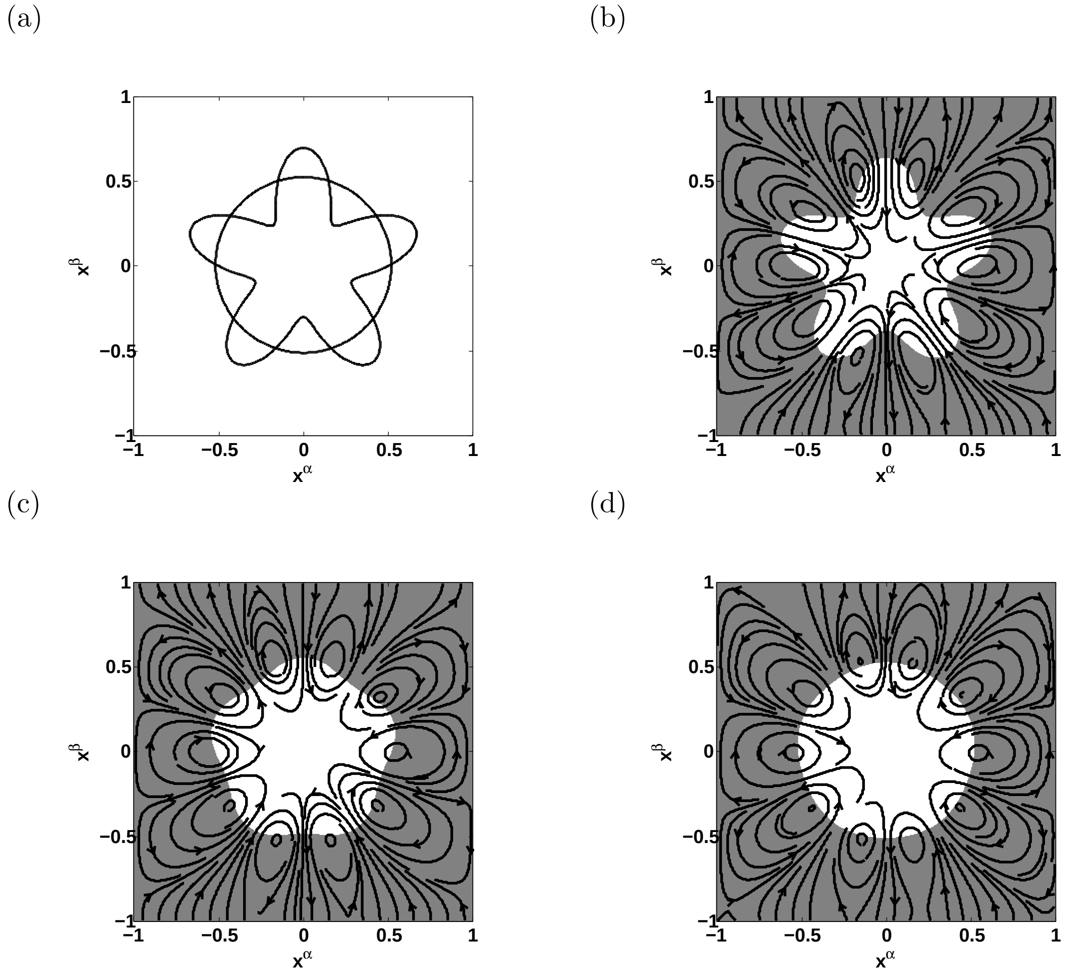

Figure 8.4: Starting from the five-star shape, the interface relaxes to a circle under surface tension. (a) The interface plotted at $t=0$ and $t=98$. The interface with streamlines of the velocity field at (b) $t=7$ (c) $t=21$ and (d) $t=35$.

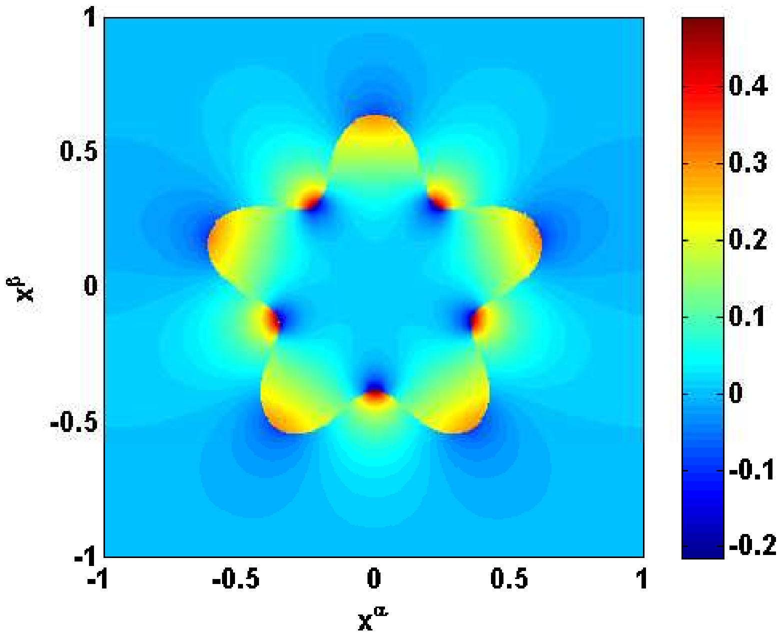

Figure 8.5: Pressure field at $t = 7$. Our algorithm captures the highly localized pressure gradient with the presence of complex five-star interface.

8.3 3D Geometry

8.3.1 Ellipsoid interface

The computational domain is $[-1, 1]^3$ with periodic boundary condition, and the grid size is 64^3. The initial condition of the interface for the two phases is chosen to be an ellipsoid

$$\varphi(x^\alpha, x^\beta, x^\gamma) = \frac{(x^\alpha)^2}{0.8^2} + \frac{\left(x^\beta\right)^2}{0.5^2} + \frac{(x^\gamma)^2}{0.4^2} - 1.0 = 0, \tag{8.3.1}$$

and the surface tension constant ξ is chosen to be 0.1. We run the simulation to equilibrium (or close to equilibrium) at $t = 100$. First we show the time evolution results for the case when $\mu^- = \mu^+ = 1.0$ in Fig. 8.6. See Fig. 8.7 for a cone plot of the velocity field at $t = 30$. Note that for the equal viscosity coefficient case, no GMRES iterations are needed.

We run the same simulations with $\mu^- = 0.5$ and $\mu^- = 2.0$. For $\mu^- = 0.5$ we have the less viscous fluid inside the interface and for $\mu^- = 2.0$ it is the opposite. GMRES iterations per time step for both cases are in the range of 5-6. The computation time for the equal viscosity case is 3079 seconds, for $\mu^- = 0.5$ is 10818 seconds and for $\mu^+ = 2.0$ is 9033 seconds.

We compare the evolved interface at $t = 50$ for these three cases and the effects of the viscosity coefficients for the fluid phase inside the interface are clearly seen.

(a) (b)

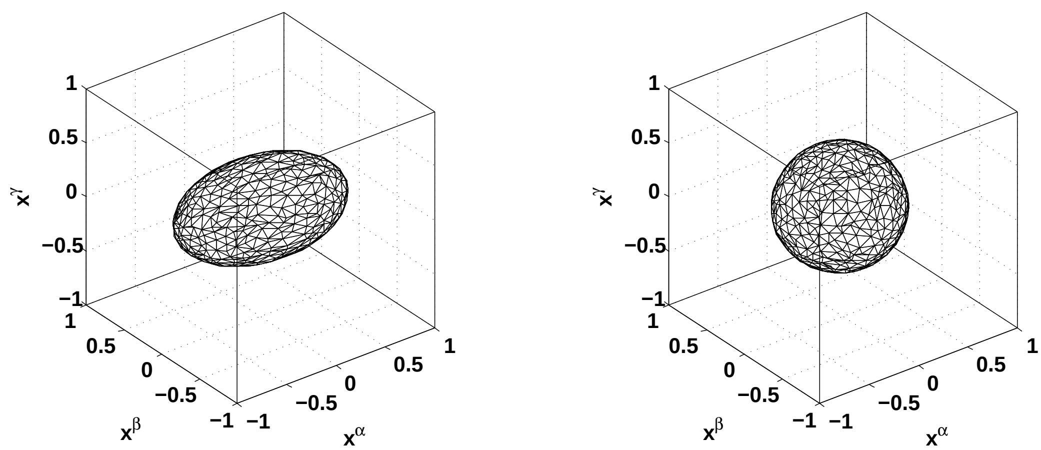

Figure 8.6: Starting from the ellipsoid, the interface evolves to a sphere under surface tension. The interface plotted at (a) $t = 0$ and (b) $t = 100$ with $\mu^- = 1.0$.

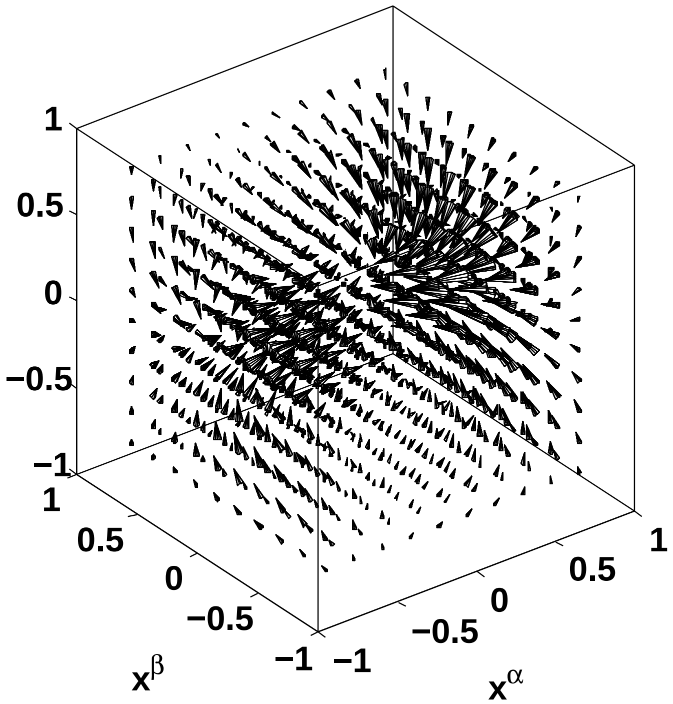

Figure 8.7: Cone plot of the velocity field at $t = 30$ with $\mu^{-} = 1.0$.

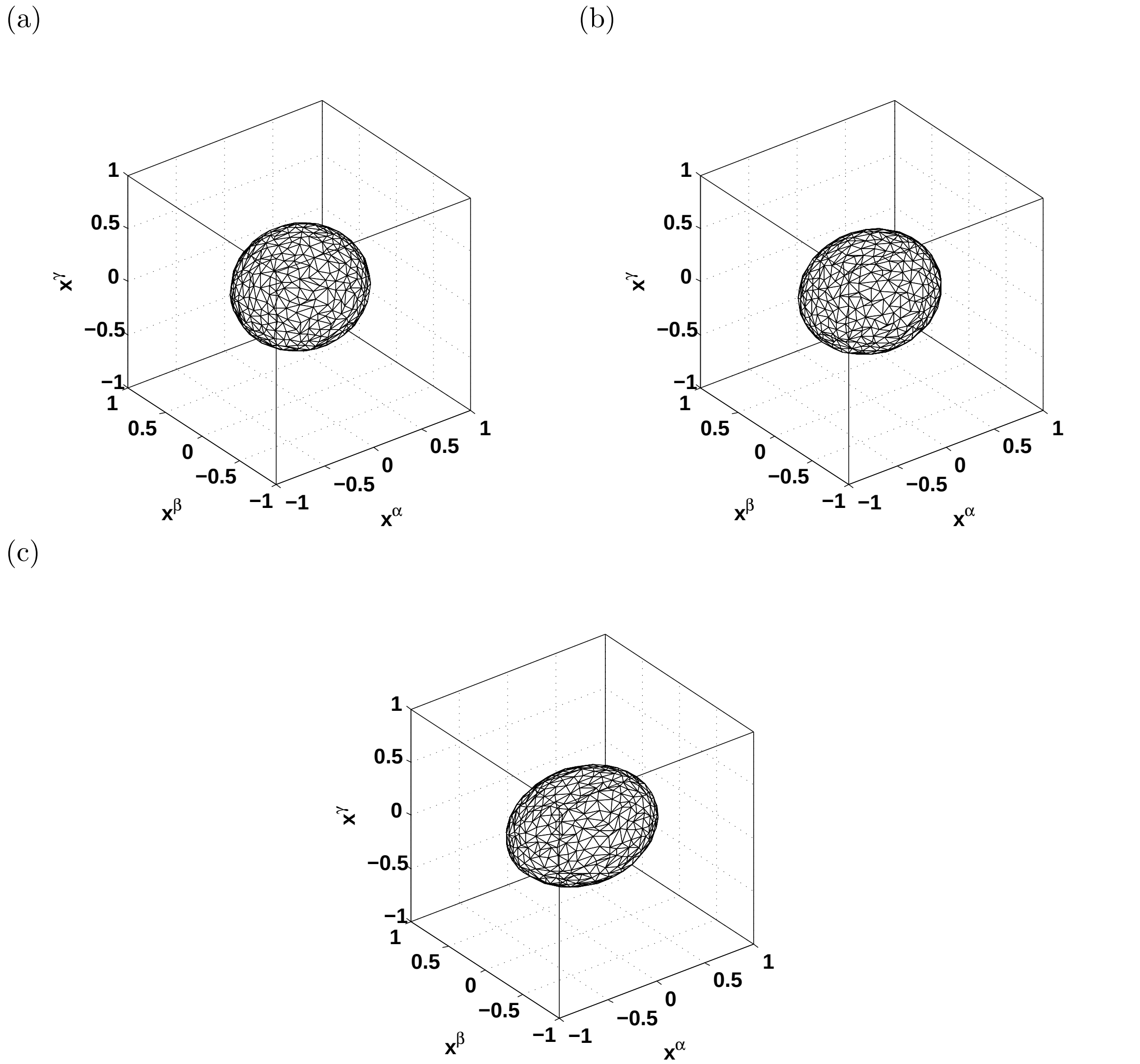

Figure 8.8: Comparison of the evolved interface at $t = 50$ for (a) $\mu^- = 0.5$, (b) $\mu^- = 1.0$ and (c) $\mu^- = 2.0$.

8.3.2 Cell aggregation implanted in a 3D model gel

Organ printing is a proposed new technology to assemble vascularized 3D soft organs using computer-aided jet-based 3D printing technology [35]. It is necessary for this new technology to show tissue tube formation as a result of cell aggregate fusion in 3D. Cell-based mathematical models have been used to predict cell aggregation behavior when implanted in a 3D model gel [39]. In this example, we start with ten attached cell aggregates and simulate the transient dynamics of these cell aggregates under surface tension.

We choose to solve the nondimensional incompressible Stokes equations. The computational domain is chosen to be $[-1,1]^3$ with periodic boundary conditions, and the grid size is 64^3. The initial condition of the interface is chosen to be 10 spheres with radius 0.2. The centers of the spheres are evenly distributed on a circle

$$(x^\alpha)^2 + (x^\beta)^2 = 0.64^2, \quad x^\gamma = 0. \tag{8.3.2}$$

See Fig. 8.9 for the interface initial condition sliced at $x^\gamma = 0.0$.

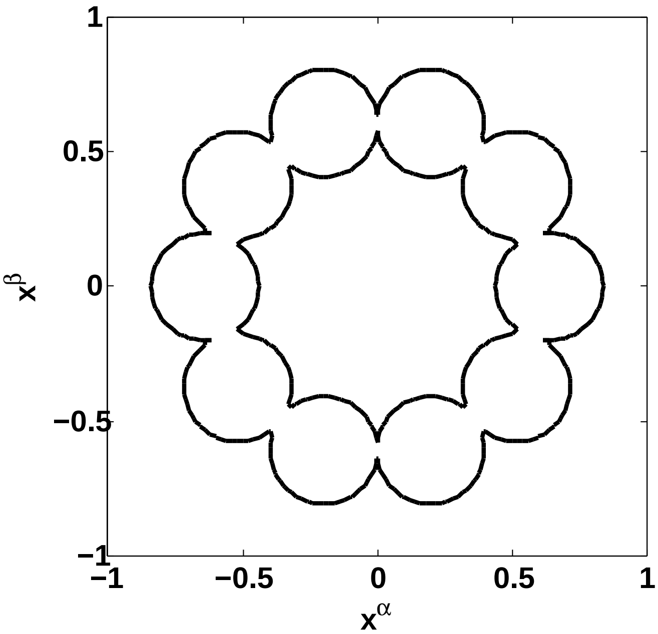

Figure 8.9: Interface initial condition sliced at $x^\gamma = 0.0$ for cell aggregation fusion simulation.

The surface tension constant ξ is chosen to be 0.1. We run the simulation to $t = 8$ for three cases where $\mu^- = 1.0, 0.5$ and 2.0 with μ^+ fixed at 1.0. See Fig. 8.10 for the initial interface and the evolved interface at end of the simulation for three different viscosity coefficient cases. Also see Fig. 8.11 for the evolved interface at $t = 2$ and $t = 4$ for the equal viscosity case. The computation cost for $\mu^- = 1.0, 0.5$ and 2.0 is 2307 seconds, 9202 seconds and 7215 seconds. The number of GMRES iterations for $\mu^- = 0.5$ is in the range of 8-24 and for $\mu^- = 2.0$ is in the range of 7-31.

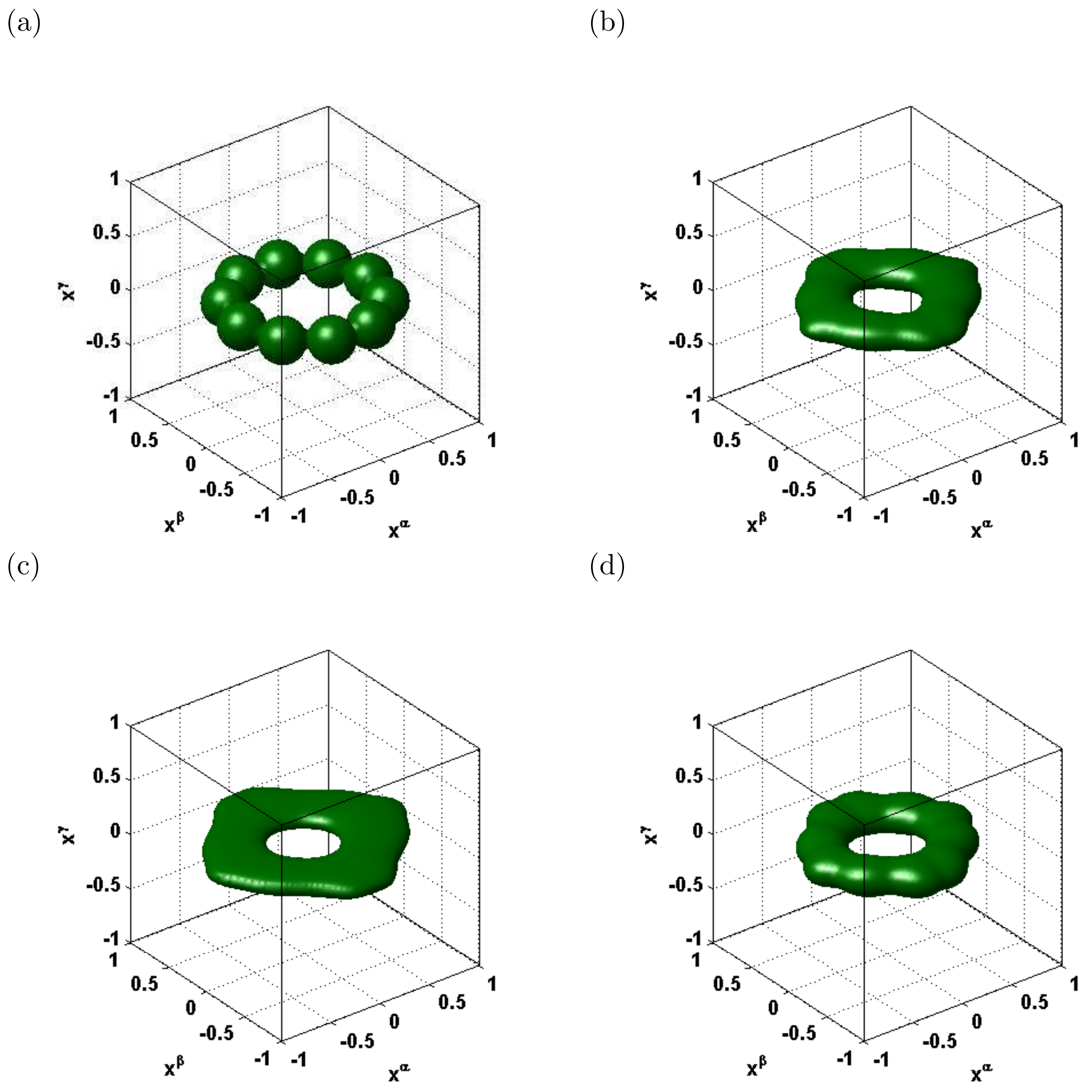

Figure 8.10: The initial interface (a) and comparison of the evolved interface at $t = 8$ for (b) $\mu^- = 1.0$, (c) $\mu^- = 0.5$ and (d) $\mu^- = 2.0$.

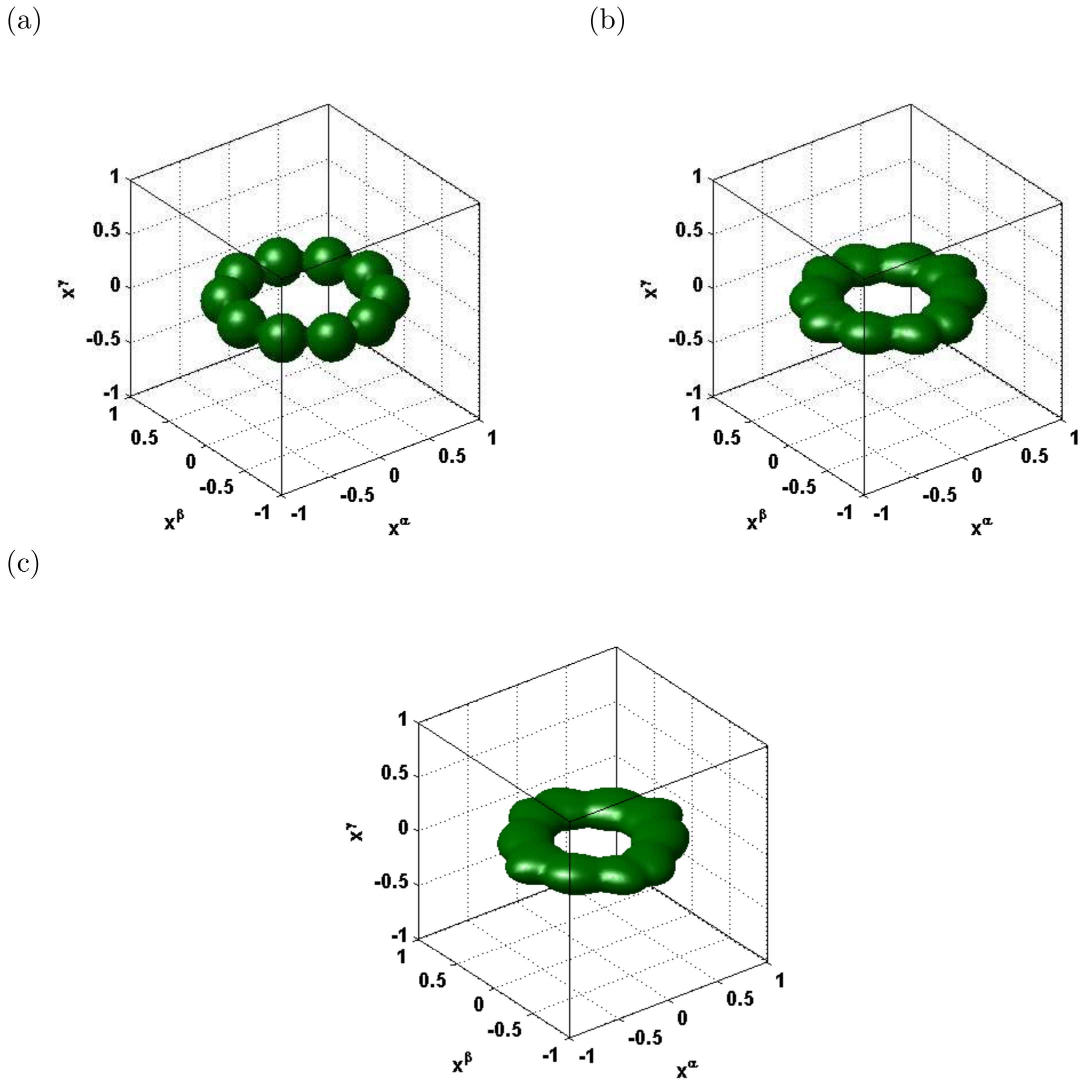

Figure 8.11: Comparison of the evolved interface at (a) $t = 0$, (b) $t = 2$ and (c) $t = 4$ for $\mu^- = 1.0$.

Chapter 9

Branching Morphogenesis: Epithelium-Mesenchyme Interactions

To simulate branching morphogenesis, we model both epithelium and mesenchyme as incompressible Stokes flow

$$-\frac{\partial p}{\partial x^i} + \frac{\partial}{\partial x^j}\left(\mu\left(\frac{\partial u^i}{\partial x^j} + \frac{\partial u^j}{\partial x^i}\right)\right) + g^i = 0, \quad \boldsymbol{x} \in \Omega^+ \cup \Omega^-, \tag{9.0.1}$$

$$\frac{\partial u^i}{\partial x^i} = 0, \quad \boldsymbol{x} \in \Omega^+ \cup \Omega^-. \tag{9.0.2}$$

Here p is the pressure, u^i is the velocity, μ is the viscosity coefficient and g^i is the body force. Across the interface Γ separating the two embryonic tissues, we have the surface force balancing condition

$$\left[\sigma_{ij} n^j\right] + f^i = 0 \tag{9.0.3}$$

where f^i is the interface force such as surface tension, n^j is the unit interfacial normal vector pointing from Ω^- to Ω^+, σ_{ij} is the stress tensor for Stokes flow defined as

$$\sigma_{ij} = -p\delta_{ij} + \mu\left(\frac{\partial u^i}{\partial x^j} + \frac{\partial u^j}{\partial x^i}\right). \tag{9.0.4}$$

We assume that some mesenchymal cells are contracting and advecting with the Stokes flow. The advection of mesenchymal cells is modeled using the advection equation

$$\frac{\partial c}{\partial t} = -u^i \frac{\partial c}{\partial x^i} \tag{9.0.5}$$

where c is the number density of contracting mesenchymal cells. The contraction force generated by those mesenchymal cells is modeled as a body force for the Stokes flow as

$$g^i = \frac{\partial(\tau c)}{\partial x^i} \tag{9.0.6}$$

where τ measures the isotropic traction force per fibroblast cell.

During branching morphogenesis, it is hypothesized [17] that some mesenchymal cells produce contraction forces which lead to clefting and further branching of epithelium. Therefore we assume that mesenchymal cells are distributed everywhere in the mesenchyme phase, but we only keep track of those cells which are contractile. We will study the two-tissue interactions given initial distributions of contractile mesenchymal cells with varying parameters. For branching morphogenesis simulations, we solve the nondimensional Stokes equations and advection equation. It is possible to estimate the parameters in the model such as tissue viscosity coefficients, mesenchymal cell number density and traction force per fibroblast cell [34].

9.1 2D Geometry

The computational domain is chosen to be $[-1,1]^2$ with periodic boundary condition, and the grid size is 200^2. The initial condition of the interface is a circle with radius 0.4:

$$\varphi\left(x^{\alpha}, x^{\beta}\right) = \sqrt{\left(x^{\alpha}\right)^2/0.4^2 + \left(x^{\beta}\right)^2/0.4^2} - 1.0, \tag{9.1.1}$$

and the initial condition for mesenchymal cell number density is chosen as

$$c(x^{\alpha}, x^{\beta}) = I_A(\boldsymbol{x}) \tag{9.1.2}$$

where $A = \{(0.42 \le r \le 0.62, -\pi/12 \le \theta \le \pi/12)\}$, and (r,θ) is the polar coordinates. $I_A(\boldsymbol{x})$ is the indicator function defined as

$$I_A(\boldsymbol{x}) = \begin{cases} 1 & \text{if } \boldsymbol{x} \in A, \\ 0 & \text{if } \boldsymbol{x} \notin A. \end{cases} \tag{9.1.3}$$

For numerical reasons, we use a diffusion smoother to filter out the roughness of the indicator function. See Fig. 9.1 for the initial mesenchymal cell number density and interface.

The surface tension coefficient is chosen as 0.001 and the traction force constant τ is chosen as 100.0. We run the simulation to $t = 1$ for $\mu^- = 1.0$, $t = 0.2$ for $\mu^- = 0.1$ and $t = 2$ for $\mu^- = 10.0$ with μ^+ fixed at 1.0. See Fig. 9.2 for the simulation results with $\mu^- = 0.1$, Fig. 9.3 with $\mu^- = 1.0$ and Fig. 9.4 with $\mu^- = 10.0$.

The computation cost for $\mu^- = 1.0, 0.1$ and 10.0 is 909 seconds, 1911 seconds and 3316 seconds respectively. The number of GMRES iterations for $\mu^- = 0.1$ is in the range of $9-15$ and for $\mu^- = 10.0$ is in the range of $10-15$. GMRES iteration is not needed for the equal viscosity case.

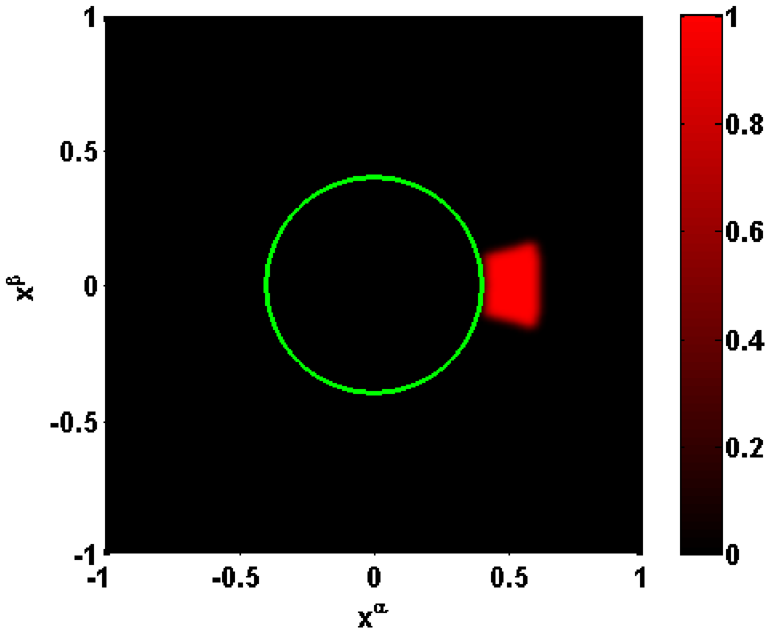

Figure 9.1: Initial number density of contractile mesenchymal cells $c\left(x^\alpha, x^\beta\right)$ (red) and initial interface (green circle) separating epithelium and mesenchyme.

It is clear from the simulation results that viscosity ratio plays a role in the interactions of the two phases across the interface. Also see Fig. 9.5 for the comparison of the interface and cell number density profile with different viscosity ratio and similar clefting depth. Note that due to the numerical inaccuracy of the discretized advection equation, the contractile mesenchymal cells may bleed into the epithelium phase, which is biologically incorrect. Also the integrated number density of contractile mesenchymal cells is non-constant due to numerical dissipations. For future work, a high order conservative scheme for the advection equation may help solve the problem. It is also desirable to solve the advection equation with the interface Γ treated as an impermeable boundary. It is seen in Fig. 9.5 that the cleft width is not monotonic with respect to the viscosity ratio. We suspect that numerical inaccuracy of solving the advection equation may be the major factor causing this result which needs further studies.

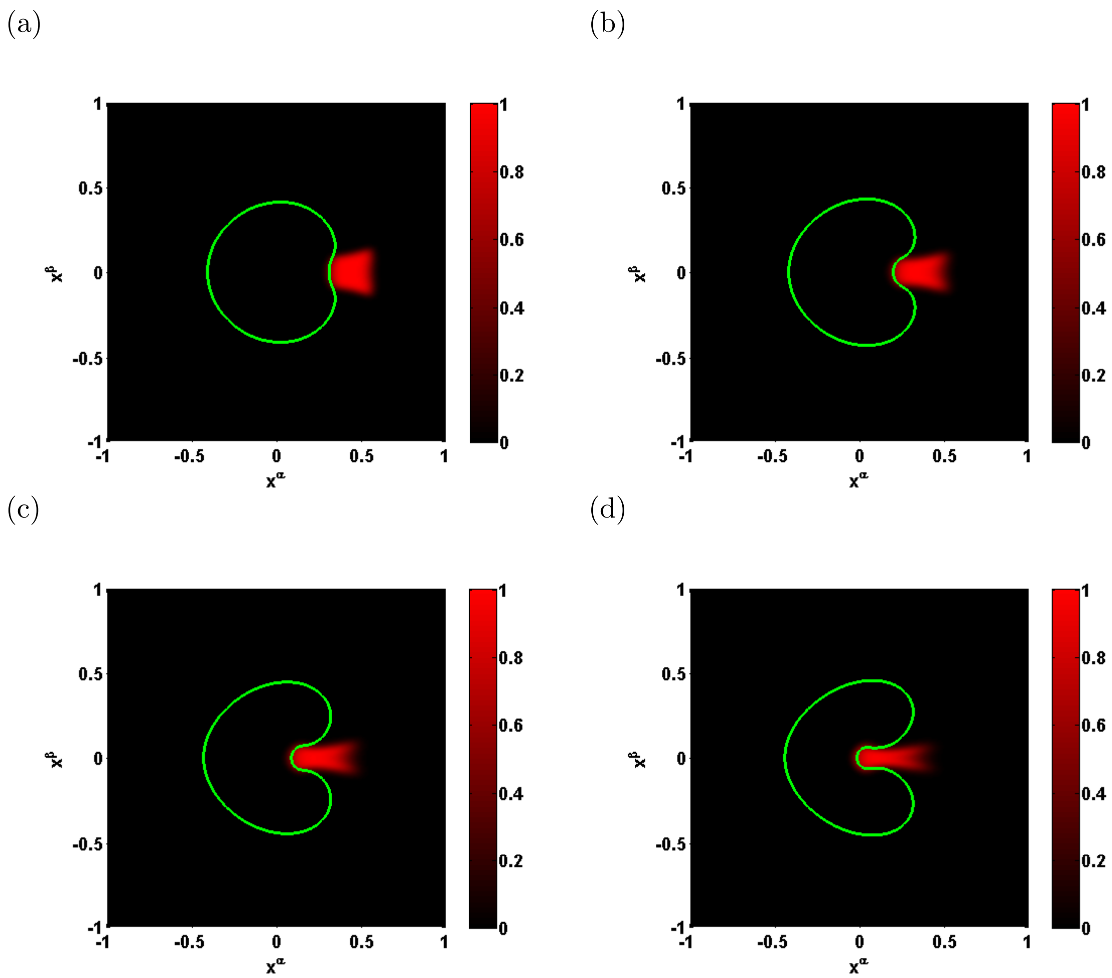

Figure 9.2: The interface with contractile cell number density profile with $\mu^- = 0.1$ at (a) $t = 0.05$ (b) $t = 0.10$ (c) $t = 0.15$ and (d) $t = 0.20$.

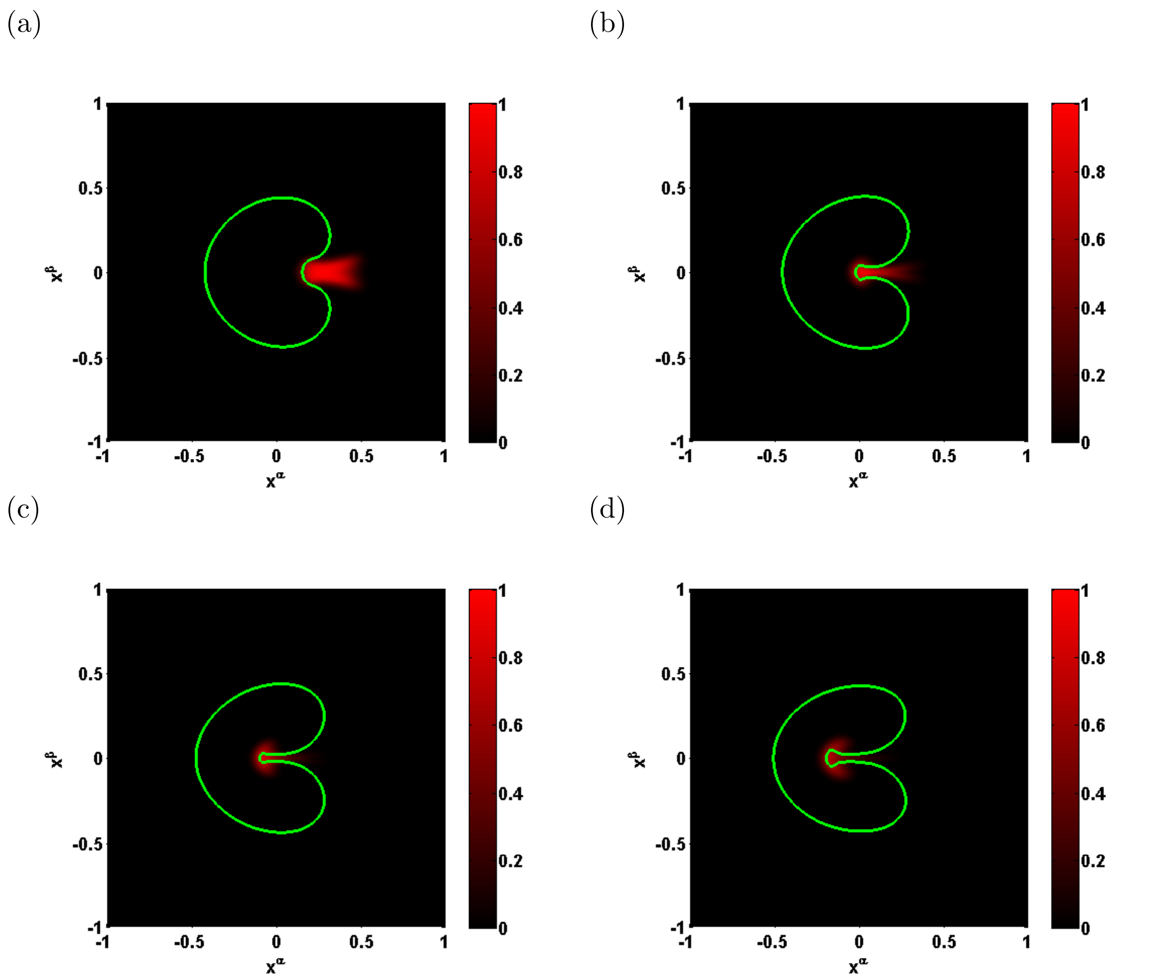

Figure 9.3: The interface with contractile cell number density profile with $\mu^- = 1.0$ at (a) $t = 0.25$ (b) $t = 0.5$ (c) $t = 0.75$ and (d) $t = 1.0$.

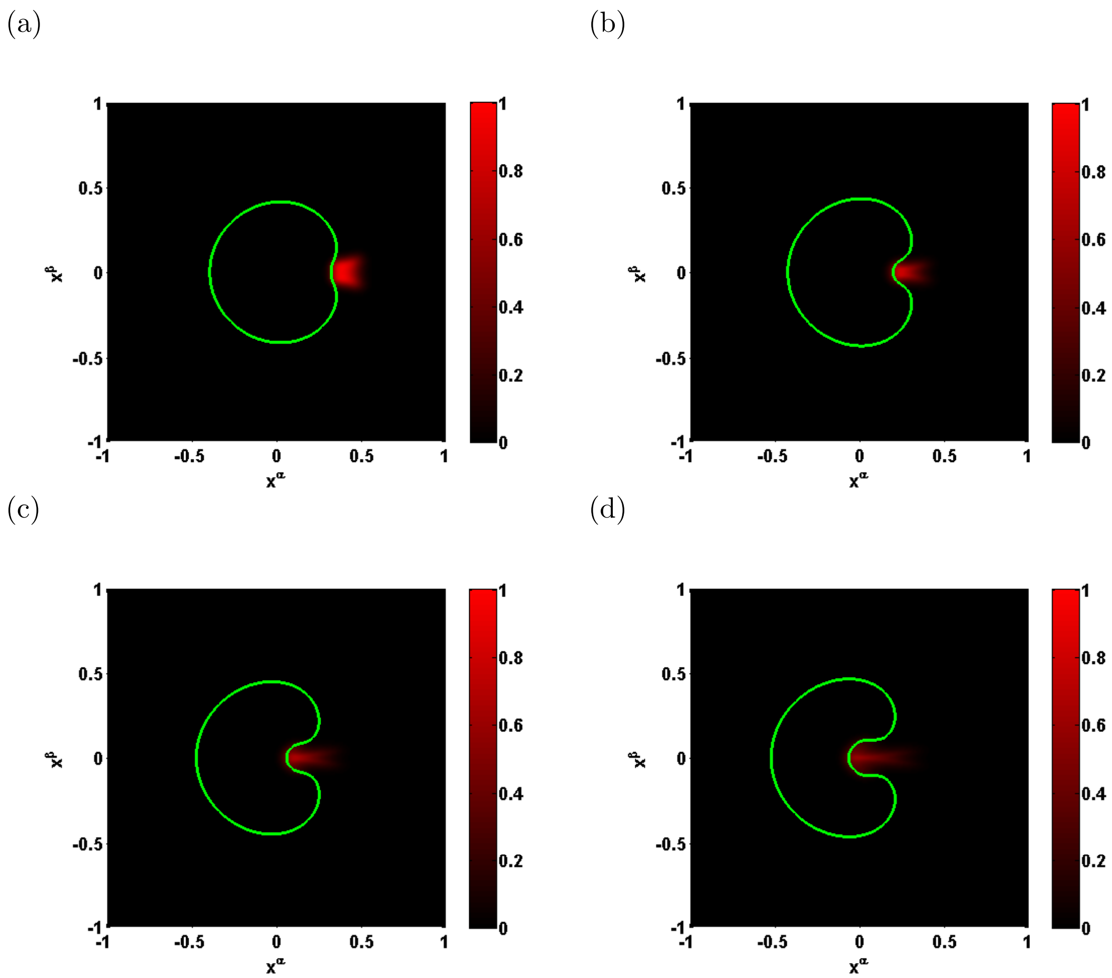

Figure 9.4: The interface with contractile cell number density profile with $\mu^- = 10.0$ at (a) $t = 0.5$ (b) $t = 1$ (c) $t = 1.5$ and (d) $t = 2$.

(a) (b)

(c)

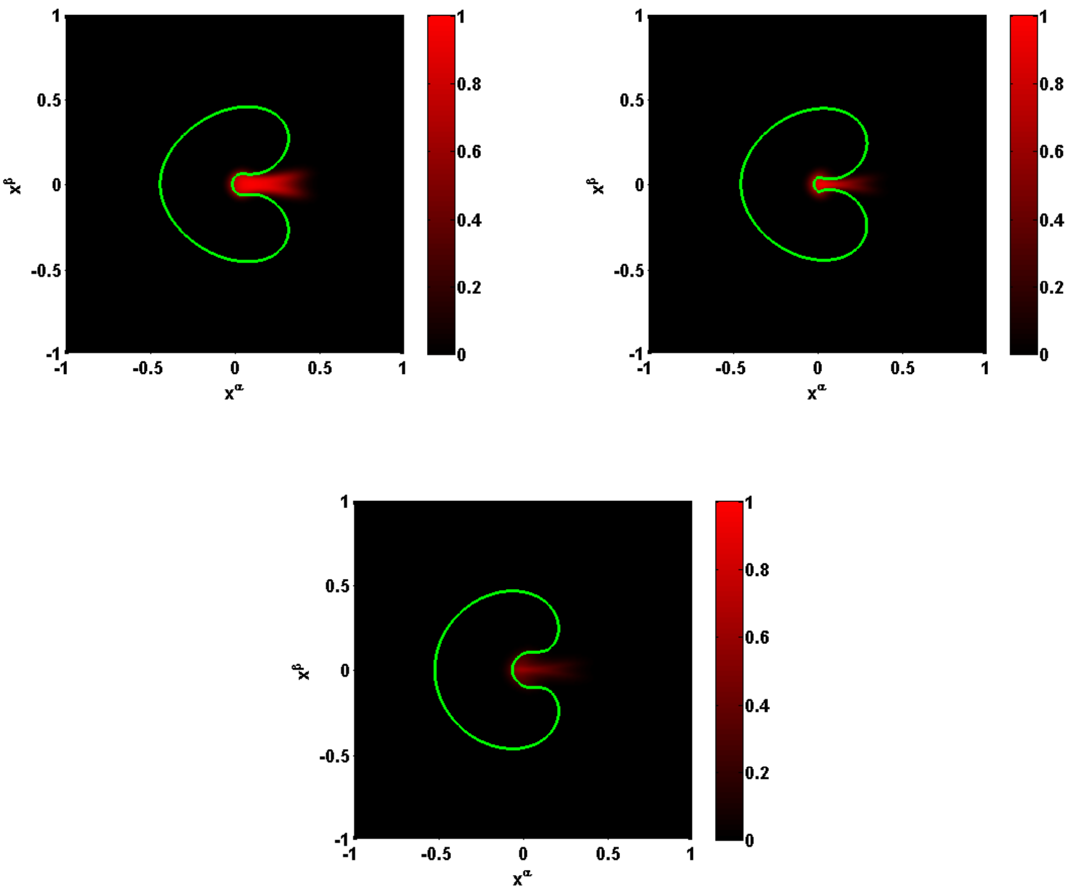

Figure 9.5: Comparison of the interface with contractile cell number density profile with (a) $\mu^- = 0.1$ at $t = 0.2$ (b) $\mu^- = 1.0$ at $t = 0.5$ (c) $\mu^- = 10.0$ at $t = 2$.

9.2 3D Geometry

The computational domain is chosen as $[-1,1]^3$ with periodic boundary condition, and the grid size is 64^3. The initial condition of the interface is a sphere with radius 0.4:

$$\varphi\left(x^\alpha, x^\beta, x^\gamma\right) = \sqrt{\left(x^\alpha\right)^2/0.4^2 + \left(x^\beta\right)^2/0.4^2 + \left(x^\gamma\right)^2/0.4^2} - 1.0, \tag{9.2.1}$$

and the initial condition for mesenchymal cell number density is chosen as

$$c\left(x^\alpha, x^\beta, x^\gamma\right) = I_A(\boldsymbol{x}) \tag{9.2.2}$$

where $A = \{(0.42 \le r \le 0.62, -\pi/12 \le \theta \le \pi/12, 0 \le \phi \le \pi)\}$, (r, θ, ϕ) is the spherical coordinates, and $I_A(\boldsymbol{x})$ is the indicator function. As in the 2D case, we use a diffusion smoother to get the approximated indicator function. See Fig. 9.6 for the initial interface and the level surface of the initial number density of the contractile mesenchymal cells.

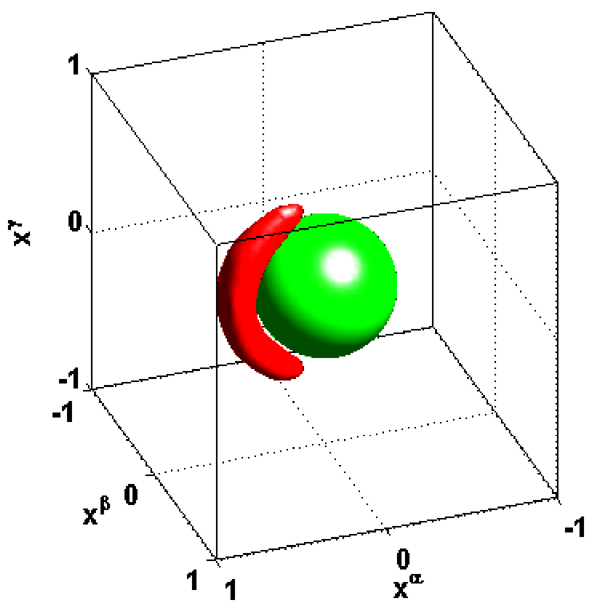

Figure 9.6: Level surface (level value: 0.5) of the initial contractile mesenchymal cell number density $c\left(x^\alpha, x^\beta, x^\gamma\right)$ (red) and initial interface (green) separating epithelium and mesenchyme.

The surface tension coefficient is chosen as 0.001 and the traction force constant τ is 100.0. We run the simulation to $t = 0.4$ for $\mu^- = 1.0$, $t = 0.2$ for $\mu^- = 0.2$ and $t = 1$ for

$\mu^- = 5.0$ with μ^+ fixed at 1.0. See Figs. 9.7, 9.8 for the simulation results with $\mu^- = 0.2$, Figs. 9.9, 9.10 with $\mu^- = 1.0$ and Figs. 9.11, 9.12 with $\mu^- = 5.0$.

The computational cost for $\mu^- = 1.0, 0.2$ and 5.0 is 1008 seconds, 3880 seconds and 7257 seconds respectively. The number of GMRES iterations for $\mu^- = 0.2$ is in the range of 9-14 and for $\mu^- = 5.0$ is in the range of 10-16. No GMRES iterations are needed for the case when $\mu^+ = \mu^-$.

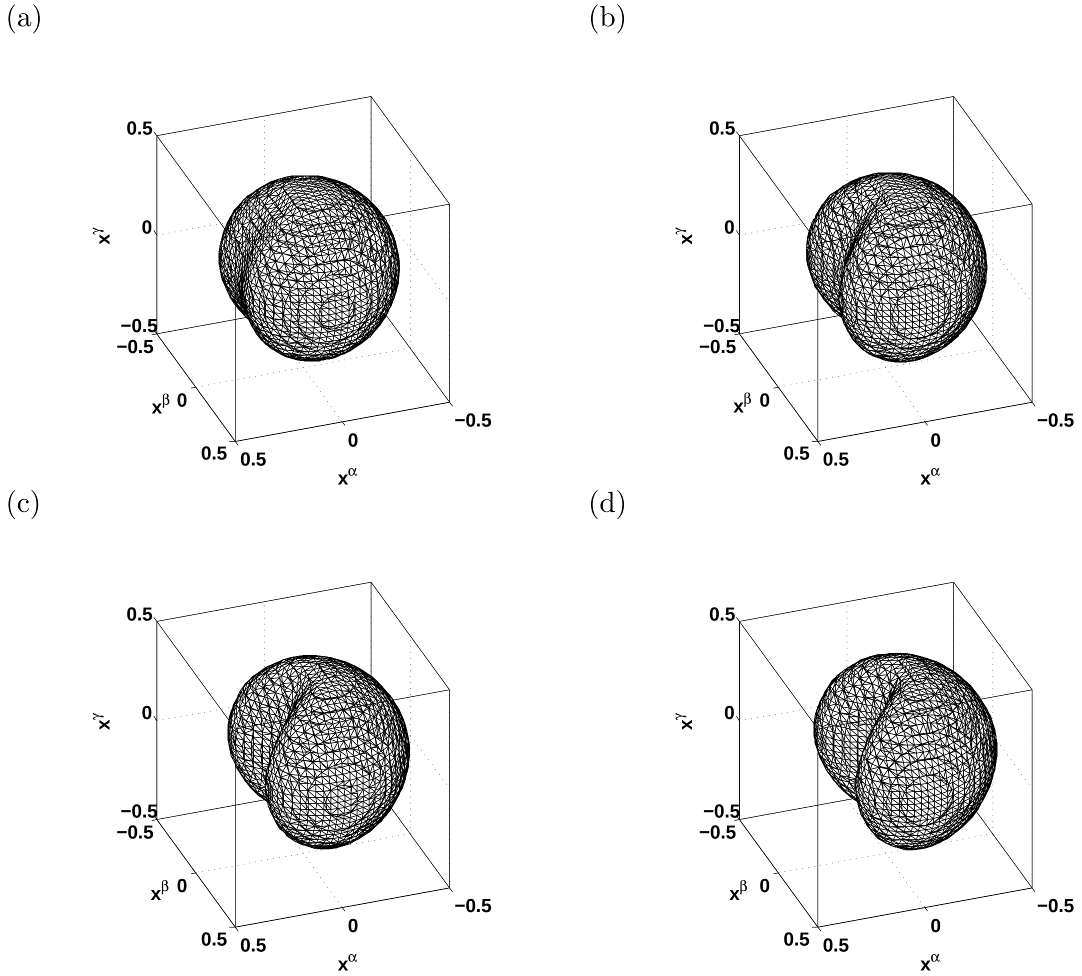

Figure 9.7: Interface evolution with $\mu^- = 0.2$ at (a) $t = 0.05$ (b) $t = 0.1$ (c) $t = 0.15$ and (d) $t = 0.2$.

To summarize, we have shown the simulation results for the interactions of epithelium and mesenchyme by solving the two-phase Stokes equations with discontinuous viscosity coefficients and singular interface force (surface tension), with the mesenchymal contraction force modeled as a body force. Our simulations show epithelium clefting due to the

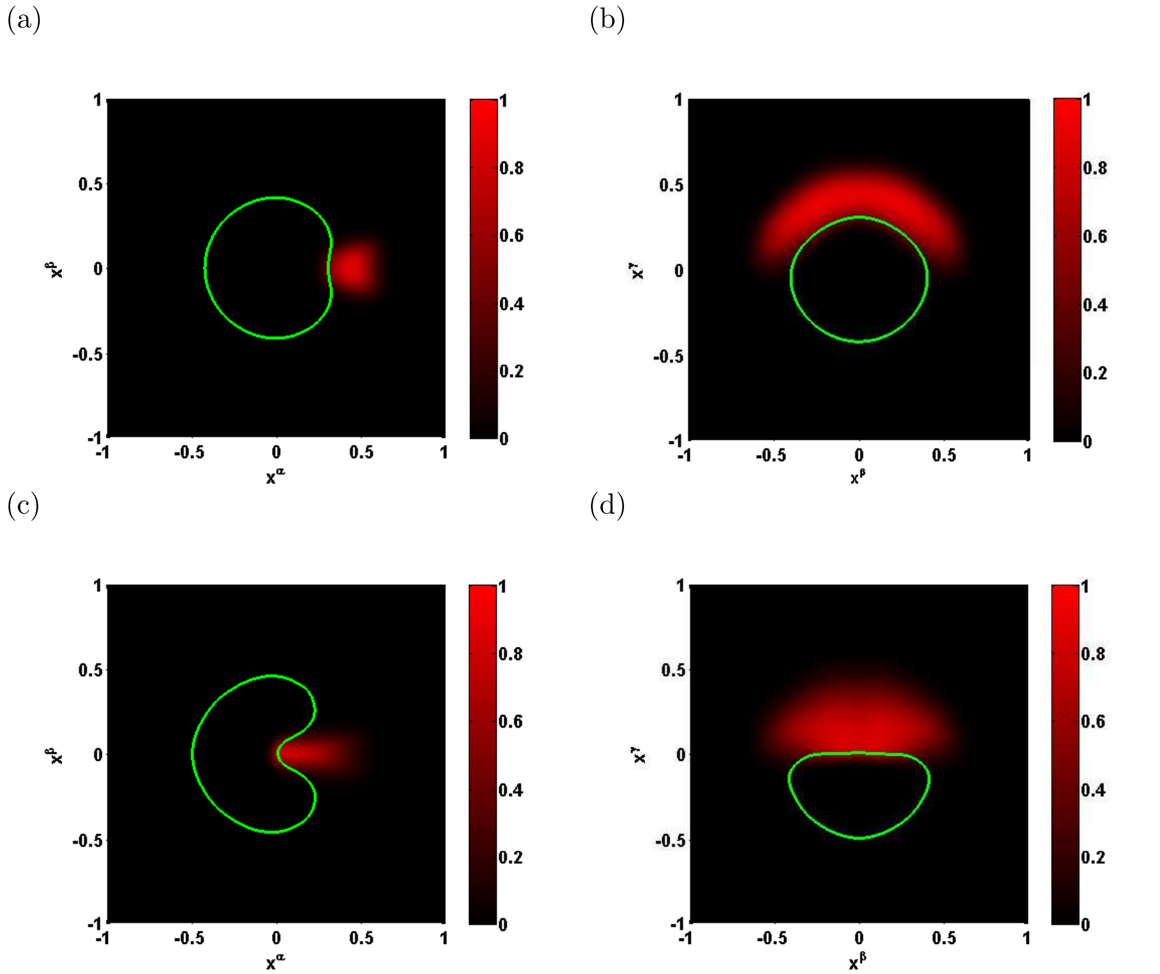

Figure 9.8: The interface sliced at $x^\gamma = 0$ (a,c) and $x^\alpha = 0$ (b,d) and sliced color plot of contractile cell number density profile (red) with $\mu^- = 0.2$ at (a,b) $t = 0.05$ (c,d) $t = 0.2$.

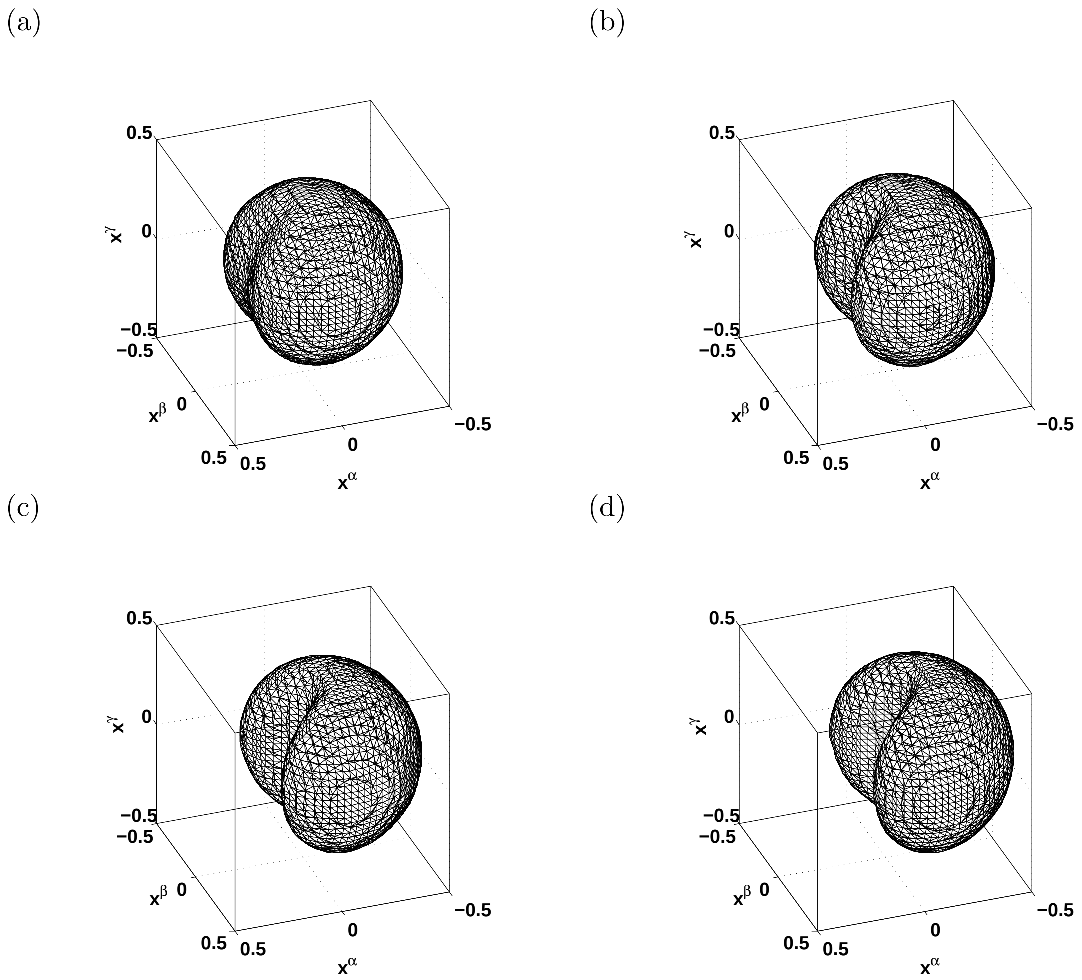

Figure 9.9: Interface evolution with $\mu^- = 1$ at (a) $t = 0.1$ (b) $t = 0.2$ (c) $t = 0.3$ and (d) $t = 0.4$.

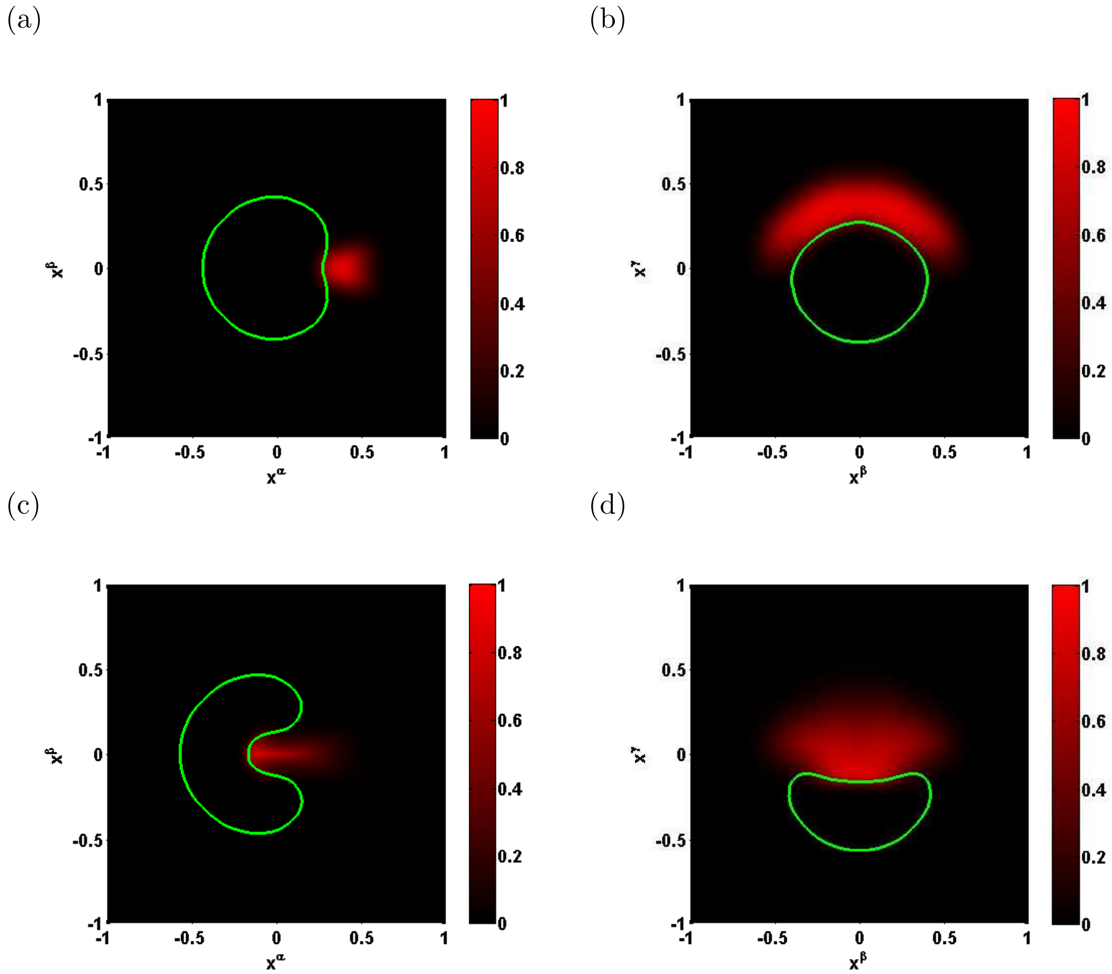

Figure 9.10: The interface sliced at $x^\gamma = 0$ (a,c) and $x^\alpha = 0$ (b,d) and sliced color plot of contractile cell number density profile (red) with $\mu^- = 1.0$ at (a,b) $t = 0.1$ (c,d) $t = 0.4$.

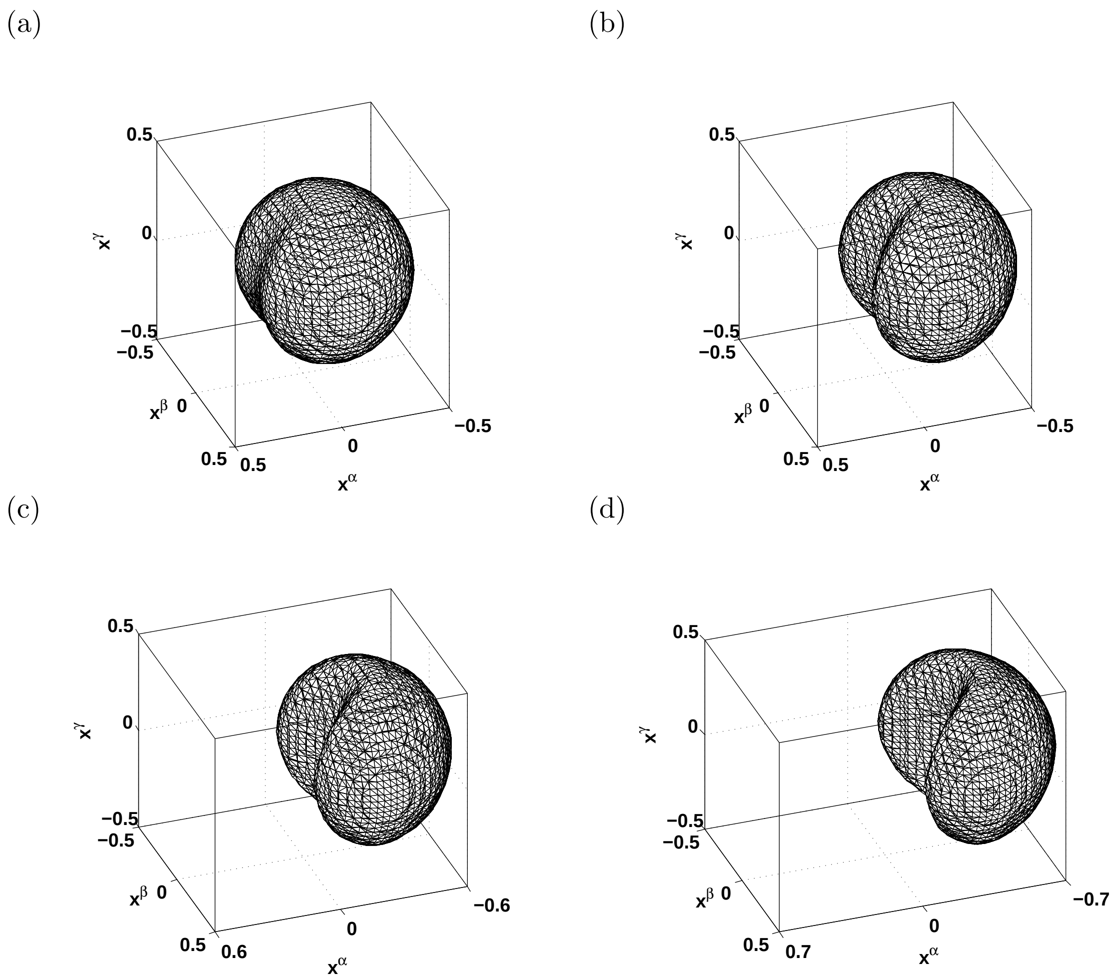

Figure 9.11: Interface evolution with $\mu^{-} = 5$ at (a) $t = 0.25$ (b) $t = 0.5$ (c) $t = 0.75$ and (d) $t = 1.0$.

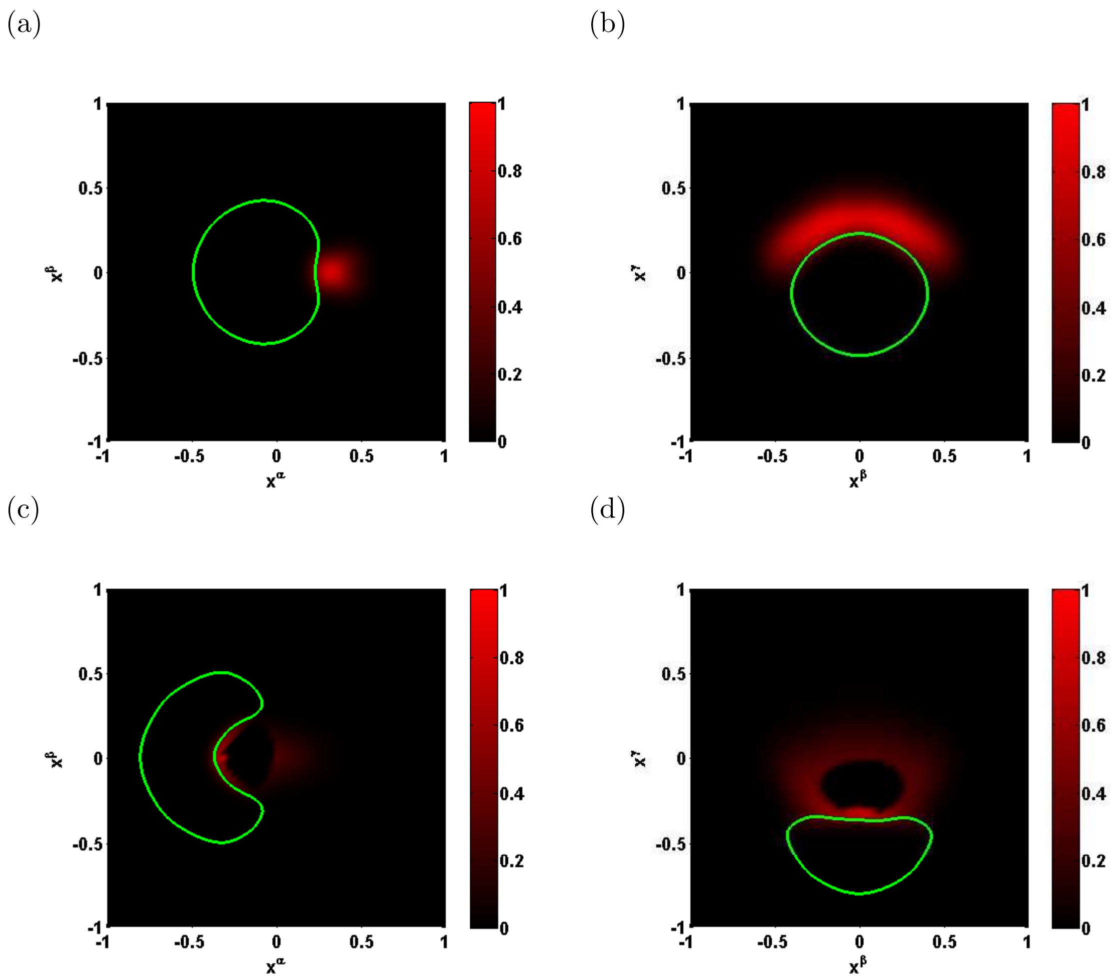

Figure 9.12: The interface sliced at $x^\gamma = 0$ (a,c) and $x^\alpha = 0$ (b,d) and sliced color plot of contractile cell number density profile (red) with $\mu^- = 5.0$ at (a,b) $t = 0.25$ (c,d) $t = 1.0$. Note that (c,d) is non-physical since the advection equation solver returns negative values for the number density c. We truncated the negative values as zero for comparison with (a,b).

mesenchymal contraction. The geometry of the cleft is consistent with the geometry in vivo.

As in the 2D case, we need to adopt a better scheme for solving the advection equation. In Fig. 9.12, we get negative values for cell number density c which is non-physical. For future work, we propose to use a high order conservative scheme for the advection equation and it is also possible to enforce the impermeable boundary condition on the interface for the cell number density c.

Chapter 10

Discussion

We have developed an immersed interface method (IIM) coupled with the level set method (LSM) for solving two-phase Stokes equations with an interface. Our numerical solver can handle two-phase flow problems with complicated interface geometry and discontinuous viscosity coefficients. Numerical experiments show the expected second-order accuracy for our method. We have applied the method to study branching morphogenesis focusing on the interactions between epithelium and mesenchyme tissues. We have presented simulation results of epithelium clefting due to mesenchymal contraction force in both 2D and 3D.

On a foundation of the immersed interface method, we have combined the local Cartesian coordinates transformation with tensor analysis to derive jump conditions for the general two-phase Stokes flow problems in Chapter 3. In Chapter 4, we have derived the IIM scheme for elliptic equations in both 2D and 3D. Approaches we have taken can be used to study various interface problems both theoretically and numerically.

Using level set functions to represent the interface implicitly, we can couple the IIM with the LSM for moving interface problems. Simulations of interface deformations due to surface tension clearly show that the numerical solver is very efficient and can capture complicated geometrical changes well.

We have tested our algorithm in Chapter 7 for general fixed interface problems where exact solutions are constructed. Numerical experiments have showed that the two-phase Stokes solver is very efficient with second-order accuracy in the infinity norm.

In Chapter 8, the two-phase Stokes solver for moving interface problems was tested using surface tension relaxation cases and our results compare favorably with existing results in the literature and also may be used to study cell aggregation dynamics in a 3D model gel. We have studied branching morphogenesis by coupling the two-phase Stokes flow with cellular advection. Clefting of epithelium is simulated with the contraction force supplied by mesenchymal cells.

Our method is based on fixed Cartesian grids and does not involve complicated and expensive meshing and re-meshing steps. Using level set functions and operations defined for those functions (e.g. union, subtraction), we can model very complicated and rather arbitrary interface deformations. The finite difference scheme we derived allows us to use existing fast Poisson solvers for interface problems and this boosts the overall performance of our algorithm. Level set methods also allow one to solve moving interface problems by simply advecting the level set functions. By deriving and incorporating the jump conditions for the Stokes equations, we are able to construct the algorithm for Stokes flow with second-order accuracy. The jump condition results are applicable to other numerical methods (e.g. finite element methods) for solving the Stokes equations.

Since the interface is implicitly defined by the level set function, it is very critical to start the simulation with a smooth level set function close to the distance function. In order to approximate the second-order derivative terms such as the mean curvature with accuracy and avoid stiffness of the moving interface problem, it is necessary to use some reinitialization schemes to maintain the level set function as a distance function. Area conservation for the level set methods still needs more investigation. Also since the immersed interface scheme uses surface derivative terms to calculate the correction term, numerical accuracy and stability depend on the adopted numerical differentiation methods. Simulations also show that for cases with unequal viscosities, because the coefficient matrix for the augmented variables has very large condition number, GMRES iterations may not be able to invert the coefficient matrix with good accuracy. Increased number of GMRES iterations due to high contrast of viscosity coefficients also slows the numerical solver. In the branching morphogenesis simulations, the epithelium center of mass drifts which may be an artifact of the area conservation scheme we used. The drifting may also be an effect of implementing the contraction force as a body force.

For future work, we first need to implement a high order conservative scheme for the advection equation. It is also possible to solve the advection equation with an irregular boundary and enforce the impermeable boundary condition. We also hope to use the same methods developed in this thesis to solve two-phase Navier-Stokes equations with interfaces. It is worthwhile to combine various numerical techniques such as staggered or/and adaptive grids with our two-phase fluid solver. We also need to adopt LSM variants such as local level set methods to improve the overall efficiency and different methods for volume conservation. Many biological problems involving cells and tissues can be modeled as multiphase flow problems and it is expected that our solver will be used for various mathematical biology problems such as cellular fluid dynamics and tissue interactions. We use periodic boundary conditions for all the moving interface problems in the thesis; we plan to extend our numerical solver for various boundary conditions.

List of References

[1] J. Adams, P. Swarztrauber, and R. Sweet. Fishpack: Efficient Fortran subprograms for the solution of separable elliptic partial differential equations. http://www.netlib.org/fishpack/.

[2] J. Bard. *Morphogenesis.* Cambridge University Press, 1990.

[3] D. A. Beysens, G. Forgacs, and J. A. Glazier. Cell sorting is analogous to phase ordering in fluids. *Proc. Natl. Acad. Sci. USA*, 97:9467–9471, 2000.

[4] A. J. Chorin. Numerical solution of the Navier-Stokes equations. *Math. Comp.*, 22:745–762, 1968.

[5] Kevin T. Chu and Masa Prodanovic. Level set method library (lsmlib). http://www.princeton.edu/ ktchu/.

[6] G. S. Davis, H. M. Phillips, and M. S. Steinberg. Germ-layer surface tensions and "tissue affinities" in Rana pipiens gastrulae: quantitative measurements. *Developmental Biology*, 192:630–644, 1997.

[7] S. Deng. *Immersed Interface Method for three dimensional interface problems and applications.* PhD thesis, North Carolina State University, 2001.

[8] F. Doljanski. The sculpturing role of fibroblast-like cells in morphogenesis. *Perspectives in Biology and Medicine*, 47:339–356, 2004.

[9] J. Dongarra, J. Bunch, C. Moler, and P. Stewart. Linpack: Library for performing linear algebra. http://www.netlib.org/linpack/.

[10] D. A. Drew and S. L. Passman. *Theory of multicomponent fluids.* Springer, 1998.

[11] H. P. Ehrlich, D. J. Buttle, and D. H. Bernanke. Physiological variables affecting collagen lattice contraction by human dermal fibroblasts. *Exp. Mol. Pathol.*, 50:220–229, 1989.

[12] D. Enright, R. Fedkiw, J. Ferziger, and I. Mitchell. A hybrid particle level set method for improved interface capturing. *J. Comput. Phys.*, 183:83–116, 2002.

[13] G. Forgacs, R. A. Foty, Y. Shafrir, and M. S. Steinberg. Viscoelastic properties of living embryonic tissues: a quantitative study. *Biophysical Journal*, 74:2227–2234, 1998.

[14] R. A. Foty, G. Forgacs, C. M. Pfleger, and M. S. Steinberg. Liquid properties of embryonic tissues: measurement of interfacial tensions. *Phys. Rev. Lett.*, 72:2298–2301, 1994.

[15] R. A. Foty, C. M. Pfleger, G. Forgacs, and M. S. Steinberg. Surface tensions of embryonic tissues predict their mutual envelopment behavior. *Development*, 122:1611–1620, 1996.

[16] S. Groß, V. Reichelt, and A. Reusken. A finite element based level set method for two-phase incompressible flows. *IGPM-Report 243, RWTH Aachen*, 2004.

[17] Y. Hieda and Y. Nakanishi. Epithelial morphogenesis in mouse embryonic submandibular gland: its relationships to the tissue organization of epithelium and mesenchyme. *Develop. Growth Differ.*, 39:1–8, 1997.

[18] M. S. Hutson, Y. Tokutake, M.-S. Chang, J. W. Bloor, S. Venakides, D. P. Kiehart, and G. S. Edwards. Forces for morphogenesis investigated with laser microsurgery and quantitative modeling. *Science*, 300:145–149, 2003.

[19] K. Ito and Z. Li. Interface conditions for Stokes equations with a discontinuous viscosity and surface sources. *Applied Math. Letters*, 19:229–234, 2006.

[20] M. Kang, R. Fedkiw, and X. Liu. A boundary condition capturing method for multiphase incompressible flow. *J. Sci. Comput*, 15:323–360, 2000.

[21] T. Kono, T. Tanii, M. Furukawa, N. Mizuno, J. Kitajima, M. Ishii, and T. Hamada. Correlation between ageing and collagen gel contractility of human fibroblasts. *Acta Derm Venereol.*, 70:241–244, 1990.

[22] M.-C. Lai and Z. Li. A remark on jump conditions for the three-dimensional Navier-Stokes equations involving an immersed moving membrane. *Applied Math. Letters*, 14:149–154, 2001.

[23] R. J. LeVeque and Z. Li. Immersed interface methods for Stokes flow with elastic boundaries or surface tension. *SIAM J. Sci. Comput.*, 18:709–735, 1997.

[24] Z. Li. *The Immersed Interface Method - A Numerical Approach for Partial Differential Equations with Interfaces.* PhD thesis, University of Washington, 1994.

[25] Z. Li. A fast iterative algorithm for elliptic interface problems. *SIAM J. Numer. Anal.*, 35:230–254, 1998.

[26] Z. Li. An overview of the immersed interface method and its applications. *Taiwanese J. Mathematics*, 7:1–49, 2003.

[27] Z. Li and K. Ito. *The Immersed Interface Method: Numerical solutions of PDEs involving interfaces and irregular domains.* SIAM (Frontiers in Applied Mathematics), 2006.

[28] Z. Li, K. Ito, and M.-C. Lai. An augmented approach for Stokes equations with a discontinuous viscosity and singular forces. NCSU-CRSC Tech. Report: CRSC-TR04-24, North Carolina State University, 2004.

[29] Z. Li and S. Lubkin. Numerical analysis of interfacial Stokes flow with discontinuous viscosity and nonlinear surface tension. *International Journal for Numerical Methods in Fluids*, 37:525–540, 2001.

[30] Z. Li, X. Wan, K. Ito, and S. Lubkin. An augmented approach for the pressure boundary condition in a Stokes flow. *Commun. Comput. Phys.*, 1:874–885, 2006.

[31] Z. Li, H. Zhao, and H. Gao. A numerical study of electro-migration voiding by evolving level set functions on a fixed cartesian grid. *J. Comput. Phys.*, 152:281–304, 1999.

[32] S. Lubkin and T. Jackson. Multiphase mechanics of capsule formation in tumors. *J. Biomech. Eng.*, 124:237–243, 2002.

[33] S. Lubkin and J. Murray. A mechanism for early branching in lung morphogenesis. *J. Math. Biol.*, 34:77–94, 1995.

[34] S. R. Lubkin and Z. Li. Force and deformation on branching rudiments: Cleaving between hypotheses. *Biomechanics and Modeling in Mechanobiology*, 1:5–16, 2002.

[35] V. Mironov, T. Boland, T. Tursk, G. Forgacs, and R. R. Markwald. Organ printing: computer-aided jet-based 3D tissue engineering. *TRENDS in Biotechnology*, 21:157–161, 2003.

[36] José C. M. Mombach, D. Robert, F. Graner, G. Gillet, G. L. Thomas, M. Idiart, and J.-P. Rieu. Rounding of aggregates of biological cells: experiments and simulations. *Physica A*, 352:525–534, 2005.

[37] J. D. Murray, G. F. Oster, and A. K. Harris. A mechanical model for mesenchymal morphogenesis. *J. Math. Biology*, 17:125–129, 1983.

[38] Y. Nakanishi, Y. Hieda, W. V. Cardoso, S. Lubkin, and C. W. Daniel. Epithelial branching. *Encyclopedia of Life Sciences, http://www.els.net/*, 2000.

[39] A. Neagu and G. Forgacs. Fusion of cell aggregates: a mathematical model. *In Biomedical Engineering. Recent Development (J. Vossoughi ed.)*, pages 241–242, 2002.

[40] S. Osher and R. Fedkiw. *Level set methods and dynamic implicit surfaces.* Springer-Verlag, 2002.

[41] B. Palsson and S. Bhatia. *Tissue engineering.* Pearson Prentice Hall, 2004.

[42] E. Palsson and H. G. Othmer. A model for individual and collective cell movement in Dictyostelium discoideum. *Proc. Natl. Acad. Sci. USA*, 97:10448–10453, 2000.

[43] H. M. Philips and M. S. Steinberg. Equilibrium measurements of embryonic chick cell adhesiveness. i. Shape equilibrium in centrifugal fields. *Proc. Natl. Acad. Sci. USA*, 64:121–127, 1969.

[44] H. M. Philips and M. S. Steinberg. Embryonic tissues as elasticoviscous liquids. i. Rapid and slow shape changes in centrifuged cell aggregates. *J. Cell Science*, 30:1–20, 1978.

[45] H. M. Philips, M. S. Steinberg, and B. H. Lipton. Embryonic tissues as elasticoviscous liquids. ii. Direct evidence for cell slippage in centrifuged aggregates. *Dev. Biol.*, 59:124–134, 1977.

[46] C. Pozrikidis. *Fluid dynamics: theory, computation, and numerical simulation.* Kluwer Academic Publishers, 2001.

[47] C. Pozrikidis. *Modeling and simulation of capsules and biological cells.* Chapman & Hall, London, 2003.

[48] J.-P. Rieu and Y. Sawada. Hydrodynamics and cell motion during the rounding of two dimensional hydra cell aggregates. *Eur. Phys. J. B*, 27:167–172, 2002.

[49] Y. Saad and M. H. Schultz. GMRES: A generalized minimal residual algorithm for solving nonsymmetric linear systems. *SIAM J. Sci. Stat. Comput.*, 7:856–869, 1986.

[50] J. A. Sethian. *Level set methods and fast marching methods.* Cambridge University Press, 2nd edition, 1999.

[51] J. G. Simmonds. *A brief on tensor analysis.* Springer-Verlag, 2nd edition, 1994.

[52] M. Sussman and E. Fatemi. An efficient, interface-preserving level set redistancing algorithm and its application to interfacial incompressible fluid flow. *SIAM J. Sci. Comput.*, 20:1165–1191, 1999.

[53] D'Arcy Thompson. *On growth and form*. Cambridge University Press, 1992.

[54] X. Wan, Z. Li, and S. Lubkin. An augmented IIM-level set method for Stokes equations with discontinuous viscosity. Electron. J. Diff. Eqns., in press.

[55] S. Xu and Z. J. Wang. An immersed interface method for simulating the interaction of a fluid with moving boundaries. *J. Comput. Phys.*, 216:454–493, 2006.

[56] S. Xu and Z. J. Wang. Systematic derivation of jump conditions for the immersed interface method in three-dimensional flow simulation. *SIAM J. Sci. Comput.*, 27:1948–1980, 2006.

Appendix

Appendix A

Note: Einstein Notation

Indicial notation, or Einstein notation is used extensively in this thesis. Einstein notation is used to (1) simplify expressions involving tensors and vectors, and (2) facilitate derivations involving tensor and vector calculus. See [51] for a short exposition of tensor analysis.

Both upper and lower indices are used. Most lower indices are used in grid discretizations. Indices we use include i, j, k and l. Major indicial notation rules we adopt here are:

(1) Unless otherwise noted, for 2D problems, all indices take on the values α and β; for 3D problems, all indices take on the values α , β and γ. For example, the Cartesian coordinate for a 2D point $\boldsymbol{x}$ takes the form of $\left(x^\alpha, x^\beta\right)$ and for a 3D point $\boldsymbol{x}$ it takes the form of $\left(x^\alpha, x^\beta, x^\gamma\right)$.

(2) Repeated indices of i, j, k and l (not index values: α, β and γ) implies summation. For example, the Laplacian operator

$$\Delta = \nabla^2 = \nabla \cdot \nabla$$

can be represented using $\dfrac{\partial^2}{\partial x^i \partial x^i}$ which in 2D is

$$\frac{\partial^2}{\partial x^\alpha \partial x^\alpha} + \frac{\partial^2}{\partial x^\beta \partial x^\beta}$$

and in 3D is

$$\frac{\partial^2}{\partial x^\alpha \partial x^\alpha} + \frac{\partial^2}{\partial x^\beta \partial x^\beta} + \frac{\partial^2}{\partial x^\gamma \partial x^\gamma}.$$

(3) Free (non-repeated) indices in each term of an expression should match. For example, i and j are both free indices in the following expression

$$\frac{\partial u^i}{\partial x^j} + \frac{\partial u^j}{\partial x^i}$$

where $\boldsymbol{u}$ is a vector-valued function.

Our notations are different from existing notations used in the literature in the following ways:

(1) Since we only use Cartesian coordinates and Cartesian transformations, we can use upper indices without worrying about covariant and contravariant tensor notations in which superscripts and subscripts may have different meanings.

(2) Because it is customary to use lower indices in finite difference discretizations, to avoid overcrowding of subscripts, we choose upper positions for Einstein indices.

(3) It is often seen that Einstein indices take on the values 1,2 and 3. We find that numbers appearing in the upper positions of a symbol can be confusing. For example,

$$\frac{\partial^2 u^2}{\partial x^1 \partial x^2}$$

may be interpreted in many different ways. Therefore we use α, β and γ for indicial values instead. For example,

$$\frac{\partial^2 u^\beta}{\partial x^\alpha \partial x^\beta}$$

is the second-order cross derivative of the second Cartesian component of a vector-valued function $\boldsymbol{u}$ with respect to coordinates x^α and x^β.

(4) For a 2×2 or 3×3 Cartesian coordinate transformation matrix $A = (a_{ij})$, we use

$$A^i_j$$

to denote the matrix element at the ith row and jth column. For example,

$$A^\alpha_\beta$$

is indeed a_{12}.